DEFINING MECHANISMS UNDERLYING CONTEXT-SPECIFIC

TCF/LEF DEPLOYMENT AT TARGET GENES

DEFINING MECHANISMS UNDERLYING CONTEXT-SPECIFIC

TCF/LEF DEPLOYMENT AT TARGET GENES

by

VICTOR GORDON

BSc Life Sciences, McMaster, 2013

A Thesis Submitted to the School of Graduate Studies in Partial Fulfilment of the

Requirements for the Degree Doctor of Philosophy

McMaster University DOCTOR OF PHILOSOPHY (2020)

Hamilton, Ontario (Biochemistry and Biomedical Sciences)

TITLE: Defining mechanisms underlying context-specific TCF/LEF deployment at target genes

AUTHOR: Victor Gordon, BSc (McMaster University)

SUPERVISOR: Bradley Doble, PhD

NUMBER OF PAGES: xxiv, 209

LAY ABSTRACT

Throughout development and adult life cells are in constant communication, using a variety of cell signaling pathways to maintain adult stem cell populations and to pattern tissues throughout the body. Communication between cells often requires one cell to release a protein molecule (called a ligand) that is recognized by a receptor molecule on the surface of another cell. These cell surface receptors, when bound by the signaling ligand become activated and often set of a cascade of internal cellular events that ultimately result in changes in gene transcription in the nucleus. These transcriptional changes are toggled by proteins known as sequence-specific transcription factors that are able to selectively regulate expression of target genes. The net effect of combinations of extracellular ligands binding cell surface receptors determines the selective recruitment of specific transcription factors that activate a cell's transcriptional program, in turn defining its fate and function.

A very important developmental signaling pathway is the Wnt signaling pathway, which employs a family of secreted Wnt molecules as ligands. The Wnt pathway is critical at all stages of organismal development and plays an essential role in tissue maintenance in mature animals. However, due to its critical role in stem cell maintenance, when mutations occur in Wnt signaling components it can have dire consequences. Wnt signaling has been found to be disrupted in more than 70-80% of all cancers. One major feature among these Wnt-related cancers is the inappropriate expression and mobilization of Wnt transcription factors. While the expression and activity of Wnt transcription factors – known as T-Cell Factor/Lymphoid Enhancer Factors (TCF/LEFs) – changes throughout

development and stem cell maintenance, their inappropriate expression is frequently associated with metastasis and poor patient outcomes.

We have used mouse embryonic stem cells (mESCs) as a model system with which to study the mechanisms employed by TCF/LEFs to regulate their target genes. Through a number of approaches, which include adding fluorescent tags to TCF/LEF factors to track their intercellular locations and expression levels or enzymatic tags to identify proteins that interact with individual TCF/LEFs during a snapshot of cell activity, we have gained new knowledge about how these critical transcription factors regulate Wnt-regulated transcriptional programs. We also describe a method for generating micropatterned growth surfaces for mESCs that forces clusters of cells to grow within small circular shapes with a diameter of 1 mm or less. We show that mESCs confined to circular micropatterns differentiate in a highly reproducible manner that allows us to study the cell populations undergoing differentiation with a focus on cell fate determination mechanisms.

ABSTRACT

The canonical Wnt/β-catenin signaling pathway is essential for the proper regulation of cell-fate decisions throughout embryogenesis and in adult issues. Activation of the Wnt signaling pathway allows for nuclear localization of the cell adhesion protein β-catenin, which then interacts primarily with members of the T-Cell Factor/Lymphoid Enhancer Factor (TCF/LEF) transcription factor family to modulate gene activity. The TCF/LEF family includes TCF7, TCF7L1, TCF7L2, and LEF1. While all four family members share a common DNA binding consensus sequence, their expression throughout embryogenesis and adult stem cell populations is unique, with their misexpression commonly occurring in Wnt related cancers and correlating strongly with metastasis and poor patient outcomes.

TCF/LEF exchange at target gene loci is a key feature of mediating context-specific cellular responses to Wnt signaling and can be observed to occur in a variety of populations throughout development and in adult stem cell populations. To model TCF/LEF exchange *in vitro* we have optimized a micropatterning fabrication and culture protocol capable of identifying and isolating discrete LEF1-only and TCF7L1-only populations during gastrulation-like processes. To characterize how complements of TCF/LEFs change during cellular divisions we have developed a novel mitotic chromatin proteomic technique. This method identifies LEF1 as the only TCF/LEF to remain associated with mitotic chromatin in Wnt-activated conditions in mouse embryonic stem cells that are transitioning out of pluripotency as a consequence of removing leukemia inhibitory factor from their culture medium. Additionally, gene targeting techniques were used to label endogenous LEF1 and TCF7L1 with different fluorescent proteins in a single

mouse embryonic stem cell line, allowing us to use TCF/LEF protein expression as a reporter of Wnt/β-catenin pathway status, which we found to be capable of identifying a unique set of compounds that are undetected by traditional Wnt activity (TOP-Flash) reporter screens.

By using gene editing technology, and novel applications of proteomic and cell culture techniques, we have been able to investigate the mechanisms driving TCF/LEF expression and exchange in mouse embryonic stem cells to identify potentially clinically relevant therapeutic targets for their potential use in addressing TCF/LEF dysregulation in cancer. We have identified a novel mechanism through which TCF/LEFs maintain cell fate over cellular division; presented a novel live-cell drug screening platform capable of identifying compounds missed by existing platforms; and presented an optimized cell culture technique for the isolation of TCF/LEF exchange events. Taken together, the work in this thesis provides new insights into the mechanisms through which TCF/LEFs regulate their gene targets during cell fate transitions and throughout mitosis.

ACKNOWLEDGEMENTS

TABLE OF CONTENTS

LIST OF TABLES

LIST OF FIGURES

LIST OF ABBREVIATIONS AND ACRONYMS

2i	CHIR99021 (GSK-3 inhibitor) + PD0325091 (MEK/ERK inhibitor)
3D-CLEM	**3D C**orrelative **L**ight and **E**lectron **M**icroscopy
A/M	**A**synchronous/**M**itotic
ABL	**Ab**elson Murine **L**eukemia (viral oncogene homologue)
AD	**A**ndrogen **D**ependent
AI	**A**ndrogen **I**ndependent
ALL	**A**cute **L**ymphoblastic **L**eukemia
AML	**A**cute **M**yeloid **L**eukemia
A-P	**A**nterior-**P**osterior
APC	**A**denomatous **P**olyposis **C**oli
ATAC-seq	**A**ssay for **T**ransposase-**A**ccessible **C**hromatin using **Seq**uencing
ATP	**A**denosine **Tri**phosphate
AVE	**A**nterior **V**isceral **E**ndoderm
BAF	**B**RG1/BRM-**a**ssociated **f**actor
βBD	β-catenin **B**inding **D**omain

BCL9	**B**-cell **C**LL/**L**ymphoma **9** protein
BCR	**B**reakpoint **C**luster **R**egion (protein)
BCR-ABL	Fusion protein between BCR and ABL gene products associated with certain leukemias
BET	**B**romodomain and **e**xtra-**t**erminal domain
BMP4	**B**one **M**orphogenetic **P**rotein **4**
BRD	**Br**omo**d**omain
BRDT	**Br**omo**d**omain **t**estis-associated
BRG (SMARCA4)	**S**WI/SNF-Related **M**atrix- **A**ssociated Actin-Dependent **R**egulator Of **C**hromatin Subfamily **A** Member **4**
BRM (SMARCA2)	**S**WI/SNF-Related **M**atrix- **A**ssociated Actin-Dependent **R**egulator Of **C**hromatin Subfamily **A** Member **2**
BSA	**B**ovine **S**erum **A**lbumin
β-TrCP	β-**Tr**ansducin repeat **c**ontaining E3 ubiquitin **p**rotein ligase
CAD	**C**omputer **A**ssisted **D**esign
CAMKII	**Ca**lcium/cal**m**odulin-dependent **K**inase **II**
CAPH	**C**hromosome **A**ssociated **P**rotein **H**
CBP	**C**yclic AMP response element-**b**inding **p**rotein

Ccnt1	**Cyc**l**in T1**
cDNA	**C**omplementary **DNA**
CHI	**CHI**R99021 (GSK-3 inhibitor)
ChiLS	**Chi**p/**L**IM-domain binding protein / **S**ingle stranded DNA-binding protein
ChIP-seq	**Ch**romatin **I**mmun**p**recipitation Followed by **Seq**uencing
CLL	**C**hronic **L**ymphoblastic **L**eukemia
Coop	**Co**repressor **o**f **P**an
CRD	**C**ontext-dependent **R**egulatory **D**omain
CtBP	**C**-**t**erminal **B**inding **P**rotein
CTTNB	Gene name for β-catenin
CUT & Run	**C**leavage **U**nder **T**argets and **R**elease **U**sing **N**uclease
CUT & Tag	**C**leavage **U**nder **T**argets and **T**agmentation
DAAM1	**D**ishevelled **A**ssociated **A**ctivator of **M**orphogenesis **1**
DNA	**D**eoxyribo**n**ucleic **A**cid
DMEM	**D**ulbecco's **M**odified **E**agle's **M**edium

DSH	**Dish**evelled
DTT	**Di**thio**t**hreitol
DVE	**D**istal **V**isceral **E**ndoderm
E1A	Adenovirus **e**arly region **1A**
E14Tg2a	Pluripotent mouse embryonic stem cell line (129/Ola strain) deficient in HPRT via transgenic manipulation
EB	**E**mbryoid **Body**
EDA	**E**quipment **D**ata **A**cquisition
EDTA	**E**thylene**d**iamine**t**etraacetic **A**cid
EGTA	**E**thylene **g**lycol-bis(β-aminoethyl ether)-N,N,N′,N′-**t**etraacetic **A**cid
EMT	**E**pithelial-**m**esenchymal **t**ransition
EpiSC	**Epi**blast-derived **S**tem **C**ell
EP300	**E**1A Binding Protein **P300**
ERK	**E**xtracellular Signal-**r**egulated **K**inase
ESRRB	**Es**trogen **R**elated **R**eceptor **B**eta
EU-RNA-seq	5-ethynyluridine (**EU**)-**RNA-seq** (transcriptome-wide sequencing of nascent transcripts)

ExE	**Ex**traembryonic **E**ndoderm
FBS	**F**etal **B**ovine **S**erum
FGF	**F**ibroblast **G**rowth **F**actor
FOXA1	**Fo**rkhead Bo**x A1**
FZD	**F**rizzle**d** (receptor)
GATA	Transcription factor family binding the consensus sequence: (T/A)**GATA**(A/G)
GO	**G**ene **O**ntology
GPCR	**G**-**p**rotein-**C**oupled **R**eceptor
Gro	**Gro**ucho (corepressor)
GSK-3	**G**lycogen **S**ynthase **K**inase-**3**
HAT	**H**istone **A**cetyl **T**ransferase
HD-EB	**H**anging-**d**rop **E**mbryoid **B**ody
HEAT	Repeat motif named after four proteins with HEAT repeats: **H**untingtin, **E**longation factor 3, Protein Phosphatase 2**A** and **T**OR1
HIC5	**H**ydrogen Peroxide-**i**nduced **C**lone **5** (corepressor)
H2A, H2B, H3, H4	**H**istone **2A**, Histone **2B**, **H**istone **3**, **H**istone **4** (the core histones)

HDAC	**Hi**stone **Deac**etylase
HDM	**Hi**stone **D**emethylase
HDMS	**H**exa**M**ethyl**Di**S**ilazane
hESC	**H**uman **E**mbryonic **S**tem **C**ell
HIPK2	**H**omeodomain **I**nteracting **P**rotein **K**inase **2**
HMG	**H**igh **M**obility **G**roup (DNA-binding domain)
HMGA1	**H**igh **M**obility **G**roup **A**T-Hook **1**
HMT	**Hi**stone **M**ethyl**t**ransferase
Hoxb9	**H**omeob**ox B9**
HRP	**H**orse**r**adish **P**eroxidase
HRP	**H**ydrophobic **R**eversed **P**hase
HPRT	**H**ypoxanthine-guanine **P**hospho**r**ibosyl**t**ransferase
IFN-β	**I**nter**f**ero**n-β**
JAK	**Ja**nus **K**inase
JNK	c-**J**un **N**-terminal **K**inase
JQ-1	Inhibitor of BRD and BET family members

KDM5a	Lysine (**K**) **Dem**ethylase **5a**
Ki-67 (MKi67)	Antigen identified by monoclonal antibody **Ki-67** (a nuclear marker of cellular proliferation)
LEF	**L**ymphoid **E**nhancer **F**actor
LIF	**L**eukemia **I**nhibitory **F**actor
LIM	Domain comprising two zinc fingers named after the first three proteins identified with the domain: **L**in11, **I**sl-1 and **M**ec-3
LRP5/6	**L**ow-density Lipoprotein **R**eceptor-related **P**rotein **5/6**
Lys-C	Protease IV from *Pseudomonas aeruginosa*
mAG	**M**onomeric **A**zami **G**reen (fluorescent protein)
MAML	**Ma**ster**m**ind-**l**ike Protein
MAPK	**M**itogen-**a**ctivated **P**rotein **K**inase
MDCK	**M**adin-**D**arby **C**anine **Ki**dney (cell line)
MEK	**M**APK/**E**RK **K**inase
mESC	**M**ouse **E**mbryonic **S**tem **C**ell
mKO2	**M**onomeric **K**usabira **O**range **2** (fluorescent protein)
MMP7	**M**atrix **M**etallo**p**roteinase **7**

MS	**M**ass **S**pectrometry
Mtgr1	**M**yeloid **T**ranslocation **G**ene **R**elated-**1**
N2B27 medium	DMEM/F12 + N2 medium : Neurobasal + B27 medium (1:1)
N2i	N2B27 + CHI + PD03
m⁶A	**N6**-methyl**a**denosine
NEAA	**N**on-**e**ssential **A**mino **A**cids
NICD	**N**otch **I**nter**c**ellular **D**omain
NLK	**N**emo-**l**ike **K**inase
NLS	**N**uclear **L**ocalization **S**ignal
OSN	**O**ct-4, **S**ox2, **N**anog (Key pluripotency TFs)
P-TEFb	**P**ositive **T**ranscription **E**longation **F**actor **b**
P2A	**P**orcine Teschovirus-1 **2A** (self-cleaving peptide)
PAGE	**P**oly**a**crylamide **G**el **E**lectrophoresis
PBS	**P**hosphate-**b**uffered **S**aline
PCP	**P**lanar **C**ell **P**olarity
PD03	PD0325091 MEK/ERK Inhibitor)

PDMS	**P**oly**dim**ethyl**s**iloxane
PFA	**P**ara**f**orm**a**ldehyde
PFI-1	Inhibitor of BRD and BET family members
PIAS4	**P**rotein **I**nhibitor of **A**ctivated **S**tat **4** (SUMO ligase)
PKC	**P**rotein **K**inase **C**
PRC	**P**olycomb **R**epressive **C**omplex
PS	**P**rimitive **S**treak
PTK7	**P**rotein **T**yrosine **K**inase **7**
PTM	**P**ost-**t**ranslational **M**odification
qRT-PCR	**Q**uantitativ**e** **R**evers**e** **T**ranscription-**P**olymerase **C**hain **R**eaction
RBPJ	**R**ecombination Signal **B**inding **P**rotein for Immunoglobulin Kappa **J** Region
RIPA	**R**adio**i**mmunopreci**p**itation **A**ssay (buffer)
RAC1	**Ra**s-related **C**3 Botinulinum Toxin Substrate **1**
RNA	**R**ibo**n**ucleic **A**cid
ROCK	**Rh**o-asso**c**iated Protein **K**inase

ROR2	**R**eceptor Tyrosine Kinase Like **O**rphan **R**eceptor **2**
RNAPII	**RNA P**olymerase **II**
SAINT	**S**ignificance **A**nalysis of **Int**eractome
SB	**SB**-431542 (Smad2/3 inhibitor)
SBE	**S**MAD **B**inding **E**lement
SDS	**S**odium **D**odecyl **S**ulfate
SMAD	*Caenorhabditis elegans* **SMA** ("small" worm phenotype) and *Drosophila* **MAD** ("Mothers Against Decapentaplegic")
SMC	**S**tructural **M**aintenance of **C**hromosomes
STAT	**S**ignal **T**ransducer and **A**ctivator of **T**ranscription
SU	**SU**-5402 (FGFR inhibitor)
SUMO	**S**mall **U**biquitin-like **Mo**difier
SWI/SNF	**SWI**tch/**S**ucrose **n**on-fermentable
TALEN	**T**ranscription **A**ctivator-**l**ike **E**ffector **N**uclease
TBST	**T**ris-**b**uffered **S**aline with **T**ween
TCF	**T**-**c**ell **F**actor

TF	**T**ranscription **F**actor
TFIID	General **T**ranscription **F**actor **IID**
TGFβ	**T**ransforming **G**rowth **F**actor **β**
TLE	**T**ransducin-**l**ike **E**nhancer of Split
YTHDF3	
TOP	**T**CF-**op**timal (binding site)
TSS	**T**ranscriptional **S**tart **S**ite
UCH37	**U**biquitin **C**arboxy-terminal **H**ydrolase **37**
Wnt	**W**ingless / **Int**egration Site
WRE	**W**nt **R**esponsive **E**lement
Xtwn	*Xenopus* homeobox gene **twin**
YEATS	A domain named after 5 proteins first discovered to contain it: **Y**af9, **E**NL, **A**F9, **T**af14 and **S**as5
YEATS2	**YEATS** Domain-containing Protein **2**
YTH	**YT**521-B **H**omology (domain)
Ythdf3	**YTH** **D**omain **F**amily **3**

DECLARATION OF ACADEMIC ACHIEVEMENT

I, Victor Gordon, declare this thesis to be my own work.

I am the sole author of this document. No part of this work has been published or submitted for publication or for a higher degree at another institution. To the best of my knowledge, the content of this document does not infringe on anyone's copyright. My supervisor, Dr. Brad Doble, and the members of my supervisory committee, Dr. Kristin Hope and Dr. Ray Truant, have provided guidance and support at all stages of this project.

I completed all of the research work.

CHAPTER 1. INTRODUCTION

1.1.   WNT/β-CATENIN PATHWAY

The Wnt signaling pathway serves a multitude of critical functions throughout embryonic development, oncogenesis, and adult stem cell maintenance (Kemp et al., 2005; Merrill et al., 2001; Tortelote et al., 2013). The best characterized Wnt signaling cascade, is often referred to as the canonical Wnt pathway, but we will use the more informative and preferred "Wnt/β-catenin pathway" designation (Fig. 1).
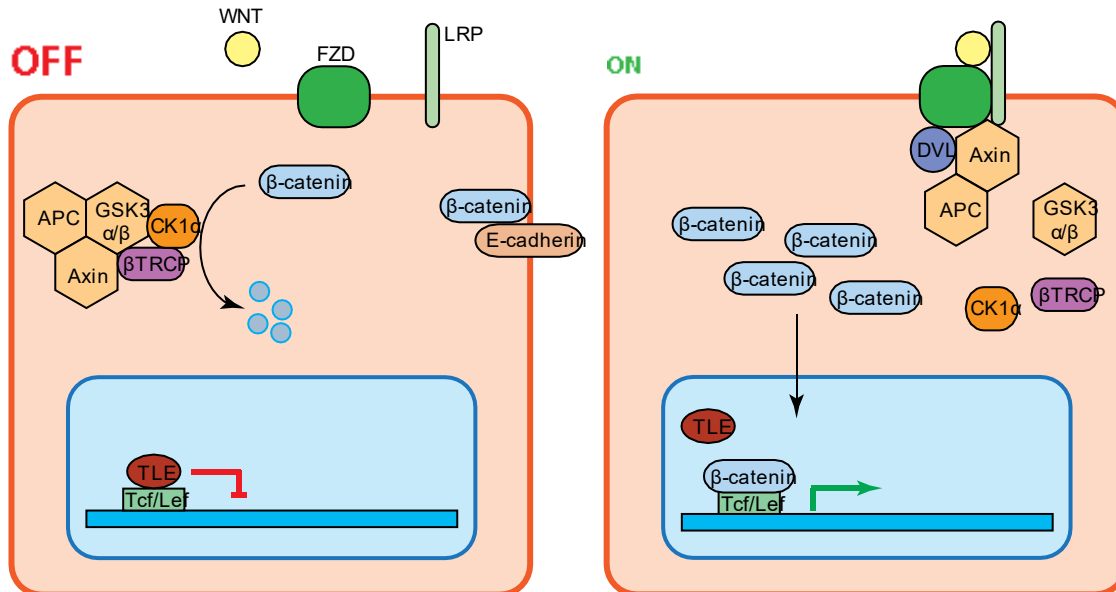
Figure 1.   Wnt/β-catenin signaling

In the absence of Wnt-activated receptors, β-catenin is targeted for degradation by a destruction complex. Wnt binding to cognate receptors results in destruction complex inactivation, which allows β-catenin to accumulate and enter the nucleus where it interacts with TCF/LEF transcription factors to activate target gene transcription.

It relies upon the stabilization of the protein β-catenin (Fagotto, 2013; Kemp et al., 2005). In epithelial cells, the majority of β-catenin resides at the inner surface of the cell membrane, associated with the cell-cell adhesion protein epithelial cadherin (E-cadherin) (Heuberger and Birchmeier, 2010). However, a small portion of total β-catenin resides in the cytosol, and this is the fraction of β-catenin that is regulated by Wnt/β-catenin signaling.

In the absence of a Wnt signal, cytosolic β-catenin is bound and targeted for degradation by a destruction complex composed minimally of adenomatous polyposis coli (APC), disheveled (Dvl), β-TrCP, and glycogen synthase kinase-3α/β (GSK-3α/β), bound to the scaffolding protein Axin (Huang et al., 2009; Kunttas-Tatli et al., 2012). In the presence of a Wnt signal, extracellular Wnt ligand is bound by transmembrane Frizzled (Fz) receptors, which then bind low-density lipoprotein 5/6 (LRP5/6) transmembrane receptors (Bhanot et al., 1996; Tamai et al., 2000). The now-colocalized intracellular domains of Fz and LRP5/6 form the Fz-Wnt-LRP5/6 complex, which interacts with the destruction complex to facilitate the dissociation of β-TrCP, preventing phosphorylation, polyubiquitination and degradation of β-catenin (Brocardo et al., 2005; Kunttas-Tatli et al., 2012). Active cytosolic β-catenin accumulates and then enters the nucleus (Brocardo et al., 2005).

Upon nuclear entry, β-catenin interacts with a wide array of transcriptional cofactors, including transcription factor-7 (TCF7), transcription factor 7-like 1 (TCF7L), transcription factor 7-like 2 (TCF7L2), and lymphoid enhancer-binding factor-1 (LEF1) of the TCF/LEF family of high mobility group (HMG) transcription factors (Graham et al., 2000). β-catenin interacts with TCF/LEFs through their highly conserved N-terminal β-catenin binding

domains (βBD) (Fig. 2), which bind the central Armadillo repeat array (ARM) of β-catenin (Graham et al., 2000). While all four members of the TCF/LEF family share a common DNA binding consensus sequence and possess some redundant functions, they each possess unique non-redundant functions. These unique functions are required for the maintenance of specific stem cell populations, the formation of entire organs, and successful gastrulation.
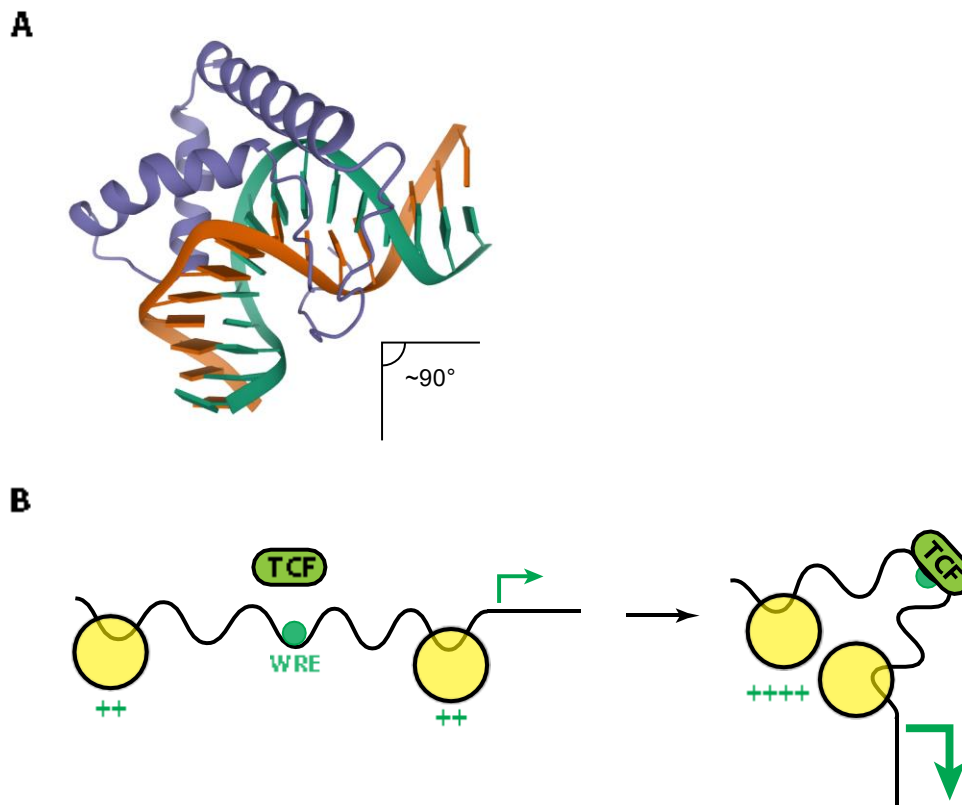
Figure 2. TCF/LEF binding to DNA can induce long-range enhancer interactions.

A) Crystal structure of LEF1 HMG domain (purple) bound to WRE, inducing a bend of roughly 90° in bound double stranded DNA (Love et al., 1995). B) Cartoon depiction of TCF/LEF binding a WRE to kink bound DNA and facilitate the interaction of two distant enhancer elements (yellow) to increase gene expression.

The common DNA binding consensus sequence shared by all four TCF/LEF family members (5' – G/CCTTTGATG/C – 3') is a product of their highly conserved HMG DNA-binding domain (Fig. 2) (Van De Wetering et al., 1997; Waterman et al., 1991).

This HMG group DNA binding domain recognizes its consensus motif in the minor groove of the DNA helix, forcing a bend in the helix of 90° – 127° (Fig. 2A), and is followed by a "basic tail motif" of nine residues carboxy terminal to the HMG (Giese et al., 1995; Love et al., 1995). While the bend introduced by HMG binding has been shown to play a role in looping distant enhancers (Fig. 2B), the basic tail enhances DNA binding affinity through contact with the positively charged DNA backbone and serves as a strong nuclear localization signal (NLS) (Giese et al., 1991; Prieve et al., 1998; Yochum et al., 2010).

The DNA binding ability of TCF7L2 and TCF7 is further modified by a domain known as the "C clamp" (Atcha et al., 2007a). This domain is also carboxy terminal to the HMG domain and confers specificity for a secondary GC-rich sequence known as a "helper site" (Chang et al., 2008). The C-clamp domain does not affect WRE binding directly, but increases TCF7/TCF7L2 binding at WREs that possess an adjacent "helper site" (Atcha et al., 2007a) . While this site can facilitate specific TCF/LEF recruitment, genome-wide ChIP studies for TCF7L2 have shown that helper sites are only enriched in a subset of targets (Hatzis et al., 2008). In the absence of nuclear β-catenin, TCF/LEFs function primarily as repressors, through association with several corepressors such as myeloid translocation gene related-1 (Mtgr1), corepressor of Pan (Coop), and hydrogen peroxide-induced clone 5 (HIC5) (Ghogomu et al., 2006a; Moore et al., 2008; Song et al., 2010). However, the most well studied of these corepressors are members of the Groucho/Transducin-like enhancer of split (Gro/TLE) repressor family. Members of the

Groucho/TLE family bind TCF/LEFs within their central context regulatory domain (CRD) and HMG domains, disrupting coactivator recruitment and suppressing downstream genes (Daniels and Weis, 2005). Motifs similar to the one in LEF1 identified to be required for TLE1 binding were also found in the other TCFs (Arce et al., 2009). Additionally, the CRD of LEF1 and TCF7 have been shown to mediate the recruitment of co-activators from the AP1 transcription factor family that allow for their β-catenin-independent activation of target genes (Sprowl and Waterman, 2013). However, despite their common structure and points of regulation, TCF/LEFs are found to be uniquely expressed throughout Wnt-active tissues during development and postnatal life. The mechanisms driving TCF/LEF selection and exchange are very poorly understood but have been shown to be critical in defining how cells respond to Wnt/β-catenin activation.

1.2. TCF/LEF ISOFORMS

Despite their common structure and points of regulation, TCF/LEFs have unique interaction partners which shape how they influence Wnt target gene expression. Additionally, TCF/LEFs are found to be uniquely expressed throughout Wnt-active tissues during development and postnatal life, with multiple isoforms having been identified for all factors other than TCF7L1, which has no identified alternative splice variants (Cadigan and Waterman, 2012; Hrckulak et al., 2016). These isoforms discretely modify TCF/LEF function and can greatly affect how they associate with and regulate Wnt target genes (Fig. 3). N-terminally truncated TCF/LEF isoforms lacking the β-catenin binding domain occur naturally, and have been shown to function as dominant-negative inhibitors of Wnt signaling activity (Hovanes et al., 2001a; Li et al., 2006; Najdi et al., 2009). Additionally, the C-tail is quite variable among TCF/LEF splice isoforms. This region can exist as one

of two broad classes, the 'B' tail which is short and has no well-defined function (Arce et al., 2006), and the longer 'E' tail which has unique interaction domains and is not found in Lef1. The E-tail harbours C-terminal binding protein (CtBP) binding sites and C-clamp activity in certain isoforms. TCF7L1 and certain TCF7L2 isoforms possess a CtBP binding sequence in their C-tail domain, which has been shown to act as a co-activator or co-repressor, critically altering their regulation of Wnt targets in different cellular contexts (Patel et al., 2014; Valenta et al., 2003). The C-clamp is a region found in E-tail isoforms of TCF7 and TCF7L2 which does not alter affinity for standard WREs, but allows the binding of GC-rich "Helper" sites upstream and downstream of the bound WRE (Atcha et al., 2007b; Hoverter et al., 2012; Hoverter et al., 2014). The presence of a C-clamp expands the transcriptome of Tcf7 and TCF7L2, allowing them to regulate critical growth-related genes that cannot be bound efficiently by C-clamp-lacking isoforms (Atcha et al., 2007b; Hoverter et al., 2012; Hoverter et al., 2014). Finally, the Lef1 N-tail and B-tail isoforms are defined by the inclusion or exclusion of exon 11, respectively (K. Hovanes, 2000; Willinger et al., 2006). While the CRD generally mediates interaction with co-regulators such as TLEs, it can be alternatively spliced to modify these interactions. All TCF/LEFs possess an alternative exon within their CRD domain, while TCF7L1 and TCF7L2 have this exon flanked by alternative splice sites, allowing the alternative exon to be flanked by short LPVQ and SxxSS amino-acid motifs. The activity of these alternative exons is not well defined but appears to recruit co-repressors in LEF1 (Ghogomu et al., 2006b). The flanking motifs have been shown to recruit co-repressors in *Xenopus* (Gradl et al., 2002).
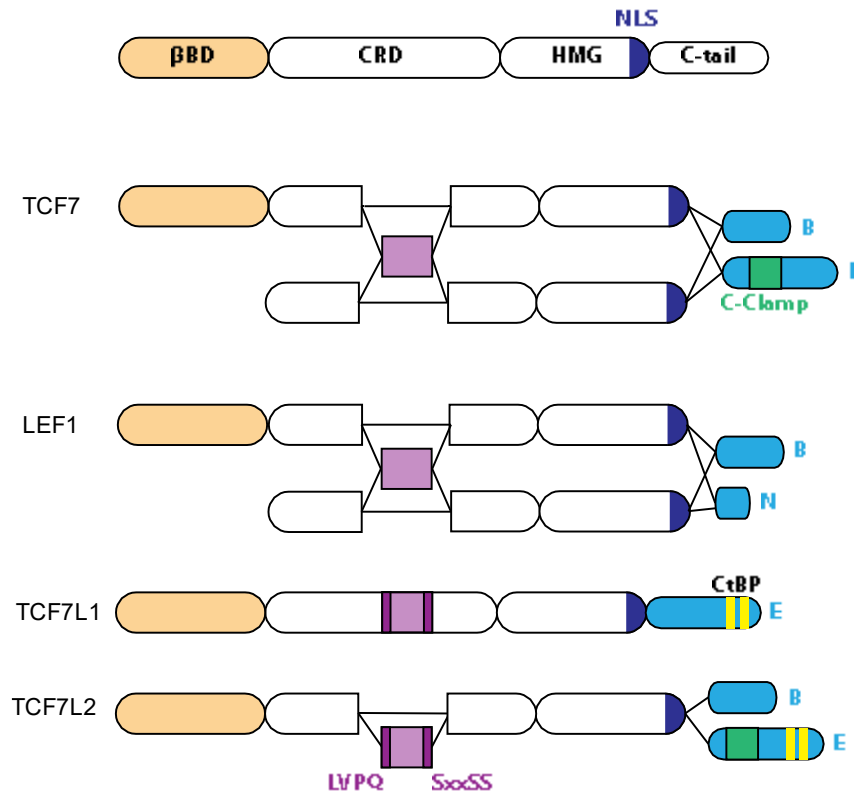
Figure 3.   Schematic representation of splice diversity among TCF/LEF family members.

A typical full-length isoform is depicted possessing an N-terminal β-catenin binding domain (orange, βBD), context-dependent regulatory domain (CRD), high mobility group DNA binding domain (HMG), nuclear localization signal (dark blue, NLS), and C-tail (light blue). Isoforms for individual TCF/LEFs depict the presence of a variable CRD exon (purple), with additional flanking motifs (dark purple), and C-tail domain variants for all family members except TCF7L1.

1.3.   β-CATENIN-INDEPENDENT WNT SIGNALING

While Wnt ligands can vary greatly in overall structure, their functions can be broadly grouped as β-catenin dependent or independent. β-catenin independent pathways are frequently referred to as "noncanonical" Wnt signaling pathways. Wnt ligands stimulating these pathways were initially identified by their ability to oppose canonical Wnt function or to affect calcium signaling in developing *Xenopus* embryos (Kohn and Moon, 2005). These Wnt ligands still bind Frizzled receptors, but they do not recruit canonical Wnt co-receptors, affect destruction complex stability, or modulate TCF/LEF transcriptional activity (Butler and Wallingford, 2017; Kohn and Moon, 2005). These β-catenin independent pathways are poorly defined due to their overlap with other signaling pathways but can be separated into three general groups: Wnt/Calcium signaling, Fzd/GPCR signaling, and the planar cell polarity (PCP) pathway.

The Wnt/calcium pathway is induced by specific Wnt and Frizzled homologs activating calcium/calmodulin-dependent kinase II (CamKII) and protein kinase C (PKC). Wnt5 and Wnt11 are well-known β-catenin-independent Wnt ligands that signal through the Wnt/Calcium pathway. As intracellular calcium release is required for body plan specification, the loss of either Wnt11 or Wnt5 function promotes hyperdorsalization of *Xenopus* or Zebrafish embryos, respectively (Kühl et al., 2000; Westfall et al., 2003). In Wnt5 loss-of-function zebrafish, this phenotype can be partially rescued by expressing constitutively active CamKII, demonstrating its functional interaction with CamKII and its ability to oppose Wnt/β-catenin signaling. Additionally, Frizzled receptors are seven pass transmembrane proteins, and have been found to function as G-protein coupled receptors

(GPCRs), further influencing the calcium pathway and broadening their role in both canonical and non-canonical Wnt signaling (Slusarski et al., 1997).

The PCP pathway is critical for the organization of structures along the perpendicular axis in the plane of flat epithelial cells (Butler and Wallingford, 2017). Defining polarity in this plane is critical for the formation of various tissues, as it allows cells to define a "front" and "back" relative to a signaling gradient. This mode of orientation is essential for the intracellular distribution of signaling components and is essential for neural tube formation. Noncanonical Wnts function by binding Fzd and recruiting a non-LRP cofactor such as PTK7 or ROR2. The receptor complex then recruits Dsh and DAAM1, which activates Rho or binds Rac1. Activated Rho then activates ROCK, and Rac1 activates JNK, which are both major mediators of cytoskeleton formation and restructuring. This restructuring allows collective orientation cellular structures, such as actin-based hairs in *Drosophila* wing cells, or organized cells in patterned tissues such as the neural tube. Mutations in PCP genes are among the most frequently identified mutations in human neural tube defects (NTDs). Robinow syndrome, which results in severe skeletal dysplasia, short limbs, and craniofacial anomalies, has been attributed to mutations in Wnt5a and its PCP co-receptor ROR2. In the context of cancer, mutations in PCP receptors or Wnt ligands such as Wnt5a or Wnt11 are frequently associated with increased cell migration, proliferation, and metastasis (VanderVorst et al., 2018).

1.4.   THE ROLE OF WNT IN DEVELOPMENT

1.4.1.   Wnt signaling and pluripotency

The maintenance of mouse embryonic stem cells (mESCs) *in vitro* requires the inhibition of multiple developmentally relevant signaling pathways to maintain a state of "naïve" pre-

implantation pluripotency (Silva et al., 2008; Ying et al., 2008). mESCs are traditionally maintained in serum-containing medium supplemented with LIF, which promotes a pluripotent state capable of self-renewal through activation of JAK/STAT3 signaling, but mESCs grown under these conditions are often heterogeneous and contain spontaneously differentiating subpopulations (Cartwright et al., 2005). Partial differentiation of pluripotent mESCs was found to arise from auto-inductive FGF4 signaling mediated by the MAPK/ERK pathway, and the inclusion of the MEK inhibitor PD0325091 was found to increase pluripotent mESC population homogeneity, but at the expense of clonogenicity (Ying et al., 2008). The inclusion of the GSK-3 inhibitor CHIR99021 (CHI), which acts as a Wnt mimetic, was found to not only rescue low clonogenicity in LIF/PD03 conditions, but also reduced apoptosis and enhanced pluripotency (Ying et al., 2008). The use of these three compounds in serum-free conditions was found to exhibit greatly increased pluripotent gene expression (Sim et al., 2017). Further characterization of this serum-free N2B27 + CHI + PD03 + LIF condition (N2i + LIF) has revealed that the addition of any two of the three supplements to basal medium can maintain pluripotent mESC self-renewal, though with slightly less efficiency than complete N2i + LIF medium.

The unique pluripotent state of embryonic stem cells is controlled primarily by the three transcription factors: Oct4, Sox2, and Nanog (OSN), that facilitate the expression of genes required for pluripotency and self-renewal (Orkin et al., 2008). However, initial characterization of Wnt regulation in pluripotency found that TCF7L1 is the most highly expressed TCF/LEF factor in pluripotent mESCs and that it co-occupies promoters throughout the genome in association with Oct4 and Nanog (Cole et al., 2008). While

TCF7L1 was first thought to contribute to the regulation of these genes as both an activator, in association with β-catenin, and repressor, in association with TLE, further genetic characterization has provided strong evidence that TCF7L1 functions as a negative regulator of pluripotent stem cell self-renewal (Martello et al., 2012; Pereira et al., 2006; Sokol, 2011; Yi et al., 2011). Characterization of TCF/LEFs within the pluripotent state revealed that TCF7L1 limits Nanog expression and promotes loss of self-renewal, as the differentiation of TCF7L1KO cells *in vitro* was heavily delayed due to excessive Nanog levels (Pereira et al., 2006). The ability of Wnt to contribute to pluripotency, was later revealed to function primarily through its derepression of TCF7L1-regulated genes (Shy et al., 2013; Wray et al., 2011). Upon Wnt stimulation, nuclear β-catenin was shown to inactivate TCF7L1 by removing it from DNA and inducing its proteasomal degradation, therefore allowing OSN to maintain pluripotency-enhancing gene expression (Shy et al., 2013). β-catenin mediated degradation of TCF7L1 was found to be sufficient for the maintenance of pluripotency, as ΔC-β-catenin lacking its transactivation domain was capable of degrading TCF7L1 and sustaining pluripotency in the presence of CHI, suggesting that Wnt contributes to pluripotency strictly through the β-catenin mediated degradation of TCF7L1 (Wray et al., 2011). Furthermore, the deletion of TCF7L1 phenocopies the deletion or inhibition of GSK-3, mimicking Wnt activation and relieving repression of the core OSN network (Wray et al., 2011). Additionally, ΔN-TCF7L1cells in which TCF7L1 can no longer bind β-catenin are insensitive to Wnt stimulation, demonstrating that this function is β-catenin specific (Wu et al., 2012). Taken together, these findings suggest that TCF7L1 functions as a repressor in the pluripotent state, and that Wnt maintains pluripotency through the β-catenin mediated degradation

of TCF7L1. Intriguingly, in the absence of the other TCF/LEF factors in genetically engineered mESCs, TCF7L1 appears to be capable of functioning as a transcriptional activator, so one must be cautious in assuming that it is a truly obligate repressor during preimplantation mouse development (Moreira et al., 2017).

1.4.2.   Wnt signaling and Gastrulation

Pluripotent conditions and mechanisms for *in vitro* maintenance of mESCs are reflective of the inner cell mass and epiblast of the pre-implantation blastocyst, between days 3.5 to 4.5 (E3.5 – E4.5) of development (Davidson et al., 2015). Multiple Wnt ligands are expressed, and *Axin2* reporter activity can be observed throughout these populations, which demonstrates a high degree of Wnt activity (ten Berge et al., 2011). However, this Wnt activity is extinguished upon implantation of the embryo (ten Berge et al., 2011). While cells of the post-implantation epiblast are still considered pluripotent, TCF7L1 is broadly expressed and Wnt signaling is inactive as determined by Wnt reporters (Guo et al., 2010; Hoffman et al., 2013; Merrill et al., 2004). However, as the developing embryo begins to posteriorize, Wnt signaling is activated and TCF/LEF expression patterns begin to change. Expression of Nodal throughout the epiblast at E5.5 promotes the expression of the BMP4 within the superjacent extraembryonic ectoderm, which in turn promotes the expression of Wnt3 within the proximal-posterior portion of the epiblast (Arnold and Robertson, 2009). Within this proximal posterior region of Wnt3 expression, cells become Wnt-active and gastrulation is initiated by E6.25. Epiblast cells beyond this Wnt-active region retain TCF7L1 expression and commit towards ectodermal fates, while Wnt-active cells lose TCF7L1 expression in favour of LEF1 expression (Merrill et al., 2004; Van Genderen et al., 1994). These LEF1-positive cells then undergo epithelial to

mesenchymal transition (EMT) and contribute towards the developing primitive streak

(PS) as they commit to a mesodermal fate (Fig. 4). At the conclusion of gastrulation by

E7.5, Wnt-inactive tissues within the anterior of the embryo exclusively express TCF7L1

and TCF7L2 in the anterior ectoderm and endoderm, respectively (Ah Cho and Dressler,

1998; Merrill et al., 2004). However, in posterior Wnt-active tissues TCF7 and LEF1 can

be found throughout mesodermal and ectodermal tissues (Mariëtte Oosterwegel, 1993;

Van Genderen et al., 1994) (Fig. 4). The anterior localization of TCF7L1/TCF7L2 in Wnt-

inactive tissues, and posterior localization of LEF1/TCF7 throughout Wnt-active tissues

highlights their general roles of repressors and activators of Wnt, respectively. How Wnt

and TCF/LEF expression affects cell fate determination and commitment is exemplified

by knockout mouse models targeting these factors.
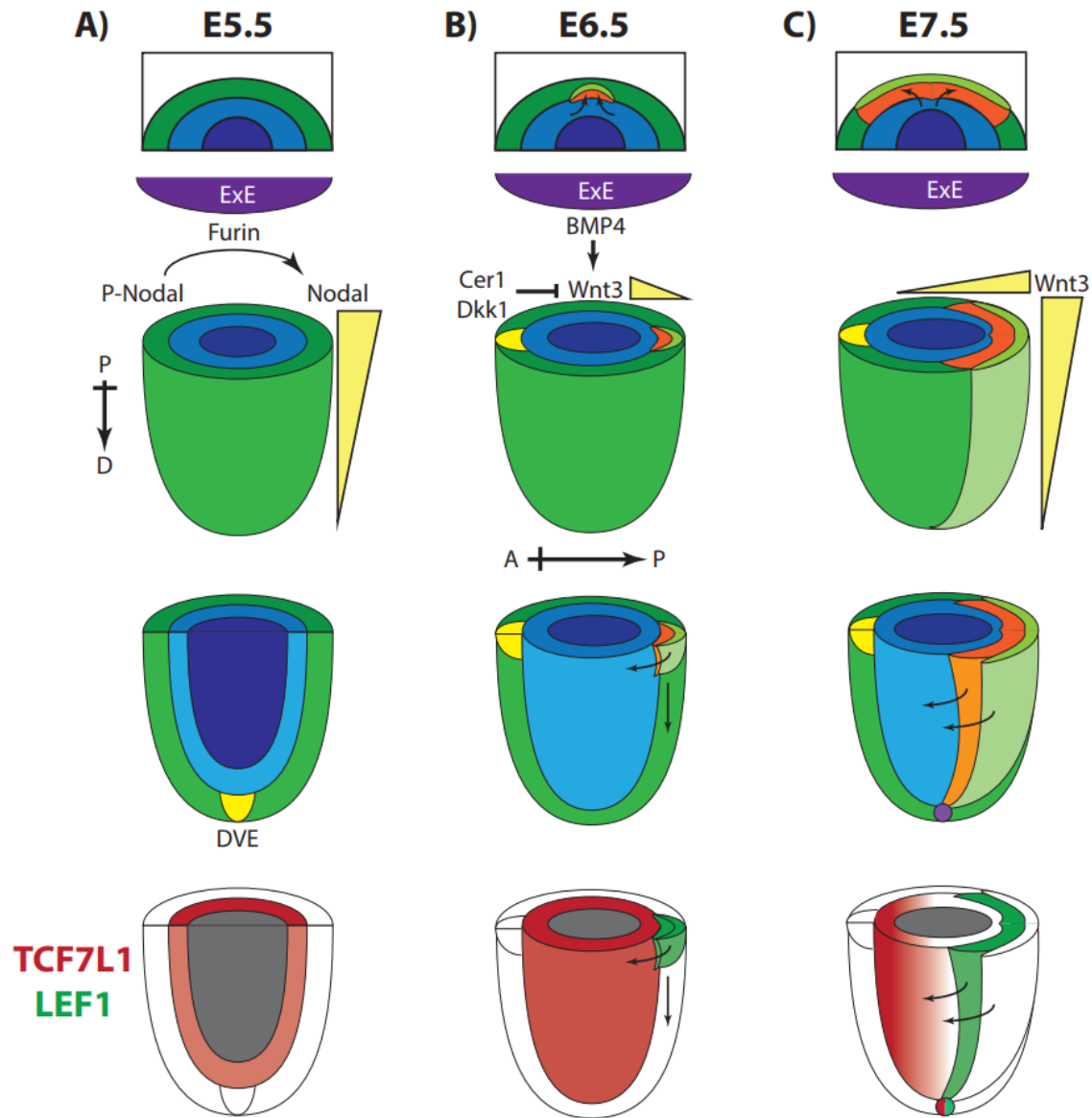
Figure 4.   TCF7L1and LEF1 expression throughout mouse gastrulation.

Figure 4. (Continued)

A) By embryonic day 5.5 (E5.5) the epiblast (light blue) of the embryo has committed towards an ectodermal fate, and broadly expresses TCF7L1(dark red). This population is overlaid by a layer of cells known as the visceral endoderm (green). Proximal-distal (P-D) asymmetry is established by the production of pro-Nodal (p-Nodal) by the epiblast, which is converted into functional Nodal by the superjacent extraembryonic ectoderm (ExE). This localized activation of Nodal patterns the subjacent embryo, establishing an organizing population of cells within the visceral endoderm known as the distal visceral endoderm (DVE). The DVE produces Wnt and BMP inhibitors, restricting Nodal to the proximal half of the embryo. B) As development continues the DVE migrates towards what will become the anterior face of the embryo by E6.5. At this time, the ExE begins producing BMP4, which promotes expression of Wnt3 within the subjacent epiblast. The presence of the DVE restricts Wnt3/BMP4/Nodal activity towards the posterior half of the embryo, establishing Anterior-Posterior asymmetry (A-P), which renames the DVE to anterior visceral endoderm (AVE). This process initiates gastrulation in the proximal-posterior portion of the embryo, causing ectodermal epiblast cells to undergo EMT and commit towards endodermal (light green) and mesodermal (orange) fates as they contribute towards the developing primitive streak (PS). Cells entering the PS rapidly lose TCF7L1(red) expression in favour of LEF1 (green) expression. C) Upon completion of gastrulation the PS has migrated distally and laterally across the embryo and established an organizing body known as the node (purple) at the distal tip of the embryo. At this point LEF1 is expressed broadly throughout Wnt-active posterior mesodermal lineages, while TCF7L1is restricted to anterior Wnt-suppressing ectodermal fates. This A-P separation of TCF7l1/LEF1 can even be observed in node cells.

1.4.3. Knockout Mouse Models

The functions of LEF1 and TCF7 are unique, yet partially redundant during early cell fate commitment. While both TCF7 and LEF1 are strongly expressed throughout the posterior mesoderm of the E7.5 mouse embryo, LEF1 expression is considerably higher, and independent knockout mice for either TCF7 or LEF1 present unique phenotypes (Mariëtte Oosterwegel, 1993; Van Genderen et al., 1994). Mice lacking TCF7 specifically lack CD4$^+$/CD8$^+$ double-positive thymocytes, but are otherwise phenotypically normal (Verbeek et al., 1995). In contrast to this specific loss of function, LEF1 knockout mice exhibit disruption in the formation of several different organs and die roughly one week

after birth (Van Genderen et al., 1994). LEF1 null mice are approximately 70% the size of WT litter mates, fail to develop teeth, mammary glands, whiskers, and body hair, and show an absence of the mesencephalic nucleus of the trigeminal nerve. Together, these findings suggest that LEF1/TCF7 function may be partially redundant during gastrulation, but they also highlight that LEF1 is essential for the proper maintenance of mesoderm-derived cell populations.

The requirement of TCF7 and LEF1 for proper mesodermal commitment is highlighted by the combined deletion of both LEF1 and TCF7. $LEF1^{-/-}/TCF7^{-/-}$ mice exhibit embryonic lethality, with embryos failing to complete gastrulation successfully, resulting in neural tube duplication, limb bud defects, and loss of mesodermal commitment (Galceran et al., 1999). This outcome closely phenocopies $Wnt3a^{-/-}$ mice (Galceran et al., 1999; Takada et al., 1994). During gastrulation, mesodermal cells exit the PS to contribute towards the lateral, paraxial, and axial mesoderm. The paraxial mesoderm then segments axially into somites that eventually form vertebrae later in development (White et al., 2003). In $LEF1^{-/-}/TCF7^{-/-}$ mice, caudal somites, which would initially be formed by posterior paraxial mesoderm, are specifically absent (Galceran et al., 1999). However, somite formation is acutely impeded in LEF1-βgal knock-in mice, where an in-frame β-galactosidase knock-in replaces the HMG domain of LEF1 in both alleles (Galceran et al., 2004). Together these findings highlight that while TCF7 alone can partially rescue the loss of LEF1, allowing embryos to successfully gastrulate without the loss of critical cell lineages, LEF1 is required for the effective maintenance cell fates derived from the paraxial mesoderm.

The expression of TCF7L2 is dispensable during gastrulation but is required for the maintenance of specific stem cell niches. While $TCF7L2^{-/-}$ mice successfully complete

gastrulation and appear phenotypically normal, they die shortly after birth (Korinek et al., 1998). Histopathological analysis of developing TCF7L2$^{-/-}$ embryos revealed that while proper intestinal epithelium is established by E14.5, no proliferative compartment was maintained in the crypts of the intestinal epithelium (Korinek et al., 1998). These findings demonstrate that TCF/LEFs can serve highly specific non-redundant functions.

In vivo, TCF7L1 is required for proper fate restriction during gastrulation, in a β-catenin-independent fashion, until E9.0. The loss of TCF7L1 has the strongest impact on early development out of all single TCF/LEF knockout mice, resulting in embryonic lethality due to disruption of gastrulation (Merrill et al., 2004). While TCF7l1$^{-/-}$ mice initiate gastrulation and undergo mesodermal commitment, they do so at the expense of ectoderm, resulting in expanded mesoderm populations and duplication of axial mesodermal structures such as the notochord (Merrill et al., 2004). Additional mesodermal structures, which were lost in LEF1$^{-/-}$ or Wnt3a$^{-/-}$ mice (such as somites), were found to be duplicated (Takada et al., 1994; Van Genderen et al., 1994). These findings are consistent with existing observations of TCF7L1functioning as a repressor, as it appears to be required for the restriction of Wnt-active regions during gastrulation. Additionally, this function appears to be β-catenin independent in developmental models, due to compensatory pathways that are absent in *in vitro* culture conditions. Mice homozygous for a TCF7L1mutant lacking its N-terminal β-catenin binding domain (TCF7L1$^{\Delta N/\Delta N}$) are capable of undergoing gastrulation without any dysregulation, but are not viable due to defects arising after E9.0 (Wu et al., 2012). These findings are consistent with those observed in the pluripotent state, where TCF7L1 is degraded upon interaction with β-catenin (Shy et al., 2013). Taken together these findings also demonstrate that repressive TCFs, such as TCF7L1,

may prime Wnt target genes for occupation and activation by "activating TCF/LEFs" and that proper regulation and exchange of TCF/LEFs is essential for delimiting and regulating populations of Wnt-active cells.

1.5.   WNT-MEDIATED TRANSCRIPTIONAL REGULATION

1.5.1.   Overview of transcriptional regulation in mammalian cells

Gene transcription is a highly ordered event regulated by the aggregation of several protein complexes and defined by specific DNA and epigenetic features. Central to this process is the recruitment and stabilization of RNA polymerase II (RNAPII). However, prior to RNAPII recruitment, genes must be epigenetically "primed" for transcription. During interphase DNA can exist in either an euchromatic or heterochromatic state. These states are defined by the association of DNA with four heterodimeric histone proteins, which includes two copies of Histone 2A (H2A), Histone 2B (H2B), Histone 3 (H3), and Histone 4 (H4) (Klemm et al., 2019; Olins and Olins, 2003). These complexes are known as nucleosomes and are encircled by ≈147 bp of DNA (Kaplan et al., 2009). Chromatin in which DNA is tightly coiled around compacted nucleosomes is considered heterochromatin, and due to its compact nature, these regions are not open to transcription (Lee et al., 2004; Thurman et al., 2012). Euchromatic regions, however, are nucleosome-poor and possess long stretches of exposed DNA upon which transcription can be initiated (Lee et al., 2004; Thurman et al., 2012). However, the organization of nucleosomes within the genome is non-uniform. While most chromatin exists in a heterochromatic state, histones are depleted at regulatory loci such as enhancers, insulators, promoters, and actively transcribed gene bodies (Thurman et al., 2012). These internucleosomal regions are often bound by transcription factors, RNA polymerases, or

architectural factors (Fyodorov et al., 2018; Thurman et al., 2012). While these regions comprise less than 3% of the genome, they account for more than 90% of transcription factor-bound regions (Thurman et al., 2012). Switching between these two chromatin states is mediated by post-translational modification (PTM) of histones within a given nucleosome (Bannister and Kouzarides, 2011). In general, the addition of charged acetyl groups promotes an euchromatic state while the addition of non-polar methyl groups promotes a compact heterochromatin state (Bannister and Kouzarides, 2011). This is a result of proximal charged acetyl groups forcing nucleosomes apart, while non-polar methyl groups promote the adhesion and compaction of nucleosomes. The proteins mediating these modifications are called epigenetic regulators. Histone acetyl transferases (HATs) and histone deacetylases (HDACs) mediate histone acetyl status while histone methyltransferases (HMTs) and histone demethylases (HDMs) mediate histone methyl status (Bannister and Kouzarides, 2011). However, a large portion of these factors lack a DNA-binding domain (Haberland et al., 2009). As a result, most of these factors function ubiquitously or are recruited by DNA binding transcription factors.

Transcription factors typically lack intrinsic histone modifying activity, and instead serve as scaffolds for the recruitment of epigenetic regulators and general transcriptional machinery (Spitz and Furlong, 2012). Activating transcription factors recruit co-activators, such as Ep300/CREB-binding protein, to promote acetylation and opening of surrounding chromatin (Merika et al., 1998; Simon et al., 2011). Repressive transcription factors recruit co-repressors, such as the polycomb repressive complex (PRC), which promotes methylation and condensation of surrounding chromatin (Chittock et al., 2017; Tan et al., 2007). While modifying surrounding nucleosomes does affect their compaction,

chromatin remodelers are required to eject or move nucleosomes from/along DNA to allow/prevent assembly of transcriptional machinery (Alver et al., 2017; King and Klose, 2017; Wapinski et al., 2017). The most well-studied chromatin remodeler is the SWItch/Sucrose non-fermentable (SWI/SNF) complex. This complex rearranges nucleosomes in an ATP-dependent manner and is ubiquitously employed by transcription factors (Alver et al., 2017). The chromatin remodeling process exposes long stretches of DNA, allowing for its transcription. However, opposing epigenetic complexes such as the Polycomb repressive complex (PRC) compete to re-establish a heterochromatic state and prevent transcription. As such, the competition between activation and suppression is highly dynamic, and its regulation is essential for proper gene expression. To ensure the stable activation of a target gene, multiple transcription factors cooperatively assemble epigenetic and transcriptional machinery into large assemblies known as "enhanceosomes". While promoters are regions within a few thousand base pairs of the transcriptional start site (TSS), enhancers can exist tens of thousands of base pairs upstream or downstream of the TSS (Andersson and Sandelin, 2020; Levine, 2010). These regions are rich in transcription factor binding sites and facilitate the assembly of enhanceosomes. The highly stereospecific assembly of transcription factors within these regions is essential for enhanceosome assembly and the efficient recruitment and concentration of co-activators, such as CBP/p300, which are required for gene activation (Carey, 1998; Levine, 2010; Panne, 2008) (Fig. 5A). Certain HMG proteins, such as HMGA1, have also been shown to play a role in enhanceosome assembly (Panne, 2008). As HMG proteins bind the minor groove of DNA they uncoil the DNA and reduce the free energy required for subsequent transcription factors to bind (Panne, 2008). Intriguingly

enhanceosomes do not appear to require direct interaction among associated transcription factors, but rather their cooperative "chelation" of coactivators, such as Ep300, is what allows them to activate downstream genes (Levine, 2010). Additionally, proximal and distant enhancer/promoter elements can be aggregated by DNA looping to further increase enhanceosome activating potential (Levine, 2010). The architectural protein CCCTC-binding factor (CTCF) is well known for its ability to bind two distant regions of DNA and loop-out the intervening region (Arzate-Mejia et al., 2018). This allows promoters and enhancers caught within the looped region to come into closer proximity and increase the potency of the assembled enhanceosomes.

A)
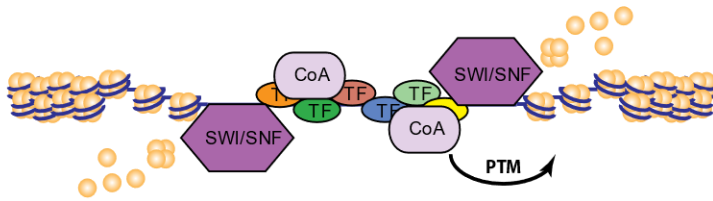
B)
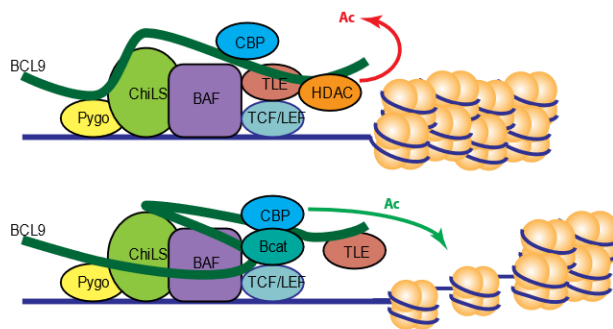
C)
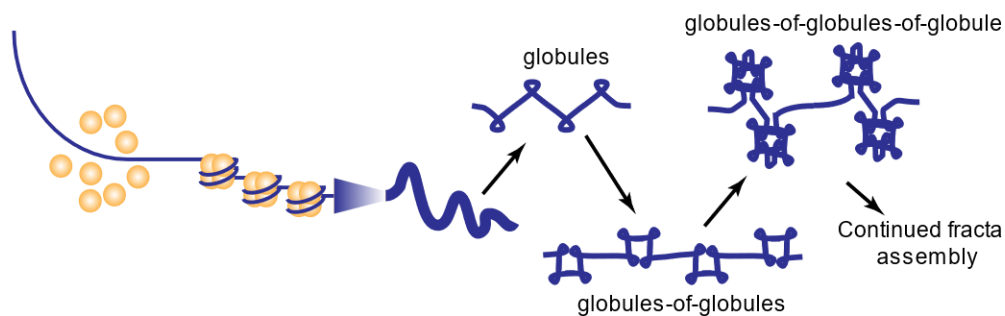
Figure 5.   Chromatin regulation and organization

A) Enhanceosomes are assembled upon a contiguous region of transcription factor (TF) binding sites to facilitate the aggregation of epigenetic and architectural complexes required to optimize target gene activation. Recruited co-activators (CoAs) typically possess catalytic domains capable of modifying proximal histones to obtain an open epigenetic state through acetylation, methylation, or a variety of other post-translational modifications (PTMs). Remodelling complexes, such as the SWI/SNF complex, are also recruited to translocate or eject nucleosomes from euchromatin regions, exposing DNA and allowing for transcription to occur. B) The Wnt assembled however the presence or absence of β-catenin is what defines its activity or inactivity, respectively. In the absence of β-catenin TLE is able to recruit HDACs and promote the compaction of adjacent chromatin (OFF). However, upon β-catenin recruitment by Bcl9 TLE binding is disrupted in such a way that it can no longer recruit HDAC. As a result the HAT activity of CBP is capable of promoting an open chromatin state through the acetylation of proximal histones. The pre-assembled nature of the Wnt enhanceosome allows for rapid changes in the regulation of target genes. C) As compacts and begins to fold into itself through intermolecular attraction it begins to crumple into discrete regions that have been termed "globules". These globules will then further collapse into each other, forming larger globules.

Enhanceosomes are large assemblies of transcription factors and epigenetic regulators that cooperatively recruit transcriptional machinery. Transcription factors regulate target genes through assembly onto cis-regulatory DNA elements known as promoters and enhancers. These features reside upstream of the transcriptional start site (TSS) and facilitate the binding of multiple transcription factors. Assembled transcription factors cooperatively assemble epigenetic regulators and transcriptional machinery to promote gene transcription. However, loss of individual factors or opposition by competing assemblies can prevent expression. In prototypical enhanceosomes, such as the interferon-β (IFN-β) enhanceosome, eight separate transcription factors assemble along a contiguous 55 bp stretch of DNA (Panne, 2008). Characterization of the IFN-β enhanceosome has revealed key insights into enhanceosome formation and stabilization. While all eight factors bind at very closely arranged DNA binding sites, they lack broad interaction faces among each other. Instead their assembly upon the enhanceosome region is stabilized by interaction with shared co-activators, such as CBP/Ep300, and specific changes in DNA conformation induced by their binding. As such, architectural factors are required to bend and open the DNA to facilitate enhanceosome assembly. HMGA1 is an architectural protein which possesses two AT-hook domains, capable of non-specifically binding the minor groove of DNA in AT-rich regions and has been shown to promote IFN-β enhanceosome assembly by reducing the free energy cost of enhanceosome factor binding. Extensive characterization of the IFN-β enhanceosome has suggested that enhanceosomes do not require direct interaction among associated transcription factors, but rather their cooperative "chelation" of coactivators, such as Ep300, is what allows them to activate downstream genes.

1.5.2. The Wnt enhanceosome

As TCF/LEFs lack intrinsic repressor or activator capacity, they rely upon the assembly of secondary factors to regulate the expression of downstream genes. In general, descriptions of this mechanism are typically reduced to the association of TCF/LEFs with repressive TLE family members in the absence of Wnt activation, and replacement of TLEs with β-catenin upon Wnt activation (Brantjes, 2001; Daniels and Weis, 2005). However, the Wnt enhanceosome is a significantly more complicated assembly of proteins than this generalization suggests.

Wnt enhanceosomes are large complexes of proteins bound to TCF/LEFs, which remain stable in both Wnt ON and OFF conditions (Van Tienen et al., 2017b). Core components of the Wnt enhanceosome in mammals include the Chip/LIM-domain binding protein (LDB)-single stranded DNA-binding protein (ChiLS) complex, BRG1/BRM-associated factor (BAF) complex, Transducin-like Enhancer of Split (TLE), Pygopus (Pygo), B-cell CLL/Lymphoma 9 protein (BCL9), cAMP response element binding protein (CREB) binding protein (CBP)/E1A associated protein 300 (EP300), and a TCF/LEF factor (Fiedler et al., 2015; Renko et al., 2019b; Van Tienen et al., 2017b). However, the recruitment of ChiLS/BAF complexes, CREB/Ep300, and TLE are known to not be Wnt-specific. The ChiLS complex is pleotropic in function, controlling multiple stages of embryonic development through cell fate commitment and maintenance (Alan D. Agulnick, 1996; Matthews and Visvader, 2003). LIM-containing proteins recruit the ChiLS complex to distant enhancers of critical lineage genes, allowing it to facilitate communication between distant enhancers and promoters by looping-out intervening sequences (Li et al., 2011; Liu and Dean, 2019; Morcillo et al., 1997). CBP and Ep300

are members of a coactivator family, frequently recruited by a large variety of transcription factors, which promote gene expression through their intrinsic HAT activity and recruitment of transcriptional machinery (Spiegelman and Heinrich, 2004). BRG1 and BRM are ATP-dependent helicases of the SWI/SNF protein family, and as such are common chromatin remodelers required to unwind DNA in preparation for transcription (Rother and Van Attikum, 2017). Members of the TLE family lack a DNA-binding domain, but are widely recruited transcriptional co-repressors (Jennings and Ish-Horowicz, 2008). The Pygopus family also possesses HAT activity and is highly specific, but not exclusive, to the Wnt pathway (David S. Parker, 2002). Finally, Bcl9 is a large flexible protein that appears to be essential for Wnt enhanceosome assembly and function (Van Tienen et al., 2017b).

While most components of the Wnt enhanceosome are not specific to the Wnt signaling pathway, their specific interactions with β-catenin:TCF/LEF complexes is what allows for the rapid regulation of Wnt target genes. Currently it is understood that β-catenin, TLE and Bcl9 mediate the transition of the Wnt enhanceosome from an OFF to ON state (Van Tienen et al., 2017b). While the Wnt enhanceosome remains constitutively assembled at WREs, there are considerable architectural changes that occur in its transition from an OFF to ON state. In the OFF state TLE binds TCF/LEF, BCL9, and recruits HDACs. The HDAC recruited by TLE opposes the HAT activity of EP300 and prevents activation of downstream target genes. However, upon Wnt activation nuclear β-catenin is recruited to the complex, inducing a conformational change in BCL9 which displaces TLE and its associated HDAC (Fiedler et al., 2015; Van Tienen et al., 2017b). Additionally, repression by TLE is further prevented by the recruitment of Ubiquitin Protein Ligase E3 Component

N-Recognin 5 (Ubr5) which ubiquitylates TLE to prevent its ability to recruit HDACs (Flack et al., 2017). Once in this ON state EP300 can freely promote activation of target genes. This retention of core components in both OFF and ON states has been shown to facilitate the rapid regulation of target genes. The assembly of an inactive Wnt enhanceosome "earmarks" target genes for rapid activation upon Wnt stimulation, which can also be rapidly inactivated upon β-catenin depletion.

1.5.3.   Co-Regulation of the Wnt signaling pathway

The interaction of TCF/LEFs with secondary transcription factors is well established, as Wnt signaling often acts in concert with a variety of developmental signaling pathways (Lei et al., 2004; Zhang et al., 2013). These interactions have been shown to cooperatively activate or suppress the expression of lineage-specific genes to guide cell fate (Klaus et al., 2012). Wnt signaling has been shown to be influenced on multiple levels by these secondary factors, which either influence the stability of Wnt signaling components such as β-catenin (Kwon et al., 2011) or directly interact with TCF/LEFs themselves (Ross and Kadesch, 2001). While influencing the stability of Wnt signaling components may potentiate overall Wnt activity, the interaction of secondary pathways with TCF/LEFs directly provides insight into how WREs are selectively occupied and regulated.

One of the most closely associated signaling pathways is the TGF-β signaling pathway which, in certain contexts, has been shown to directly influence WRE activity and Wnt target gene expression (Etienne Labbe, 2000; Jain et al., 2015). TGF-β target genes are regulated by "receptor Smads" (R-Smads) such as Smad2/3 for TGF-β ligands, and Smad1/5 for BMP ligands (Gaarenstroom and Hill, 2014). However, these Smads require co-Smads, such as Smad4, to enter the nucleus and affect target gene expression. In the

absence of a TGF/BMP signal both R-Smads and co-Smads remain unphosphorylated and are cytosolically localized. However, upon ligand binding by TGF-β Receptor 1/2 (TGFR1/2), TGFR1/2 are autophosphorylated and recruit the appropriate R-Smad group. These associated R-Smads are then phosphorylated by TGF-B R1/2 and their affinity for co-Smads is greatly increased. The phospho-R-Smad/co-Smad complex is then capable of entering the nucleus and regulating target gene expression. While capable of independently influencing gene activity, Smad2/3/4 complexes have been shown to interact with LEF1 (Etienne Labbe, 2000), while Smad1/5/4 complexes have been shown to interact with TCF7L1 (Sierra et al., 2018). In the *Xenopus* model system LEF1 has been shown to directly interact with Smad2/3 to directly influence the expression of the developmentally relevant gene Xtwn (*Xenopus* homeobox gene twin) (Labbe et al., 2000). In this context two Smad binding elements (SBEs) were found to exist ≈200bp upstream of three concatenated WREs in the *Xtwn* promoter (Etienne Labbe, 2000). Through use of reporter assays it was shown that the loss of either SBEs or WREs could shut down *Xtwn* expression, whereas both Smad2/3 and β-catenin/LEF1 complexes were required for maximal activation (Etienne Labbe, 2000). In human embryonic stem cells (hESCs) Smad2/3 have been shown to promote Wnt-mediated mesodermal differentiation (Estaras et al., 2015). Mesodermal Wnt target genes were shown to recruit β-catenin/LEF1 complexes and enrich for Ser5-phosphorylated RNA polymerase 2 (RNAPII), indicating initiation of transcription. However, it was shown that recruitment of Smad2/3 to these target genes was required for the subsequent recruitment of phospho-Transcription Elongation Factor b (P-TEFb) to promote Ser7-RNAPII accumulation and complete transcriptional elongation. Together, these studies show that cooperative gene

regulation by Wnt and TGF-β signaling requires LEF1/Smad2/3 interactions for maximal activation of target genes.

Similar mechanisms of cooperative gene regulation have been observed for the FGF, Notch, and Hippo signaling pathways. Coordinated Wnt/Notch signaling events have been shown to be critical for specific fates such as intestinal epithelium (Ogaki et al., 2013). Patterning of broad progenitor-rich tissue groups such as those found in the developing limb bud or tooth bud have been shown to be the product of Wnt/FGF coordination (Kratochwil et al., 2002; Sasaki et al., 2005; Ten Berge et al., 2008). The expansion or restriction of these, and other, progenitor populations has in turn been shown to be a product of Wnt/Hippo cooperative regulation (Aragona et al., 2013). However, these various pathways have been shown to interact with Wnt at multiple levels of the signaling pathway. Transcriptional effectors of Hippo signaling have been shown to directly interact with TCF/LEFs, whereas additional Hippo signaling components have been found to directly affect β-catenin stability and localization (Azzolin et al., 2014). Similarly, LEF1 has been found to function as a co-activator for Notch transcription factors, and Notch activation has been shown to mediate β-catenin stability (Kwon et al., 2011; Ross and Kadesch, 2001). However, FGF and Wnt signaling have been shown to more indirectly affect each other through cross-regulation of each other's signaling components (Yin et al., 2008).

The ability of Wnt to interact closely with so many other developmentally critical pathways demonstrates its importance in cell fate determination and maintenance. However, as majority of these interactions are directly mediated at the transcriptional level, the TCF/LEF complement may define a cell's ability to participate in crosstalk events. Thus,

how cells determine, maintain, and change TCF/LEF expression status is a critical aspect of Wnt signaling.

1.6.   MITOSIS AND WNT

1.6.1.   "Bookmarking" transcription factors

The retention of transcription factors upon mitotic chromatin, and its role in cell fate determination, is becoming better understood. Initial models of mitotic chromatin asserted that transcription and translation halted until mitosis was complete and all transcription factors and transcriptional machinery were ejected into the cytosol during mitosis (Marian A. Martinez-Balbas, 1995; Parsons and Spencer, 1997). However, these assertions were supported by experiments that relied upon formaldehyde crosslinking prior to immunofluorescent imaging of transcription factors and associated machinery during mitosis. When these observations were compared to experiments using live cell fluorescence microscopy of fluorescently labelled factors, it was determined that many transcription factors (Liu et al., 2017; Palozola et al., 2019) and much transcriptional machinery (Chen et al., 2002; Xing et al., 2008) remain associated with mitotic chromatin. The artifactual loss of mitotic association observed in studies employing formaldehyde crosslinking methods is thought to be due to the fluid-like nature of mitotic chromatin, which results in chromatin-associated factors only interacting transiently, thereby preventing efficient crosslinking (Maeshima et al., 2020a). Mitotically associated factors include:

Table 1. Experimentally confirmed bookmarking factors

Factor	Context	Reference
TFIID	HeLa (human, cervical cancer)	(Christova and Oelgeschlager, 2002; Xing et al., 2008)
TFIIB	HeLa (human, cervical cancer)	(Christova and Oelgeschlager, 2002; Xing et al., 2008)
TBP	HeLa (human, cervical cancer)	(Christova and Oelgeschlager, 2002; Xing et al., 2008)
CTCF	HeLa (human, cervical cancer)	(Burke et al., 2005)
FOXI1	PAC2 (Zebrafish, fibroblasts)	(Yan et al., 2006)
RUNX2	Saos-2 (human, osteosarcoma)	(Daniel W. Young, 2007)
BRD4	NIH3T3 (mouse, fibroblasts)	(Anup Dey, 2003)
MLL	HeLa (human, cervical cancer)	(Blobel et al., 2009)
GATA1	G1E (mouse, erythroid precursors)	(Kadauke et al., 2012)
FOXA1	HUH7 (human, hepatocarcinoma)	(Caravaca et al., 2013)
RBPJ	F9 (mouse, testis)	(Lake et al., 2014)
PARP1	HEK293 (mouse, kidney)	(Lodhi et al., 2016)
ORC1	U2OS (human, osteocarcinoma)	(Kara et al., 2015)
RING1	HeLa (human, cervical cancer)	(Arora et al., 2016)
BMI1	HeLa (human, cervical cancer)	(Arora et al., 2016)

ESRRB	Embryonic stem cells (mouse/human)	(Festuccia et al., 2016)
SOX2	Embryonic stem cells (mouse/human)	(Deluz et al., 2016)
OCT4	Embryonic stem cells (mouse/human)	(Liu et al., 2017)
KLF4	Embryonic stem cells (mouse/human)	(Liu et al., 2017)

Characterization of mitotically associated transcription factors has revealed that these factors play a critical role in cell fate maintenance through the rapid reactivation of lineage-specific target genes following mitosis (Kadauke et al., 2012; Sekiya et al., 2009). This ability to "bookmark" lineage genes for preferential post-mitotic expression has led to these factors being referred to as "bookmarking" factors. Rapid reactivation of bookmarked target genes has been quantitatively demonstrated in studies of the transcription factor GATA1 (Kadauke et al., 2012). ChIP-seq analyses examining GATA1 localization in both interphase and metaphase populations revealed that GATA1 remains associated with a specific set of target genes in both conditions. The preferential reactivation of these bookmarked targets was then demonstrated by mitotically arresting cells and following the reactivation of bookmarked versus non-bookmarked targets upon mitotic release by using qPCR. Consistent with the theorized role of bookmarking factors, the bookmarked target genes were activated significantly faster than non-bookmarked targets. Further structural characterization of bookmarking factors, such as FOXA1 (Caravaca et al., 2013) and ESRRB (Festuccia et al., 2016), also revealed that bookmarking factors both scan and specifically bind DNA during metaphase. While their

ability to scan mitotic chromatin is what leads to their total decoration of mitotic chromatin when observed microscopically, it has also been shown to directly affect their ability to find and bind specific target genes (Caravaca et al., 2013; Sekiya et al., 2009). These specific binding events have been shown to play a critical role in bookmarking activity.

Global analysis of histone methylation and acetylation status during interphase and metaphase has revealed that while repressive histone marks are consistently retained across interphase and metaphase, activating acetylation marks are significantly reduced during metaphase (Liu et al., 2017; Valls et al., 2005). However, many housekeeping and lineage marker gene promoters appear to retain their acetylation status during mitosis (Liu et al., 2017). Consistent with this observation, the working model for bookmarking factors was that they remained associated with target genes and retained their euchromatin status so that they could be more easily reactivated following mitosis (Caravaca et al., 2013; Kadauke et al., 2012). This model followed the long-held notion that transcription halted during metaphase (Prescott and Bender, 1962).

The recently developed EU-RNA-seq technique has allowed for increased sensitivity in determining transcriptional activity during metaphase (Palozola et al., 2017). To label nascent transcripts the culture medium is spiked with 5'ethynyluridine (EU), which is able to enter cells in a matter of minutes and become incorporated in nascent mRNA (Palozola et al., 2017). After recovering RNA from the treated population, click chemistry is then used to conjugate the EU-incorporated RNAs to biotin. Purification of biotin-EU-RNA is then accomplished by using streptavidin-sepharose beads, followed by on-bead cDNA synthesis and high-throughput DNA sequencing. When performed on asynchronous HeLa cells ≈28 000 transcripts were identified, while ≈8 000 transcripts were detected in

mitotic populations (Palozola et al., 2017). While mitotic transcripts were on average 5-fold less abundant than asynchronous equivalents, there was up to 100-fold difference in expression among mitotic targets. Together these findings demonstrate that transcription is selectively maintained during mitosis for roughly 30% of interphase target genes. When considered with existing knowledge that RNA Pol II (Liang et al., 2015a) and basal transcription factors (TFIID, TFIIB, etc.) (Teves et al., 2018) remain associated with mitotic chromatin, this has updated the current view of mitotic bookmarking. In the current model, bookmarking factors and transcriptional machinery remain associated with target genes during mitosis, maintaining promoter/enhancer euchromatin status and providing a pool of mRNA for translation during early G1, respectively (Palozola et al., 2019) (Fig. 6). Following mitosis this accumulation of transcript and retention of epigenetic status allows bookmarked genes to reactivate significantly faster than non-bookmarked genes, which must first regain their epigenetic status and then recruit transcriptional machinery before resuming transcription.
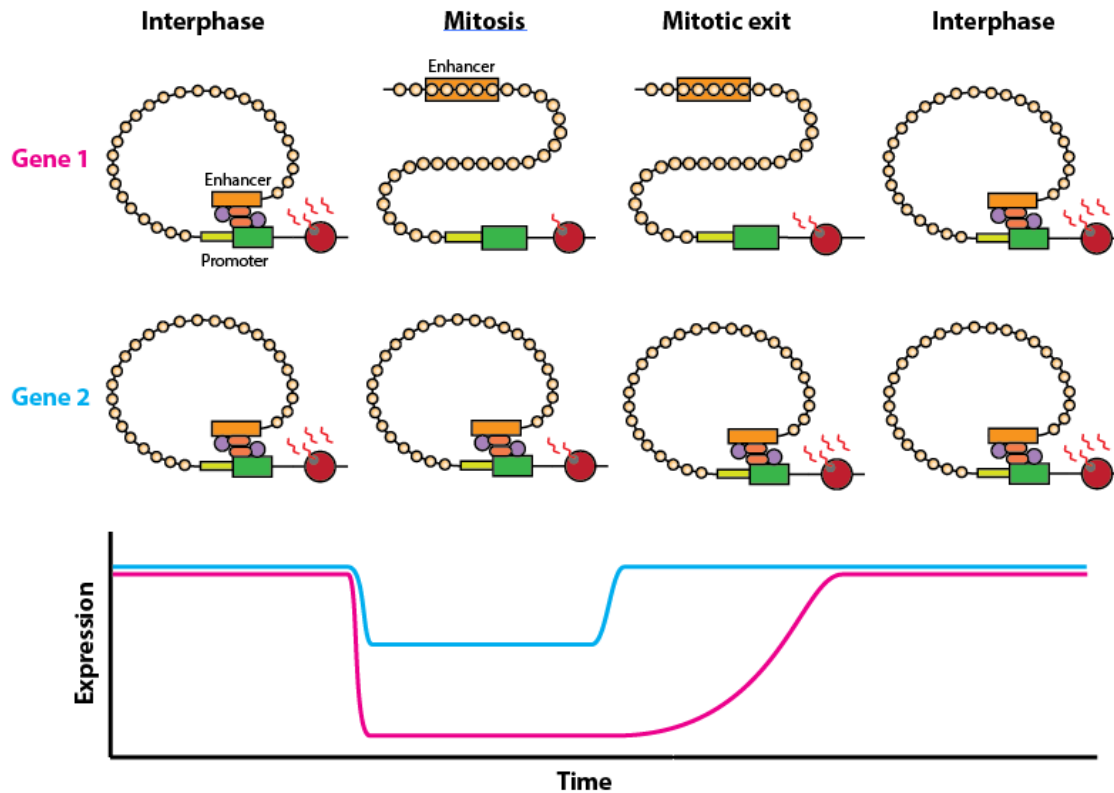
Figure 6.   Bookmarking factors maintain gene structure throughout metaphase.

Typical genes regulated by transcription factors that are ejected from mitotic chromatin (e.g. gene 1) have greatly reduced activity throughout metaphase and are slow to reinitiate transcription following mitotic exit. This is due to the loss of enhancer looping and occupation during mitosis (orange box). When not maintained, these enhancer regions adopt a heterochromatin state (beige circles) as mitotic chromatin condenses. While RNA Polymerase II (red circle) has been found to remain associated with the promoter of many genes during mitosis, its activity is greatly reduced (fewer red squiggles). As a result, typical genes must restore their euchromatin status before resuming maximal activity, producing a considerable lag phase following mitosis. Bookmarked genes (gene2) however retain their epigenetic status throughout mitosis. Bookmarking transcription factors maintain the open status of bound enhancers, retaining gene structure and reducing the impact of metaphase on transcription rates. Upon mitotic exit maximal transcriptional activity is restored, and due to the retained epigenetic structure of bookmarked genes, maximal transcriptional activity is rapidly restored. This allows bookmarked genes to resume transcriptional activity significantly faster than non-bookmarked genes.

While bookmarking is an observed function for an increasing number of transcription factors, there is still very little understanding as to why one DNA binding transcription factor can bookmark, and another cannot. A recent live-cell fluorescence imaging screen assessed 501 transcription factors for their ability to remain associated with mitotic chromatin, and found 112 of those factors to become enriched on mitotic chromatin during metaphase (Raccaud et al., 2019). Unfortunately, mitotically enriched proteins showed no considerable enrichment in common sequences or domains that correlated with mitotic retention. However, by using various imaging and transcriptomic techniques, Raccaud et al. determined that their findings supported a model in which non-specific DNA binding properties play a critical role in determining whether a transcription factor is capable of mitotic association. While this model supports the ability of a transcription factor to remain associated with mitotic chromatin, it is not entirely consistent with proper bookmarking functionality. As previously mentioned, EU-RNA-seq has revealed that only ≈30% of interphase genes appear to be active during mitosis (Palozola et al., 2017). This finding would suggest that while transcription factors appear to decorate total mitotic chromatin, it is their specific association with discrete target genes that affects their rapid reactivation following mitosis. Mitotic chromatin is an incredibly complicated milieu of proteins and DNA, meaning that the increased DNA scanning trait proposed by Raccaud *et al.* may just predispose these factors to non-specifically adhere to mitotic chromatin without promoting proper bookmarking activity. To understand how transcription factors establish islands of transcriptional activity through mitosis, we must first understand the composition and structure of mitotic chromatin.

1.6.2.   Mitotic Chromatin Structure

Organization of chromatin during interphase is a carefully regulated aspect of cellular fate determination. However, during mitosis, chromosomes undergo a variety of equally precise topological and epigenetic changes as they begin to form cylindrical chromosomal bodies. These gross morphological changes and the segregation of factors between the mitotic chromosomes, perichromosomal layer, and cytosolic fraction of the dividing cell have been shown to be critical regulators of cellular fate and function.

To understand the 3D structure of chromatin, a variety of chromatin conformation capture techniques have been developed (Abou El Hassan and Bremner, 2009; Dostie et al., 2006; Lieberman-Aiden et al., 2009; Zhao et al., 2006). However, the most robust approach is Hi-C, which is capable of mapping inter-/intra-chromosomal interactions throughout the entire genome with a one megabase resolution. In this technique, cells are crosslinked, and DNA is then digested with a restriction enzyme. The resulting sticky ends are then filled in with biotinylated nucleotides, which can then be ligated under dilute conditions to favour ligation of DNA fragments within the same crosslinked complex. Biotinylated fragments are then purified using streptavidin beads and identified by paired-end sequencing. Mapping these ligated fragments reveals regions of inter/intra-chromosomal contact across the entire genome. By using these interaction matrices as a foundation, Lieberman-Aiden et al. were able to use polymer simulation models to determine how distant interactions reflected on the overall structure of interphase chromosomes. Building off previously proposed models, Lieberman-Aiden *et al.* found that interphase chromosome interactions most closely fit a "fractal globule" model (A. Grosberg, 1993; Grosberg et al., 1988) (Fig. 5C). In this model each chromosome is a

considered to be an unentangled polymer which crumples into a series of small globules, similarly to "beads-on-a-string". As the polymer compacts further, these globules serve as monomers until a single globule of globules-of-globules-of-globules is formed. The fractal nature of these condensed globules would facilitate easy unfolding and refolding, which would be a requisite of gene regulation (S.K.Nechaev). However, compaction of these interphase structures into ordered linear mitotic chromosomes requires further organizational mechanisms.

Upon entering prometaphase, individual chromosomes are condensed into chromatids through the linear arrangement of loops in the mitotic chromatin (Earnshaw and Laemmli, 1983; Gibcus et al., 2018b). Characterization by microscopy has shown that chromosomes become recognizable by prophase (Ohnuki, 1968), shortening and condensing further during prometaphase (Liang et al., 2015b) until chromosomes are fully condensed in metaphase. This process is mediated by gross intermolecular forces within the chromatin favouring compaction, with Condensin complexes organizing this compaction, and topoisomerase II alpha relieving torsion as the DNA is compacted (Liang et al., 2015b). Condensin complexes are essential for compaction and are assembled from five proteins, which belong to three different protein families (Hirota, 2004). The Structural Maintenance of Chromosomes (SMC) family contributes SMC2 and SMC4 to both Condensin I and II complexes (Hirota, 2004). The Kleisin family contributes Chromosome Associated Protein H (CAPH) to the Condensin I complex, and CAPH2 to the Condensin II complex (Schleiffer et al., 2003). Finally, two HEAT repeat subunits are also present in Condensin I (CAP-D2, CAP-G) and Condensin II (CAP-D3, CAP-G2) complexes (Miguel A. Andrade, 1995). The HEAT domain is named after the proteins it

was initially found in: **H**untingtin, elongation factor 3 (**E**F3), protein phosphatase 2A (PP2**A**), and the yeast kinase **T**OR1 (Miguel A. Andrade, 1995).

Once assembled, both Condensin complexes have been shown to function as mechanochemical motors, capable of translocating along DNA in an ATP-dependent manner (Terakawa et al., 2017) (Fig 6A). This motor function has been thought to be responsible for chromosome condensation for many years (Earnshaw and Laemmli, 1983; Hirota, 2004; Ohnuki, 1968). Characterization of this process by performing Hi-C analysis on metaphase populations has confirmed this notion, finding that the motor function of Condensin II allows it to introduce ≈50kb loops into prometaphase chromatin during early prophase, which grow in size to become up to ≈700 kb loops by prometaphase (Gibcus et al., 2018b) (Fig. 7B). These loops are then subdivided by Condensin I which introduces smaller ≈80 kb loops (Gibcus et al., 2018b). These nested loop sections are non-random, and are instead arranged around a central helical axis, similar in structure to a spiral staircase (Gibcus et al., 2018b). This central helical structure is thought to be a result of stacked HEAT domains within CAP-D3 and CAP-G2 of the Condensin II complex (Gibcus et al., 2018b; Yoshimura and Hirano, 2016). While Condensin I and II are responsible for the ordered compaction of mitotic chromatin, they rely on secondary factors to segregate individual chromosomes during metaphase. To achieve this, a surfactant layer of protein is deposited upon the surface of condensing chromosomes
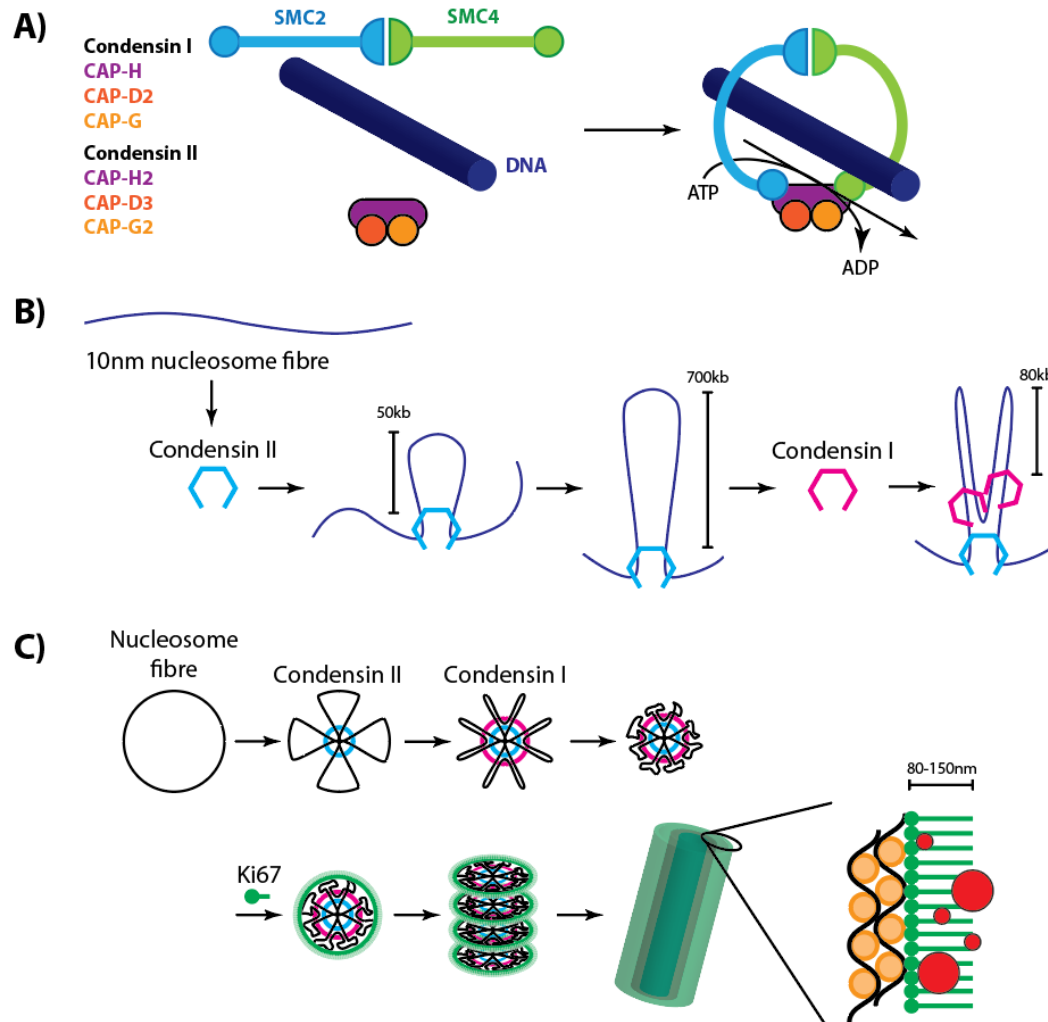
Figure 7.   Condensin I and II mediate the compaction of mitotic chromatin.

A) Condensin I and II share two common SMC2/4 components but vary in the composition of their HEAT and Kleisin subunits. However, both Condensin I/II translocate across DNA in an ATP-dependent manner. B) Condensin II initiates the formation of large chromatin loops, which are then further subdivided into nested loops by the recruitment of Condensin I. C) Overview of mitotic chromatin condensation mediated by Condensin I/II. Cross section shows mitotically associated factors (red circles) adhering to Ki67 perichromosomal layer or directly to mitotic chromatin (yellow circles).

This surfactant layer has been termed the "perichromosomal layer" and is an ionically charged milieu of proteins that prevent metaphase chromatin from collapsing into a single congealed mass (Cuylen et al., 2016). Characterization of this mitotic compartment by using 3D-CLEM, a combination of light microscopy and serial block-face scanning electron microscopy, has revealed that this perichromosomal layer comprises 30-47% of the entire chromosome volume (Booth et al., 2016). These observations are further supported by quantitative proteomics that has found the perichromosomal layer to account for more than 33% of mitotic chromosomal protein mass (Booth et al., 2016).

Research into this specific mitotic fraction over a timespan of more than 10 years has identified >50 specific components, including proteins, antigens, and RNAs (Booth and Earnshaw, 2017). Although the list of proteins in the perichromosomal layer continues to grow, the main constituents appear to be fibrillarin, nucleolin, nucleophosmin, peripherin, and Ki-67 (Booth and Earnshaw, 2017; Van Hooser et al., 2005). These perichromosomal components reside in the nucleolus during interphase and are released upon nucleolar degradation during mitosis to form a layer around the mitotic chromatin that is approximately 80-150 nm thick (Booth et al., 2016) (Fig. 7C).

The most well-studied component of the perichromosomal layer is Ki-67, which is a large linear protein with a C-terminal domain that has high affinity for heterochromatin, a long flexible central domain, and a polar N-terminal domain (Booth and Earnshaw, 2017; Cuylen et al., 2016). This structure has been proposed to allow Ki-67 to assemble on metaphase chromatin like ≈80 nm long bristles on a brush (Cuylen et al., 2016). However, the heterogeneity of the perichromosomal layer is thought to allow many proteins to "piggyback" on mitotic chromatin through non-specific interactions (Ginno et al., 2018;

Ohta et al., 2010). As such, many existing proteomic methods have omitted RNA polymerase II and translational machinery from their results, suggesting that they would adhere non-specifically, and that their absence is a result of pure mitotic chromatin preparations (Ginno et al., 2018; Ohta et al., 2010). However, these claims conflict with previously discussed observations that RNA polymerase II is not only present, but also still active, on mitotic chromatin (Festuccia et al., 2019; Palozola et al., 2017). This would suggest that novel proteomic tools are required to properly bridge these two techniques so that we may comprehensively investigate how bookmarking complexes are assembled and maintained during mitosis.

1.7.   TCF/LEF SELECTION AND EXCHANGE

Asymmetry in cell fates following mitosis is a common feature of progenitor cell populations, such as those observed in the intestinal crypt epithelium (Qi and Chen, 2015; Qi et al., 2017). However, beyond changes in signaling ligand concentrations, the transcriptional mechanisms governing these abrupt cell fate changes remain poorly defined. In the context of Wnt signaling, fate-related transcriptional changes can be observed as changes in TCF/LEF status. An excellent example of such an event is in the hair follicle, where TCF7L1 and LEF1 have been found to regulate the differentiation of multipotent skin stem cells (Merrill et al., 2001). As Wnt-inactive TCF7L1-positive skin stem cells differentiate and contribute towards the hair follicle, they begin to lose TCF7L1 expression and instead express LEF1 as they become Wnt-active. A similar process has been observed in pluripotent mESCs, where an exit from pluripotency caused by Wnt stimulation is associated with the loss of TCF7L1 expression and gain of LEF1 expression (Moreira et al., 2017; Shy et al., 2013). These examples demonstrate that the complement

of TCF/LEFs expressed in a cell can be altered in response to Wnt activation and changes in cellular context. However, while there is no well-defined mechanism for how rapid changes in the occupancy of target genes by different TCF/LEFs occurs, many potential mechanisms have been proposed.

1.7.1.   Post-Translational Modification (PTM) of TCF/LEFs

Post-translational regulation of TCF/LEFs has been shown to be a crucial aspect of Wnt signal regulation. Phosphorylation of TCF/LEFs has been shown to selectively deplete or activate TCF/LEFs. In *Xenopus,* the phosphorylation of TCF7L1/TCF7L2/LEF1 by HIPK2 has been shown to dissociate them from target genes, allowing TCF7 to selectively occupy and regulate WREs in response to a Wnt signal (Hikasa and Sokol, 2011b). By contrast, LEF1 is specifically regulated by Nemo-like Kinase (NLK), which in some contexts promotes the transcriptional activity of LEF1 and in others facilitates the degradation of LEF1 (Ota et al., 2012; Yamada et al., 2006). Further, modification by ubiquitin has been shown to impede DNA binding of TCF/LEFs, which can be countered by the selective deubiquitylation of TCF7 by Uch37 (Han et al., 2017). Both TCF7L2 and LEF1 have been shown to be sumoylated by PIAS4, which affects their transcriptional activity and localization (Ihara et al., 2005; Sachdev, 2001). This complex network of TCF/LEF post-translational regulation highlights a means through which TCF/LEF status can be finely tuned. The presence or absence of these modifying enzymes could determine the TCF/LEF status of a Wnt-responsive cell, defining the effect of a Wnt ligand on the cell's biology. Although not the sole source of regulation for TCF/LEF exchange, post-translational modification of TCF/LEFs is likely to serve as an important mechanism of TCF/LEF control.

1.7.2.   TCF/LEF Selection via Abundance or Coregulation

As previously discussed, TCF/LEFs can recruit secondary non-Wnt transcription factors to cooperatively regulate target genes. However, not all TCF/LEFs function equally in this regard. Cooperative factors may favour one or more TCF/LEFs over the others. As the cellular context changes, these cooperative factors may then be lost or changed to select for alternative TCF/LEFs. In the absence of coregulators or regulation by PTM, the simplest mechanism of exchange may be through sheer abundance. If there are multiple TCF/LEFs present, the most abundant TCF/LEF may have the greatest impact on how Wnt signals are transcriptionally executed. However, this mechanism seems unlikely in scenarios where TCF/LEF exchange events occur rapidly. In the transition from ectoderm (TCF7L1-positive) to primitive streak mesoderm (LEF1-positive), the region of TCF7L1/LEF1 double-positive cells is quite limited (Merrill et al., 2004; Van Genderen et al., 1994). The tight delineation of different TCF/LEF populations would suggest that exchange events are mediated by more active mechanisms than competitive expression. In our lab, by employing ChIP-seq, we have found clear cases where individual TCF/LEFs, specifically TCF7, bind specific WREs exclusively, despite their having dramatically lower expression than another TCF/LEF (TCF7L1) (Moreira et al., 2018b).

1.7.3.   TCF/LEF Selection via Mitotic Depletion

In a variety of adult stem cell niches, such as the hair follicle (Merrill et al., 2001) or intestinal crypt (Davies et al., 2008), Wnt signaling has been shown to play a crucial role in tissue patterning. However, in these contexts cell fates change as cells divide and move from their niches to surrounding environments. Similar to processes observed in development, TCF/LEF complements change as Wnt status changes (Merrill et al., 2004;

Van Genderen et al., 1994). In proliferative stem cell niches, there is a zone of transition where asymmetric cell divisions are likely to occur. These events provide an opportunity where daughter cells may inherit an asymmetric distribution of TCF/LEFs, providing them with unique transcriptional states. If some TCF/LEFs are capable of remaining associated with mitotic chromatin while others are not, they may be able to bookmark Wnt-responsive genes. Understanding this potential mechanism could provide insight into how Wnt-driven progenitor states are maintained or lost as cells divide within a given niche.

Although an increasing number of transcription factors have been observed to remain associated with mitotic chromatin, many of these factors do not rapidly reactivate target genes following mitosis and are therefore not true bookmarking factors. Despite this, there may be a function in mitotic loading beyond bookmarking target genes. The mitotic chromatin, perichromosomal layer, and cytoplasm could be considered different compartments with different regulatory functions. If, for instance, a cytoplasmic factor constitutively degraded TCF/LEF members, but mitotically associated TCF/LEFs were sequestered from its activity through association with mitotic chromatin, then this differential association could define a method of selective degradation of TCF/LEFs. Following division, only mitotically retained TCF/LEFs would be available to modulate Wnt target genes, promoting a renewed Wnt-responsive state in resulting daughter cells.

A gradient of Wnt ligand could further serve to pattern cells if activating TCF/LEFs like TCF7 and/or LEF1 were mitotically retained. Cells with less Wnt exposure would have attenuated Wnt signaling and would tend towards a Wnt OFF state. However, cells engaging more Wnt ligand could enter a feed-forward loop, as activating TCF/LEFs such as LEF1 promote the expression of Wnt ligands and are themselves Wnt target genes.

Thus, mitotic bookmarking by activating TCF/LEFs like LEF1 provides a tantalizing potential mechanism for stem cell fate determination in the context of a Wnt ligand gradient.

1.8.   IN VITRO MODELS AND REPORTERS OF THE WNT PATHWAY

Although studying the role of Wnt in development in animal models is the gold standard, in higher organisms like mammals, these techniques are very time consuming, technically challenging and fraught with issues related to the ethical use of experimental animals. To overcome these limitations, multiple *in vitro* techniques employing pluripotent stem cells have been developed to study developmental processes. While these techniques are generally limited to modelling early developmental events, they provide a scalable and reproducible platform with which to study these events.

1.8.1.   TCF/LEF Optimal Promoter (TOP)-based Reporter Systems

To better characterize and define regions of Wnt activity throughout development, and in *in vitro* conditions, reporter genes and systems have been used extensively. Immunofluorescence techniques were first used to identify Wnt-active cells based on nuclear translocation of β-catenin. Following the identification of constitutive Wnt target genes, such as *Axin2* and *Cyclin-D1*, the increased expression of these genes was used as a reporter for increased Wnt activation (McCormick, 1999; Morikawa et al., 2016; Yan et al., 2001). Changes in expression were followed by using qPCR or *in situ* hybridization to define regions of Wnt activity. However, to track Wnt activity in live cell populations and to establish an unbiased reporter system, a reporter system based on TCF/LEF optimal binding sites (TOP) was developed (Van De Wetering et al., 1997).

The TOP reporter system consists of several concatenated TCF/LEF binding sites positioned upstream of a minimal promoter fragment and a chosen reporter gene. To track Wnt activity in live cell populations, GFP or GFP-H2B have been used widely as chosen reporter molecules (Ferrer-Vaquer et al., 2010b; Varga et al., 2007). For high sensitivity, a luciferase enzyme was used as a reporter for the original TOP/FOP system and for subsequent reporters with larger numbers of TCF/LEF binding sites (Korinek et al., 1997; Veeman et al., 2003). To easily define regions of Wnt activity in tissue samples β-galactosidase was used with the TOP reporter to generate TOP-Gal reporter mouse lines (Ramanuj DasGupta, 1999). The versatility of the TOP reporter lead to its broad application in the field of Wnt signaling, however its synthetic nature fails to fully capture the nuances of Wnt signaling.

1.8.2.   3D Models of Gastrulation

Initially developed as an alternative to the teratoma assay of pluripotency, embryoid bodies (EBs) were used to determine if cell lines were capable of trilineage differentiation (Kurosawa, 2007). This assay allowed for small populations of cells to aggregate while in suspension and to stochastically differentiate over a 7 – 14 day period. However, due to considerable inconsistency among EBs, it was difficult to accurately quantify trilineage capacity beyond "present" or "absent". Additionally, heterogeneity between EBs meant that it was not possible to investigate sequential fate decisions over time, as each EB lacked axial organization and would have differing proportions of cells of a given fate. However, van der Brink et al. found that by stimulating EBs with a pulse of CHI they could induce a reproducible axial elongation of EBs, forming structures resembling gastrulating embryos, which they termed "gastruloids" (van den Brink et al., 2014).

Gastruloids are initially formed by a spherical ≈800 cell mESC or hESC aggregate which, after an initial culture period, is pulsed with CHI to induce polarization (Turner et al., 2017; van den Brink et al., 2014). Following this pulse of Wnt activation, gastruloids adopt an anteroposterior asymmetry, which is marked by an asymmetrical TOP activity and expression of gastrulation-associated factors such as Brachyury, Sox2, and Sox17 (Beccari et al., 2018; Turner et al., 2017). Gastruloids then adopt a sausage-like morphology as they elongate along this established axis of asymmetry. This loss of symmetry demonstrates that cells in a gastruloid are capable of spontaneous organization. Such organizational events reflect gastrulation more accurately than traditional EBs. Additionally, chemical inhibition or activation of developmentally relevant pathways such as Wnt, TGF-β , or Notch signaling during gastruloid formation provides an excellent platform with which to investigate developmental signaling circuitry (Turner et al., 2017; van den Brink et al., 2014). Single cell sequencing of developing gastruloids has also revealed that somitogenesis may occurring during gastruloid extension, further broadening the role of this platform in modelling developmental processes (Van Den Brink et al., 2020). However, while all gastruloids in a given experiment will undergo extension, their overall morphology is quite heterogeneous (van den Brink et al., 2014). In combination with their 3D nature, this makes gastruloids quite laborious to gather and to obtain standardized data from, despite their excellent recapitulation of gastrulation. As such, 2D micropatterned surfaces provide an alternative platform for truly quantitative analysis of early gastrulation events, while gastruloids are more suited as a mid-gastrulation model.

1.8.3.   2D Micropattern Models of Gastrulation

Standard culture protocols rely upon the random deposition and culture of mESCs upon uniform plastic surfaces coated with extracellular matrix components, such as laminin or gelatin. As cells grow in these conditions, colonies of varying size are formed, and these colonies populate the culture surface at non-uniform densities. This lack of defined colony size or distribution results in a culture condition where each colony behaves uniquely, depending on the number of cells in each colony and the number and proximity of surrounding colonies (Thery, 2010b). As a result, while careful manipulation of culture conditions can induce directed differentiation towards a chosen cell fate, there is little consistency in this process between individual colonies of the same culture plate. If our goal is to follow TCF/LEF exchange events throughout these early differentiation processes, using standard culture plates would yield inconsistent data (e.g., imaging data) between different colonies. Alternatively, characterization by flow cytometry would lose the spatial context of TCF/LEF exchange events. To overcome these limitations, 3D aggregation, and alternative 2D culture techniques, can be used to homogenize cellular populations during gastrulation-like differentiation *in vitro*.

Cellular populations can be discretely organized on 2D culture surfaces using micro-engineering techniques. Commonly employed techniques include microcontact printing, laser-patterning, and photo-patterning (Thery, 2010b). These techniques can be used to restrict the regions in which cells can adhere by manipulating the chemical nature of the culture surface on a subcellular scale (Thery, 2010b). By taking advantage of these chemical differences, regions of the surface can be made selectively adhesive for cells. Characterization of cells differentiating on these surfaces has shown that micropattern

shape (McBeath et al., 2004), size (Morgani et al., 2018), the distance between micropatterns (Miyamoto et al., 2016), and the ECM used (Joo et al., 2015) all affect the differentiation of cells captured within them.

By manipulating micropatterning parameters, it was found that mESCs and hESCs can undergo gastrulation-like events when confined to 1000 µm diameter circles (Deglincerti et al., 2016; Martyn et al., 2018; Morgani et al., 2018). Further immunofluorescent characterization of these circular micropatterns revealed that mesodermal fates exist at the periphery of the circle, with endodermal cells just interior to them, and ectodermal fates present only in the centre (Deglincerti et al., 2016; Morgani et al., 2018). Critically, EMT is also observed during this process, with central E-cadherin expression being lost, and N-cadherin expression being gained, in peripheral mesoderm cells (Morgani et al., 2018). However, cells grown on micropatterns do not typically retain confined to their pattern longer than 72 hours, as cells begin to overgrow their pattern and lose their organization (Miyamoto et al., 2016; Morgani et al., 2018). This short-lived, but highly organized, nature of micropatterns makes them ideal for the characterization of early developmental events.

1.9.   DYSREGULATION OF WNT IN CANCER

1.9.1.   Prevalence of Wnt in Cancer

Due to the role Wnt signaling plays in the maintenance of stem cell populations throughout the body, dysregulation of Wnt signaling is a common feature of many different cancers (Zhan et al., 2017). Wnt dysregulation is most prominently observed in colorectal cancer (CRC), where constitutive Wnt activation is observed in ≈90% of cases (Giles et al., 2003). Characterization of patient samples demonstrated that constitutive Wnt activation was

due to APC loss of function mutations in 90% of these cases. This is consistent with Wnt signaling being required for the proper maintenance, expansion, and differentiation of stem cell populations of the intestinal crypt (Farin et al., 2016; Qi and Chen, 2015). The reliance of Wnt-driven CRC upon APC destabilization was demonstrated by using a mouse model in which APC could be inducibly knocked out with a specific shRNA (Dow et al., 2015). By inducing a loss of APC, constitutively activating Wnt signaling, mice developed polyps throughout their colon, which resulted in death within 2 weeks. However, by halting anti-APC shRNA expression, restoring proper Wnt function after 1 week of treatment, defined polyps successfully de-differentiated and contributed towards healthy tissue. No mortality was observed in mice that had APC function restored.

In breast cancer, constitutive Wnt activation is observed in more than 50% of cases, with high Wnt activity and nuclear β-catenin staining correlating significantly with poor patient outcome (Lin et al., 2000). Interestingly, only a small fraction of breast cancers harbor a mutation in key Wnt regulators such as β-catenin or APC (Geyer et al., 2011; Pohl et al., 2017). Instead these cancers exhibit an increased expression of Wnt ligands and receptors, due to aberrant epigenetic regulation of these genes (Howe and Brown, 2004; Klarmann et al., 2008). Although the exact mechanisms surrounding or driving these mutations are poorly understood, Wnt signaling is undoubtably a core aspect of breast cancer.

Wnt signaling also plays a significant role in both hematopoiesis and the development of hematological malignancies (Staal et al., 2016). Hematopoietic stem cells (HSCs) found in the bone marrow give rise to all blood cells, through a carefully regulated step-wise series of differentiation events. Wnt signaling appears to play a critical role in this process,

being required not only for specific fate commitment, but also for the proper maintenance and expansion of differentiated populations (Malhotra and Kincade, 2009; Staal and M. Sen, 2008). This role is well demonstrated by TCF7$^{-/-}$ knockout mice, in which T-cells fail to fully commit to CD4$^+$/CD8$^+$ double-positive T-cells (Verbeek et al., 1995). The proper balance of TCF/LEF factors is also critical to hematopoiesis, as the loss of TCF7 in mouse model systems results in spontaneous T-cell malignancies, which resemble T cell acute lymphoblastic leukemia (Yu et al., 2012).

Among the various classes of hematopoietic malignancies, Wnt signaling has been found to play a crucial role in the initiation and maintenance of the malignant populations. Characterization of these hematopoietic cancers has found that Wnt can facilitate these changes through five major mechanisms: over production of Wnt ligand, hypersensitization to Wnt ligand through receptor overexpression, epigenetic dysregulation of Wnt signaling components, mutations in β-catenin or APC which constitutively activate the pathway, and imbalances in the TCF/LEF complement (Staal et al., 2016). Any of these events will disrupt proper HSC differentiation and result in malignancy. These same mechanisms of Wnt dysregulation can be found in almost all Wnt-driven cancers, highlighting the potency of Wnt signaling and its common points of failure.

1.9.2. Wnt and EMT in Cancer

Along with the role Wnt plays in fate determination and maintenance, Wnt also plays a critical role in epithelial to mesenchymal transitions (EMT). Epithelial cells are typically columnar in shape and tightly adhered to each other through adherens junctions, which are assembled from cadherin proteins (Wheelock et al., 2008). Epithelial cells express

primarily E-cadherin, but as they transition towards a mesenchymal phenotype, E-cadherin expression is lost in favour of N-cadherin (Wheelock et al., 2008).

This cadherin switch causes cells to lose their columnar phenotype, become squamous in phenotype, and promotes metastasis (Cao et al., 2019). Loss of epithelial phenotype and metastasis is further promoted by N-cadherin driving the expression of matrix metalloproteinase 9 (MMP-9), which degrades extracellular matrix (ECM) components (Hsu et al., 2016; Walker et al., 2014). Suppression of E-cadherin is required for the initiation of EMT, and is primarily mediated by the zinc finger transcription factor Snail (Carver et al., 2001). However, Wnt signaling plays a crucial role in this process.

Snail has been found to be destabilized and degraded after its phosphorylation by GSK3β, in a mechanism similar to β-catenin, such that Wnt stimulation simultaneously stabilizes Snail and β-catenin (Yook et al., 2005). Additionally, as β-catenin is a structural protein, it can interact with E-cadherin at adherens junctions (Tian et al., 2011). The loss of E-cadherin frees bound β-catenin, adding to the cytoplasmic pool of β-catenin available for Wnt signal transduction. The increase in free β-catenin further drives EMT, as Snail and LEF1 are direct Wnt target genes capable of generating a positive feedback loop (Hovanes et al., 2001b; Kim et al., 2002; Yook et al., 2005). While EMT is critical for gastrulation and development, it is commonly dysregulated in cancer, resulting in increased rates of metastasis.

During gastrulation, ectodermal epithelial cells of the epiblast must undergo EMT as they adopt a mesenchymal phenotype and migrate through the primitive streak to contribute towards mesodermal fates (Carver et al., 2001). Throughout development, EMT is tightly

controlled by TGFβ, Notch, and Wnt signaling (Medici et al., 2006; Nawshad et al., 2007; Zavadil et al., 2004). However, the dysregulation of EMT in the context of cancer has been shown to be a major driver of metastasis (Chaffer and Weinberg, 2011; Seyfried and Huysentruyt, 2013).

Metastasis, an event in which cells from the primary tumour spread to adjacent tissues or distant organs, such as the brain, lungs, or liver, and has been estimated to be the cause of ≈90% of cancer-related deaths (Chaffer and Weinberg, 2011). For a cancer cell to undergo metastasis it must be capable of regenerating a tumour population at its secondary location. As such, successfully metastatic cells are considered cancer stem cells (CSCs) by nature. These CSCs are pluripotent or multipotent progenitors capable of undergoing asymmetric cell division and giving rise to tumour progenitors (Pardal et al., 2003). Characterization of metastatic breast and pancreatic cancer cells has revealed rare populations of CSCs expressing both stem cell and EMT marker genes (Al-Hajj et al., 2003; Hermann et al., 2007). How these metastasized CSCs maintain cell fate and EMT capacity throughout this process is a topic of intense research. Understanding these underlying mechanisms has potential to provide insight into novel treatment options for a wide variety of cancers.

1.10. LEF1 AS A CRITICAL REGULATOR OF METASTASIS

LEF1 has been found to directly mediate the expression of EMT-related genes in a wide variety of cancers. An outstanding example of this is in the CRC cell line DLD1, which possesses nuclear β-catenin but has an epithelial phenotype. By infecting DLD1 cells with an adenovirus expressing LEF1, cells rapidly undergo EMT. Furthermore, this EMT event is reversed upon LEF1 withdrawal (Kim et al., 2002).

Further characterization of EMT has shown that LEF1 independently and cooperatively regulates EMT-related genes. LEF complexes with activated phospho-Smad2/Smad4 heterodimers in medial edge epithelium cells during embryonic palate development to directly bind the E-cadherin promoter and suppress its expression (Nawshad et al., 2007). Another marker of EMT and metastasis is the over expression of Vimentin, a type III intermediate filament protein found in mesenchymal cells and migratory epithelial cells (Brzozowa et al., 2015; Liu et al., 2010). In human breast cancers LEF1 has been implicated in the overexpression of Vimentin, as β-catenin-TCF/LEF complexes were found to directly bind the Vimentin promoter and drive its expression (Christine Gilles, 2003). Additionally, Slug mRNA expression was found to increase as a result of LEF1 in human osteoblasts, further suppressing E-cadherin expression (Lambertini et al., 2010).

Curiously, LEF1 has also been shown to mediate EMT-related genes in a β-catenin independent fashion in both cancer and developmental contexts. In Madin-Darby canine kidney (MDCK) cells, the expression of ΔN-LEF1, which lacks its β-catenin binding domain, was capable of increasing EMT potential and the expression of EMT-related genes such as Slug (Kobayashi and Ozawa, 2013). This function of LEF1 was also observed in β-catenin$^{-/-}$ MDCK cells (Kobayashi and Ozawa, 2018). Consistent with these findings, β-catenin is not found to be nuclear before, during, or after the EMT of palate cells during mouse development (Nawshad and Hay, 2003). Taken together, these findings demonstrate that while Wnt signaling plays a critical role in EMT regulation, LEF1 is not only a key mediator of this function, but it is also capable of facilitating EMT independent of Wnt status in both developmental and cancer contexts.

Complementary to its role in EMT promotion, LEF1 has been closely associated with pluripotency maintenance. Wnt signaling has been shown to directly promote the expression of core pluripotency factors including Oct4, Nanog, c-Myc, and Cyclin D1 (He, 1998; Huang and Qin, 2010; Kim et al., 2011; Shtutman et al., 1999). However, the main Wnt effector used in the regulation of Oct4 and Nanog is LEF1. LEF1/β-catenin complexes have been found to directly occupy WREs within the Oct4 and Nanog promoters (Huang and Qin, 2010; Kim et al., 2011). Furthermore, LEF1 has been shown to bind DNA targets in association with Nanog, to further activate their expression (Huang and Qin, 2010).

While these findings were demonstrated in human stem cell populations *in vitro*, this role of Wnt and LEF1 in pluripotency maintenance has been observed across a variety of cancers. Altered, often overexpressed, LEF1 levels are a common feature across several cancers including lung adenocarcinomas, colon cancer, endometrial carcinomas, prostate cancer, and leukemia (Santiago et al., 2017). Additionally, in many of these cancers, increased LEF1 expression strongly correlates with increased metastasis and poor patient outcomes (Santiago et al., 2017). The overexpression of Hoxb9 and LEF1 in lung adenocarcinoma potentiates invasion and outgrowth, while increasing metastasis towards bone and brain regions (Nguyen et al., 2009). In LEF1-high endometrial cancers, the expression of ECM-degrading MMP7 is increased by 30-fold relative to surrounding healthy tissue (Shelton et al., 2012). While LEF1 is required for proper T- and B-cell differentiation, there is a roughly 13-fold increase in LEF1 expression in acute lymphoblastic leukemia (ALL) (Petropoulos et al., 2008). In murine models exogenous LEF1 expression has been shown to induce ALL (Petropoulos et al., 2008).

Not only can exogenous LEF1 induce EMT in cancer, its withdrawal has been shown to halt EMT in certain LEF1-high cancers. There are multiple prostate cancer cell lines with varying phenotypes, although in androgen-dependent (AD) cell lines, LEF1 expression is found to be 100-fold greater than in androgen-independent (AI) cell lines (Li et al., 2009). By exogenously expressing LEF1 in AI prostate cancer cell lines, a 2.5-fold increase in matrigel invasiveness was observed, and this feature was lost when these same cells were treated with a LEF1 shRNA (Li et al., 2009). Taken together, these findings demonstrate that LEF1 is a potent mediator of EMT and metastasis. With the knowledge that LEF1 is itself a Wnt target gene, aberrant Wnt activation not only establishes a positive feedback loop, LEF1 overexpression enforces and maintains a pro-EMT and pro-metastasis cell state.

Due to the strong correlation between LEF1 overexpression and metastasis, LEF1 has been used as a biomarker in a wide variety of cancers. In chronic lymphoblastic leukemia, a 2011 study found LEF1 to be overexpressed in 100% of 92 tested neoplastic samples (Tandon et al., 2011). Additionally, while LEF1 is absent in mature B-cells, LEF1 was found to be overexpressed in ≈70% of B-cell CLL samples (Menter et al., 2015). In oral squamous cell carcinoma (OSCC) LEF1 is overexpressed, while TCF7L2 expression is constant between surrounding tissue and OSCC cells (Su et al., 2014). Additionally, higher LEF1 expression correlates strongly with lymphovascular invasion and reduced survival (Su et al., 2014). In healthy colon crypt tissue TCF7L2 is the only TCF/LEF expressed. However, LEF1 is frequently overexpressed. This overexpression of LEF1 in CRC cells is associated with shorter survival time, and increased metastasis (Lin et al., 2011). While these correlations allow LEF1 to function as an informative biomarker for

patient outcome and treatment options, the mechanisms underlying this function are poorly understood. While LEF1 promotes and maintains the expression of pluripotency- and EMT-related genes, how does it maintain this transcriptional network following metastasis? How does LEF1 maintain this pro-metastatic function over multiple divisions in the absence of Wnt activation? My unbiased opinion: bookmarking.

1.11. Hypothesis

We hypothesize that TCF/LEF exchange at Wnt target genes is mediated by factors bound to co-regulatory elements flanking WREs in the genome and the selective depletion of mitotic TCF/LEFs upon cellular division.

We will address our hypothesis by generating endogenous TCF7L1/LEF1 reporter cell lines and by using micropatterning to isolate mESC populations before, during, and after TCF/LEF exchange events occur during gastrulation-like differentiation *in vitro*. These populations will be examined by techniques that will allow us to determine genome-wide changes in chromatin occupancy by TCF7L1, LEF1 and undetermined factors and concomitant changes in global transcriptional outputs. We will also address potential bookmarking roles for TCF7L1 and LEF1 by employing techniques that will allow us to identify the network of proteins associated with TCF7L1 and LEF1 in asynchronous and mitotically arrested mESCs. These interaction networks will also assist us in building models for the mechanisms regulating TCF7L1/LEF1 exchange at target genes.

CHAPTER 2. ENDOGENOUS TCF7L1 AND LEF1 EXPRESSION AS A REPORTER OF WNT ACTIVITY

2.1.   SUMMARY OF INTENT

Despite the broad role that Wnt signaling plays throughout development and adult stem cell maintenance, our understanding of the mechanisms regulating dynamic changes in TCF/LEF status is far from complete. However, TCF/LEF exchange events appear to correlate strongly with abrupt cell fate changes. The most well-documented events occur during: i) early gastrulation, when TCF7L1-positive ectodermal epiblast cells become mesodermal LEF1-positive cells as they contribute to the PS (Merrill et al., 2004; Van Genderen et al., 1994); ii) T-cell maturation, when a TCF7 to LEF1 exchange is observed (Xing et al., 2016); and, iii) hair follicle cycling, when a TCF7L1 to LEF1 exchange is observed (Merrill et al., 2001).

In general, TCF/LEF-expressing populations during development are restricted to the static expression of one or two TCF/LEFs, with activating (TCF7/LEF1) and repressive (TCF7l1/TCF7L2) TCF/LEFs typically being paired (Ah Cho and Dressler, 1998; Ferrer-Vaquer et al., 2010a; Mariëtte Oosterwegel, 1993; Merrill et al., 2004). Furthermore, TOP-GFP reporter mice have revealed that not all of these populations are Wnt-active, as measured by TOP activity (Ferrer-Vaquer et al., 2010a). However, as these cells differentiate towards more specific cell fates and organize into larger structures, their TCF/LEF status changes accordingly. The appropriate selection of TCF/LEFs is critical during these processes, as TCF/LEF knockout mice show acute loss of specific stem cell populations dependent on the lost TCF/LEF (Korinek et al., 1998; Zhou et al., 2010). These findings demonstrate that while TCF/LEFs share some redundant functions, their

appropriate expression and exchange are required for development and postnatal survival.

The absence of TOP activity in regions of exchange suggests, not only that the TOP reporter fails to fully capture Wnt regulation, but also that TCF/LEF exchange may be regulated cooperatively with secondary pathways. However, characterization of these TCF/LEF exchange events is limited not only by insufficient existing reporter systems, but also by technical limitations associated with isolating these highly specific populations.

While the TCF/LEF optimal promoter (TOP) reporter system is the most commonly used method of assessing Wnt activity in live cell populations, it does not reflect TCF/LEF status. The TOP reporter is ideal for capturing events of strong Wnt activation, but it fails to capture the nuanced changes in Wnt transcriptional machinery that occur during Wnt activation. The Super 8X TOPFlash reporter possesses seven concatenated TCF/LEF binding sites upstream of a minimal promoter driving the expression of a luciferase reporter gene (Molenaar et al., 1996). As such, the TOP reporter is effectively reporting only the formation of transcriptionally activating nuclear β-catenin:TCF/LEF complexes.

Changes in TCF/LEF status cannot be accurately inferred from changes in TOP activity. Changes in TOP activation are therefore binary and not reflective of the changes in TCF/LEF status that are integral to facilitating these changes. This lack of biological relevance can be observed in drug screening efforts aimed at identifying Wnt modulating compounds by using TOP-based reporter systems. With more than three million compounds estimated to have been screened for Wnt activity via TOP-based reporter systems, only 3 are currently in phase 2 clinical trials (Jung and Park, 2020; Lu et al.,

2016). Additionally, these TOP-based screening efforts appear to preferentially identify compounds that target either cell surface Wnt receptors or destruction complex components (Jung and Park, 2020; Lu et al., 2016). As these Wnt signaling components would most directly affect nuclear β-catenin levels, this preference is understandable, but has limited the clinical translation of identified compounds.

Since potent Wnt activators/inhibitors identified by TOP-based reporters typically target core regulators of Wnt activation, their use *in vivo* will influence nearly all Wnt-active tissues. However, more biologically nuanced screens should be able to select for inhibitors of disease-specific Wnt-states, thereby limiting off-target effects *in vivo*. To overcome this limitation, individual Wnt transcriptional components such as the TCF/LEFs themselves, would need to be tracked directly.

Additionally, the characterization of TCF/LEF exchange events during gastrulation is complicated by the limitations of *in vivo* systems. While adaptive light-sheet microscopy platforms have been developed for time-lapse imaging of live embryos, this approach is technically difficult (McDole et al., 2018). Alternative live cell microscopy approaches are similarly difficult to implement (Yamanaka et al., 2007), while the characterization of fixed samples greatly reduces temporal resolution and reproducibility. To bypass these limitations, 2D and 3D *in vitro* culture techniques can be used to capture early gastrulation-like events. By combining these 2D and 3D techniques with an updated Wnt-reporter mouse embryonic stem cell (mESC) line we can capture and quantitatively characterize TCF/LEF gastrulation-like events *in vitro* while bypassing the technical limitations associated with *in vivo* techniques.

2.2.   ABSTRACT

The canonical Wnt/β-catenin signaling pathway is essential for the proper regulation of cell-fate decisions throughout embryogenesis and in adult issues. However, due to its role as a critical signaling pathway it is very frequently dysregulated in variety of cancers. As such there have been numerous high throughput/high content screening efforts put forward to identify modulators of Wnt activity. The most prominent platform used by more than 90% of these screens in the past decade is the TCF/LEF Optimal Promoter (TOP) reporter assay, which relies upon several concatenated TCF/LEF binding sites to drive the expression of a downstream reporter gene. While this reporter system is very sensitive to changes in Wnt activity, very few identified compounds have successfully translated to clinical use. Additionally, inhibitors of epigenetic regulators have recently been found to have excellent specificity for cancer populations. Unfortunately, this class of inhibitor would very likely be missed by an exogenous TOP reporter system. To overcome these limitations, and to provide a more biologically relevant screening platform, we have used TALEN-facilitated homologous recombination to fluorescently label endogenous TCF7L1 and LEF1, two key transcriptional regulators of Wnt signaling that play critical roles in the maintenance of pluripotency and EMT, respectively. By tracking TCF7L1/LEF1 expression status through live cell fluorescence imaging, we have been able to identify epigenetic inhibitors capable of altering TCF7L1/LEF1 status without affecting TOP activity, demonstrating our novel platform's ability to identify inhibitors that would otherwise have been missed by traditional TOP screens.

2.3. Introduction

The dysregulation of Wnt signaling is a common feature among a wide variety of cancers, where its aberrant activation or suppression can have either tumour suppressor or oncogenic activity in a context-dependent manner (Kim et al., 2002; Santiago et al., 2017; Zhan et al., 2017). There have been continuous drug screening efforts for the discovery of novel small molecule, RNA-mediated, antibody, or protein-based modulators of Wnt signaling activity (Lu et al., 2016). Currently, slightly more than half of all patents held for Wnt modulators have been protein based, while the second and third most prevalent modulators are antibody and small molecule mediated, respectively (Lu et al., 2016).

The targets of these modulators are prominently extracellular components of Wnt signaling, which function through the sequestration or stimulation of Wnt ligands and receptors (Lu et al., 2016). While targeting these components of the Wnt signaling pathway is viable, tightly regulated Wnt signaling is required for the proper maintenance and differentiation of many adult stem cell populations throughout the body; by globally affecting Wnt signaling activity there may be a considerable risk of off-target effects (Chiurillo, 2015; Lu et al., 2016). Additionally, while extracellular Wnt ligands and regulators are often epigenetically silenced during progression of Wnt related cancers, the most frequent initiating mutations are those that occur in intracellular regulators of β-catenin stability (Chiurillo, 2015; Lu et al., 2016; Rodenhizer et al., 2018).

The biased identification of inhibitors of extracellular components is not ideal, as these inhibitors can only indirectly affect β-catenin transcriptional activity. However, this apparent bias for identification of extracellular Wnt modulators may be an artifact of the

TOP-driven Wnt reporter, which lacks the biological nuance required to fully reflect Wnt signaling status.

The TOP reporter possesses seven concatenated TCF/LEF binding sites upstream of a minimal promoter driving the expression of a chosen reporter gene. As such the TOP reporter is effectively reporting only the formation of transcriptionally activating nuclear β-catenin:TCF/LEF complexes. This functional bias results in the selective identification of compounds affecting β-catenin stabilization, which is clearly reflected in the bias for receptor/destruction complex targets of current Wnt-targeting therapeutics (Jung and Park, 2020; Lu et al., 2016).

While β-catenin is a potent transcriptional regulator of the Wnt signaling pathway, TCF/LEFs are responsible for the selection of target genes, and their selective expression and exchange is critical for cell fate determination. As previously discussed, TCF/LEF dysregulation is a common feature among Wnt-driven cancers. In breast cancers both TCF7L1and LEF1 have been found to be drastically upregulated (Slyper et al., 2012; Zheng et al., 2017), while LEF1 is over expressed in most colorectal cancers and B-cell lymphomas (de la Roche et al., 2014; Menter et al., 2015). Additionally, the exogenous and synthetic nature of the TOP reporter system prevents it from capturing epigenetic changes affecting cells.

Epigenetics is known to play a critical role in differentiation, as demonstrated by global changes in DNA and histone acetylation and methylation status that can be observed within differentiating embryonic or adult stem cell populations (Gyuris et al., 2009; Shang et al., 2009). Additionally, major regulators of histone status such as histone deacetylases

(HDACs) and histone acetylases (HATs) have been shown to mediate the activity of a growing list of non-histone proteins, including the oncosuppressor p53 (Juan et al., 2000). The impacts of HDAC/HAT activity on non-histone proteins can impact their stability by mediating acetylation of lysines to prevent or promote ubiquitylation and degradation, or altering protein-protein interactions to affect gene expression (factors such as signal transducer and activator of transcription 3 (STAT3) require acetylation for dimerization and subsequent nuclear translocation) (Zhuang, 2013).

As such, the dysregulation of HDACs/HATs is a common feature across many types of cancer, often resulting in or promoting aberrant epigenetic or transcriptional changes through the post-translational modification of histone and non-histone proteins (Chunaram Choudhary, 2009; Minucci and Pelicci, 2006; Parbin et al., 2014). Due to their importance in differentiation and cancer development, considerable effort has gone into finding chemical inhibitors of HDAC/HAT activity, resulting in a multitude of specific or pan HDAC/HAT inhibitors (HDACi/HATi) becoming commercially available. The most striking feature of HDACi compounds is their apparent selective toxicity for tumour cells, with normal cells displaying a considerable degree of resistance to the toxic effects of these compounds (Minucci and Pelicci, 2006; Parbin et al., 2014).

Though Wnt signaling has been known to influence epigenetic status, through the direct recruitment of epigenetic regulators by β-catenin, current research has continued to strengthen the link between Wnt signaling and epigenetic regulation (Jiang et al., 2008; Wolf et al., 2002; Zaidi et al., 2010). While LEF1 and TCF1 were found last year to have intrinsic HDAC activity, required for the proper maturation and maintenance of CD8+ T-cells, the acetylation or trimethylation of K49 in β-catenin by members of the polycomb

repressive complex 2 (PRC2) was shown to be a critical mediator of β-catenin transcriptional activity (Hoffmeyer et al., 2017; Xing et al., 2016). While β-catenin K49A mutants were found to have major differentiation defects, mutations in K49 of β-catenin have also been found frequently in Wnt-associated cancers (Hoffmeyer et al., 2017). Additionally, Hoffmeyer et al. demonstrated that the K49Me3 versus K49Ac status of β-catenin at target genes was a stronger determinant of transcriptional activity than overall β-catenin localization.

It appears that the interaction of Wnt components with epigenetic machinery is critical, not only for regulating Wnt target gene activity and histone status, but also for modulating the activity of Wnt signaling components themselves (Hoffmeyer et al., 2017). As the weight of these interactions between epigenetic regulators and Wnt signaling continues to gain significance, it is becoming clear that a new generation of more biologically relevant reporters will be required to interrogate and understand Wnt signaling mechanisms.

2.4.   RESULTS

2.4.1.   Targeting Endogenous LEF1, TCF7L1, and ROSA26 loci by using TALENs

To directly assess the expression of TCF7L1and LEF1 in E14Tg2A mESCs by using live cell imaging, each gene locus was targeted by employing transcription activator-like effector nuclease (TALEN)-facilitated homologous recombination. Through co-transfection of an appropriate targeting vector (Supp. Fig. 1) the LEF1 gene was N-terminally fused with monoAzami Green (mAG) and the TCF7L1 gene was N-terminally fused with mono-Kusabira-Orange2 (mKO2) through homologous recombination. The resulting mAG-LEF1/mKO2-TCF7L1 cell line is referred to as **G**reen-**L**EF1/**O**range-

TCF7L1 (GLOT3). Integrations were confirmed by PCR and then validated by western

blotting, and imaging analysis. Bands for WT and labelled TCF7L1/LEF1 were identified

by western blotting, confirming their hemizygous integration (Fig. 8).
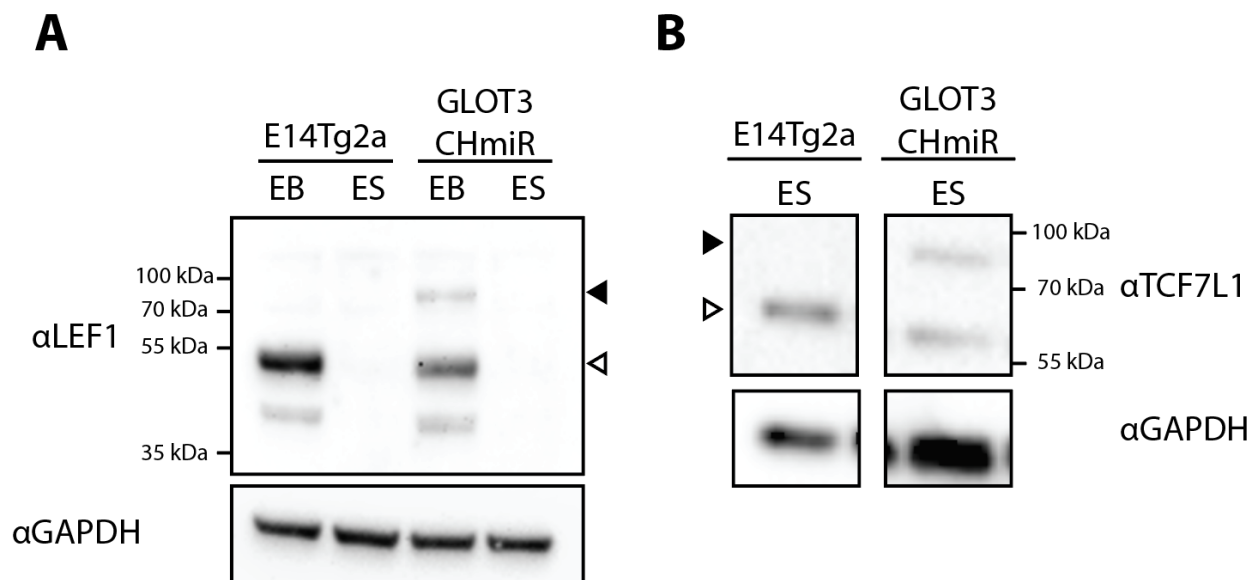
Figure 8.   GLOT3-CHmiR validation by western blot analysis.

Wild (E14Tg2a) and GLOT3-CHmiR cells were probed for LEF1 in differentiation (EB)
and pluripotent (ES) conditions. Bands were identified at the expected full length
(empty arrowhead) and fusion (filled arrowhead) sizes for LEF1 and TCF7L1. A)
Samples were blotted for LEF1 and GAPDH loading control separately. B) Samples
were blotted for TCF7L1 and GAPDH separately.

**2.4.2.   Characterizing mKO2-TCF7L1/mAG-LEF1 Expression in EB Medium and
Potential Effects on Wnt function or mESC Differentiation**

To a determine a time point at which LEF1 and TCF7L1 are most highly expressed, and

to ensure our GLOT3 cell line did not impede Wnt activity or differentiation, we assessed

mKO2-TCF7L1/mAG-LEF1 fluorescence and lineage marker expression over three days

of differentiation in EB medium (Fig. 9A). Wild-type E14TG2a cells grown in identical

conditions were collected for analysis by qRT-PCR (Fig. 9B). Consistent with our GLOT3

observations, expression of established Wnt target genes Wnt3 and Brachyury was lowest when repressive TCF7L1 expression is high, and highest when activating LEF1 expression is low. These consistencies suggest that differentiation of the GLOT3 mESC line is not impeded by our endogenous LEF1/TCF7L1 fluorescent tags.

2.4.3. Constitutive H2B-miRFP670 Expression as an Endogenous Nuclear Marker

To facilitate rapid and consistent nuclear identification of cells during live imaging, the epigenetically stable ROSA26 locus was targeted by using TALENs to introduce histone 2B (H2B) fused to a fluorescent nuclear marker. To avoid spectral overlap and aggregation of our H2B nuclear marker, we chose the monomeric far-red fluorescent protein miRFP670 (miR) (Shcherbakova et al., 2016). As the ROSA26 locus has moderate constitutive activity, we attempted to target our cassette with or without a CAG promoter. However, due to the poor quantum yield of miRFP670, the resulting moderate expression without a CAG promoter was insufficient for robust nuclear identification (Fig. 10A). The presence of an upstream CAG promoter facilitated robust expression and consistent nuclear identification (Fig 10B). As such, our CAG-driven H2B-miRFP670 cell line was used in all future experiments.

A

B
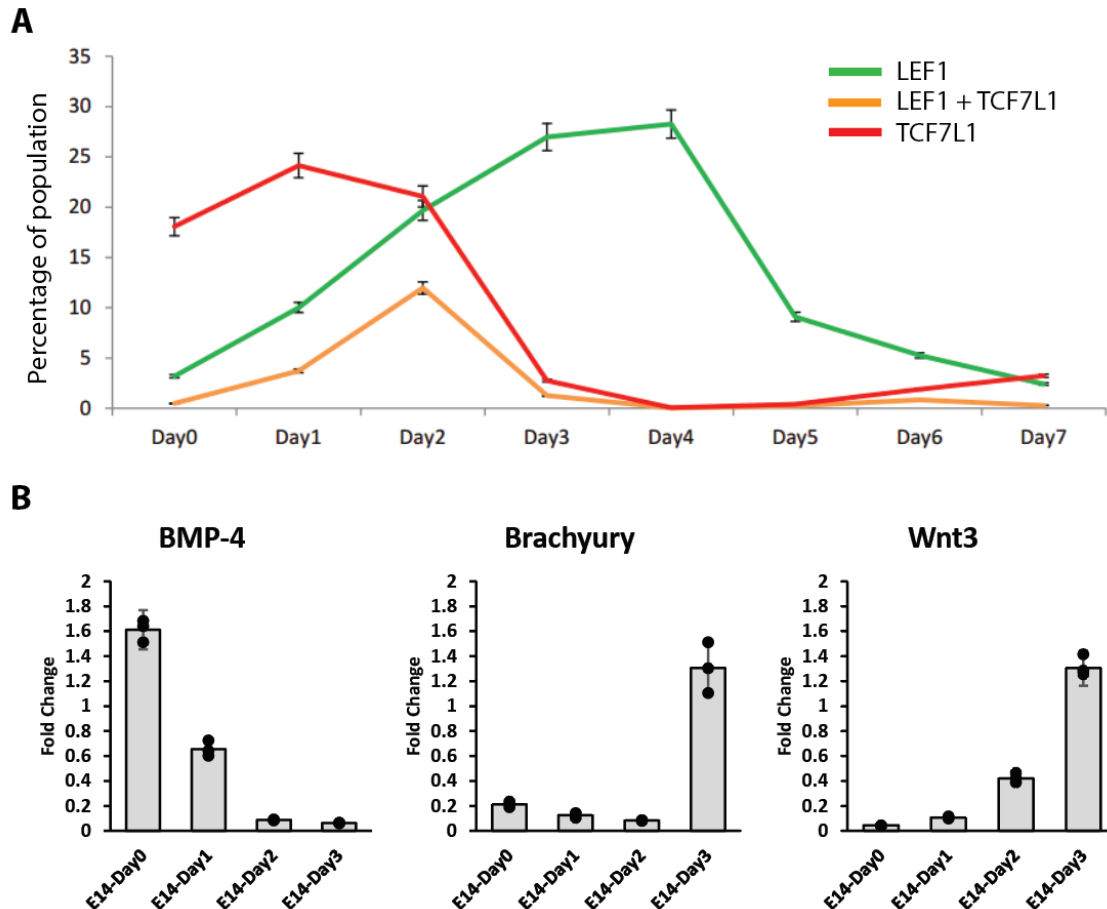
Figure 9. Dynamic expression of TCF7L1/LEF1 during mESC exit from pluripotency.

The expression of TCF7L1/LEF1 is most dynamic after 48 hours of culture in EB conditions, where cells are primed for Wnt activation and mesodermal commitment. A) GLOT3 cells cultured as hanging drop EBs were collected every 24 hours and characterized by flow cytometry to determine mAG-LEF1/mKO2-TCF7L1 fluorescence levels using flow cytometry (n = 3). B) Wild-type E14Tg2a cells cultured as hanging drop EBs were collected every 24 hours to determine mesoderm (Brachyury), ectoderm (BMP4), and Wnt activity (Wnt3) marker gene expression by using qPCR (n = 3).

2.4.4. Optimizing Imaging and Treatment Conditions with Wnt Modulators

To automate image processing, a pipeline was generated using Cell Profiler (McQuin et al., 2018) for image analysis and Python for data processing. Our H2B-miRFP670 signal

was used to identify nuclei, and this area was then used to determine mean mAG-LEF1 and mKO2-TCF7L1 fluorescence intensity for each cell. Images were acquired at the 48-hour mark, which has been shown in hanging drop EBs and adherent cultures to have large LEF1- and TCF7L1-positive populations (Moreira et al., 2017). Hex bin graphs were then used to compare TCF7L1/LEF1 expression for all cells identified in each condition (Fig. 11).

To optimize dosage and image quantification, we chose to first characterize a set of three known inhibitors. As LEF1 is a known Wnt target gene that is strongly activated by the potent GSK3 inhibitor, CHIR-99021 (CHI), we treated our GLOT3-CHmiR cell line with 1, 5, or 10 µM CHI, with the first robust change in TCF/LEF expression being observed at 5 µM (Fig. 11).

The Smad2/3 inhibitor SB-431542 (SB) and FGFR inhibitor SU-5402 (SU) were also tested at 5 and 10 µM concentrations (Fig. 12A). A similar trend was observed where 5 and 10 µM doses were similar in effect, while 5 µM was less cytotoxic. As such, 5 µM was chosen as our initial screening concentration when working with larger libraries. To quantify these changes, the percent of change of LEF1/TCF7L1 fluorescence in each well was quantified over its respective DMSO control (Fig. 12B).
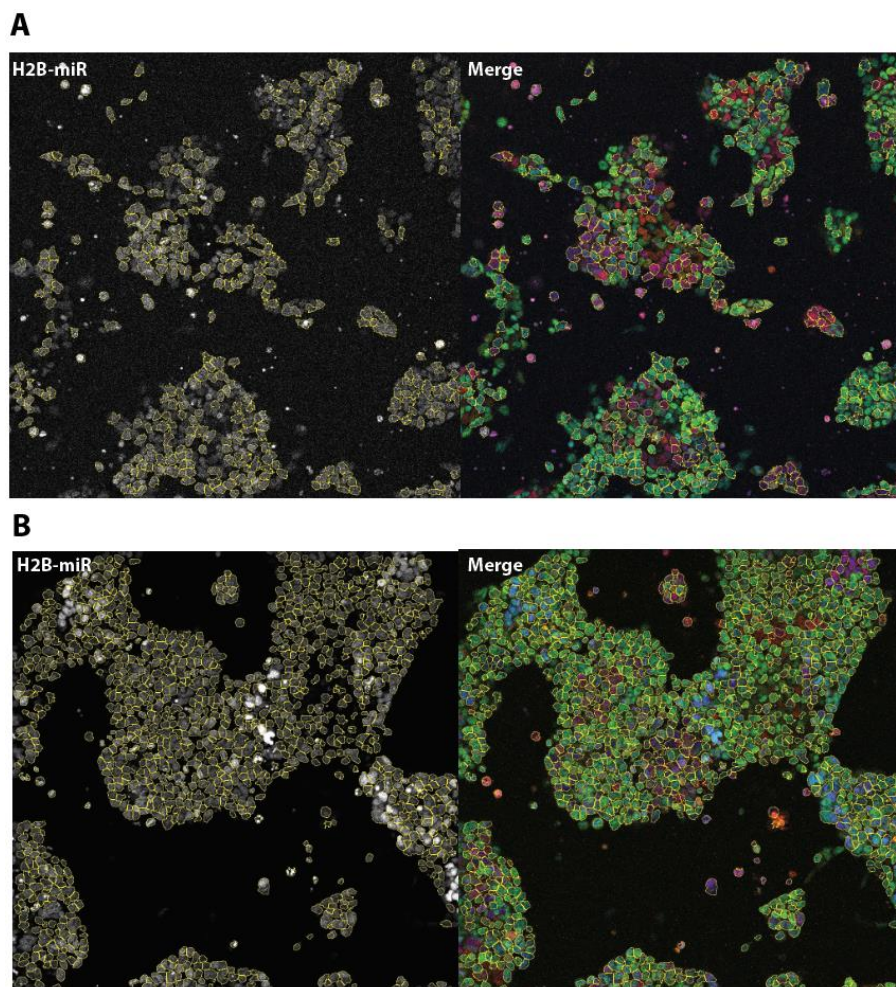
Figure 10. Detection of nuclei with H2B-miRFP670.

The inclusion of a CAG promoter in our ROSA26-targeted H2B-miRFP670 cassette allows for robust nuclear detection. GLOT3 cells with an endogenously driven (A) or CAG-driven (B) H2B-miRFP670 cassette were plated at equal density and grown in EB medium conditions for 48 hours prior to imaging and image analysis using identical settings. Nuclear H2B-miRFP670 fluorescence is shown on the left panels (H2B-miR), with nuclei identified by our CellProfiler pipeline outlined in yellow. These images are then shown as a merge with Green (mAG-LEF1) and Red (mKO2-TCF7L1) channels. GLOT3-CHmiR seeding, treatment, imaging, and quantification protocols were optimized by using a small library of known Wnt modulators.
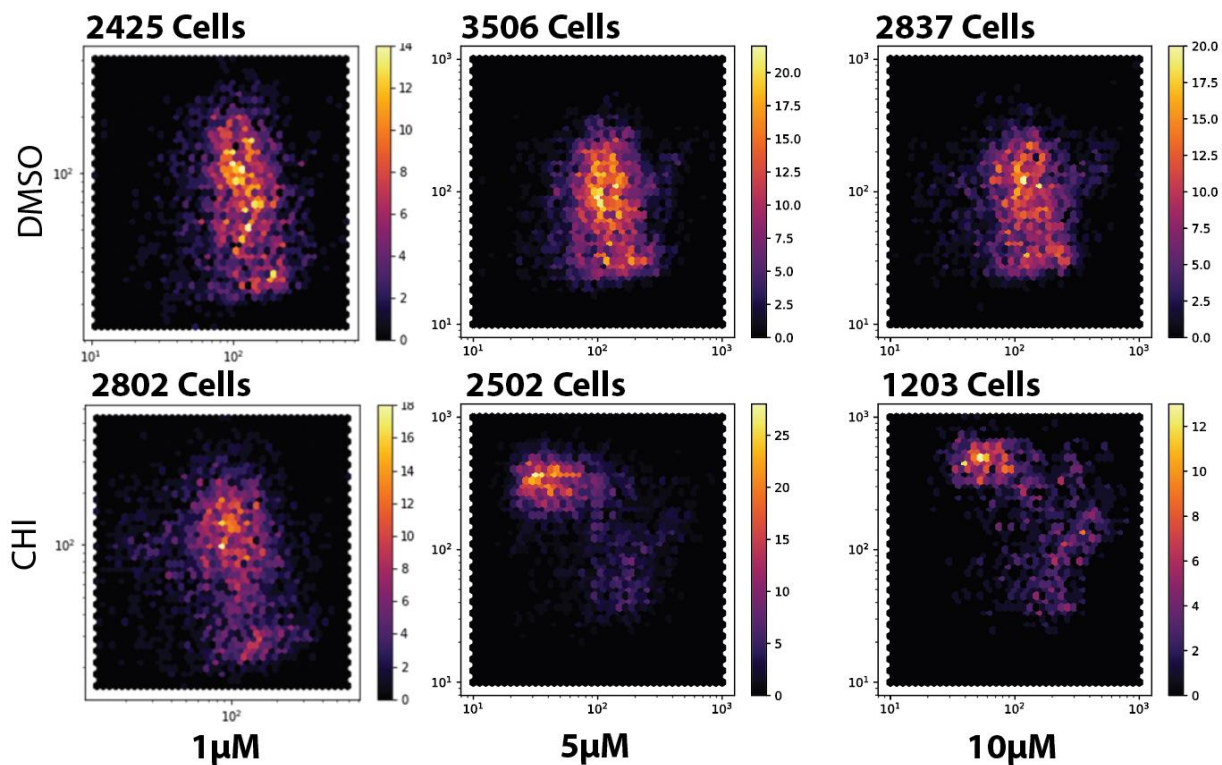
Figure 11. Dynamic LEF1/TCF7L1 states are recapitulated in adherent culture and can be influenced by chemical inhibitors.

GLOT3-CHmiR cells were grown for 24 hours in EB medium before CHI (CHI99021) was added at the indicated concentrations and grown for an additional 24 hours. Equivalent volumes of DMSO were added as vehicle controls. Images were acquired from each well at the 48-hour mark and mean nuclear intensity was scored for mAG-LEF1 (y-axis) and mKO2-TCF7L1 (x-axis). Data is presented on a log scale hex bin scatter plot for each identified nucleus, with average cell count per run listed above each plot (n = 3).
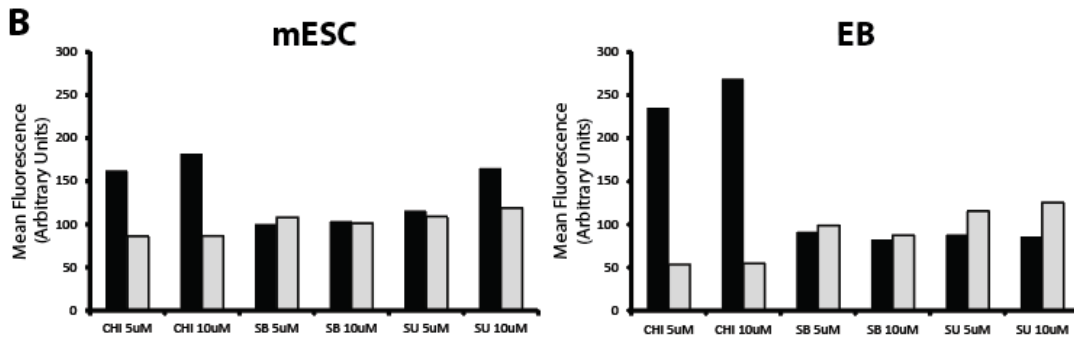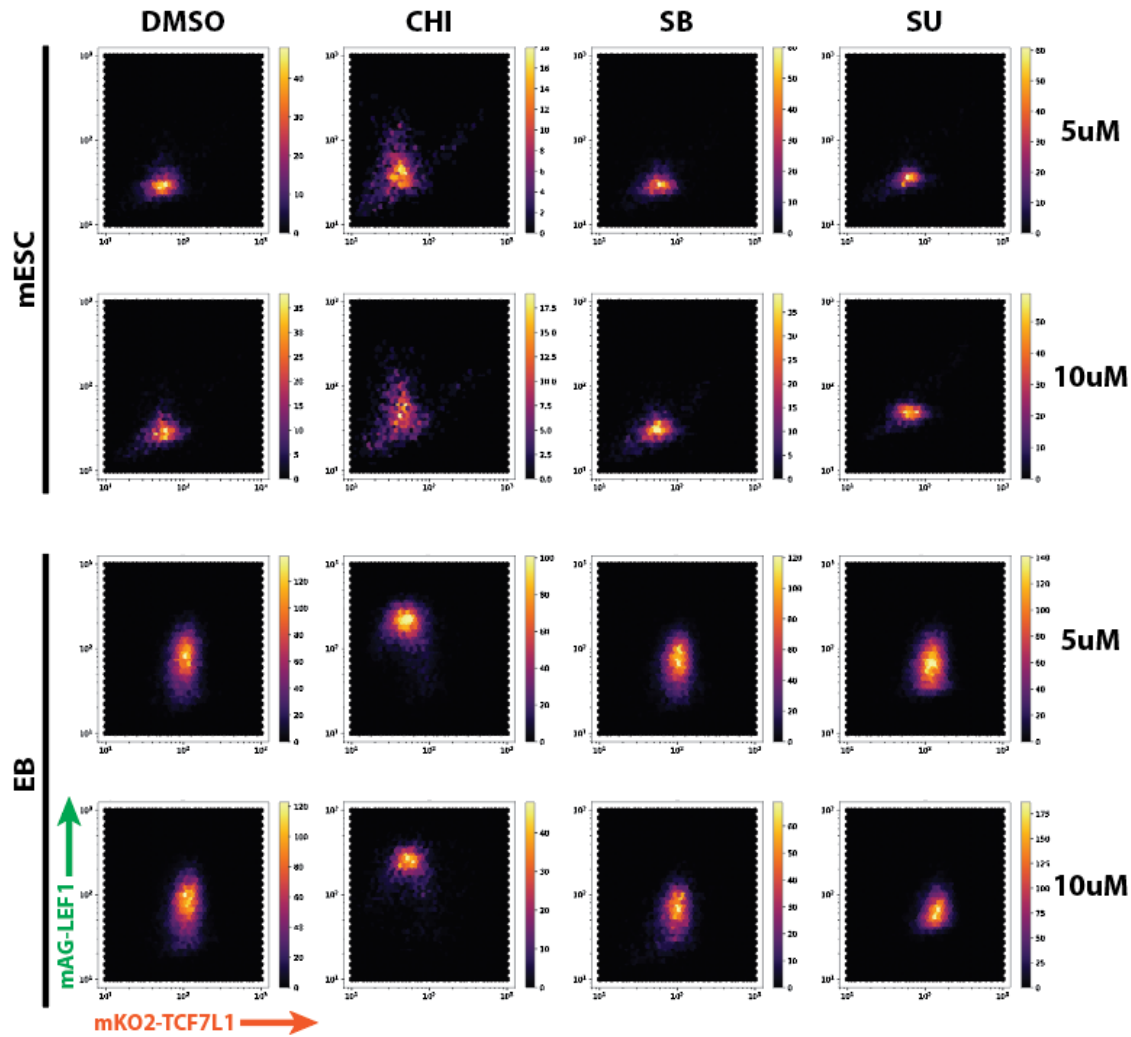
Figure 12. LEF1 and TCF7L1 protein expression in mESCs is more responsive to small molecule treatments in the absence of LIF.

Figure 12. (Continued) A) GLOT3-CHmiR cells were cultured for 24 hours in the absence of drugs and an additional 24 hours in medium containing the indicated concentration of CHI (CHI99021), SU (SU5402), SB (SB431542), or DMSO vehicle control. Medium used was either mESC or EB, as indicated. Images were acquired at the 48h mark and mean nuclear fluorescence was plotted as hex bin scatter plots for mAG-LEF1 (y-axis) and mKO2-TCF7L1 (x-axis) as a log scale. B) Mean nuclear mAG-LEF1 (black) and mKO2-TCF7L1 (grey) fluorescence intensity for each condition was plotted as a percent of change relative to DMSO vehicle control.

2.4.5. Identifying Wnt-modulating Epigenetic Inhibitors by Changes in TCF7I1/LEF1 Status

Our characterization of TCF7L1/LEF1 expression during differentiation demonstrated that TCF7L1 and LEF1 expression was most prolific throughout the population at 48h (Fig. 9A). To observe changes in this dynamic TCF7L1/LEF1 state, GLOT3-CHmiR cells were imaged after 48h in EB conditions, with probes added at the 24h mark (Fig. 13A). Thirty probes were chosen from the Epigenetic Probe Collection (Structural Genomics Consortium, Toronto), based on their ability to affect their target in <= 24h and have activity at 5 µM or less, to fit our chosen timeline and to reduce cytotoxicity, respectively (Fig. 13B). In the 30-probe screen, 11 were found to have a Z-score > 1.0 or < -1.0 in either the green (LEF1) or red (TCF7L1) channel (Fig. 13C). From these 11 probes, we chose to move forward with JQ-1, PFI-1, NVS-1, UNC038, UNC0642, and GSKJ4 as they were the most well documented, and their targets were known to be involved in early developmental regulation. While most compounds were not found to significantly modulate mKO2-TCF7L1/mAG-LEF1 fluorescence relative to a DMSO control in follow-up screens, the Bromo- and Extra-Terminal domain (BET) family inhibitors JQ-1 and PFI-1 were found to significantly reduce LEF1 expression, and the JMJD3/UTX inhibitor GSK-J4 was found to significantly increase TCF7L1 expression (Fig. 14A). Additionally, JQ-1 and PFI-1 were found to increase mean H2BmiRFP670 fluorescence, which is indicative

of G2/M phase arrest. However, JQ-1 and PFI-1 treatment has only ever been associated

with G1/G0 arrest (Alghamdi et al., 2016; Picaud et al., 2013) (Fig. 14A). To determine if

these six compounds could have been identified by a traditional TOP-based reporter

system, E14Tg2A mESCs were transfected with an 8xTOP-FLASH reporter and

incubated for the same 48h timeline before luminescence was read. While the addition of

CHI successfully activated the TOP reporter, none of our epigenetic probes induced a

change that was significantly different from the DMSO control (Fig. 14B). Our chosen

probes were then re-screened in the presence of 5 µM CHI, using both GLOT3-CHmiR

imaging and TOPFLASH (Fig. 14). While CHI increased TOP activation and LEF1

expression, this effect was shown to be suppressed by all probes. Intriguingly, the

suppression of TCF7L1 expression by CHI was inhibited in the presence of GSK-J4 (Fig.

14A).
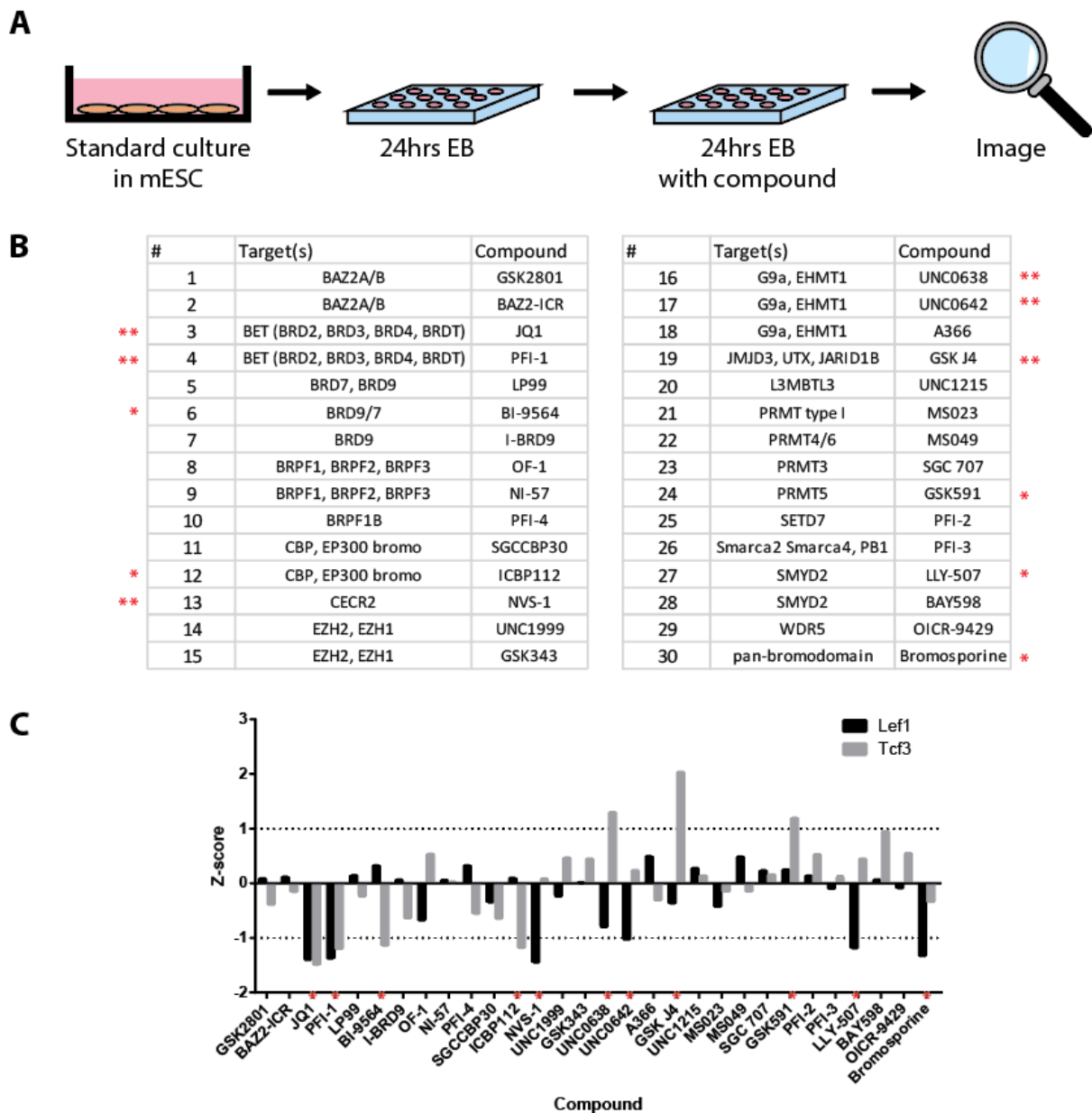
Figure 13. Epigenetic modulators influence LEF1/TCF7L1 expression status.

A) GLOT3-CHmiR cells were seeded at equal density in EB medium for 24 hours, medium was then replaced with EB medium containing our desired drug and incubated for an additional 24 hours. Images were then taken of each well at the 48-hour mark, processed using CellProfiler, and then analysed with custom Python scripts (n = 3). B) A list of probes, provided by the SGC, used in our initial screen. C) A plot of Z-scores for each probe. Red asterisks denote probes with a Z-score > 1 or < -1 for either LEF1 or TCF7L1. These noted compounds were then used in subsequent assays.
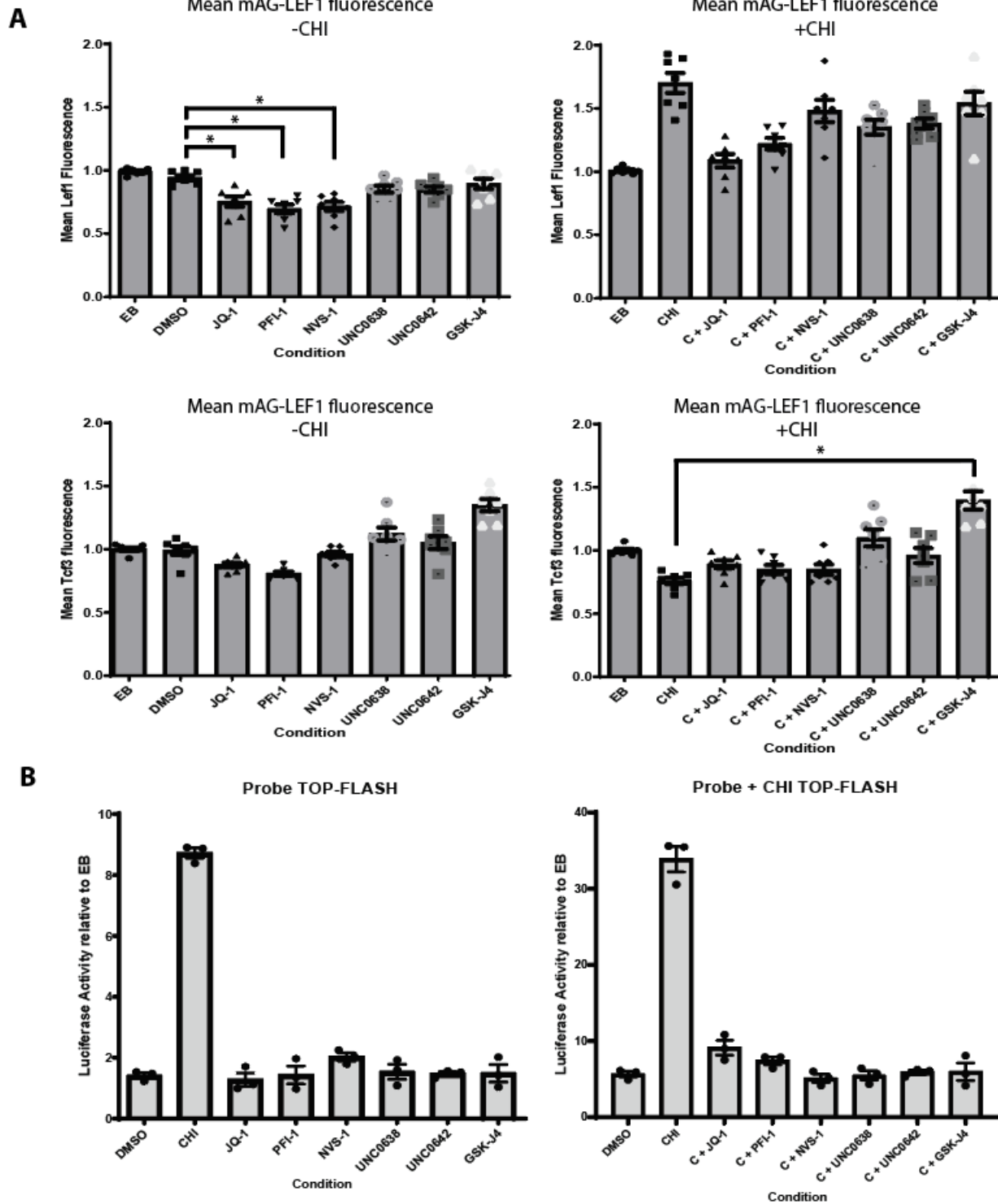
Figure 14. GLOT3-CHmiR cells can detect changes in Wnt state better than TOP-FLASH assays in the absence of CHI.

Figure 14. (Continued) Epigenetic inhibitors were chosen based on previously determined activity. A) GLOT3-CHmiR cells were treated with select epigenetic inhibitors in the absence (name) or presence (C + name) of CHI and scored by mean nuclear fluorescence (n = 7). JQ1 and NVS1 were found to be capable of significantly reducing LEF1 expression in the absence of CHI (p < 0.0005) and GSKJ4 was found to be capable of maintaining TCF7L1 expression in the presence of CHI (p < 0.0005). B) The screen was then repeated with WT mESCs transiently transfected with TOP-FLASH reporter constructs (n = 3). CHI was found to significantly increase TOP activity relative to DMSO, while all tested probes were only found to significantly reduced TOP activity when tested in the presence of CHI (p < 0.0005).

2.5.   DISCUSSION

2.5.1.   GLOT3-CHmiR mESCs provide a more biologically nuanced albeit less sensitive, screening platform compared to TOP-based screens.

Our GLOT3-CHmiR platform can identify Wnt modulators that would have otherwise been missed by traditional TOP-based assays. However, when TOP activity was assessed in the presence of both our small molecule inhibitor and CHI it was found that the TOP-FLASH assay could detect a strong suppression of Wnt activity relative to CHI-only control, with much greater fold change than our GLOT3-CHmiR cell line (Fig. 14). Current Wnt modulators available to the field and in clinical use tend to target extracellular Wnt ligands or receptors, which typically results in binary activation or suppression of Wnt activity (Lu et al., 2016).

That our GLOT3-CHmiR screen could identify nonbinary Wnt modulators suggests that compounds identified by our screen could be more clinically relevant, as they may more finely tune Wnt activity. Importantly, these nuances could help identify compounds capable of modulating TCF/LEF selection. In a wide variety of cancers, aberrant LEF1 expression is associated with increased EMT and poor patient prognosis (Santiago et al.,

2017). Finding compounds capable of reverting these misexpression events could potentially provide a mechanism with which to improve patient outcomes.

Consistent with this aim of TCF/LEF regulation, our GLOT3-CHmiR screening platform has found JQ-1 and PFI-1 to be capable of suppressing LEF1, and GSK-J4 to be capable of increasing TCF7L1 expression. JQ-1 and PFI-1 are potent inhibitors of Bromodomain (BD) and extra-terminal domain (BET) family members. These include BD-containing 2 (BRD2), BRD3, BRD4, and BD testis-associated (BRDT) which is found specifically in the testis. Members of the BET family specifically recognize acetylated lysine on histones through two N-terminal domains (BD1 and BD2) (Belkina and Denis, 2012; Dhalluin et al., 1999). Among these members, BRD2 and BRD4 are the most well-studied, as they have been found to play a critical role in transcriptional regulation through their interactions with various protein complexes within active promoters and enhancers (Jang et al., 2005). This has been shown to occur through BRD4 binding acetylated histones within active promoters and recruiting positive transcription elongation factor b (P-TEFb) to promote RNA polymerase II (RNAPII) extension (Jang et al., 2005; Wu and Chiang, 2007). While BRDs have been shown to function quite ubiquitously throughout the genome, their activity has also been shown to be critically enriched at lineage-specific enhancers and super-enhancers (Chapuy et al., 2013; Jiang et al., 2020b). Inhibitors of BET family members, such as JQ-1 and PFI-1, inactivate BRDs by competitively occupying their acetyl-histone binding domain to prevent their binding to acetylated histones, reducing their association with, and activation of, oncogenic targets, promoting terminal differentiation and apoptosis of cancer cells (Filippakopoulos et al., 2010; Jiang et al., 2020b).

As such, JQ-1 and similar BRD inhibitors have been found to exhibit promising therapeutic effects in a variety of cancers. These inhibitors have been found to be particularly effective in targeting hematopoietic malignancies, including acute myeloid leukemia (AML) (Dawson et al., 2011; Roe et al., 2015), diffuse large B-cell lymphoma (DLBCL) (Chapuy et al., 2013), and Burkitt lymphoma (BL) (Mertz et al., 2011). Interestingly, LEF1 is over expressed so frequently in these cancers that it is often used as a biomarker of AML (Petropoulos et al., 2008), DLBCL (Tandon et al., 2011), and BL (Walther et al., 2013). In these contexts, LEF1 expression correlates with worse patient outcomes due to its ability to promote EMT and consequential metastasis (Medici et al., 2006; Nawshad and Hay, 2003). Our finding that JQ-1 suppresses LEF1 expression may provide a novel avenue for the investigation of therapeutic treatments in cancers where LEF1 is known to be overexpressed.

2.5.2. The GLOT3-CHmiR platform selects for direct transcriptional regulators of Wnt signalling.

As previously mentioned, compounds found to directly modulate the activity of TCF/LEFs are very limited. However, our system uses LEF1/TCF7L1 as a readout of Wnt activity, allowing it to specifically track an aspect of Wnt signaling that is poorly captured by existing platforms. While the driving mutation in a majority of Wnt-related cancers are related to the constitutive stabilization of β-catenin, mutations in TCF/LEFs are considerably less frequent (Tate et al., 2019). By selecting for modulators capable of activating or suppressing TCF/LEF transcriptional activity, compounds identified by our GLOT3-CHmiR system may be applicable to a wider variety of Wnt-related cancers.

In contrast to existing inhibitors that promote broad Wnt activation/suppression, resulting in considerable off-target effects *in vivo*, inhibitors capable of targeting and modulating TCF/LEF status may have reduced off-target effects. This potential for enhanced sensitivity is supported by the contrast in therapeutic efficacy of existing kinase-targeting compounds versus epigenetic inhibitors in the treatment of cancers.

In cancers where translocation events or mutation produce unique constitutively active kinases, such as the BCR-ABL translocation in AML (Deininger et al., 2000), kinase inhibitors are exquisitely sensitive for cancer populations. However, targeting WT kinases that are upregulated in cancer populations results in the inactivation of kinases within healthy populations long before cancer populations are significantly suppressed. By contrast, a wide variety of epigenetic inhibitors have been found to be significantly more selective for cancer cell populations than healthy cell populations, despite targeting WT epigenetic regulators (Minucci and Pelicci, 2006; Parbin et al., 2014; Perez-Salvia and

Esteller, 2017). This heightened sensitivity is not yet fully understood, but it demonstrates that cancer cell populations are more sensitive to modulators of their epigenetic/transcriptional status. As TCF/LEF dysregulation is a common feature in Wnt-related cancers, inhibitors capable of reverting or alleviating this dysregulation at the epigenetic/transcriptional level have the potential to overcome the off-target limitations of kinase or cell surface receptor inhibitors.

The efficacy of BRD inhibitors in certain cancers has been attributed to their ability to inhibit the epigenetic maintenance of critical lineage and self-renewal genes by BRDs (Jiang et al., 2020a). Similarly, LEF1 overexpression in a variety of cancers has been found to strongly correlate with the upregulation of EMT-related genes (Santiago et al., 2017). Compounds identified by our GLOT3-CHmiR platform capable of suppressing LEF1 expression should similarly impede the expression of these EMT-related targets, sensitizing the cancer population to apoptosis or at least inhibiting metastasis. Congruent with this hypothesis, and our findings, JQ-1 has previously been shown to inhibit the proliferation of colorectal cancer cells through the suppression of Wnt signaling (Zhang et al., 2018). As such, we hope that the use of our GLOT3-CHmiR platform in the identification of novel epigenetic regulators will identify compounds capable of selectively disrupting TCF/LEF dysregulation in Wnt-related cancers.

2.6. MATERIALS AND METHODS

2.6.1. Culture Methods

E14tg2a mESCs (ATCC CRL-1821), and derived cell lines, were maintained in mESC medium containing high glucose Dulbecco's Modified Eagle's Medium (DMEM), 15% Fetal Bovine Serum (FBS), 2 mM L-glutamine, 1 mM Sodium Pyruvate, 100 µM non-

essential amino acids, 0.1 mM 2-mercaptoethanol, and 10^3 units/mL leukemia inhibitory

factor (LIF). Cultured cells were passaged every 48h at a 1:6 ratio on 10 cm 0.1% gelatin-

coated culture dishes. During imaging experiments, and to induce LEF1 expression, cells

were cultured in embryoid body (EB) medium, which is identical in composition to mESC

medium but lacks LIF.

2.6.2.   TALEN Design and Transfection

TALENs were designed with TAL Effector Nucleotide targeter 2.0 (Cermak et al., 2011;

Doyle et al., 2012) using default settings, a spacer of 15-20 nt, and 15-20 RVDs per

TALEN. The plasmid kit used for generation of TALENs was a gift from Daniel Voytas

and Adam Bogdanove (Addgene kit # 1000000024). The TALEN pair made to target the

endogenous LEF1 locus was designed to cut roughly 500 bp upstream of the TSS. LEF1

Forward TALEN RVD sequence: NH HD NH HD NH NI HD HD NI HD NH NH NG NH NH

HD HD NI NG. LEF1 Reverse TALEN RVD sequence: NG NI NG NG HD HD HD HD NI

HD HD HD NI NH HD HD HD NH HD NH. The TALEN pair made to target the endogenous

TCF7L1 locus was designed to cut between the third and fourth TCF7L1 exon. TCF7L1

Forward TALEN RVD sequence: NG HD HD HD NH NH NI NH NI NG NG NH NH NG

HD NI NH HD. TCF7L1 Reverse TALEN RVD sequence: HD HD NI NH NH HD HD HD

NG NG NH HD HD HD NI NI HD NG NG NG HD NG. Regions of homology required for

homologous recombination were amplified from either locus using PCR and assembled

into a final repair template vector through digestion and ligation. A LoxP-flanked neomycin

resistance cassette was also included within the recombination region of the repair

template to select for successful integration via resistance to the drug G418. To target the

mouse Rosa26 locus we employed TALEN-mROSA26 KKR and ELD constructs gifted

by Radislav Sedláček (Addgene plasmid # 60025, 60026). A repair template was made by using pDonor MCS Rosa26, which was a gift from Charles Gersbach (Addgene plasmid # 37200). This repair template was then engineered to contain either the CAG-H2B-miRFP670 or H2B-miRFP670 reporter cassettes.

All TALEN targeting transfections were performed using 2 x 10^6 cells, 2 µg of either TALEN and 1 µg of repair template and the transfection reagent Lipofectamine 2000 (Thermo, Cat# 11668030). Transfected cells were seeded equally across four 10 cm culture dishes in mESC medium for 24h before 2 µg/mL puromycin was added to select for cells successful transfected with the TALEN expression constructs. After a 24h incubation with puromycin, medium was removed and cells were washed twice in PBS before being transferred to mESC medium containing 250 µg/mL G418. Cells were then allowed to grow for roughly 5 – 7 days until individual colonies formed. Once individual colonies could be identified without the aid of a microscope, they were isolated and expanded. Putative clones were then screened by using PCR to determine if desired fusion protein cassettes were successfully integrated into the correct genomic locations. Following PCR validation, putative clones were then Cre excised. 2 x 10^6 cells were transfected with 2 µg of Cre-IRES-PuroR, which was a gift from Darrell Kotton (Addgene plasmid # 30205). As before, individual clones were isolated, successful excision was validated by PCR, and successful expression of fusion proteins was determined by western blotting and sequencing. This process was repeated for LEF1, TCF7L1, and CAG-H2B-miRFP670 using E14tg2a mESCs as our initial cell line.

2.6.3. Hanging Drop Embryoid Body Formation and Flow Analysis

Hanging drop embryoid bodies (HD-EBs) were generated by using the protocol described by Wang and Yang 2008, but modified to initiate HD-EB formation using 800 cells rather than 500 cells (Wang and Yang, 2008). HD-EBs were collected every 24 hours over seven days of differentiation, gently singularized with Trypsin, and analyzed by using flow cytometry (n=3). To account for the endogenous expression of mAG-LEF1/mKO2-TCF7L1 in our GLOT3 cells, E14tg2a cells were transfected with CAG-mAG or CAG-mKO2 for use in fluorescence compensation, rather than fluorphore conjugated beads.

Flow cytometry control plasmids were based on pCAG:H2B-EGFP, a gift from Anna-Katerina Hadjantonakis & Virginia Papaioannou (Addgene plasmid # 32599 ; http://n2t.net/addgene:32599 ; RRID:Addgene_32599).

2.6.4. qPCR Analysis

E14tg2a cells were grown as HD-EBs and samples were collected every 24 hours for three days. RNA was then collected (RNeasy kit, Qiagen) from samples and converted to cDNA using qScript (Quantbio). The expression of each of the listed genes was determined using SsoAdvanced Universal SYBR Green Supermix (BioRad), with expression being shown relative to the expression of Rpl13a (n=3). Primers used for qRT-PCR:

RPL13a   Fwd: 5'-TCCCTCCACCCTATGACAAG-3'
              Rev: 5'-GTCACTGCCTGGTACTTCC-3'

Wnt3   Fwd: 5'-TGGAACTGTACCACCATAGATGAC-3'
              Rev: 5'- ACACCAGCCGAGGCGATG-3'

T/Brachyury Fwd: 5'-AGCTCTCCAACCTATGCGGACAAT-3'

Rev: 5'-TGGTACCATTGCTCACAGACCAGA-3'

BMP4   Fwd: 5' - GCCGAGCCAACACTGTGAGGA - 3'
Rev: 5' - GATGCTGCTGAGGTTGAAGAGG - 3'

2.6.5. Western Blot Analysis

To promote LEF1 expression, cells were grown in EB medium for 48 hours, while cells were grown for 24h in mESC medium to promote TCF7L1 expression. Protein was extracted by lysing cells in RIPA buffer with HALT protease/phosphatase inhibitor cocktail (Thermo). Samples were then quantified by using DC protein assay (BioRad) and 20 µg of total protein was separated by using SDS-polyacrylamide gel electrophoresis with Bolt bis-tris gels (Thermo Fisher). Proteins were then electrophoretically transferred to nitrocellulose membrane and blocked for 1 hour at room temperature in 5% non-fat milk/TBS, and then incubated overnight at 4°C in 5% nonfat dry milk in TBS with 0.1% Tween-20 (TBST) containing diluted primary antibody. Primary antibodies against LEF1 (Cell Signaling Technologies C12A5) or TCF7L1 (Abcam ab86175) were used at a 1:1000 dilution, while antibody against GAPDH (Abcam ab9485) was used at 1:40 000. The membrane was washed to remove excess antibody and incubated in secondary antibodies diluted 1:20 000 (BioRad) in 5% nonfat dry milk in TBS with 0.1% Tween-20 for 1 hour at room temperature. Blots were then developed with enhanced chemiluminescence substrate (Immobilon Forte, Sigma) and imaged using a BioRad ChemiDoc system.

2.6.6. Drug Library Preparation

For initial optimization and validation of our GLOT3-CHmiR screening system we used CHIR99021 (Sigma), SU5402 (Sigma), and PD0325901 (Sigma). Our library of epigenetic inhibitors was generously gifted to us from the Structural Genetics Consortium of Toronto.

All compounds were resuspended in DMSO to a final concentration of 500 mM and split across multiple 96-well round-bottom plates. These master stocks were then stored at -80°C. Aliquots were prepared in 96-well round-bottom plate format and stored at -20°C for use in treatments of live cell imaging populations. Each aliquoted plate was used a maximum of three times before disposal and preparation of a fresh aliquot plate.

2.6.7. Plate Seeding, Maintenance, and Imaging

Cultured GLOT3-CHmiR cells were singularized by using Accutase for 5 minutes at 37°C and seeded onto 0.1% gelatin-coated uPlate 96-well plates (IBIDI, 80826) at 10 000 cells/well and cultured for 24 hours in EB medium. After 24 hours, medium was aspirated, and cells were washed once in PBS before 5 µM of each drug in EB medium was added to each well to a final volume of 200 µL. Control wells in which no drug was added, or an equivalent volume of DMSO alone was added, were included in each run. Following an additional 24 hours of culture, cells were imaged by using a Nikon A1 scanning laser confocal microscope. Images were acquired at 20x magnification over 10 equally spaced fields within each well with a 488 nm laser and FITC filter to image mAG-LEF1 (492/505), a 560 nm laser and TRITC filter to image mKO2-TCF7L1 (551/565), and a 647 nm laser and Cy5 filter to image H2B-miRFP670 (642/670). Images were converted from NIS2 format (Nikon) and annotated using FIJI (Schindelin et al., 2012). Converted images were then processed with CellProfiler (McQuin et al., 2018) to identify nuclei and score mean nuclear fluorescence. Fluorescence data was then processed with Python 3.7 (Oliphant, 2007) using Pandas (McKinney, 2010) for data structuring, Matplotlib (Hunter, 2007) for graphing, and SciPy (McKinney, 2010) for statistical analyses.

2.6.8.   TOP-FLASH Transfection and Quantification

E14Tg2a mESCs were transfected with M50 Super 8x TOPFlash, which was a gift from

Randall Moon (Addgene plasmid #12456) and pRL-CMW (Promega) in a 20:1 ratio using

Lipofectamine 2000 (Thermo) and seeded at 50 000 cells/well in a 0.1% gelatin-coated

96-well flat-bottom plate. Plated cells were then incubated for 24h in EB medium, washed

once with 1X PBS, and then incubated for an additional 24h in EB medium containing

selected drugs. Samples were then prepared and collected for the Dual-Luciferase

Reporter Assay System (Promega E1980), and resulting luminescence was quantified

using a plate reader with recommended settings.
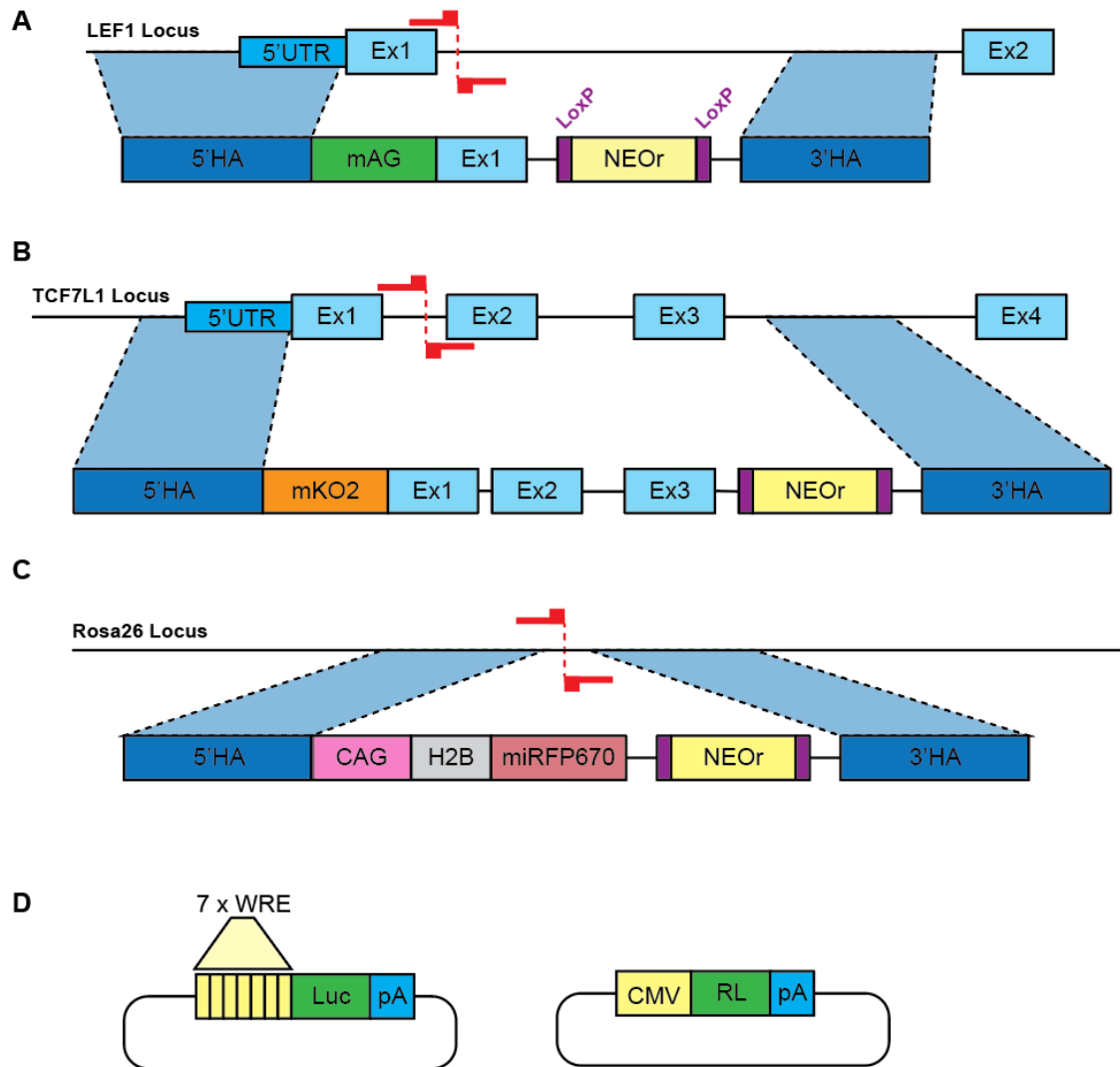
Supplementary Figure 1. **TALEN-based targeting strategy for GLOT3-CHmiR cell line generation and TOP-FLASH reporter constructs.** A-C) TALENs depicted in red yield double-strand breaks in the indicated endogenous loci. Targeting constructs are shown below. 5'/3' homology arms are designated as blue boxes (5'/3'HA) and are mapped back to homologous regions of targeted loci (dotted box). All targeting constructs contained a LoxP-flanked (purple) neomycin resistance cassette (NEOr) for selection of successful integration. D) Plasmid map of TOP-FLASH construct with several WREs driving luciferase (Luc) expression, and CMV-driven renilla (RL) transfection control plasmid.

CHAPTER 3. DEVELOPING A 2D MICROPATTERNED CULTURE PLATFORM FOR THE CHARACTERIZATION AND ISOLATION OF TCF/LEF EXCHANGE EVENTS

3.1.   ABSTRACT

Directing the differentiation of stem cell populations towards a given fate has long been a goal of stem cell biologists. Differentiation protocols often rely upon selection of a desired fate from a heterogeneous population and serve as poor models with which to study mechanisms underlying cell fate determination. By contrast, seeding pluripotent stem cells onto micropatterned culture surfaces, which contain geometrically defined shapes in which cells selectively adhere, induces highly consistent organization of differentiating populations. The consistent organization of micropatterned populations not only makes them amenable to a variety of automated imaging techniques, but also provides a means to isolate homogeneous populations for use in downstream mechanistic studies. However, the techniques and equipment required for the fabrication of micropatterns are typically restricted to biomedical engineering groups. To make micropatterning more accessible to a wider range of stem cell biologists we present here a fabrication technique that requires minimal technical experience. The primary limitation is a requirement for a specialized UV-ozone cleaner, but this small piece of equipment is affordable for many labs (approximately $5000 USD). Alternatively, it should be possible to gain access to this instrument through biomedical engineering facilities available at many academic institutions. We demonstrate the efficacy of our micropatterning protocol by using it to reproducibly generate precisely timed cellular differentiation states that we can detect by using mouse embryonic stem cells in which LEF1 and TCF7L1 genes have had fluorescent proteins introduced into their endogenous loci to generate N-terminal fusion

proteins. We discuss how this platform could be used to isolate pure populations for downstream analyses.

3.2.   INTRODUCTION

Directed differentiation has long been a goal for the field of stem cell biology (Chambers et al., 2009; Spater et al., 2014; Torres et al., 2012). However, the majority of the efforts towards coaxing stem cells to differentiate towards a desired fate have been carried out by using traditional culture techniques. Characterization of these techniques has revealed that differentiation under these conditions occur less through directed fate commitment of the total population, and more through subpopulation selection (Oh and Jang, 2019). These findings demonstrate that the means of differentiation in traditional culture plates is through selection for a given cell fate by medium conditions, rather than organizing and guiding the population through a series of cell fates. As a result, cell fate yield is often quite low, reaching as little as 10-50% of the starting population, requiring cell sorting to obtain pure (>90%) populations (Oh and Jang, 2019). Low yields and lack of uniform cellular organization limit secondary characterization, making it quite difficult to track cell fate events that occur throughout *in vitro* differentiation.

To overcome these limitations of traditional culture, a variety of microfabrication techniques have been employed to better organize 2D culture populations (Ermis et al., 2018). These techniques allow for the capture and consistent geometric organization of discrete cell populations. By chemically modifying defined regions of the culture surface, researchers can selectively coat regions of these surfaces with extracellular matrix (ECM) proteins, allowing them to selectively capture cell populations (Joo et al., 2015). These techniques have been employed to capture individual cells to investigate cytoskeletal

architecture or hundreds of cells to capture gastrulation-like events. In addition, modified post-seeding techniques can be used to investigate cellular migration and epithelial to mesenchymal transition (EMT) (Kusuma et al., 2017; Morgani et al., 2018; Thery, 2010a). However, the fabrication techniques required to generate these surfaces is often quite technically difficult and require experience with, and access to, specialized equipment.

The most frequently used fabrication approaches include microcontact printing, laser-patterning, and photo-patterning (Ermis et al., 2018). Microcontact printing is performed by coating a polydimethylsiloxane (PDMS) stamp etched to possess the desired micro-features. ECM proteins can be applied to the stamp and then imprinted onto a desired culture surface. However, the technical limitations associated with stamp microfabrication limits its accessibility, and variations in efficient protein transfer limit its reproducibility. Laser-patterning and photo-patterning both take advantage of high-energy light, such as deep ultraviolet (<200 nm) light, which can generate localized plasma to directly oxidize culture substrates or dissociate hydrophobic coatings. When used in combination with hydrophobic culture substrates, these approaches allow for the generation of discrete hydrophilic regions that permit the selective deposition of ECM proteins (Ermis et al., 2018; Strickland et al., 2012). While laser-patterning approaches allow for excellent control over pattern design, which can be rapidly changed and adjusted as protocols are optimized, the systems required to implement them are quite specialized. Alternatively, photo-patterning uses similar principles to laser-patterning, but the equipment required is significantly cheaper and easily accessible in most university settings (Carpi et al., 2011).

Here, we describe a highly accessible photopatterning technique that requires minimal knowledge of microfabrication techniques. Our technique uses freely available software

and common fabrication equipment that many labs will be able to afford, but which is also available in most engineering departments. The basic principles of the technique can be built upon as users gain experience. While services exist to purchase prefabricated micropatterned chips or plates, our technique is considerably more cost-effective and customizable for those intending to use micropatterned growth substrates routinely. With the technique we describe, we hope to lower the barrier of entry for cell biology labs and promote the use of these powerful micropatterning platforms in investigating cell signaling and differentiation.

3.3.   DEVELOPMENT OF METHOD

Much of the existing literature describing micropatterning techniques is highly specialized and focuses upon fabricating and analyzing cellular behaviour by using intricate micropatterned fabrication and analysis techniques. While these publications serve their intended engineering audience well, they rarely see translation into general use within the fields of biochemistry and cell biology. However, these techniques can provide exquisite control of cellular environments and differentiation, and as such, warrant consideration by those in the fields of developmental and cancer biology. To make this technique more accessible for non-experts we chose to assemble a scalable, cost-effective, and simple technique that relies upon access to readily accessible materials and equipment.

In developing this protocol, we had three main aims: i) minimize reliance on specialized equipment, ii) minimize material cost, and iii) provide experience with techniques that can be independently expanded upon. To this end we chose a photolithographic fabrication technique that requires only a UV/Ozone Cleaner as a light source, and no prior chemical preparation of the seeding surface (Fig. 15). As UV/Ozone cleaners are common in micro-

engineering lab spaces, these devices should be quite accessible through collaborations with engineering lab groups. The use of a positive photomask and omission of a pre-coating reduces complexity and avoids the requirement of additional equipment. Finally, photolithography is a remarkably flexible technique. By using our protocol to establish a basic microfabrication and analysis pipeline, we hope to provide cell biology and biochemistry labs with a point of entry into the field of micropatterning and help them foster future collaborations across multiple disciplines.

3.4. APPLICATION OF METHOD

Our technique can be used as a platform for the generation of homogeneous cell populations for downstream analysis using microscopy or transcriptomic techniques such as Assay for Transposase-Accessible Chromatin using sequencing (ATAC-seq) (Buenrostro et al., 2015), Cleavage Under Targets and Release Using Nuclease (CUT & RUN) (Skene and Henikoff, 2017), or Cleavage Under Targets and Tagmentation (CUT & Tag) (Kaya-Okur et al., 2019). Cells grown on micropatterned surfaces spontaneously organize into ordered populations as they differentiate. As a result, gene expression patterns are highly organized within micropatterns, and are highly consistent between micropatterns on the same plate and across experiments. This can be taken advantage of by using fluorescent imaging of live or fixed samples. Since all micropatterns will be consistent in their shape and dimensions, patterns in gene expression can be averaged across many micropatterned populations to define these patterns of expression with great confidence. Additionally, transcriptomic approaches such as ATAC-seq or Tag & Run can be performed on cell populations of less than 100 000 cells (Buenrostro et al., 2015; Kaya-Okur et al., 2019; Skene et al., 2018). Performing Tag & Run against a given transcription

factor in a large micropatterned population will ensure that the obtained results are reflective of a consistent cellular context, reducing the noise incurred by assessing a heterogeneous population grown on standard un-patterned culture plates.
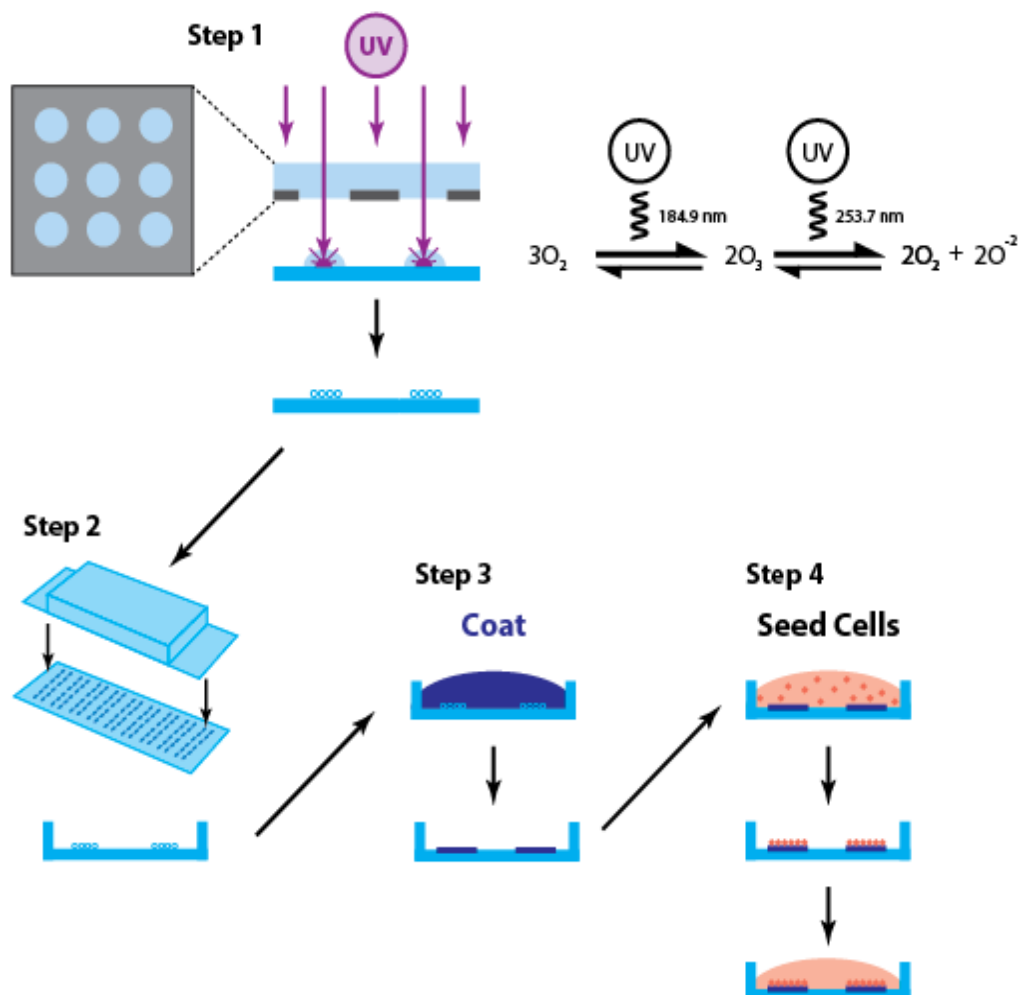
Figure 15. Overview of micropatterning protocol

Step 1: Etch hydrophobic coverslips using a photomask and a deep UV light source. This process takes advantage of the molecular oxygen produced by deep UV light to specifically oxidize regions of the culture surface that were exposed through the photomask. Step 2: Assemble a full culture slide using the photopatterned coverslip and adhesive slide wells. Step 3: Coat assembled coverslip wells with ECM protein of choice. ECM proteins will selectively deposit upon oxidized (hydrophilic) micropattern regions. Step 4: Seed cells onto the coated micropatterned coverslip, wash away excess un-patterned cells, add desired medium and begin micropattern assay.

3.5.   DESIGNING A PHOTOMASK

3.5.1.   Materials

- **Software**

There are a variety of software programs that will allow for the design of mask features. However, the files produced by these programs must be compatible with the mask manufacturer's factory equipment. For most manufacturers, Equipment Data Acquisition (EDA) standard formats such as GDS-II or OASIS files are ideal, but computer-assisted design (CAD) file formats such as DWG or DWX may also be acceptable. EDA format files can easily be produced using free design programs such as LayoutEditor (https://layouteditor.com/). Alternatively, CAD programs such as AutoDesk Fusion 360 (https://www.autodesk.com/) can be obtained by using a free student licence. It is best to contact your chosen manufacturer before designing a photomask, to ensure that your photomask is designed using their preferred file format. However, most manufacturers can convert files between different formats, though this may produce artifacts in your converted file, which may cost extra for them to correct.

When submitting completed photomask design files, one must be sure to specify if one has designed a "positive" or "negative" photomask, and if one's design will read-right with the chrome facing up or down (Fig. 16B). Most manufacturers will also ask for you to define your minimum feature size, which is the smallest shape that you require them to produce for your photomask. Typically, the lower limit of these production techniques is around 0.5 μm, but for the purposes of our larger circle or ellipse patterns 5-10 μm is sufficient.

- **Photomask**

Deep UV irradiation generates molecular oxygen by using 184.7/249.8 nm light (Fig. 15). It is critical that your photomask is mounted on a material that is transparent to wavelengths below 200 nm. The ideal material for this application is fused-silica quartz, as glass has much worse transparency below 200 nm, and plastic film is similarly opaque and will be damaged by this process. A thickness of 2-3 mm is typically sufficient for this application. However, most photomask manufacturers don't use fused-silica quartz as their default material, so one must be certain to specify that it is required. The dimensions of your photomask should also be defined based on the dimensions of your UV/Ozone cleaner. Typically, these will be between 3x3 and 5x5 inches. Finally, the mask type should be specified as ≈1 µm chrome. This is the material that your mask will be made of. We have had great success with photomasks obtained from PhotomaskPortal (https://www.photomaskportal.com/) in Texas, USA. Additionally, their website has excellent resources available to help learn and understand their photomask design and ordering process. An alternative company, which is present in most countries, is Toppan Photomasks (https://www.photomask.com/).

3.5.2. Designing Features

Photomasks are typically much larger than coverslips, allowing multiple coverslips to be patterned at once. As such, the photomask can be subdivided into regions with different types of patterns. Including larger features easily visible by eye, such as a 1-2 mm thick line, make it easy to distinguish different subdivisions one may want to employ. In order to optimize micropattern dimensions for a chosen experiment, it is best to first order a "test" mask capable of assessing a variety of dimensions. By filling each subdivision with

a different set of test patterns, it is possible to rapidly assess a wide variety of potential patterns of interest (Fig. 16A). However, it is important to note that larger micropatterns containing hundreds to thousands of cells can influence the organization of adjacent patterns if packed too closely. To avoid these confounding influences, it is best to separate individual micropattern shapes by 500-750 µm (Fig. 16A). Once an ideal pattern has been identified, a second photomask containing a single selected pattern can be obtained, which will increase patterned coverslip production rates. Alternatively, carefully designed test plates can be used as-is to produce micropatterns for low throughput assays.
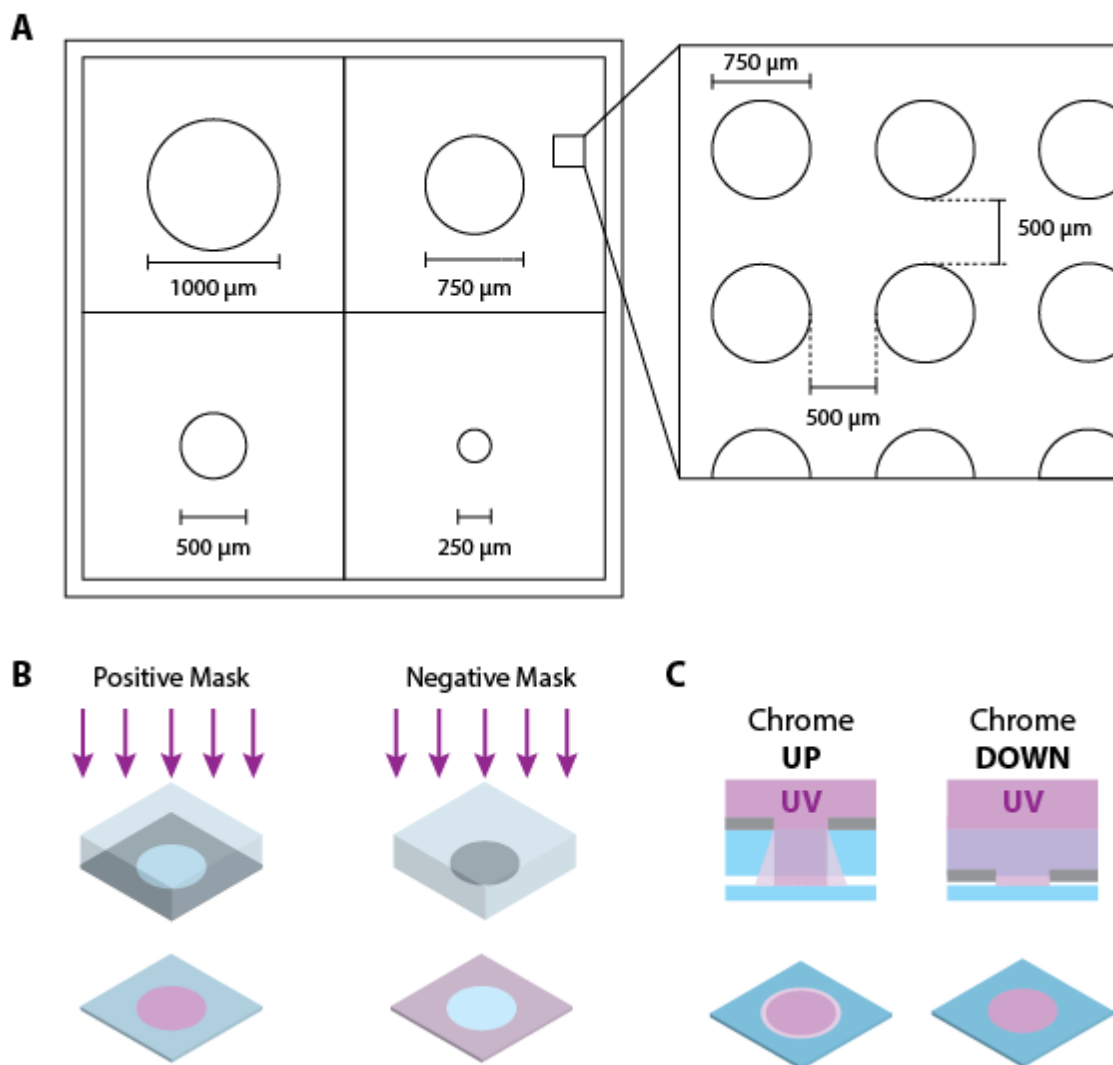
Figure 16. Photomask design guidelines

A) Demonstration of subdivision and feature separation for a 5x5 inch photomask. Large shapes in each quadrant represent the designs present in each. The blow-out image shows the actual designs present in each section. B) Positive photomasks leave an intended design feature uncovered, patterning just a selected feature. Negative photomasks are filled only by a designed feature, exposing the surrounding space to the light source. C) Photomasks should always be used chrome side down to prevent exposing more than your intended area (light purple).

3.6.   MICROPATTERN FABRICATION

3.6.1. Materials

- **UV/Ozone cleaner**

While we have used Bioforce (ProCleaner™ Plus, SKU 1062) and Jelight (UVO cleaner, 342-220) models, UV/Ozone cleaners with peaks in emission at $\lambda = 185$ nm and 254 nm are sufficient for micropatterning applications. However, UV/Ozone cleaners must have an exhaust system installed or must be used in a chemical hood or biosafety cabinet (BSC) to avoid exposure to toxic ozone.

While a UV/Ozone cleaner can be purchased online for a moderate price, they can typically be found in microengineering clean rooms. Through collaboration with these engineering groups, and by following clean room protocols, it should be possible to gain access to this equipment.

Photomasks should be placed within $0.5 – 5$ cm of the UV/Ozone cleaner bulbs while patterning is in progress. If the support tray in the instrument is not close enough to the UV light source, the photomask assembly can be placed on a glass block to bring it closer to the bulbs.

- **Photomask**

To avoid fouling or contamination from microparticles, photomasks should only ever be handled or removed from their case in a BSC or clean room setting. Prior to use, the chrome face of the photomask should be cleaned by gently rinsing it, or cautiously wiping it down with a wetted lint-free and non-abrasive tissue such as a Kimwipe (Kimberly-Clark). This should be done first using acetone to remove any potentially contaminating

organic residues, and then using isopropanol to remove inorganic contaminants and residual acetone. After cleaning, the photomask is placed back into its open case, chrome face up, and allowed to fully air dry before use

Note: Always be sure to use the photomask chrome side down when patterning. This ensures the closest possible contact between your chrome photomask and the patterning surface. If placed chrome side up, light will be able to scatter as it passes through the fused silica-quartz backing, weakly patterning a small area surrounding your intended design (Fig. 16C). This will result in cells adhering weakly around your micropattern, resulting in a poorly defined boundary around the patterned cell cluster.

- **Uncoated, hydrophobic, polymer coverslips** (IBIDI, cat.# 10813)

Coverslips should never be removed from their packaging or handled while outside of a BSC or clean room setting.

- **Fine pair of tweezers**
- **Scissors**
- **200 μL Plastic pipette tips** (Frogga Bio, Cat# 4TI-2105)
- **Sterile Petri dishes** (Frogga Bio, Cat# 6139-00)
- **Glass stage block**

This is a roughly one-inch thick piece of glass that is included with the UV/Ozone cleaner and matches the dimensions of its loading tray.

3.6.2. Method

1. Fully wipe down and sterilize your working area using 70% ethanol and a lint-free wipe to remove any potential microparticle contaminants.

2. Turn on the UV/Ozone cleaner and allow it to run for 5 minutes to fully warm the bulbs before use.

3. Prepare polymer coverslips:

   a. Hydrophobic polymer coverslips will have a film covering their hydrophobic face. This face is difficult to identify visually so, using a fine pair of tweezers, scratch at the top right corner of the coverslip. If performed on the correct face, this will begin to tear the film covering. Once torn, use the fine tweezers to delicately pull away and remove the remaining film. To keep track of which side of the coverslip is hydrophobic, place it hydrophobic face up and use scissors to cut off a small portion of the top right corner. Now, whenever held in that same orientation, the hydrophobic face will always be facing up if the top right corner is missing. This is important to remember when placing your coverslips under the photomask.

   b. Place your prepared coverslips into a sterile Petri dish, hydrophobic face up.

   c. Prepare as many coverslips in this way as needed.

4. Create the photopatterning assembly:

a. Wipe down and clean your glass stage block using 70% ethanol and lint-free non-abrasive wipes. Allow to air dry before continuing.

b. Open the loading tray of your UV/Ozone cleaner and place your cleaned glass stage block onto the loading tray.

c. Using a fine pair of tweezers, place coverslips on top of the glass stage block, hydrophobic face up. Use a minimum of two coverslips to be sure your photomask is prevented from making direct contact with the glass stage block. However, be careful to leave enough space between coverslips to prevent them from laying on top of each other.

d. Using both hands, carefully place the photomask chrome face down, on top of your coverslips that have been placed onto the glass stage. Use caution to avoid knocking the photomask against the glass stage block, as this will damage the chrome photomask. Be sure to visually confirm that your assembled photomask, coverslips, and glass stage block assembly are less than 5 cm away from the bulbs of the UV/Ozone cleaner but does not collide with the bulbs or any internal components of the UV/Ozone cleaner.

5. Photopatterning coverslips:

a. Carefully close the UV/Ozone loading tray and lock it shut.

b. Turn on the UV/Ozone cleaner and let it illuminate your photopatterning assembly for 10 minutes.

c. Turn off the UV/Ozone cleaner and carefully open the loading tray. Note: If using a UV/Ozone cleaner that does not have an exhaust system installed, wait an additional 2-3 minutes after turning off the device to allow any remaining ozone to dissipate.

d. Carefully remove the photomask from the photopatterning assembly. If any coverslips remain stuck to the photomask, hold the photomask over an open sterile Petri dish and use a plastic pipette tip to carefully nudge the coverslips off into the Petri dish. Use a fine pair of tweezers to any remaining coverslips from the glass stage block into the same Petri dish. **Do not** use metal tweezers to remove coverslips stuck to the photomask, as there is a very high risk of damaging the photomask.

e. Photopatterned coverslips can be stored in a sterile Petri dish at room temperature for roughly two weeks before being used. When held for longer periods of time pattern quality appears to diminish.

6. Repeat steps 3 to 5 until the desired number of coverslips have been patterned.

7. Once photopatterning has been finished and the photomask is no longer needed, wash it with acetone and isopropanol as previously described. Carefully place the photomask back into its storage case and return it to storage. Photopatterned coverslips can be stored and held in a sterile Petri dish for up to two weeks at room temperature.

3.7.   COVERSLIP COATING

3.7.1.   Materials

- **Laminin** (Sigma, Cat# L2020-1MG)

We have found Laminin coatings to produce the best results, but it is also possible to use alternative extracellular matrix (ECM) proteins. Fibronectin or gelatin are two common alternatives, and their working concentration can be optimized by testing serial dilutions.

- **P10 and P1000 pipettes and associated tips** Frogga Bio, Cat# 4TI-2105, L1250F)

- **Sterile Petri dishes** (Frogga Bio, Cat# 6139-00)

- **A fine pair of tweezers** (Sigma, Cat# T5415-1EA)

- **0.1% (w/v) Pluronic acid F127 in PBS without Ca^{2+}/Mg^{2+}**

Pluronic acid is a very efficient antifouling molecule which will prevent non-specific adhesion of proteins/cells to nonirradiated regions.

- **Dulbecco's PBS without Ca^{2+}/Mg^{2+}** (Thermo, Cat# 14190250)

Pluronic acid is slow to dissolve. A 10 mL sample will need to be rocked at room temperature for ≈20 minutes for the pluronic acid to fully dissolve. Filter the solution by using a syringe and 0.2 μm filter before use. The final sterilized solution can be stored at 4°C for several months.

- **Sticky-slide 8-well** (IBIDI, cat# 80828)

    o   These are bottomless 8-well slides that match the dimensions of Ibidi patterned coverslips and come with adhesive pre-applied to their bottom surface.

- **Photopatterned coverslips from previous section**

- **Plastic container with lid**

- **Class II Biosafety Cabinet (BSC)**

- **4°C fridge**

3.7.2. Method

1. Prepare the BSC by wiping down your working area with 70% ethanol using a lint-free non-abrasive wipe.

2. Use 70% ethanol and lint-free non-abrasive wipes to decontaminate your plastic container and place it aside in the BSC to air dry.

3. Remove the sticky-slide 8-wells from their individual packaging and place them in the BSC in a sterile Petri dish, adhesive side up, along with a matching number of photopatterned coverslips in a separate Petri dish, hydrophobic side up.

4. Using a fine pair of tweezers remove the film from the adhesive side of the sticky-slide.

5. Holding the sticky-slide in one hand, and the photopatterned coverslip in tweezers with the other, align them corner-to-corner and carefully start adhering the coverslip to the sticky-slide. **Note:** Be sure that the coverslip is adhered with the photopatterned hydrophobic face up, towards the sticky-slide.

6. Using the blunt back end of the tweezers, carefully push out any remaining air bubbles that may be present between the coverslip and the adhesive surface of

the sticky-slide. **Note:** It is very important that one not apply any pressure to the bottoms of the wells themselves, as this will tear the coverslip. Only apply a gentle force to the regions directly adhered to the sticky-slide.

7. Set the assembled micropatterned slide aside.

8. Calculate the surface area for each of the wells you wish to coat, referred to as TotalA, and the recommended fill volume for each of these wells, which will be referred to as TotalV.

9. Resuspend 1-10 µg of laminin per cm^2 of TotalA in a volume of 0.1% pluronic acid/PBS equal to TotalV. Use this solution to fill each desired well with their recommended fill volume. In the case of an 8-well sticky-slide this will be 300 µL/well. Gently pipette up and down in each well to mix.

    a. Note: The amount of laminin used for coating is highly dependent on micropattern design and density, and as such must be optimized for each micropattern used.

10. Place assembled and coated sticky-slide assemblies into a sterilized plastic container and incubate for 18-24 hours at 4°C.

    a. Coated sticky-slides should be used immediately after coating. Leaving the plates for an additional 18-24 hours will allow laminin to adhere non-specifically, greatly increasing non-specific cell adhesion.

3.8.   CELL DEPOSITION

3.8.1.   Reagents

- **Mouse embryonic stem cell (mESC) medium**

  - **Dulbecco's Modified Eagle Medium (DMEM)** (Thermo, Cat# 11960051)

  - **Fetal Bovine Serum (FBS)** (Gibco, Cat# LS10082147)

  - **Non-essential amino acids (NEAA)** (Thermo, Cat# 11140050)

  - **Sodium pyruvate** (Thermo, Cat# 11360070)

  - **L-glutamine** (Thermo, Cat# 25030081)

  - **β-mercaptoethanol** (Pierce, Cat# 35602BID)

  - **Leukemia Inhibitory Factor (LIF)** (Gibco, Cat# PMC9484)

- **N2B27 medium**

  - **DMEM/F12 medium** (Gibco, Cat# 21041025)

  - **Neurobasal medium** (Gibco, Cat# 21103049)

  - **N-2 supplement** (Gibco, Cat# 17502048)

  - **B-27 supplement without vitamin A** (Gibco, Cat# 12587010)

  - **Non-essential amino acids (NEAA)** (Thermo, Cat# 11140050)

  - **Sodium pyruvate** (Thermo, Cat# 11360070)

- o **L-glutamine** (Thermo, Cat# 25030081)

- o **β-mercaptoethanol** (Pierce, Cat# 35602BID)

- o **CHIR-99021** (Stemcell Technologies, Cat# 72052) and **PD0325901** (Stemcell technologies, Cat# 72182) are added as required to yield complete N2B27 + 2i medium (add inhibitors just prior to using complete medium).

- **Accutase** (Stemcell Technologies, Cat#. 07922)

- **Dulbecco's Phosphate Buffered Saline, without Ca^{2+}/Mg^{2+}** (Stemcell Technologies, Cat# 37350)

- **300 mM EGTA** (ethylene glycol-bis(β-aminoethyl ether)-N,N,N′,N′-tetraacetic acid) (Sigma, Cat# P3075) resuspended in Ca^{2+}/Mg^{2+} free PBS.

- **Rho Kinase Inhibitor (ROCKi)** CAS 872543-07-6 (Sigma, Cat# 555550)

3.8.2. Equipment

- **Incubator**

- **Benchtop centrifuge**

- **Class II Biosafety Cabinet**

- **P10 and P1000 pipettes, with respective tips**

- **15 mL centrifuge tubes**

- **Semi-confluent 10 cm dish of cultured mESCs**

- **Benchtop microscope**

- **Automated cell counter or hemocytometer**

3.8.3.   Method

1. Remove a semi-confluent 10 cm plate of mESCs from the incubator, aspirate medium, wash once with 1X PBS and aspirate 1X PBS.

2. Add 2 mL of Accutase, incubate for 5 minutes at 37°C.

3. While cells incubate with Accutase, retrieve micropatterned sticky-slides.

4. Wash the micropatterned slides:

   a. Using a P1000 pipettor, gently aspirate the coating solution from a well of the sticky-slide and add 300 µL of 1X PBS to the same well. Repeat this step for each coated well of the micropatterned sticky-slide. Note: The bottoms of the sticky-slide are quite delicate, so care must be taken no to damage the bottoms of the wells. However, this process must be done quickly for each well, as exposing the micropatterns to air for too long will damage their laminin coating.

   b. Repeat step 4a) three times for each well.

   c. Once washes are finished, add 300 µL of 1X PBS to each well.

5. Using a P1000 pipettor, add 1 mL of mESC medium to the Accutase-treated plate of mESCs and dissociate them by gently pipetting up and down.

6. Count mESCs:

   a. Transfer dissociated mESC to a 15 mL centrifuge tube and top to 10 mL total volume using 1X PBS.

   b. Centrifuge cells at 1200 x g for 3 minutes.

   c. Aspirate the supernatant and resuspend the cell pellet in 8 mL of mESC medium.

   d. Use this resuspension to acquire an accurate cell count.

7. Seed mESCs onto micropatterns:

   a. Using a P1000 pipettor, remove all PBS from each well of the micropatterned sticky-slide.

   b. Seed each well with 300 µL of cells suspended in mESC medium supplemented with 10 µM ROCKi and 100 µM EGTA and seeded at 100 000 to 500 000 cells/cm^2.

      i. The inclusion of ROCKi helps prevent cell death. EGTA is also included to chelate divalent cations such as Ca^{2+}. This prevents caherin-based adhesion, which causes cells to clump together, and promotes integrin-based adhesion to laminin-coated micropatterns.

    ii. The number of cells/cm^2 required is dependent on micropattern design and density and will need to be optimized for each condition independently.

c. Allow the seeded micropatterns to sit at room temperature in the BSC for 3-5 minutes to allow cells to settle.

d. Transfer the seeded micropatterns to a 37°C incubator and allow them to incubate for an additional 1 – 2 hours for the cells to fully adhere.

    i. Note: This step is the most variable point of the entire protocol and will need to be optimized for each cell line, micropattern, and slide type used. In optimization runs, the micropatterns can be viewed under a microscope every 20-30 minutes to look for signs of adhesion. As cells begin to adhere, they will change from a spherical to flattened phenotype, which can help gauge how much seeding time is required. Additionally, seeded populations require roughly 12-24 hours to completely fill their micropattern, so assessments of initial seeding densities should be made after this interval. Seeding too many cells will crowd the micropattern, reducing the 2D quality of micropatterns and resulting in clumping. Seeding too few cells will underpopulate the micropattern, resulting in clusters of smaller colonies growing within the micropatterned space.

e. Once seeding is complete, move the micropatterned coverslip to the BSC.

i. At this point, to confirm that cells have adhered to the micropattern, gently tap the sides of the coverslip and view the micropatterns using a microscope. If cells have adhered properly, the micropatterned areas should be quite obviously enriched for adherent cells, while cells will be seen to move readily across unpatterned areas.

f. For each well independently: use a P1000 pipettor to gently aspirate medium from the well and gently wash 2-3 times with 300 μL of 1X PBS. PBS should be added gently to either a corner, or along the walls, of each well. Between each wash, be sure to assess adhesion under the microscope to determine if additional washes are necessary.

i. Note: Aspirating with a P1000 pipettor is strongly recommended, as aspirating with a vacuum pump has a higher likelihood of removing cells from micropatterns. Additionally, PBS or culture medium should never be added directly on top of the micropatterns as this is almost guaranteed to remove large numbers of cells from the micropatterns.

g. Once all washes have been completed, carefully remove any remaining PBS and add your chosen culture medium.

i. Note: Larger micropatterns for gastrulation-modeling permit stable growth for 48-72 hours, depending on culture conditions and initial seeding density. Beyond this time frame, cells begin to overgrow their micropatterns and lose organization. As such, early runs should focus on identifying media conditions and seeding densities that are

appropriate for your chosen timeline. Live cell fluorescence or bright-

field imaging is ideal for these assessments.

3.9.   RESULTS

3.9.1.   UV-Ozone passivation of polymer surfaces allows for micropatterning of mESC populations.

Assembled micropatterned 8-well culture slides were found to facilitate mESC adhesion

and growth within our intended micropattern region without any colonies forming within

unpatterned hydrophobic regions (Fig. 17B). Morphology of cells grown in micropatterns

appeared homologous throughout the population, with cell growth remaining confined to

the micropatterned region for up to 72h after the initial seeding. Beyond 72h of growth,

cells overfilled the micropatterns and began to assume a spherical EB-like structure which

no longer adheres to the surface and enters suspension beyond ≈72h of initial seeding.
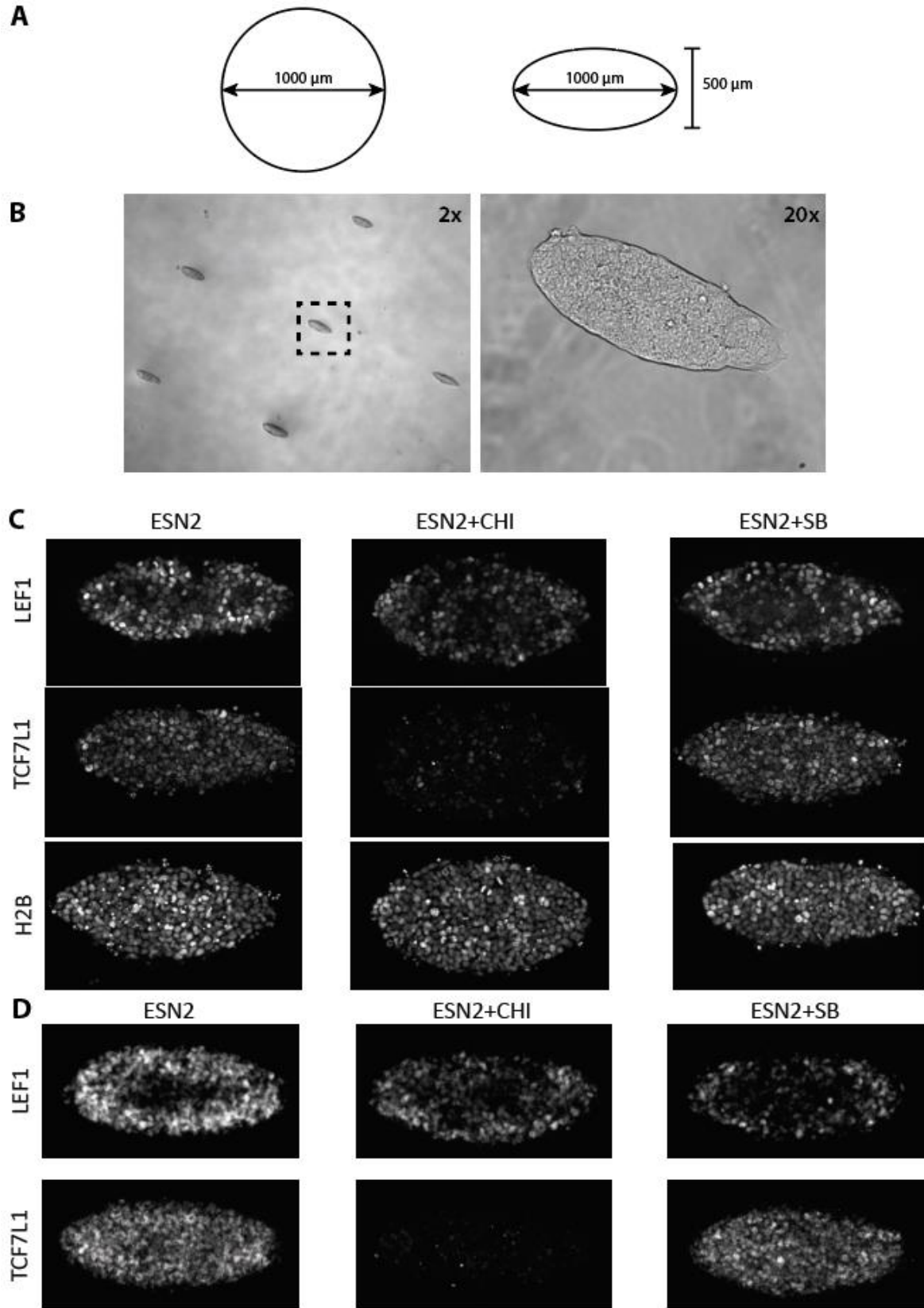
Figure 17. GLOT3-CHmiR cells organize reproducibly when cultured in micropatterns.

Figure 17. (Continued) A) Tested micropatterns include 1000 μm diameter circles, or ellipses 1000 μm in length and 500 μm in width. B) Representative bright field images of GLOT3-CHmiR cells cultured on ellipse micropatterns taken at 2X (left) or 20X (right) magnification 24 hours after seeding. No colonies are observed within unpatterned regions. C) Micropatterned populations were passaged in mESC medium before being micropatterned for 48 hours in N2B27 medium (ESN2). LEF1/TCF7L1 expression patterns were influenced by the addition of 5 μM CHI99021 (ESN2+CHI) or 5 μM SB431542 (ESN2+SB) at the 24-hour mark. D) To demonstrate consistent micropattern organization, eight separate colonies were imaged in each condition, and Z-sum stacks were produced using each channel.

3.9.2. Micropatterned GLOT3-CHmiR cells display consistent ordered TCF7L1/LEF1 expression.

GLOT3-CHmiR cells maintained in mESC conditions and then seeded onto micropatterns and grown for 24h in N2B27 displayed robust LEF1 expression, localized mainly towards the edge of the pattern, while TCF7L1 expression was modestly expressed throughout the full population (Fig. 17C). When grown for 24h in N2B27 + 5 μM CHI, micropatterned populations were found to lose TCF7L1 expression, while LEF1 expression was greatly reduced yet no longer excluded from the centre of the pattern as observed in N2B27 alone (Fig. 17C). The 24h N2B27 + 10 μM SB condition was found to reduce LEF1 expression to CHI-like levels yet restrict it towards tips of the ellipse pattern, while TCF7L1 expression was still global and slightly less intense than in N2B27 alone. These observed patterns become more evident by averaging multiple micropattern images (Fig. 17D).

3.9.3. Micropatterned GLOT3-CHmiR populations distribute more reproducibly with better spatial separation of TCF7L1/LEF1 populations when maintained in N2B27 + 2i conditions.

Micropatterned populations were previously generated from GLOT3-CHmiR cells maintained in mESC conditions (15% FBS, LIF, DMEM) prior to seeding onto micropatterns. When seeded onto ellipse micropatterned surfaces, cells were grown for

48h in N2B27, with 5 µM CHI added at 24h. In this combination of maintenance and seeding conditions, LEF1 expression was moderately expressed within peripheral cells while TCF7L1 was expressed weakly throughout the full population at the 48h mark (Fig. 18B). However, when GLOT3-CHmiR cells were maintained in N2B27 + 2i conditions prior to micropatterning, the expression of TCF7L1/LEF1 was much more robust after 48h of micropatterned growth (Fig. 18C, D). While the distribution of TCF7L1/LEF1 was similar to mESC preconditioned micropatterns, discrete LEF1-only and TCF7L1-only populations were much more apparent (Fig. 18C). However, TCF7L1 expression was lost more completely at the periphery of the pattern, and a "knot" of TCF7L1-only cells was also observed near the tip of ellipse micropatterns, which was not observed when cells were maintained in mESC conditions (Fig. 18D). Additionally, circular micropatterns 1 mm in diameter failed to induce organization of TCF7L1/LEF1 populations when cells were maintained in mESC medium prior to patterning (Fig. 19B). However, cells maintained in N2B27 + 2i consistently organized TCF7L1/LEF1 populations across the periphery of circular micropatterns (Fig. 19C, D). In these micropatterns LEF1 was expressed loosely throughout the centre of the circle, and in a tight band of cells along the periphery of the circle, with a moderate space of LEF1-negaive cells between the two populations. TCF7L1 was expressed predominantly at the periphery of these patterns as well, but in a thicker band of cells interior to the LEF1-positive peripheral band.
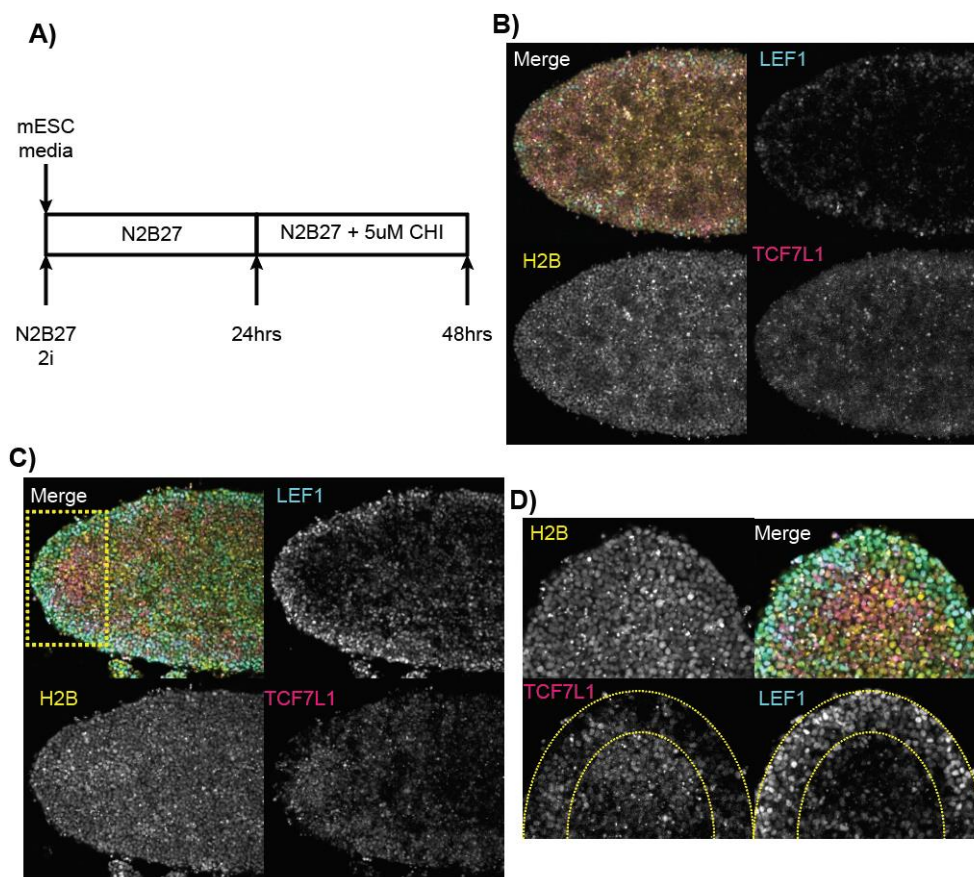
Figure 18. Maintaining cells in N2B27 + 2i conditions greatly improves LEF1/TCF7L1 expression and organization within ellipse micropatterns.

A) Cells cultured in either mESC or N2B27 + 2i conditions for 3 passages were used to seed ellipse micropatterns. Micropatterned populations were then cultured for 24h in N2B27, and then 24h in N2B27 + 5 µM CHI (CHI99021), before images were acquired at the 48hr mark. Representative images were acquired at 20X magnification with mAG-LEF1 (cyan), mKO2-TCF7L1 (magenta), and H2B-miRFP670 (yellow) channels are shown independently and as a merged image for each condition. B) GLOT3-CHmiR cells cultured in mESC conditions before micropatterning. C) GLOT3-CHmiR cells cultured in N2B27 + 2i conditions before micropatterning. D) Magnified image of the boxed region in panel C with dotted lines denoting regions of LEF1/TCF7L1 segregation.
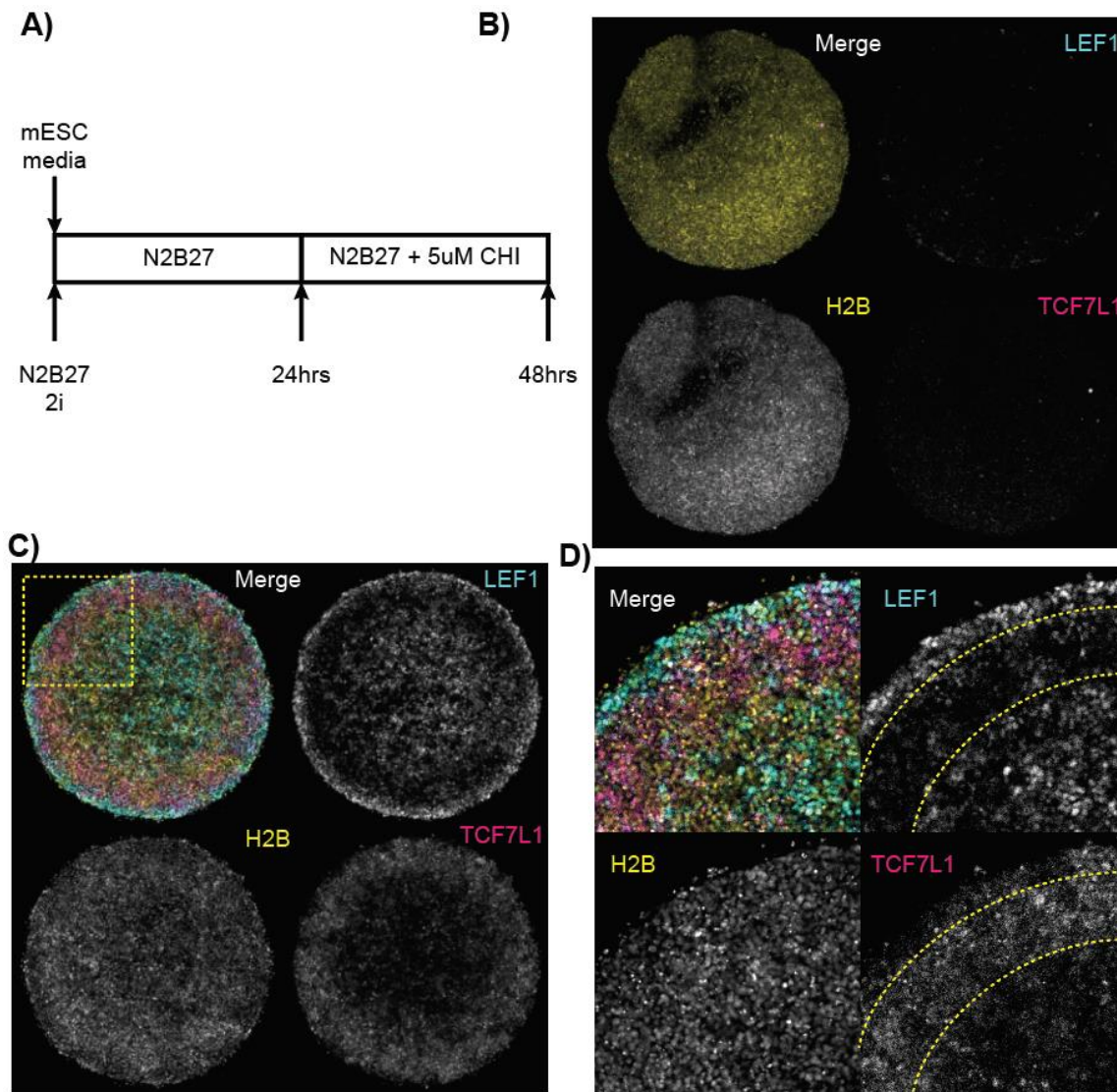
Figure 19. Maintaining cells in N2B27 + 2i conditions greatly improves LEF1/TCF7L1 expression and organization within circle micropatterns.

A) Cells cultured in either mESC or N2B27 + 2i conditions for 3 passages were used to seed circular micropatterns. Micropatterned populations were then cultured for 24h in N2B27, and then 24h in N2B27 + 5 µM CHI (CHI99021), before images were acquired at the 48h mark. Representative images were acquired at 20x magnification with mAG-LEF1 (cyan), mKO2-TCF7L1 (magenta), and H2B-miRFP670 (yellow) channels are shown independently and as a merged image for each condition. B) GLOT3-CHmiR cells cultured in mESC conditions before micropatterning. C) GLOT3-CHmiR cells cultured in N2B27 + 2i conditions before micropatterning. D) Magnified image of the boxed region in panel C) with dotted lines denoting regions of LEF1/TCF7L1 segregation.

3.9.4. Quantitative image analysis reveals consistent micropattern organization across large micropattern arrays.

To quantify micropattern organization across different culture conditions, CellProfiler (McQuin et al., 2018) was used to define X/Y coordinates to all imaged nuclei, and a custom Python pipeline was used to represent all identified nuclei from all imaged micropatterns on a single graph (Figs. 20, 21). Stratifying LEF1/TCF7L1 mean intensity across quantiles allowed us to correlate nuclear LEF1/TCF7L1 expression with pattern organization. Representation of first quantile nuclei demonstrates that very low-level expression of LEF1/TCF7L1 can be observed in all regions of the micropattern (Fig. 20-Q1, 21-Q1). The low fluorescence intensity of these nuclei, however, may be a product of autofluorescence caused by the depth of cells present, or the micropattern substrate itself. Second quantile nuclei reveal a consistent, if slightly noisy, pattern of LEF1/TCF7L1 localization within either micropattern with a considerable portion found to be positive for both LEF1/TCF7L1 (Fig. 20-Q2, 21-Q2). Finally, the third quantile population reveals that cells most highly expressing LEF1/TCF7L1 organize into discrete regions of the micropattern with minimal overlap (Fig. 20-Q3, 21-Q3). Additionally, stimulation of micropatterned populations with 5 µM CHI appears to favour more rapid and accurate organization of LEF1/TCF7L1 populations. However, 5 µM and 10 µM CHI treatments provided best separation at 72 h.
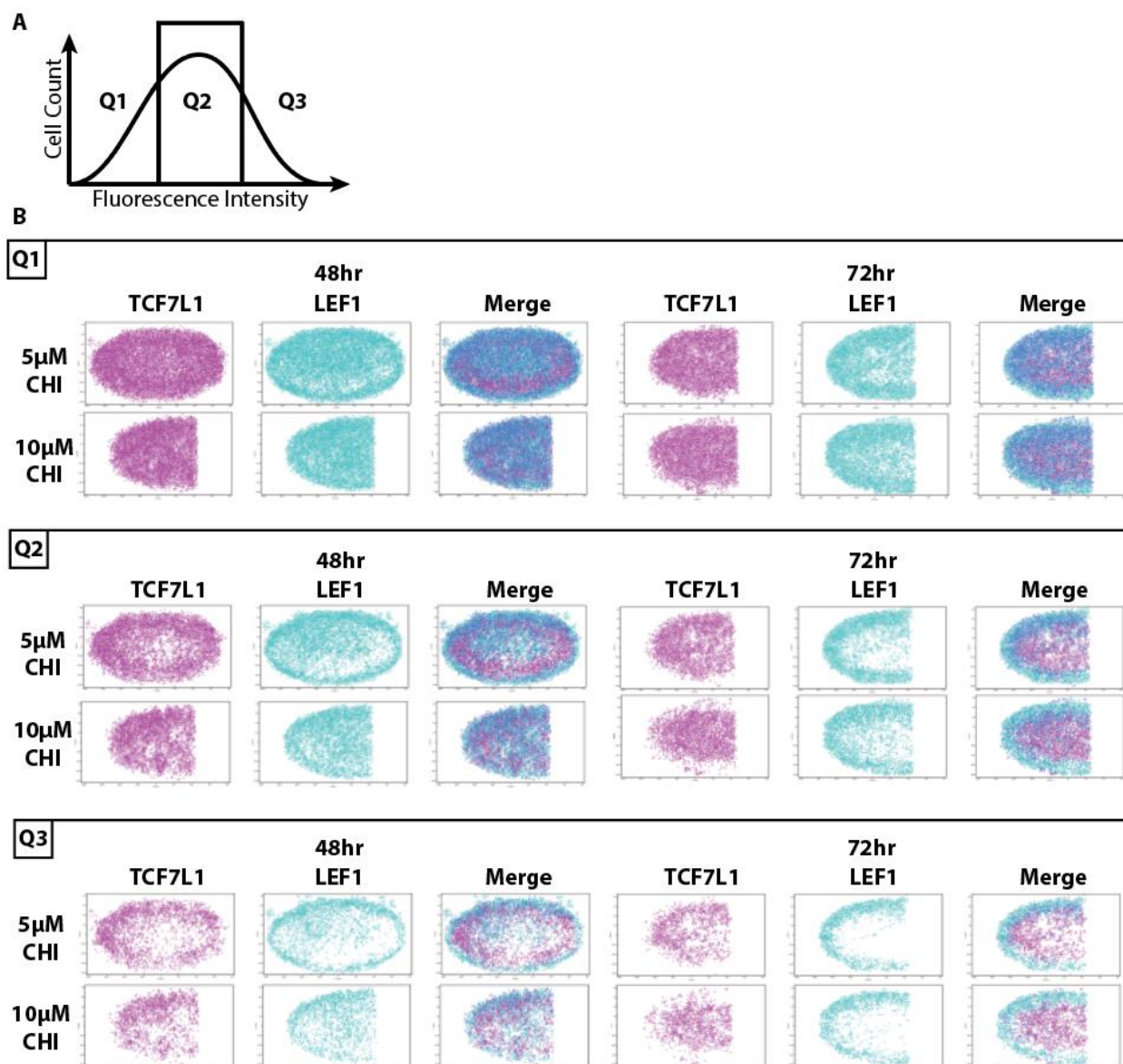
Figure 20. Plotting identified nuclei based on LEF1/TCF7L1 fluorescence intensity better reflects population distributions in ellipse micropatterns.

A) Identified nuclei were stratified into quartiles based on mean nuclear mAG-LEF1 or mKO2-TCF7L1 fluorescence. Q1: The lowest 25% of fluorescent cells. Q2: The mediumn 50% of fluorescent cells. Q3: The highest 25% of fluorescent cells. B) GLOT3-CHmiR cells cultured in micropatterns for 24h in N2B27 and then 48h in N2B27 supplemented with 5 or 10 µM CHI (CHIR99021), were imaged at 48h and 72h. Nuclear fluorescence intensity of mAG-LEF1 (cyan) and mKO2-TCF7L1 (magenta) were recorded for each nucleus and their X/Y coordinates were recorded relative to the centroid of the micropattern population. Nuclear LEF1/TCF7L1 intensities were then stratified into first, second, and third quantiles and plotted, by X/Y coordinate, for each quantile. Image data presented here were acquired from three separate micropatterns in each defined condition and plotted onto a single graph for each condition.
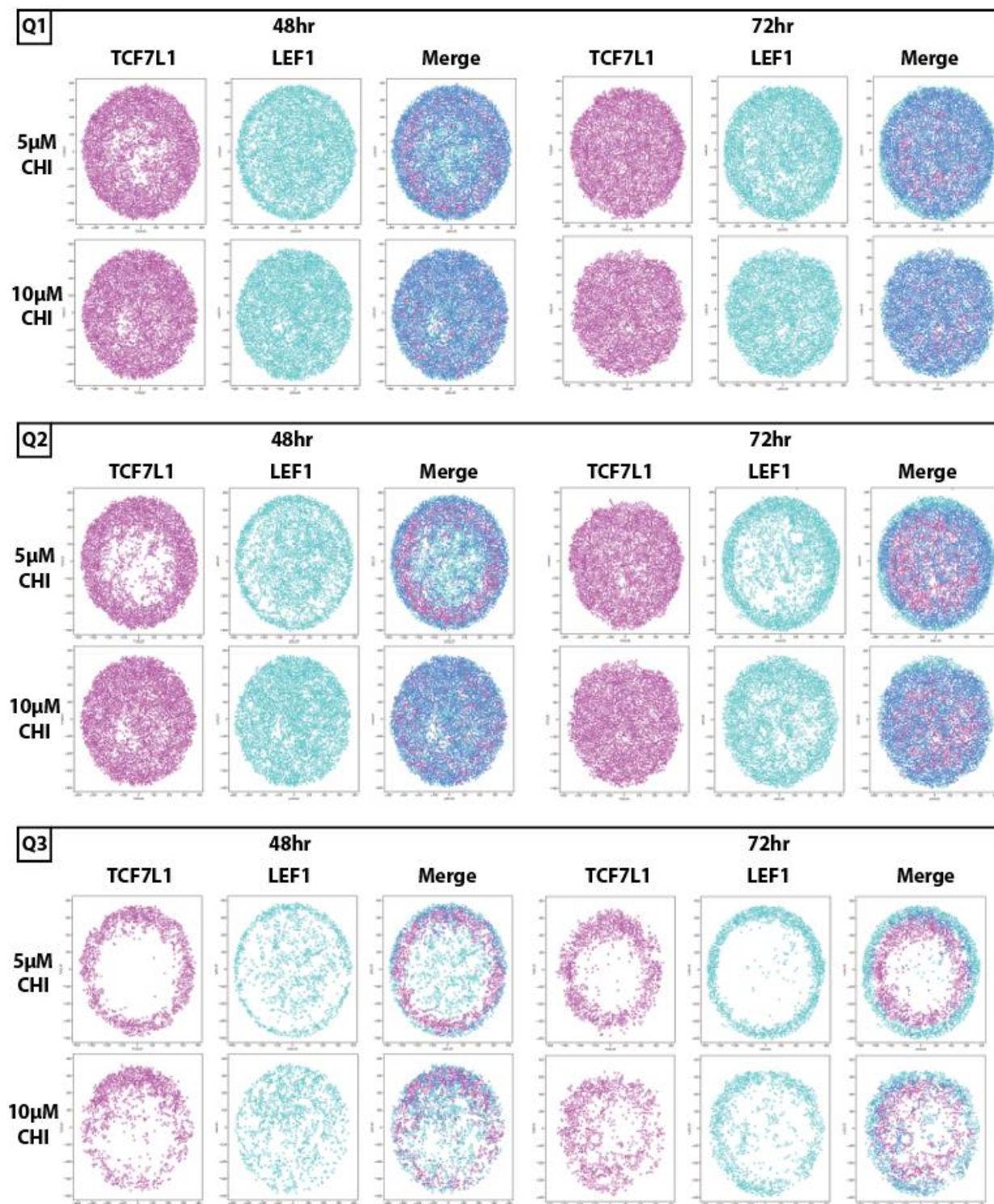
Figure 21. Plotting identified nuclei based on LEF1/TCF7L1 fluorescence intensity better reflects population distributions in circular micropatterns.

Figure 21. (Continued) GLOT3-CHmiR cells cultured in micropatterns for 24h in N2B27 and then 48h in N2B27 supplemented with 5 or 10 µM CHI (CHI99021), were imaged at 48h and 72h. Nuclear fluorescence intensity of mAG-LEF1 (cyan) and mKO2-TCF7L1 (magenta) were recorded for each nucleus and their X/Y coordinates were recorded relative to the centroid of the micropattern population. Nuclear LEF1/TCF7L1 intensities were then stratified into first, second, and third quantiles and plotted, by X/Y coordinate, for each quantile. Image data presented here were acquired from three separate micropatterns in each defined condition and plotted onto a single graph for each condition.

3.10. DISCUSSION

3.10.1. Culture Conditions Affect Micropatterning

The conditions in which cells are maintained once micropatterned will directly affect their differentiation and organization within the micropattern. However, it is important to note that the conditions in which cells are maintained prior to micropatterning can directly affect their ability to respond to these micropattern conditions. To demonstrate this, we have used our previously reported mAG-LEF1/mKO2- TCF7L1/H2B-miRFP670 (GLOT3-CHmiR) mESC cell line capable of reporting the expression of two key Wnt signaling transcriptional regulators, T-cell factor 7 like 1 (TCF7L1) and lymphocyte enhancer factor 1 (LEF1). Wnt signaling is a critical regulator of gastrulation, with LEF1 being expressed throughout the mesoderm and TCF7L1 expressed throughout the ectoderm. By following these two transcription factors, we can identify regions of mesodermal and ectodermal fate commitment in differentiating populations. We chose to maintain these GLOT3-CHmiR cells in either mESC or N2B27 + 2i conditions prior to micropatterning them in a common culture condition. While cells maintained in mESC medium could display weak LEF1/TCF7L1 expression and organization, the cells maintained in N2B27 + 2i medium had considerably increased LEF1/TCF7L1 expression and organization (Figs. 17-19). However, other labs investigating early trilineage differentiation on similar micropattern

culture substrates have found that priming mESCs towards an epiblast-like stem cell (EpiSC) state prior to micropatterning produces more consistent patterning (Morgani et al., 2018). Similar preconditioning protocols could be used with our GLOT3-CHmiR cell line to optimize organization within micropatterned areas. Additionally, while our micropattern culture protocol used small molecule inhibitors to induce Wnt activation, most micropatterning protocols make use of recombinant ligands such as Wnt (Martyn et al., 2018; Morgani et al., 2018). In micropatterned hESC populations Wnt and Nodal signalling ligands have been found to be produced by the micropatterned cells to induce organization within the micropattern (Martyn et al., 2018). As such, use of CHI in our system could bypass these self-organizing networks and induce a global artificial Wnt-ON state, delaying or impeding organization. While our system appears most ordered at the 72-hour mark, other systems have observed similar levels of organization by the 24- or 48-hour marks (Deglincerti et al., 2016; Martyn et al., 2019; Nemashkalo et al., 2017). As such, preconditioning and micropattern culture conditions will be a primary point of optimization in future efforts.

3.10.2. Our micropattern platform allows for robust image analysis and reproducible LEF1/TCF7L1 organization.

The majority of micropatterning publications have relied upon the use of immunofluorescent staining to define regions of lineage commitment (Deglincerti et al., 2016; Martyn et al., 2019; Morgani et al., 2018; Nemashkalo et al., 2017). While these efforts have been foundational in establishing micropatterns as a model system for gastrulation, IF staining only provides a snapshot of these developmental decisions. By contrast, the use of our GLOT3-CHmiR cell line with our micropattern platform will allow us to perform time-course live cell imaging to track LEF1/TCF7L1 expression and

exchange as cells spontaneously organize in our micropatterns (Fig. 22A). This will allow us to identify key points of LEF1/TCF7L1 co-expression or separation, allowing us to determine ideal sample collection times for our chosen downstream experiments. Additionally, *in vivo* studies describing LEF1 and TCF7L1 expression patterns during gastrulation relied upon IF and in situ hybridization (ISH), which impose similar limitations (Merrill et al., 2004; Van Genderen et al., 1994). While it is well understood that LEF1-positive mesodermal cells arise from TCF7L1-positive ectodermal cells, we may be able to capture this event for the first time in live cells by using our endogenous fluorescence system. Additionally, Wnt signaling activity has been shown to oscillate in intensity during mesodermal tail segmentation in the mouse (Sonnen et al., 2018). As this work was done using a Wnt reporter, our system may be able to capture LEF1/TCF7L1 expression oscillation during our time course. However, capturing and quantifying these changes will require appropriate image and data processing pipelines.

The CellProfiler and Python pipelines described in this chapter have been designed for processing small image batches but can be easily scaled up for time-course image sets. To analyze our images we have produced a CellProfiler pipeline to identify nuclei, assign their X/Y position within the image, and quantify their mean LEF1/TCF7L1 fluorescence intensity. As CellProfiler is designed for high-throughput imaging applications, our existing pipeline can be adjusted to accommodate larger time-course imaging sets, while our existing Python pipeline will only need to be adjusted to work with larger batches of image data. Once optimized, this pipeline will allow us to rapidly identify time points at which LEF1/TCF7L1 separation is most ideal for our downstream assays.

3.10.3. CUT & Tag analysis of micropatterned populations will allow us to characterize WRE occupation by LEF1/TCF7L1 in unique populations.

To investigate WRE occupation in distinct LEF1-only and TCF7L1-only populations generated by our micropatterning platform we will make use of the recently described Cleavage Under Targets and Tagmentation (CUT & Tag) (Kaya-Okur et al., 2019). This technique is a hybridization of Cleavage Under Targets and Release Using Nuclease (CUT & RUN) (Skene and Henikoff, 2017) and Assay for Transposase-Accessible Chromatin using sequencing (ATAC-seq) (Buenrostro et al., 2013). By gently permeabilizing live cells and incubating them with a primary antibody against a transcription factor of interest, this interaction can be amplified by secondary antibodies, and finally targeted with a Protein A fused Transposase 5 (pA-Tn5) preloaded with sequencing adapters. Through recognition of the primary and secondary antibodies by Protein A, the pA-Tn5 fusion protein is able to efficiently integrate sequencing adapters in a region of roughly 80 bp centred upon the bound transcription factor. These fragmented regions can then be enriched from purified DNA and analyzed using standard high-throughput sequencing approaches. The main advantages of CUT & Tag are its high sensitivity, with nearly twice the peak calling efficiency of CUT & RUN or ATAC-seq at low read counts, and its ability to be used with single-cell platforms or with as few as 60 000 cells per run (Kaya-Okur et al., 2019). These qualities make CUT & Tag ideal for investigating the occupation of WREs within well segregated LEF1-only and TCF7L1-only populations.

By performing live cell imaging on our micropatterned GLOT3-CHmiR cells, we can optimize culture conditions to generate concentric LEF1-only and TCF7L1-only populations, similar to those observed in our previous optimization efforts (Fig. 18, 19).

As our current micropattern designs have been found to accommodate ≈2000 cells/pattern, with each well holding 25 patterns, we should be able to obtain roughly 50 000 cells/well. These populations can then be gently singularized and processed using CUT & Tag against either LEF1 or TCF7L1. A unique feature of our micropatterned populations is that regions of LEF1/TCF7L1 co-expression have been found to resolve into distinct regions of LEF1-only and TCF7L1-only populations (Fig. 20, 21). Not only does this provide us with pure populations, but it will also allow us to capture populations before and after TCF7L1/LEF1 exchange has occurred (Fig. 22B). This important distinction will allow us to make novel insights into how WRE occupation changes as cells change their fate, and to inform further investigations of how WRE-proximal factors change between unique TCF/LEF states.
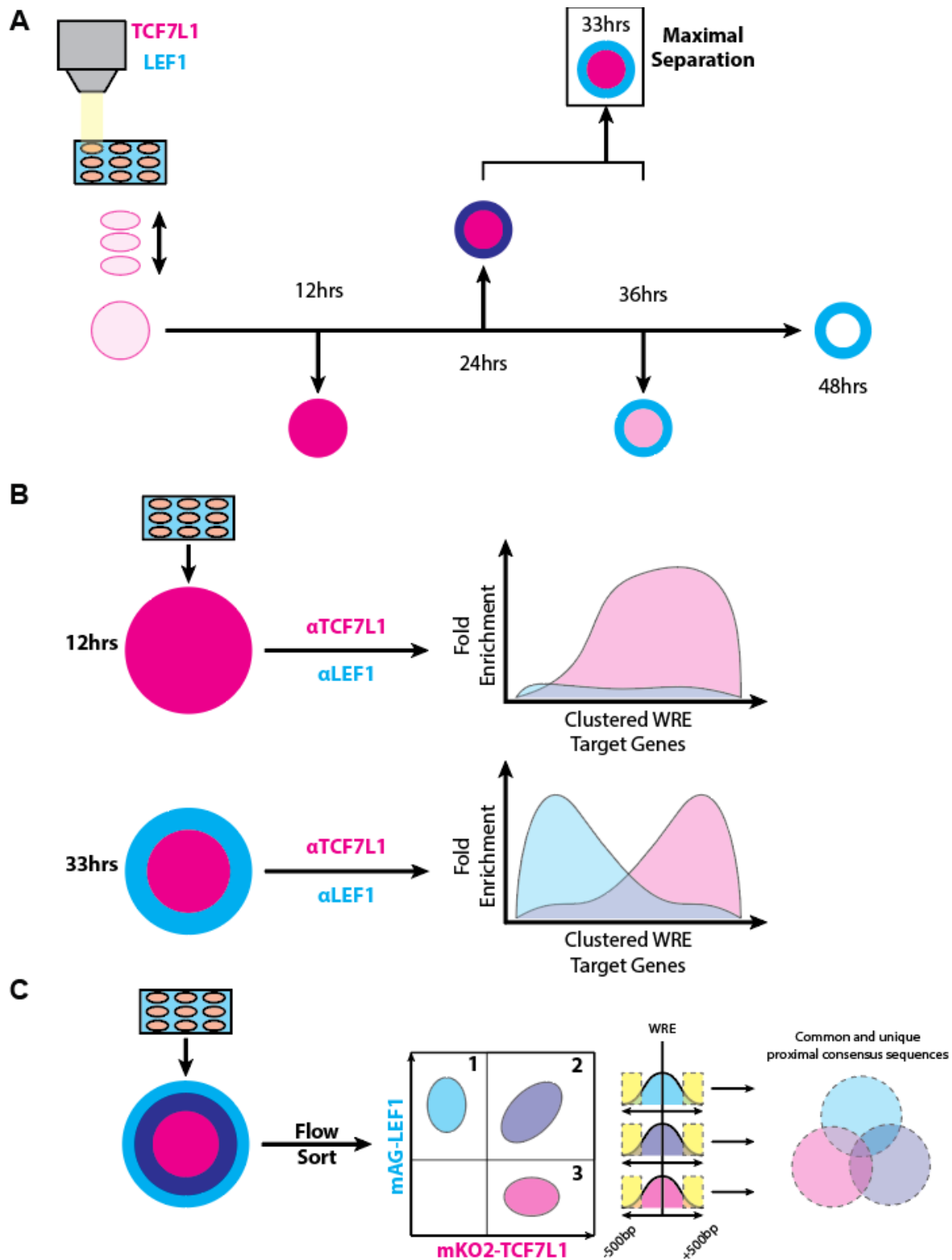
Figure 22. Optimization of culture conditions through live cell imaging will facilitate the isolation of unique LEF1/TCF7L1 populations for future analysis.

Figure 22. (Continued) A) Automated time-course live cell imaging will allow for quantitative image analysis to identify ideal culture time points for desired LEF1 (Cyan) and TCF7L1 (Magenta) separation or co-expression (Blue) within micropatterned surfaces. Images will initially be taken at wide 6-hour intervals, and when an interval or interest has been identified shorter 30 minute intervals will be used to determine an optimal culture time. B) Performing CUT & Tag analysis against LEF1 and TCF7L1 in TCF7L1-only, or segregated TCF7L1-only and LEF1-only populations will allow for the characterization of changes in WRE occupation by either factor before and after exchange occurs. C) The isolation of LEF1-only, TCF7L1-only, and co-expressing population will allow each population to be characterized by flow cytometry to determine how common or unique WRE-flanking transcription factors may affect TCF/LEF exchange.

3.10.4. Assessing micropatterned populations by flow cytometry and ATAC-seq allows for investigation of LEF1/TCF7L1 co-occupation.

Another key feature of our micropatterned populations was the extensive co-expression of TCF7L1 and LEF1 observed as micropatterns underwent spontaneous organization (Fig. 18, 19). While our CUT & Tag approach will provide excellent insight into two unique, yet static, TCF/LEF states, the use of ATAC-seq will allow us to investigate factors co-occupying WREs during this exchange. The use of ATAC-seq will allow us to identify not only TCF/LEF-occupied WREs, but also occupied consensus sequences found proximal to these WREs. By optimizing micropattern culture conditions to produce regions of LEF1-only, TCF7L1-only, and LEF1/TCF7L1 co-expression, we can then sort out these populations by using flow cytometry and characterize each with ATAC-seq (Fig. 22C). By scanning WRE-proximal regions in TCF7L1- and LEF1-dominant states and comparing these to the factors identified in co-expressing populations, we can identify factors which promote or prevent TCF/LEF exchange.

However, a caveat associated with this approach is the successful isolation of fluorescent protein-tagged populations via flow cytometry. To optimize mKO2-TCF7L1 fluorescence

for use with common flow cytometry cubes alternate GLOT3-CHmiR cell lines were produced in which mKO2-TCF7L1 was replaced with mRuby3-TCF7L1 or mScarlet-TCF7L1. Additionally, as our fluorophores are endogenously expressed, commonly used antibody conjugated fluorescent controls may be too bright for use as compensation controls with our endogenous cell lines. To overcome this, individual Rosa-targeted H2B-miRFP670 and H2B-mAG lines were produced, with mRuby3 and mScarlet lines in development. If isolation of these populations by flow cytometry is deemed too difficult, paired-seq can be used to simultaneously perform RNAseq and ATAC-seq on single cells (Zhu et al., 2019). This technique would allow the total population to be characterized at once, with transcriptomic analysis allowing us to confirm LEF1/TCF7L1 status based on relative transcript levels.

3.10.5. Optimization of Micropatterning Method

While a polymer culture substrate is ideal for a simplified fabrication pipeline, it is not as optically ideal as glass. During optimization of our system, we found that images taken in-plane with the polymer substrate produced excessive background, specifically within the micropatterned area (data not shown). While this can be mitigated by limiting the depth of our focal plane on confocal microscopes, it may impede our ability to investigate the basal cells of our micropatterned populations. This specific population is not of concern for our current research objectives, but further optimization can overcome this limitation. The autofluorescence observed in our polymer micropatterns is likely a product of UV/Ozone passivation, as similar levels of autofluorescence were observed when laminin, gelatin, or fibronectin coatings were tested (data not shown). However,

micropatterning publications describing the use of glass substrates report no such autofluorescence (Deglincerti et al., 2016; Kusuma et al., 2017; Nemashkalo et al., 2017).

To optimize glass as a micropatterning substrate we would first need to determine if a pre-coating is required. Glass substrates do not possess the same degree of hydrophobicity found in our polymer substrates (Carpi et al., 2011). As a result, typical PLL-g-PEG pre-coatings and ECM coatings are likely to adhere weakly without a pre-coating to increase adhesion. Commonly used adhesion promoters are **H**exa**M**ethyl**Di**Silazane (HDMS), which must be evaporated in a 120°C oven containing a glass substrate, and Ti Prime (MicroChemicals) which is an organic titanium compound that is applied by spin-coating before a 1-2 minute bake at 120°C. This increased complexity, and equipment requirements, associated with the use of glass culture substrates were deterrents in our initial efforts. However, with our current micropatterning experience, they could potentially be adopted to provide a more optimal imaging substrate.

3.11. MATERIALS AND METHODS

3.11.1. mESC Medium Cell Culture

GLOT3-CHmiR cells were maintained in mESC medium containing high glucose Dulbecco's Modified Eagle's Medium (DMEM), 15% Fetal Bovine Serum (FBS), 2 mM L-glutamine, 1 mM Sodium Pyruvate, 100 µM non-essential amino acids, 0.1 mM 2-mercaptoethanol, and 10^3 units/mL leukemia inhibitory factor (LIF). Cultured cells were passaged every 48h at a 1:6 ratio on 10 cm 0.1% gelatin-coated culture dishes.

3.11.2. N2B27 + 2i Cell Culture

GLOT3-CHmiR cells were maintained in N2B27 made with a 1:1 mix of DMEM/F12 medium and Neurobasal medium containing 2 mM L-glutamine, 1 mM Sodium Pyruvate, 100 µM non-essential amino acids, 0.1 mM 2-mercaptoethanol, 1X N2 supplement, and 1X B27 supplement, with 3 µM CHI99021 and 1 µM PD035901 added prior to use in culture. Cultured cells were passaged every 48h at a 1:6 ratio on 10 cm 0.1% gelatin-coated culture dishes.

3.11.3. Live Cell Imaging

Live cell images were obtained by using a 63X oil immersion lens on a laser scanning confocal microscope (LSM-880, Zeiss). Mono-Azami Green (mAG) was stimulated by a 488nm laser and mono-Kusabira Orange 2 (mKO2) was stimulated by a 561nm laser.

3.11.4. Image Processing and Analysis

Multichannel images acquired by the microscope were converted to single channel TIFFs using FIJI, and then processed using a custom CellProfiler pipeline to identify nuclei based on H2B-miRFP670 fluorescence, assign X/Y coordinates based on nuclear centroids, and quantify mAG-LEF1 and mKO2-TCF7L1 mean nuclear fluorescence. The resulting data were then processed by using a custom Python script to generate nuclear position plots.

CHAPTER 4. MITOTIC TURBOID IDENTIFIES NANOG AND LEF1 AS NOVEL BOOKMARKING FACTORS WHICH REMAIN ASSOCIATED WITH TRANSCRIPTION AND TRANSLATION MACHINERY IN MITOTIC CHROMATIN.

4.1.   ABSTRACT

Mitotic cell division ensures that resulting daughter cells inherit identical genetic material. However, asymmetric cell fates can result from these divisions and are indeed required for the successful patterning and maintenance of tissues throughout the body. One of the most prominent mechanisms found to drive these asymmetries is mitotic bookmarking. In this process, lineage-specific transcription factors have been shown to remain associated with specific genes during mitosis, whereupon they maintain enhancer-promoter loops and associated transcriptional machinery to facilitate basal transcription throughout mitosis. By contrast, non-bookmarked genes have been shown to lose enhancer-promoter loops and maintain little to no transcriptional activity. While this bookmarking activity has been observed by a variety of key transcription factors, including Oct4, Esrrb, and Sox2, characterization of bookmarking activity is technically difficult, as it relies upon mitotic ChIP-Seq analysis. To improve the rate of bookmarking factor detection we performed mitotic TurboID using an H2B-TurboID fusion protein to profile the full interactome of mitotic chromosomes in Wnt-activated mESCs. While a variety of well-established bookmarking factors were identified by mitotic H2B-TurboID, we also observed the novel mitotic retention of Nanog and LEF1. Through fusion of LEF1 and Nanog with TurboID we were able to identify considerable overlap between their mitotic interactomes and the mitotic interactomes of TurboID fusions with well-known bookmarking factors. Intriguingly, the selective mitotic association with transcription and translation machinery was common to all TurboID-fused bookmarkers tested, including

LEF1 and Nanog. These findings suggest not only that LEF1 and Nanog possess bookmarking activity, but that bookmarking factors maintain translation in addition to the transcription of bookmarked targets. Additionally, mutational analysis of LEF1 revealed that sumoylation at Lys-267 is required for its mitotic stability.

4.2.   INTRODUCTION

Asymmetrical cell division is essential for the proper patterning of various tissues throughout the body, allowing stem cell niches to retain their identity while producing single differentiated daughter cells over multiple divisions (Ng and Alexander, 2017; Qi and Chen, 2015). While there are multiple mechanisms of asymmetry that have been identified, including asymmetric cell membrane (Paridaen et al., 2013) or transcription factor inheritance (Fuentealba et al., 2008), mitotic bookmarking appears to be a commonly employed mechanism. During mitosis the majority of transcription factors are ejected from mitotic chromatin, rendering them inactive. However, "bookmarking" transcription factors remain associated with their gene targets throughout mitosis, allowing them to maintain enhanceosomes and enhancer-promoter loops at their bound genes (Festuccia et al., 2019; Kadauke et al., 2012). Additionally, RNA polymerase II has been shown to remain associated and active at these bookmarked loci (Palozola et al., 2017). While typical non-bookmarked genes lose their assembled enhancers and halt transcription as mitotic chromatin compacts, bookmarked genes retain a basal level of transcription, and resume maximal transcription significantly faster upon mitotic exit, affording these genes a competitive advantage in establishing cellular fate (Festuccia et al., 2019; Kadauke et al., 2012). As such, bookmarking factors play a critical role in cell

fate maintenance, and understanding the mechanisms guiding their recruitment and retention is critical to understanding cell fate determination.

However, mitotic chromatin is a highly complex cellular compartment that is difficult to isolate or investigate by using traditional techniques (Maeshima et al., 2020b). As interphase chromatin compacts, the majority of the genome becomes heterochromatic and non-bookmarking transcription factors are ejected from their bound enhancer or promoter regions (Gibcus et al., 2018a). As compaction continues, chromatin is then assembled into nested loops around a core of condensin I and II complexes (Gibcus et al., 2018a).

To prevent individual chromosomes from condensing into a single disordered mass, MKi67 and other nucleolar proteins form a surfactant-like layer around each chromosome termed the perichromosomal layer (Booth and Earnshaw, 2017; Cuylen et al., 2016). This region is highly charged, and accounts for roughly 40% the chromosomal volume and 33% of chromosomal protein mass (Booth et al., 2016).

It is the stratified nature of mitotic chromosome that confounds traditional techniques used to identify mitotic chromatin-associated proteins. Immunofluorescence crosslinking techniques are impeded by the perichromosomal layer, rendering IF results unreliable and inconsistent (Festuccia et al., 2017). The highly charged nature of the perichromosomal layer, and its tight adherence to mitotic chromatin, make it exceptionally difficult to isolate from mitotic chromatin in proteomic analyses as well. Additionally, while live cell fluorescence imaging bypasses crosslinking, it cannot distinguish between mitotic

association and true specific gene bookmarking, requiring technically difficult mitotic ChIP-seq validation assays (Deluz et al., 2016; Festuccia et al., 2016; Wong et al., 2014).

Taken together, these complications have greatly slowed the investigation of mitotically associated transcription factors. To overcome these limitations, we have optimized a mitotic TurboID protocol for the rapid proteomic investigation of transcription factors and nucleosome components associated with mitotic chromatin.

TurboID is a genetically engineered derivative of the BioID promiscuous biotin ligase, capable of saturating proximal interactors with only a 45-minute biotin pulse (Branon et al., 2018), while previous BioID versions have required an incubation time of 18 – 24 hours (Roux et al., 2018). This reduced incubation time has allowed us to investigate chromatin-associated interactions in nocodazole-arrested metaphase mouse embryonic stem cell (mESC) populations, which would otherwise become highly cytotoxic over the 24-hour incubation period required by traditional BioID enzymes.

By transiently expressing an H2B-TurboID fusion protein, we were able to capture interactions throughout the volume and surface of mitotic chromosomes, capturing several well-defined bookmarking transcription factors, as well as Nanog and LEF1 as novel bookmarking factors. Additionally, our H2B-TurboID data suggests that transcriptional and translational machinery are greatly enriched upon mitotic chromatin, and not just associated with the perichromosomal layer non-specifically, as previously thought. Subsequent TurboID fusions with Oct4, Esrrb, Rbpj, Nanog, and LEF1 were able to capture mitotic associations with, not only enhanceosome and transcription factors, but also translation-associated factors, suggesting that bookmarking factors not only maintain

transcription but also prime translation of bookmarked genes. The novel bookmarking activity of LEF1 was further characterized by directed mutation analysis, suggesting that mitotic LEF1 is selectively stabilized by K267 sumoylation and constitutively degraded in an apparently TLE3-dependent manner when this site is ablated. The findings presented here demonstrate that mitotic TurboID is a robust, yet technically straightforward, approach to rapidly identifying and characterizing mitotically associated proteins.

4.3.   RESULTS

4.3.1. H2B-TurboID Identifies Proximal Interactors in Asynchronous and Metaphase mESCs

To detect nucleosome-associated proteins in both interphase and metaphase, we chose to tag H2B with TurboID. To identify H2B interactors, a transient expression vector was generated containing a CAG-driven H2B-TurboID fusion protein, followed by a P2A self-cleaving peptide and EGFP to serve as a transfection reporter. Control vectors containing a CAG-driven TurboID-P2A-EGFP cassette were also generated to serve as an experimental control by identifying non-specific TurboID interactors. Wild-type E14Tg2a mESCs were then transfected with either vector, cultured for 48 hours in EB medium + 5 µM CHI, and then pulsed with 500 µM Biotin for 45 minutes before sample collection (Fig. 23A). Metaphase populations (M-phase) were collected after adding 150 ng/mL Nocodazole 7 hours prior to biotin addition and collection, while asynchronous populations (A-phase) were kept in EB + 5 µM CHI for the full 48h culture period. Proximal H2B interactors from M or A populations were then identified through mass spectrometry. Putative protein-protein interactions in either condition were determined by using SAINT (Significance Analysis of INTeractome). Comparison of peptide counts among these interaction lists revealed that while 263 interactors saw a 2-fold increase in peptide counts

in interphase conditions, and 203 interactors saw a 2-fold increase in peptide counts under metaphase conditions, 497 interactors were found to exhibit no significant change in association between either condition (Fig. 23B). Our H2B-TurboID fusion protein was confirmed to successfully integrate into nucleosomes and mitotic chromatin by its ability to selectively enrich for mitotic chromatin markers such as condensin components, chromatin scaffolding factors, and topoisomerases in M-phase samples (Fig. 23D). Similarly, Sumo2 peptides were exclusively identified, and chromatin remodeling factors were significantly reduced, in M-phase samples (Cubenas-Potts et al., 2015). Interestingly, a considerable number of transcriptional machinery components remained associated with H2B-TurboID during metaphase, and translation-associated factors were selectively enriched in M-phase samples. Finally, while a number of known bookmarking factors were found to remain associated with mitotic H2B-TurboID, both NANOG and LEF1 were also found to remain associate with mitotic chromatin, which has not yet been reported.
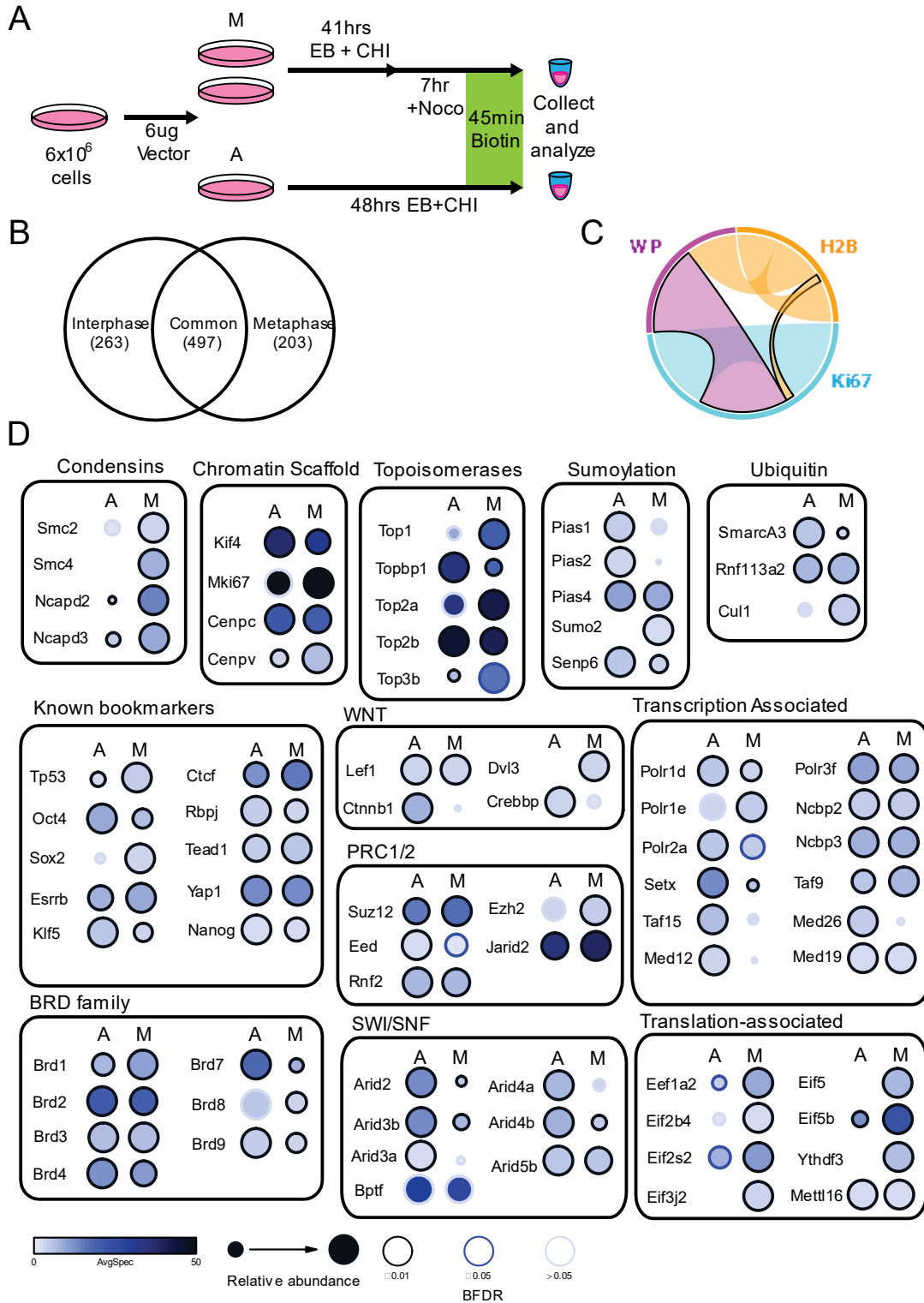
Figure 23.   Proximal H2B-TurboID interactors identified in asynchronous and metaphase populations that are unique from whole mitotic proteome approaches.

Figure 23. (Continued) A) Overview of asynchronous (A) and metaphase (M) sample preparation. Wild-type E14Tg2a mESCs are transfected with a chosen transient expression vector and grown for 48 hours in EB + 5 μM CHI. Mitotic samples are arrested for 7 hours in prometaphase using 150 ng/mL nocodazole. Both samples are pulsed with 500 μM biotin for 45 minutes before collection, lysis, and analysis. B) Distribution of identified H2B-TurboID interactors, based on peptide counts, found to be enriched in asynchronous interphase populations (A >= 2*M), metaphase populations (M >= 2*A), or common to both conditions. D) Dot plot of H2B-TurboID interactors identified after 48 hours of transient vector expression.

4.3.2. Mitotic H2B-TurboID Detects Few Perichromosomal Components

To determine if our identified H2B-TurboID interactors were consistent with known mitotic chromatin components, our mitotically enriched interactors were compared to mitotic interactors identified by whole-proteome mitotic analysis and MKi67 ChIP-MS data sets (Fig. 23C). Our whole proteome (WP) data set was taken from mitotically enriched factors identified by Ginno et al., where a sucrose density gradient was used to isolate a mitotic chromosome fraction from cell lysates (Ginno et al. 2018). This list was then compared to a list of mitotically enriched factors identified by MKi67 ChIP-MS reported by Sobecki et al. (Sobecki et al. 2016). While 43% of MKi67 ChIP-MS targets were also identified by WP, only 14% of targets were identified by H2B-TurboID, demonstrating nearly a 4-fold reduction in contamination by perichromosomal components.

4.3.3. Mitotic TurboID Using Mitotically Associated Transcription Factors

To investigate the interactome of mitotically enriched transcription factors, TurboID fusions with LEF1, OCT4, NANOG, RBPJ, and ESRRB were generated. Mitotic association of our chosen transcription factors was confirmed by generating EGFP fusions of each factor and performing live cell fluorescence imaging (Fig. 24A). All products displayed mitotic enrichment. Transient expression vectors for each of the

chosen transcription factors were then transfected into E14Tg2a mESCs and collected under conditions identical to those used for our previous H2B-TurboID analysis. Protein-protein interactions for both asynchronous (A) and metaphase (M) conditions were once again determined by using SAINT. Bait-bait comparison of interaction profiles revealed that the interaction profiles of LEF1 and NANOG cluster strongly as independent A/M sample pairs (Fig. 24B). However, while OCT4 and ESRRB A/M interactomes cluster together, RBPJ clusters most strongly with H2B A/M samples (Fig. 24B). To further investigate these common interactions between all samples, a chord diagram was generated using significant (BFDR < 0.05) interactors from all A/M samples (Fig. 24C).

Most strikingly, RBPJ was found to share 76% of its interactome (573/748) with H2B, while all other transcription factors have only ≈60% of their interactions in common with H2B interactors. Additionally, while the other selected transcription factor-TurboID fusions had 70-80% of their interactions in common with each other, RBPJ only displayed ≈50% of its interactions in common with other transcription factors. Very similar trends are also observed when looking at mitotically enriched (M >=2*A) or asynchronous-enriched (A>=2*M) interactors. However, a considerable portion of these interactions appear to be unique to each factor (Fig. 24D).
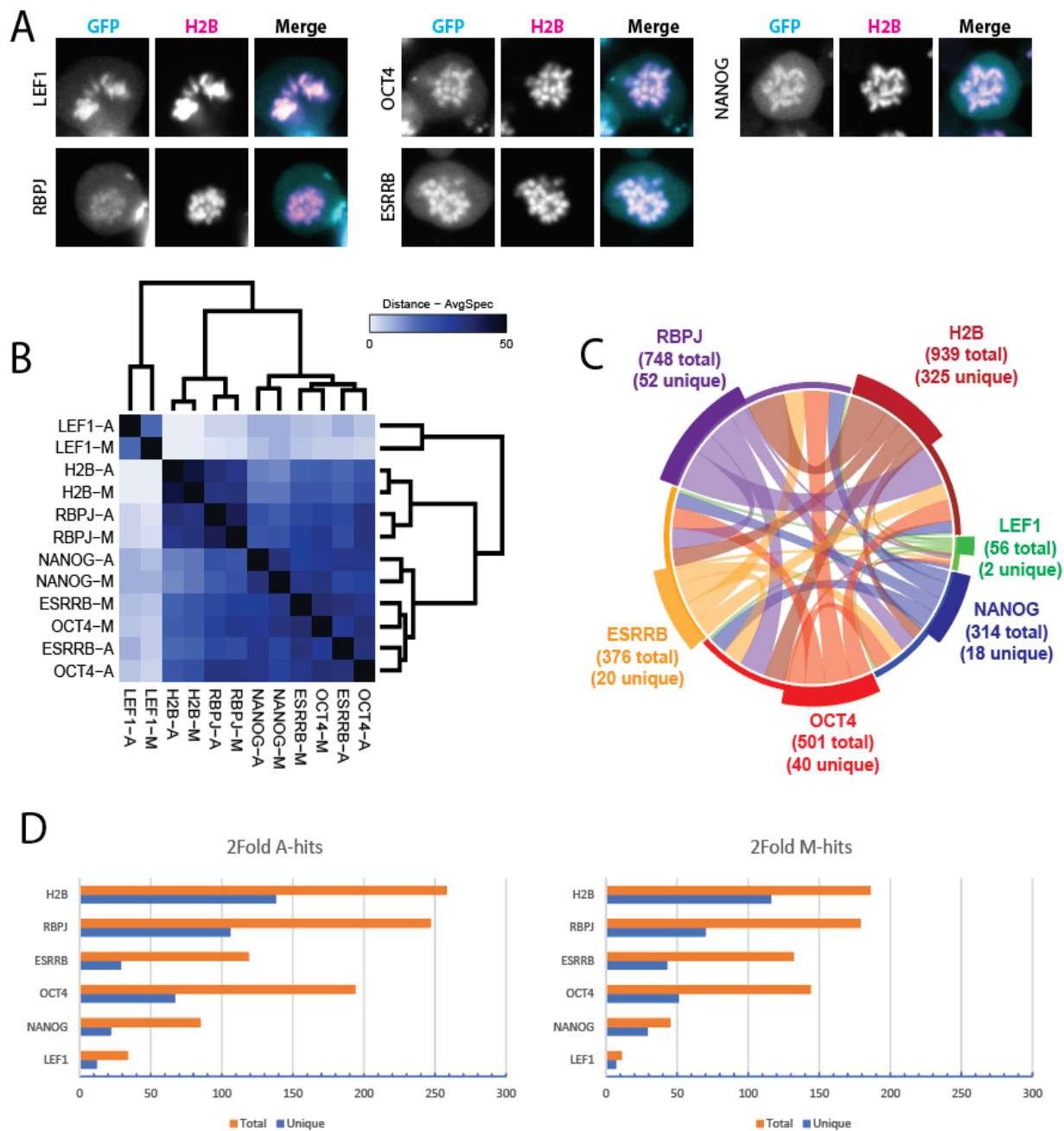
Figure 24. Mitotically enriched transcription factors share more common interactions with each other than H2B.

A) Live cell fluorescence imaging of mESCs transiently transfected with EGFP-tagged OCT4, ESRRB, RBPJ, NANOG, or LEF1 expression vectors. Transient expression vectors also expressed H2B-mKO2 to mark mitotic chromatin.

Figure 24. (Continued) B) Bait vs bait hierarchical comparison of identified factors among TurboID asynchronous (A) and metaphase (M) data sets. C) Chord diagram of all significant interactions (BFDR <= 0.05) identified in A and M conditions for each TurboID fusion. D) Unique and total identified A-enriched (A >= 2*M peptide count) and M-enriched (M >= 2*A peptide count) interactors in each sample.

4.3.4.   NANOG, OCT4, ESRRB, RBPJ, and H2B Possess Unique Interactomes

Gene ontology (GO) analysis was performed on lists of identified interactors from each condition to determine if TurboID fusions with H2B or transcription factors (LEF1, NANOG, OCT4, ESRRB, RBPJ) recognized unique interactomes in asynchronous or metaphase populations. As would be expected from transcription factors during interphase, a majority of GO terms were associated with transcription or epigenetic regulation (Fig. 25A). Asynchronous H2B-associated GO terms were primarily associated with histone acetylation or methylation, which would be expected of heterochromatic regions, where H2B is expected to reside (Fig. 25A). Interestingly, M-phase transcription factor GO terms are primarily associated with RNA polymerase II binding, and even ribosome binding (Fig. 25B). While M-phase H2B GO terms do include helicase activity, that would be expected in compacting mitotic chromatin, the majority of enriched GO terms are associated with transcription and translation associated processes (Fig. 25B). Together, these findings demonstrate that M-phase and A-phase interactomes are unique for both H2B and our chosen transcription factors.
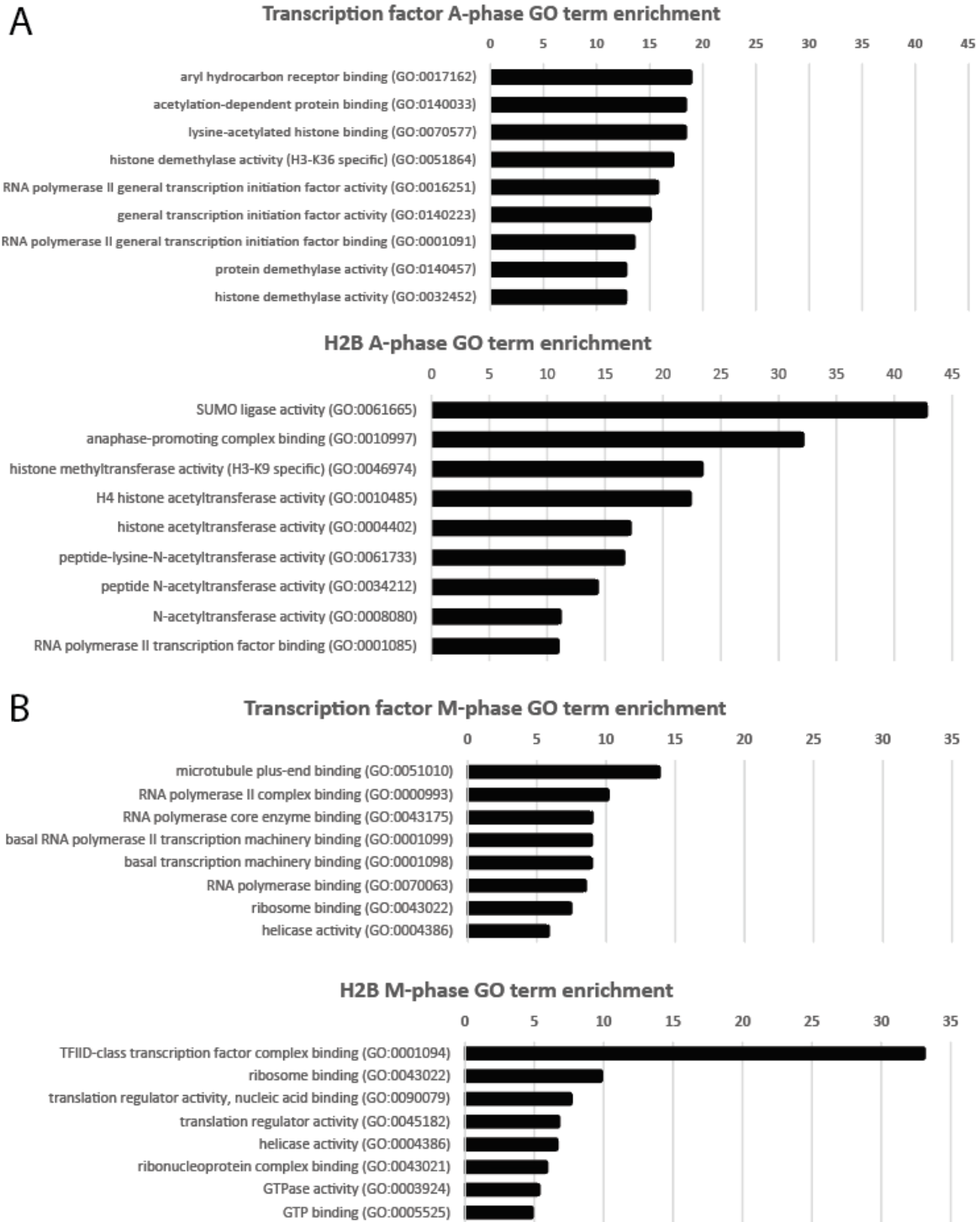
Figure 25. H2B and bookmarking transcription factors have unique interactomes in both asynchronous and metaphase populations.

Figure 25. (Continued) Interaction lists of mitotically (M >= 2*A peptide counts) or asynchronously (A >= 2*M) enriched interactors from H2B alone, or all pooled transcription factors, were assembled. GO term analysis was then performed on A) asynchronous or B) metaphase interaction lists, with the top 8 GO-terms based on fold enrichment being displayed.

4.3.5. Mitotically Enriched Transcription Factors and Enhanceosome Components

Direct comparison of interactor peptide counts between A and M conditions among our assessed factors revealed that there are key regulatory components common among most factors. While a variety of E3 ubiquitin and sumo ligases can be found to associate With H2B, ubiquitin ligase, Trim33, and Sumo ligase, Pias4, were found to be common interactors with most factors (Fig. 26A). While it is logical that H2B associates with a variety of nucleosome remodeling factors in both interphase and metaphase, as chromatin remains dynamic in both contexts, it is interesting that our assayed transcription factors remain associated with remodeling complexes during metaphase. All assayed transcription factors remain associated with core SWI/SNF complex components Arid1a/b during metaphase (Fig. 26B). As the SWI/SNF complex is a core enhanceosome component, this may suggest that our assayed transcription factors retain enhanceosome structure during metaphase. Consistent with this observation, our assayed transcription factors mitotically associate with Yeats2, which specifically binds histone H3 crotonylated Lys-27, a marker of active promoters and enhancers.

In further support of our GO analysis, all assayed transcription factors mitotically associate with Ccnt1 and Ythdf3. Ccnt1 is an activator of p-TEFb, promoting transcript elongation, while Ythdf3 binds N6-methyladenosine (m^6A)-containing RNAs and

promotes RNA translation efficiency. Additionally, all assayed transcription factors interact with a variety of Wnt enhanceosome components (Fig. 26D). While CTNNB is identified by H2B only in interphase, all transcription factors associated with β-catenin during metaphase. Interestingly, while TCF7 and TCF7L1 are recognized only during interphase, LEF1 remains associated with H2B, Nanog, and RBPJ during metaphase.
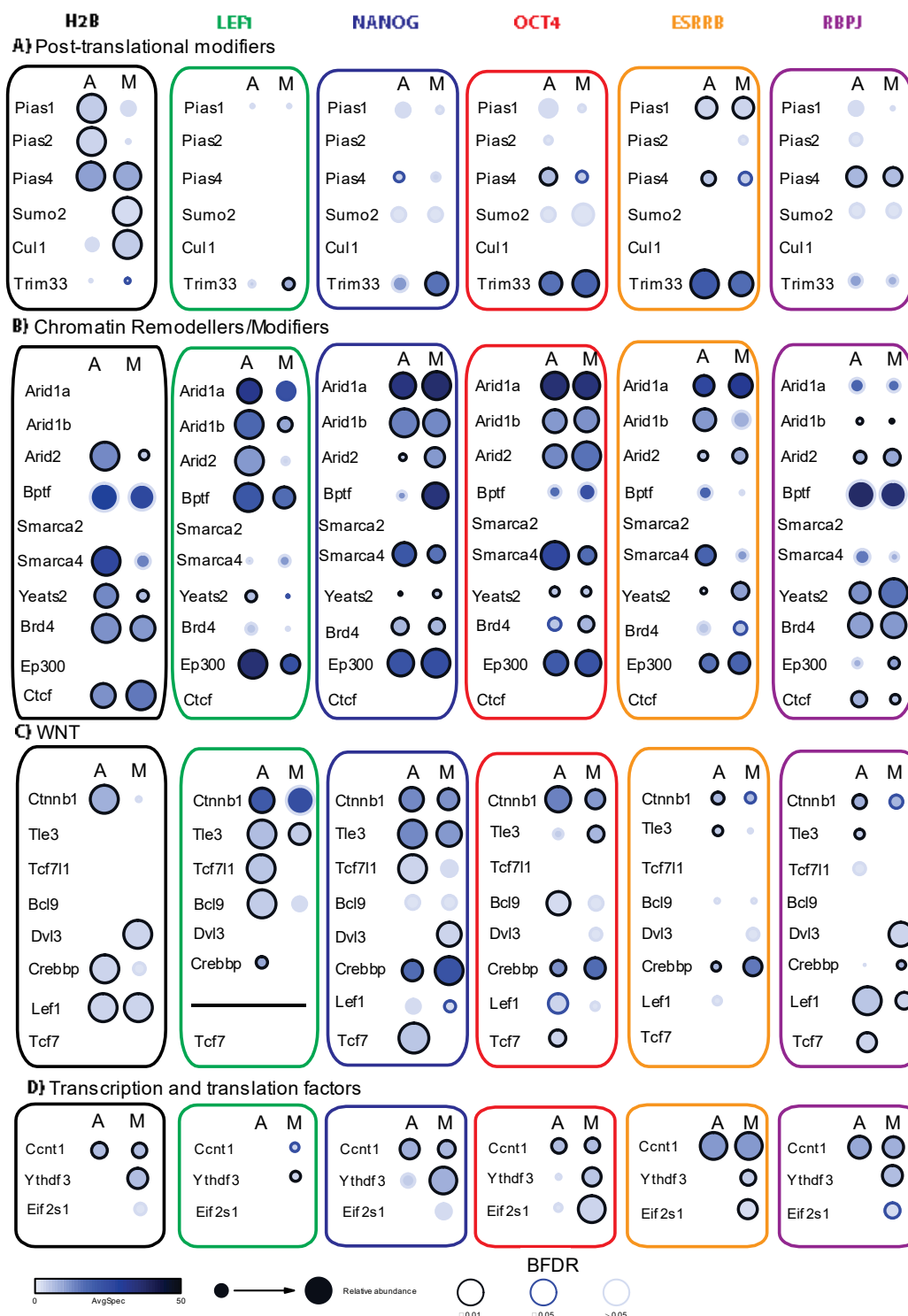
Figure 26. Bookmarking factors remain associated primarily with chromatin remodeling factors during metaphase.

The most frequently enriched A) post-translational modifiers, B) chromatin remodelers, C) Wnt signaling components, and D) translation factors identified by each TurboID fusion were chosen and presented here. Average peptide spectral counts were capped at 50.

4.3.6.   Potential Mitotic LEF1 Stabilization by K267 Sumoylation

While TCF7, TCF7L1, and LEF1 were all identified by one or more factors in our TurboID screen, LEF1 appeared to be the only TCF/LEF capable of remaining associated with mitotic chromatin in mESCs maintained as described. To determine which domains of LEF1 are responsible for this unique function, targeted LEF1 truncations were generated and assessed by live cell fluorescent imaging. While full length (FL) and Δβ-catenin binding domain (Δβ) LEF1 isoforms are capable of strongly associating with mitotic chromatin, this enrichment is greatly reduced by the loss of the C-tail domain (ΔC) (Fig. 27A). The first fifteen residues of the C-tail domain contain a nuclear localization signal (NLS) and are also tightly associated with bound DNA (boxed region), likely causing the loss of mitotic enrichment observed in our ΔC mutants (Fig. 27A). To assess the impact of post-translational modifications on LEF1 mitotic enrichment we chose to perform a conserved Lys-267-Arg mutation to disrupt the previously reported sumoylation of Lys-267 by PIAS4 (Sachdev et al. 2001). Both FL-K267R-LEF1 (K267R) and ΔC-K267R-LEF1 (K267RΔC) point mutants resulted in attenuated fluorescent signal, suggestive of increased degradation of the protein (Fig. 27B). As sumo proteins have been shown to influence protein-protein interactions, and the sumo site of LEF1 (K267) is proximal to the TLE binding domain of LEF1 (235 – 255), a LEF1 deletion was generated targeting the TLE-binding domain (ΔT). The loss of the TLE binding site alone did not appear to considerably affect LEF1 localization or abundance (Fig. 27C). However, in the absence of a TLE binding domain K267R mutants were no longer capable of inducing attenuation of LEF1 fluorescent signal (Fig. 27C). These findings suggest that K267 sumoylation is

required for the stabilization of mitotic LEF1, which is otherwise constitutively degraded

in a TLE-dependent manner, although this remains to be confirmed by further mechanistic

studies.
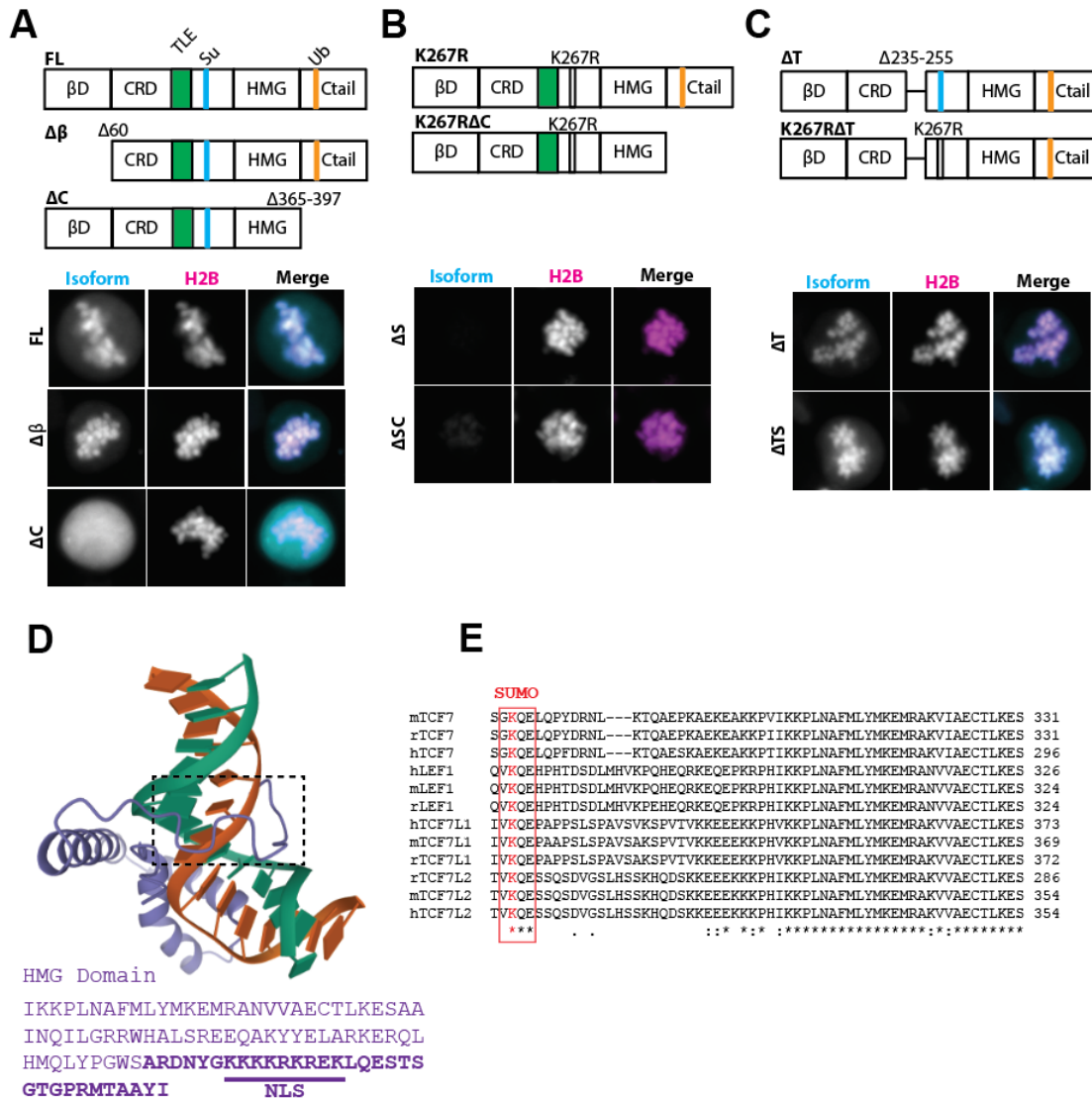
Figure 27. Constitutive mitotic degradation of LEF1 requires TLE binding and is inhibited by sumoylation at K267.

Wild-type mESCs were transiently transfected with expression vectors containing LEF1 mutants and grown for 48 hours in EB + 5 µM CHI before imaging. mAG-LEF1 isoforms (cyan) and H2B-mKO2 (magenta) nuclear marker are shown as single channel and merged images for each isoform. βD marks the β-catenin binding domain (residues 1 -60), CRD marks the central regulatory domain (residues 61 – 356), HMG marks the high mobility group DNA binding domain (residues 357 – 425), C-tail marks all residues C-terminal to the HMG (residues 326 – 397), TLE marks the TLE binding site (residues 235 – 255), and Su marks the sumoylation site (K267).

Figure 27. (Continued) A) Full length LEF1 (FL) was found to be enriched upon mitotic chromatin and weakly present within the cytoplasm, while β-catenin binding domain truncations (Δβ) saw no significant change in localization, the loss of the C-tail domain (ΔC) prevented mitotic enrichment and resulted in strong cytoplasmic localization. B) The conserved point mutation of K267R preserves the chemical profile of lysine but prevents sumoylation, resulting in the constitutive degradation of K267R-FL-LEF1 (K267R) and truncated ΔC-K267R-LEF1 (K267RΔC) isoforms. C) While loss of the TLE binding domain (ΔT) had minimal effect on LEF1 localization, it prevents the degradation of FL-K267R-LEF1 (K267RΔT). D) Crystal structure of LEF1 (purple) bound to DNA fragment containing a WRE (orange and green) with boxed region outlining the first 15 residues of the C-tail that are lost in our ΔC isoform (Love et al., 1995). The HMG Domain and full C-tail domain (bolded) sequence is listed below, with the nuclear localization signal (NLS) underlined. E) Multiple sequence alignments of all four TCF/LEF factors from human, mouse, and rat reveal a high degree of conservation at the sumoylation site (Red box) identified in LEF1, with mouse K267

4.4.   DISCUSSION

4.4.1.   Mitotic H2B-TurboID Captures Metaphase Heterochromatin Interactors

Existing techniques for proteomic analysis of mitotic chromatin rely upon the isolation of mitotic chromatin through density gradient or size exclusion chromatography (Ginno et al., 2018; Heusel et al., 2020). While such techniques have provided excellent insights into the composition of the mitotic proteome, they are not capable of excluding targets that associate non-specifically with mitotic chromatin (Van Hooser et al., 2005). These non-specific interactions have largely been attributed to the perichromosomal layer.

This space is defined as a charged surfactant-like coating covering all mitotic chromosomes, which prevents the aggregation of individual chromosomes during metaphase, and is comprised primarily of MKi67 and several other nucleolus-associated proteins (Booth and Earnshaw, 2017; Cuylen et al., 2016). Further characterization of this space by serial block-face scanning electron microscopy has shown that 30-47% of chromosomal volume during metaphase is comprised of perichromosomal proteins

(Booth et al., 2016). However, bookmarking factors have been shown to bypass this space and interact directly with enhancer and promoter regions within the genome. To better understand how bookmarkers localize and mediate these interactions it is important to generate proteomic data that is not contaminated by non-specific perichromosomal interactions.

To overcome perichromosomal contamination, we performed TurboID analysis using a H2B-TurboID fusion protein in asynchronous and nocodazole-arrested metaphase mESC populations. The inclusion of an asynchronous condition allowed us to identify metaphase-specific interactions, and to identify factors that are retained in either condition. Identification of core architectural mitotic chromosome components, such as Smc2/4 and several helicases, confirmed that our H2B-TurboID product is capable of labeling interactors even in tightly compacted heterochromatin states. Additionally, the perichromosomal marker protein MKi67 was more robustly detected in metaphase samples.

Together, these findings demonstrate that our H2B-TurboID approach can identify interactors throughout the volume and surface of mitotic chromosomes. Additionally, surface interactions identified by H2B-TurboID should only include factors capable of closely interacting with mitotic heterochromatin. While the perichromosomal layer has been shown to have a depth of ≈150nm, TurboID only has a range of 10-20 nm when linkers between the "bait" and TurboID proteins, such as the GGSGG linker we used, are employed (Booth et al., 2016; Branon et al., 2018). Specifically, this aspect of our H2B-TurboID system suggests that the observed abundance of transcriptional and

translational machinery is due to intentional mitotic loading, and not contamination by perichromosomal pull-down.

Whereas bookmarking factors are typically characterized by mitotic enrichment observed by live cell fluorescence, H2B-TurboID can capture the mitotic enrichment of multiple transcription factors simultaneously. Screening large numbers of transcription factors for bookmarking function has been done before by using live cell imaging platforms, but it is a very laborious process, which limits the number of cell lines or contexts that can be feasibly assessed. As all known bookmarking factors have been found to possess chromatin-scanning activity, our H2B-TurboID system could be used to rapidly investigate the full complement of bookmarking factors present in any TurboID-amenable cell type or culture context. However, in our study we chose to investigate the mitotic association of OCT4, ESRRB, RBPJ, NANOG, and LEF1 in Wnt-activated mESCs.

4.4.2. Selected TF Baits Reveal Unique Aspects of Mitotic Enrichment

As OCT4 has previously been shown to remain associated with 61.5% of its interphase genes during metaphase (Liu et al., 2017), and RBPJ has been shown to remain associated with ~60% of its interphase gene targets (Lake et al., 2014), we chose to tag these proteins to represent broadly associated bookmarking factors. While CCCTC-binding factor (CTCF) was initially a candidate to represent topological regulators of mitotic chromatin, it has previously been shown to strongly impede proliferation upon over expression in multiple cell lines (John E. J. Rasko, 2001). Additionally, CTCF has been confirmed by multiple techniques to lose tight association with chromatin in prometaphase (Oomen et al., 2019). However, RBPJ has been shown to directly bind CTCF, and nearly 20% of mitotic RBPJ targets are enriched for adjacent CTCF binding motifs (Lake et al.,

2014; Owens et al., 2019). Additionally, the depletion of CTCF results in the loss of enriched CTCF motifs in mitotic RBPJ targets, suggesting that RBPJ and CTCF collaborate in establishing chromatin domains and mediating long-range chromatin interactions during mitosis (Lake et al., 2014).

As such, RBPJ was chosen as a bait to overcome the limitations associated with CTCF, while still providing insight into the role of CTCF during mitosis. Consistent with our intention, CTCF was selectively identified by H2B and RBPJ baits in asynchronous and metaphase conditions, demonstrating the association of RBPJ with CTCF (Fig. 26B). The RBPJ interactome was also shown to cluster most strongly with the H2B interactome, suggesting that these interactions occur predominantly in nucleosome-rich regions such as heterochromatin (Fig. 24B).

During metaphase, mitotic chromatin is highly compacted, with non-bookmarked promoters becoming silenced (Patel et al., 2018). However, GO analysis of our mitotic H2B-TurboID interactome found TFIID-class transcription factor complex binding factors to be enriched by 35-fold, suggesting that these promoters are heterochromatic but still bound by TFIID-associated factors (Fig. 25B). Interestingly, RBPJ has been shown to be capable of suppressing target genes through direct contact with TFIID and TFIIA components (Ivan Olave, 1998). While RBPJ has also been shown to activate genes through recruitment of Mastermind-like protein (MAML) and the intracellular domain of the Notch receptor (NICD), neither component was identified by RBPJ-TurboID (Andersson et al., 2011; Borggrefe and Oswald, 2009; Vasquez-Del Carpio et al., 2011).

Instead we found RBPJ to interact strongly with KDM5a, a co-repressor directly bound by RBPJ (Liefke et al., 2010), in both metaphase and asynchronous conditions. While we did find RBPJ to interact with certain co-activators, the close association of RBPJ with heterochromatin and TFIID components suggests a unique role for RBPJ among our tagged transcription factors. While our other bookmarking baits had interactomes indicative of transcriptional activation, RBPJ appears to associate predominantly with epigenetically silenced promoters to maintain their silenced status by inhibiting associated TFIIA/D components and recruiting co-repressors to promote a heterochromatin state. This would suggest that RBPJ functions as a "negative" bookmarking factor, ensuring that target genes remain suppressed during mitosis (Fig. 28C).

By contrast, Esrrb was chosen to represent a highly selective bookmarking factor, as it has been shown to only remain associated with ~13% of its interphase targets during mitosis (Festuccia et al., 2016). However, ~55% of all ES-specific super-enhancers associated with key pluripotency genes are mitotically bound by Esrrb (Festuccia et al., 2016; Warren et al., 2013). If these super-enhancer regions are also bound by Oct4 in our chosen condition, it may be for this reason that the ESRRB-TurboID interactome clusters most closely with the OCT4-TurboID interactome.

As it has previously been reported by multiple sources to be excluded from mitotic chromatin in live cell images of ES cells (Deluz et al., 2016; Festuccia et al., 2016), Nanog was chosen to be tagged as a control for mitotic depletion. While our H2B-TurboID data found Nanog to remain associated with mitotic chromatin, it was assumed that this interaction was likely to be transient in nature, given the aforementioned imaging data. However, in our E14Tg2a mESC line, overexpressed EGFP-NANOG fusion protein

appeared enriched upon mitotic chromatin, and our TurboID-NANOG fusion generated robust interphase and metaphase interactomes.

While this consequentially eliminated our mitotic depletion control, leaving us with only our independent TurboID control, it allowed us to identify a novel function of Nanog as a potential bookmarking factor. The bookmarking activity of Nanog may be Wnt-activity dependent, as no other sources assessed mitotic enrichment in the presence of CHI, or could have been unmasked due to our choice of using an N-terminal fusion (Deluz et al., 2016; Liu et al., 2017). However, the critical role of Nanog in the maintenance of pluripotency, and its expression within the posterior ectoderm of gastrulating embryos, immediately adjacent to cells undergoing EMT and mesodermal commitment, both strongly suggest that Nanog bookmarks to maintain cellular identity (Hart et al., 2004; Hatano et al., 2005).

Finally, LEF1 was chosen to be tagged as it has not yet been reported to be capable of mitotic enrichment and was the only TCF/LEF found to be present on mitotic chromatin by our initial H2B-TurboID run (Fig. 26C). While its interactome was quite limited, it identified key Wnt enhanceosome components and shared some of the most highly conserved interactors of the other transcription factors. TurboID-LEF1 was also able to detect TCF7L1 in asynchronous populations (Fig. 26C).

While the Wnt enhanceosome has previously been shown to remain constitutively assembled at target genes, regardless of Wnt status (Fiedler et al., 2015; van Tienen et al., 2017a), this observation suggests that TCF/LEFS may actively compete for, or co-occupy, Wnt enhanceosomes at target genes.

The greatly reduced interactome of LEF1 compared to other baits is also an interesting finding, suggesting that LEF1 is quite specific in its interactions. Previous characterization of TCF/LEF occupation of WREs by CHiP-seq analysis has shown that even in the face of total TCF/LEF depletion, WRE occupation is not proportionally depleted (Moreira et al., 2018c). Additionally, BioID has previously been used to characterize the interactome of TCF7L1 in asynchronous populations before and after CHI treatment (Moreira et al., 2018a). In this study the interactomes of endogenously versus exogenously expressed BioID-TCF7L1 were compared, finding a total of 43 and 146 proximal interactors, respectively. Although this assay used BioID instead of TurboID, the scale of these interactomes are much more similar to the 56 total interactors identified by our TurboID-LEF1 analysis, than to the 300 – 500 interactors identified by OCT4, NANOG, or ESRRB.

As such, the reduced number of LEF1 interactions is not overly surprising. This disparity in interactome scale suggests that LEF1, and potentially TCF/LEFs in general, are more discrete in their interactions than comparable transcription factors. While all transcription factors participate in enhanceosomes to promote gene expression, TCF/LEFs do so with very little promiscuity. While OCT4, NANOG, and ESRRB are known to interact with a wide variety of transcription factors, supporting their larger interactomes (Festuccia et al., 2016; Horne et al., 2015; Mulas et al., 2018), TCF/LEFs may only associate with different factors in the presence of core Wnt enhanceosome components.

The range of BioID, and in turn TurboID, biotinylation has been estimated to be 10-20 nm, which corresponds to roughly 30 nt of DNA or a protein complex of roughly 3000 – 4000 kDa (Astori et al., 2020). While this range is sufficient to capture proximal enhanceosome components for most promiscuous factors, the constitutive presence

closely associated of Wnt enhanceosome components would prevent TCF/LEFs from reporting a rich interactome by BioID analysis (Renko et al., 2019a; van Tienen et al., 2017a). As such, our reduced TurboID-LEF1 interactome is reflective of constitutive TCF/LEF association with Wnt enhanceosome components, suggesting that TCF/LEFs do not contribute promiscuously to non-Wnt enhanceosomes.

While our aim was to use TurboID to characterize mitotically associated bookmarking factors in differentiating mESC populations, a recent study has used BioID to characterize the interactome of eight lineage-restricted T lymphocyte transcription factors (Astori et al., 2020). While these experiments were only performed in asynchronous populations, they were able to identify AT-rich interactive domain-containing protein 1a (ARID1a), a core component of the BAF (SWI/SNFA) complex as a highly conserved interactor among all tested transcription factors (Astori et al., 2020). T cell-specific ARID1a knockout mice were then generated, which resulted in a significant depletion of mature T cells and a 20-fold reduction in thymic cellularity (Astori et al., 2020). Complementary knockout mice for transcription factors assessed in this study, such as TCF7 and PAX5, also result in the depletion of mature thymic populations (Horowitz et al., 2004; Sjef Verbeek, 1995).

Together, these findings demonstrate the requirement of specific chromatin remodeling factors, such as ARID1a, in the maintenance of cell fate by lineage-specific transcription factors. Interestingly, while ARID1a was strongly enriched in both asynchronous and metaphase samples for LEF1, NANOG, OCT4, and ESRRB no peptides were detected by H2B in either context (Fig. 26B). By contrast RBPJ, which appears to associate predominantly with heterochromatin regions, only recognizes ARID1a with very low confidence (Fig. 26B). This would suggest that ARID1a is selectively enriched within

nucleosome-free regions, and that lineage-maintaining transcription factors such as bookmarkers may require associated SWI/SNF components such as ARID1a to maintain an open status at their target genes.

4.4.3. Bookmarking Transcription Factors Remain Associated With Transcriptional and Translational Machinery

In the current model of bookmarking, transcription factors are thought to facilitate the retention of enhancer-promoter loops throughout metaphase, allowing target genes to retain their association with transcriptional machinery and maintain basal expression (Palozola et al., 2019). All five of the TurboID-tagged transcription factors assessed here appear to be consistent with this theory, as multiple remodeling factors and transcriptional regulators were recognized by each. Specifically, a core component of p-TEFb, Ccnt1, was identified in the mitotic fraction of all tested transcription factors (Fig. 26D). However, all five factors were also found to specifically interact with Ythdf3 in metaphase. This is a point of significant note because Ythdf3 binds mRNA and interacts directly with 40S and 60S ribosome subunits, promoting translation efficiency of the bound mRNA transcripts (Shi et al., 2017). While none of our assessed transcription factors were found to interact directly with any ribosomal components, mitotic samples of Oct4, Esrrb, and Rbpj were all found to interact with one or more Eukaryotic translation initiation factor (EIF). When considered in the context of translation machinery found to be enriched on mitotic chromatin by H2B-TurboID, this may suggest that bookmarked genes not only maintain transcription during metaphase, but also maintain a state of active translation.

While early characterization of mitotic translation rates found protein synthesis to decrease by 70% upon mitotic entry (Fan and Penman, 1970), more recent techniques

have shown that rates of translation are largely unaffected by the cell cycle (Coldwell et al., 2013; Stonyte et al., 2018). While this observation is quite unexpected, it offers an even stronger potential mechanism in guiding cell fate maintenance than the retention of transcriptional activity alone. Through mitotic translation, bookmarked genes would be able to rapidly outcompete non-bookmarked targets, no longer requiring an advantage in transcript levels alone to re-establish lineage-specific gene network output. Additionally, while MKi67 was one of the most abundant interactors of H2B-TurboID, due to MKi67 interacting extensively with heterochromatin during mitosis (Sobecki et al., 2016), only RBPJ identified MKi67 peptides with low confidence while no other transcription factors recognized any MKi67 peptides.

While the total mitotic decoration observed by fluorescence imaging would suggest that bookmarkers coat mitotic chromatin, our observation that they fail to identify a major component of the perichromosomal layer would suggest that bookmarking factors permeate through the volume of mitotic chromatin, and not along the surface. However, this permeation is not complete, as core chromosomal components such as Condensin factors were only identified by RBPJ. As transcription and translation components have previously been identified as major components of the MKi67 interactome (Booth and Earnshaw, 2017; Sobecki et al., 2016) it would suggest that they are dispersed throughout the perichromosomal layer, while their recognition by our transcription factors suggests that these components may be directly recruited to active "bubbles" of transcription and translation at bookmarked genes within mitotic chromatin (Fig. 28). LEF1 appears to be selectively enriched upon mitotic chromatin, and it is likely that alternative TCF/LEFs can be similarly enriched in different cellular contexts.

While all four TCF/LEFs share a high degree of sequence homology, and compete for common WREs, knockout mouse models have shown that their individual functions are quite unique. Throughout development there are frequently regions of overlap in the expression of these factors, but as cells differentiate their TCF/LEF expression profile is often reduced to a single factor (Courtney van Genderen, 1994; Merrill et al., 2001; Sjef Verbeek, 1995). Despite these observations, very little is known about the mechanisms governing such events of TCF/LEF selection or exchange. However, our mitotic TurboID approach has found that LEF1 is selectively maintained on mitotic chromatin in Wnt-active conditions, and that LEF1 stability in these mitotic cells is potentially mediated through K267 sumoylation and interaction with TLEs (Fig. 27A, B, C).

From previously published findings, it is likely that LEF1 is sumoylated at K267 by Pias4 (Sachdev et al., 2001). The consensus site for this sumoylation event, [KVQE], is quite highly conserved among all four TCF/LEF family members (Fig. 27E). Additionally, LEF1 was found to interact quite strongly with TLE3 in both asynchronous and metaphase samples, which our truncation screen found to be required for LEF1 depletion. Taken together, these observations provide novel insight into the mechanisms governing TCF/LEF exchange. Characterization of the Wnt enhanceosome has shown that Wnt enhanceosome components, including TLE3 and TCF/LEFs, remain constitutively associated with Wnt target genes (Fiedler et al., 2015; Renko et al., 2019a; van Tienen et al., 2017a). However, it appears that upon mitotic entry TLE3 may mediate the degradation of Wnt-enhanceosome-bound TCF/LEFs that lack sumoylation. As TLE3 lacks intrinsic kinase or E3 ligase activity, it would appear that this degradation event is mediated by an interactor of TLE3. To better investigate this mechanism further, LEF1

truncations are needed to determine the PTM sites that may be required for this function,

and additional TLE3-TurboID analyses will be needed to identify this secondary factor.
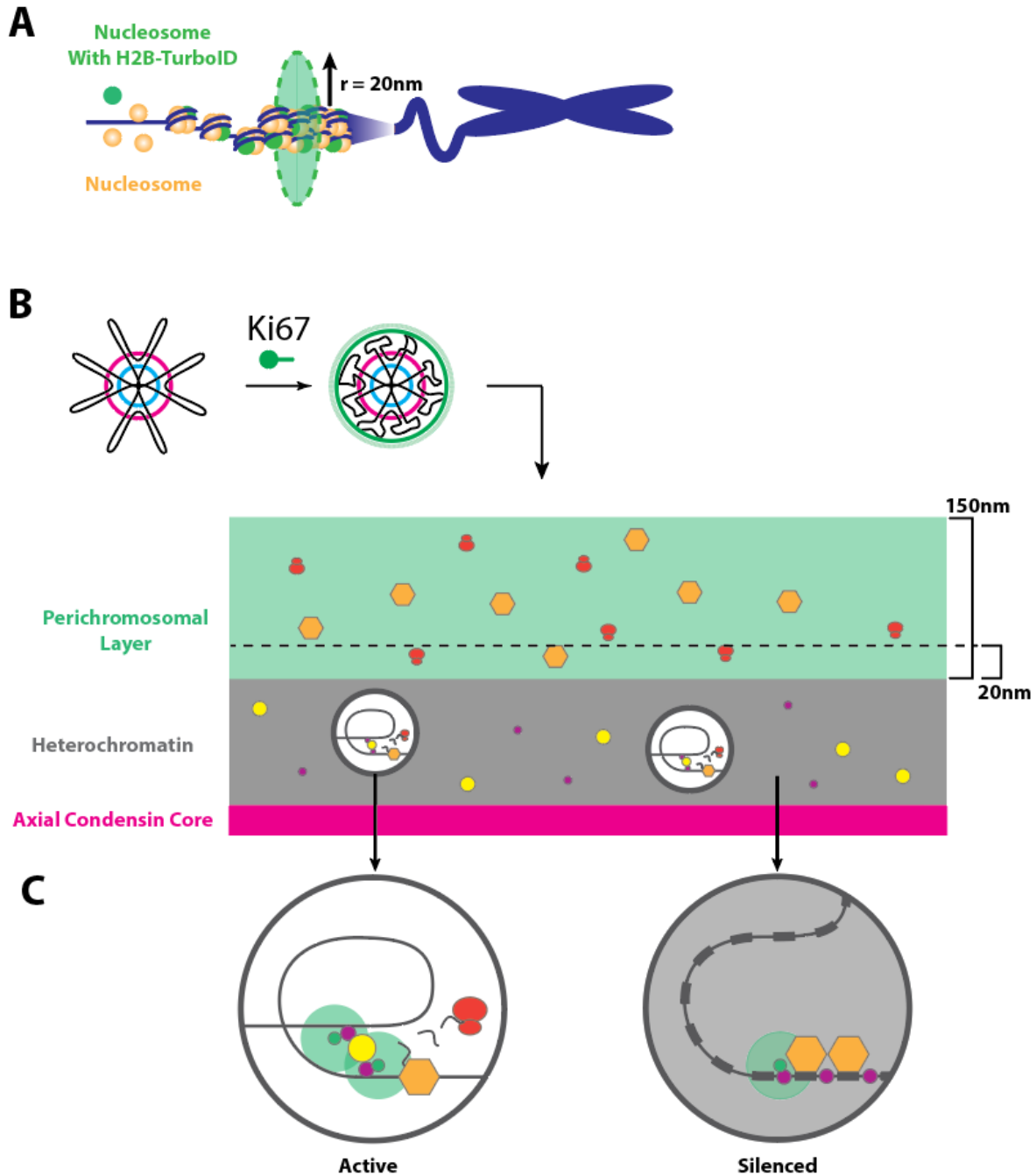
Figure 28. Physical location and functional role of bookmarking factors.

Bookmarking factors diffuse through the volume of mitotic chromatin and maintain "bubbles" of active transcription and translation at bookmarked target genes within mitotic heterochromatin. A) H2B-TurboID incorporates into nucleosomes throughout the genome. These incorporated nucleosomes detect proximal interactors within a 20 nm radius at all stages of chromatin compaction.

Figure 28. (Continued) B) As chromatin condenses into individual chromosomes heterochromatin is arranged in tightly packed nested loops around a Condensin I (cyan) and Condensin II (magenta) core. Heterochromatin looped beyond this Condensin core folds in onto itself and is coated by a surfactant-like perichromosomal layer roughly 150 nm thick and composed primarily of Mki67. A medial view through mitotic chromatin demonstrates that transcriptional machinery (orange) and translational machinery (red) are distributed primarily throughout the 150 nm thick perichromosomal layer. H2B-TurboID embedded throughout the mitotic heterochromatin will capture interactions throughout the volume of mitotic chromosomes and up to 20 nm into the perichromosomal layer. While bookmarking transcription factors (purple) and enhanceosome components (yellow) diffuse throughout the mitotic chromatin, they also assemble into euchromatic "bubbles" of active transcription and translation. C) These euchromatic bubbles are where "activating" bookmarking factors retain enhancer-promoter looping and enhanceosome assembly, to which transcription and translation factors are recruited. Alternatively, "silencing" bookmarkers such as RBPJ retain heterochromatin status and inactivate transcriptional machinery upon select promoters. Our TurboID (green) tagged factors were able to identify interactors within 20 nm (light green) in these "bubbles".

4.5. MATERIALS AND METHODS

4.5.1. Cell culture

E14tg2a mESCs (ATCC CRL-1821), and derived cell lines, were maintained in mESC medium containing high glucose Dulbecco's Modified Eagle's Medium (DMEM), 15% Fetal Bovine Serum (FBS), 2 mM L-glutamine, 1 mM Sodium Pyruvate, 100 µM non-essential amino acids, 0.1 mM 2-mercaptoethanol, and 10^3 units/mL leukemia inhibitory factor (LIF). Cultured cells were passaged every 48 h at a 1:6 ratio on 10 cm 0.1% gelatin-coated culture dishes. During experiments, and to induce LEF1 expression, cells were cultured in embryoid body (EB) medium, which is identical in composition to mESC medium but lacks LIF.

4.5.2. Plasmids

Full-length mouse LEF1 and TCF7L1 were PCR-amplified from mESC cDNA. The PCR products were blunt-end ligated into pJET3.4 (Thermo, K1231) and validated by sequencing. Using a vector generously provided by Dr. Jonathan Draper's lab (McMaster University), containing CAG-H2B-mKO2-pA we used multiple InFusion (Takara) reactions to generate CAG-H2B-mKO2-P2A-mAG-LEF1-pA, and CAG-H2B-mKO2-P2A-mAG-TCF7l1-pA vectors. 3xHA-TurboID-NLS was PCR amplified from 3xHA-TurboID-NLS-pcDNA3 (Addgene 107171) and integrated into our previously described CAG-H2B-mKO2-P2A-mAG-LEF1-pA vector to generate CAG-3xHA-TurboID-NLS-P2A-H2B-mAG-pA (TurboID), CAG-H2B-TurboID-P2A-mAG-pA (H2B-TurboID), and CAG-H2B-mAG-P2A-TurboID-LEF1-pA (TurboID-LEF1) vectors. To assess mitotic association by live cell fluorescence TurboID was excised by restriction enzyme digest and replaced with EGFP to produce CAG-H2B-mKO2-P2A-EGFP-LEF-pA vectors. A similar protocol was followed for the generation of EGFP- and TurboID-fusion vectors for OCT4, ESRRB, RBPJ, and NANOG

4.5.3. Cell lines and Transfection

Mouse E14Tg2a embryonic stem cells were maintained in an incubator with 5.0% CO_2 at $37^{\circ}C$ in mESC medium. To generate cells transiently expressing TurboID and mAG fusion proteins, mESCs were transfected by using lipofectamine 2000 according to the manufacturer's recommended protocols. For TurboID runs 9×10^6 cells were transfected with 9 μg of H2B-TurboID or TurboID-LEF1, seeded equally across three 10 cm plates, and were maintained in EB medium (mESC medium without LIF) supplemented with 5 μM of CHIR99021 (StemCell Technologies) for 41 hours. Medium was aspirated from all

plates, which were then washed once with 1X PBS. EB medium supplemented with 5 µM CHI was added to one plate, and EB medium with 5µM CHI and 150 ng Nocodazole (Sigma, M1404) was added to the other two. After 47 hours and 15 minutes, biotin-D (Sigma, B4639) was added to all plates at a final concentration of 500 µM. Cells were incubated for an additional 45 minutes after the addition of biotin (37˚C, 5% CO_2). Mitotically arrested cells were collected from nocodazole treated plates by mitotic shake-off, collected in 15 mL centrifuge tubes, and washed twice with PBS. Untreated cells were dissociated using Accutase (Stemcell Tech., 07922), collected in 15 mL centrifuge tubes, and washed twice with PBS. Excess PBS was aspirated, and samples were then snap-frozen and stored at -80ºC until all runs were completed.

4.5.4.   TurboID On-Bead Protein Digestion, and Identification by 1D LC-MS/MS

Samples were thawed on ice and lysed with 1 mL of 1 x RIPA [20 mM Tris-HCl, pH 7.5; 150 mM NaCl; 1 mM EDTA-Na_2; 1 mM EGTA; 1% NP-40; 1% sodium deoxycholate; 2.5 mM sodium pyrophosphate; 1 mM β-glycerophosphate; 1 mM Na_3VO_4, 1X Halt™ Protease/Phosphatase inhibitor (Thermo Scientific™)] for 5 minutes. Samples were then sonicated over 10 x 5s pulses at 50% load to shear DNA (Fisher Scientific sonicator FB50 with micro probe). Lysed samples were clarified by centrifugation at 16 000 x g for 10 minutes at 4°C. The supernatant of each sample was quantified by using the Bio-Rad DC Protein Assay. Following quantification, 20 µL aliquots of streptavidin-sepharose bead slurry for each sample was washed once in 1 mL of 1X RIPA. Washed bead aliquots were then resuspended in 1 mL of 1X RIPA containing 1 mg of quantified protein supernatant and rotated overnight at 4°C. Samples were then centrifuged at 1000 x g for 5 minutes, and bead pellets were washed thoroughly three times by resuspending in 1 mL Wash

Buffer (50 mM Tris-HCl pH 7.4, 8 M Urea) and rotating for 8 minutes at room temperature. Samples were then resuspended in 285 µL of ammonium bicarbonate (50 mM) and 15 µL of 1 mM biotin to saturate streptavidin binding and to prevent peptide recapture during on-bead digestion. Protein-bound beads were washed with Tris buffer 3 times, and protein reduction was performed by using 10 mM dithiothreitol (DTT) for 30 minutes at 57°C. Protein alkylation was then performed with 50 mM iodoacetamide (IAA) and quenched with 17 mM DTT at room temperature. Digestion was then performed by using 1 µg trypsin/Lys-C mix (Promega) overnight at 37°C. Peptides were collected the next day, desalted by using Sola HRP cartridges (Thermo), and samples were then lyophilized and quantified prior to mass spec analysis.

4.5.5. Data Analysis

Mass spectrometric data was obtained with an Orbitrap Q Exactive HF-X mass spectrometer (Thermo Fisher Scientific, Bremen, Germany). Peptides were identified by using instrument standard settings: 2 missed cleavage tryptic peptides were permitted, with a parent and fragment mass tolerance of 0.02 Da and 15 ppm, respectively. A fixed post-translational modification of C+57.021 was applied, and variable PTMs including N-terminal acetylation, deamidation, methylation, phosphorylation, oxidation and ubiquitylation were permitted. Peptides were then assigned into source proteins with Proteome Discoverer 2.2 (Thermo Fisher) using a mouse protein sequence database (Uniprot, 2019). SAINTexpress was then used to calculate the probability of each potential proximal protein interaction from background contaminants using default parameters (Choi et al., 2011). Two experimental replicates were used for control and experimental samples. Two unique peptides and a minimum iProphet probability of 0.95

were required for protein identification. SAINTexpress data were analyzed and visualized by using ProHits-Viz (Knight et al., 2017).

4.5.6. Live Cell Imaging

Mouse E14Tg2a stem cells were transfected as previously described using $5x10^5$ cells and 1 µg of plasmid DNA. Transfected cells were then seeded in EB medium with 5µM CHI at 5×10^4 cells/well onto µ-Slide 8 well chamber slides (IBIDI, 80826) and grown for 48 hours prior to imaging. Live cell images were obtained using a 63x oil immersion lens on a laser scanning confocal microscope (LSM-880, Zeiss). Mono-Azami Green (mAG) was stimulated by a 488 nm laser and mono-Kusabira Orange 2 (mKO2) was stimulated by a 561 nm laser.

A
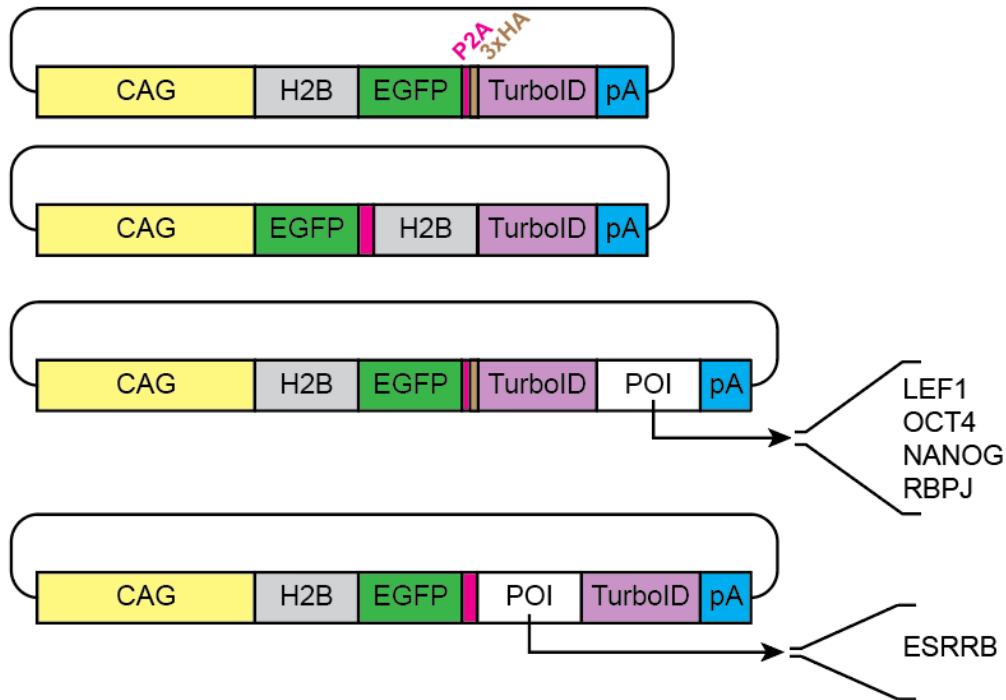
B
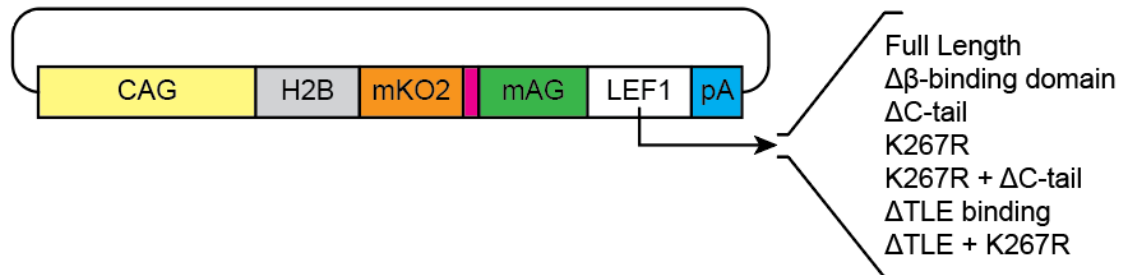
Supplementary Figure 2. **TurboID and LEF1 mutant plasmids.** A) TurboID-only control plasmid and all vectors used for the expression of proteins of interest (POIs). B) Transient expression vector used to investigate LEF1 mitotic association. All LEF1 isoforms were inserted at the indicated LEF1 position in separate vectors.

CHAPTER 5. Discussion and future directions

5.1.   Applications for mitotic TurboID

Functional characterization of mitotic chromatin has classically relied upon transcriptomic, immunofluorescent, and whole-proteome analyses that are impeded by the chemical complexity of mitotic chromatin. The reliability of paraformaldehyde and other fixation techniques have been shown to be inconsistent in their capture of mitotic chromatin interactions, resulting in the inaccurate assessment of bookmarking activity for many factors (Teves et al., 2016). While mitotic ChIP-Seq analyses have successfully identified mitotic gene targets of bookmarking factors, due to the reliance on a chemical crosslinking step, true bookmarking efficiency may be inaccurately reported (Festuccia et al., 2017; Teves et al., 2016). Additionally, inefficient mitotic chromatin fraction isolation techniques result in proteomic samples that are contaminated by perichromosomal components that require considerable post-processing to define mitotic components with confidence (Ginno et al., 2018; Heusel et al., 2020).

More recent efforts to identify bookmarking factors have relied upon the transient transfection of fluorescently labelled factors to allow for assessment by live cell imaging (Raccaud et al., 2019). While this approach bypasses the complications associated with handling or isolating mitotic chromatin, the data it provides is mostly qualitative in nature. To overcome the technical limitations associated with classical techniques, while providing quantitative *in situ* proteomic data, we chose to perform mitotic TurboID analysis (Branon et al., 2018). By using H2B to define the mitotic heterochromatin interactome, and multiple known bookmarkers to define a bookmarking interactome, we were able to

identify and strongly support the putative bookmarking activity of LEF1 and Nanog, which have not yet been shown to remain associated with mitotic chromatin.

While mitotic transcriptome techniques are more absolute in their ability to define the bookmarking capacity of a given factor, mitotic H2B-TurboID can identify the entire mitotic interactome in a given cellular context in a single experiment, rapidly informing follow-up assays. As such, this technique has broad application in the characterization of transcription factors associated with maintaining a given cell state. This could provide excellent insight into changes in mitotically associated factors as cells differentiate from a given precursor state to a defined terminal cell state, such as in the differentiation of MC3T3 osteogenic progenitor cells (Almeida et al., 2005; Kahler et al., 2006).

Additionally, there is growing evidence that bookmarking plays a functional role in maintaining cellular identity to oppose a cancer state, and maintaining a cancer state once it has been obtained (Fritz et al., 2019; Zaidi et al., 2018). The ease of mitotic TurboID could allow for the characterization of the mitotic interactome for many cancer and normal tissue samples, potentially identifying common mitotically associated factors that could serve as future therapeutic targets. Additionally, epigenetic regulator inhibitors have already seen clinical application in a variety of cancers (Cheng et al., 2019; Perez-Salvia and Esteller, 2017). One of the most frequently discussed epigenetic inhibitors is JQ-1, which is a potent inhibitor of the Bromodomain and Extra-Terminal motif (BET) family, specifically targeting BRD2/4 (Da Costa et al., 2013; Filippakopoulos et al., 2010; Handoko et al., 2018; Jiang et al., 2020a). As acetyl-lysine binding factors, BRDs have been shown to maintain the active state of key lineage and pluripotency genes (Horne et al., 2015; Jiang et al., 2020a). However, in the presence of JQ-1, however, BRDs can no

longer bind acetyl-lysine, losing their affinity for these key target genes, which then become repressed, resulting in apoptosis (Jiang et al., 2020a). Interestingly, our H2B-TurboID dataset identified nearly the entire BET protein family. Use of our mitotic TurboID technique for characterizing how BET family members and associated chromatin factors change in response to JQ-1 could shed novel insight into how JQ-1 affects BRD function and mitotic association. Additionally, as more factors are tagged and used in mitotic TurboID experiments, bookmarker interactomes will become more well defined, allowing for more confident bookmarker validation.

However, care must be taken in the preparation of fusion constructs. In our H2B-TurboID dataset, we found endogenous Nanog to be significantly enriched on mitotic chromatin. When reviewing existing publications to determine if this observation was novel, two prior publications were found in which Nanog was assessed for bookmarking capacity through transient expression and live cell imaging (Deluz et al., 2016; Festuccia et al., 2016). In both publications Nanog was C-terminally fused to a chosen fluorescent protein and convincingly excluded from mitotic chromatin. While both the N- and C-terminal regions of Nanog have been shown to possess transactivation potential the C-terminal domain was found to possess seven times greater transactivation potential (Pan and Pei, 2003). For this reason, our Nanog, GFP and TurboID fusions were assembled as N-terminal fusions. However, while our intention was to have Nanog as a negative control (a non-bookmarking transcription factor), our N-terminal fusions revealed robust mitotic association. While this was a pleasant surprise, it did deprive us of a non-bookmarking control. Although the interactomes identified by each of our chosen bookmarkers appear convincingly consistent and are implied to be euchromatic by their absence from the H2B-

interactome, a follow-up run must be done to confirm that these regions are not open to non-specific interaction by mitotically excluded factors.

Despite the extensive characterization of bookmarking factors, and their common role in cell fate, there has been no obvious commonality identified among them that might confer or predict bookmarking ability. A recent live cell imaging screen assessed the mitotic enrichment of 501 transcription factors, and while a correlation was observed between high non-specific DNA binding and mitotic enrichment, no significant protein sequence feature was found to correlate with mitotic enrichment (Raccaud et al., 2019). These findings led them to suggest then that mitotic enrichment may be mediated by specific interaction partners or post-translational modifications. Consistent with this viewpoint is our observation that LEF1 is the only TCF/LEF to be enriched upon mitotic chromatin, and that this ability may require LEF1 to be sumoylated at Lys-267. While LEF1 has previously been reported to be sumoylated at this site by PIASy, our finding that it may modulate mitotic association is entirely novel (Sachdev et al., 2001).

However, Lys-267 and its associated PIASy consensus site is very highly conserved among TCF/LEF family members, suggesting that this modification may have different effects on other TCF/LEFs, or that this PTM is applied to a chosen TCF/LEF in a context-dependent manner. Both possibilities are intriguing, and while additional experiments are required to investigate this topic further, insights can be made from our existing TurboID-LEF1 data. The first observation is that while TLE1/3/4 were identified by OCT4 and NANOG, TLE3 is the only TLE identified by LEF1. As the depletion of K267R LEF1 is rescued by the deletion of TLE binding domain of LEF1, it is likely that TLE3 is specifically involved in the modulation of LEF1 levels. However, as TLEs remain associated with the

Wnt enhanceosome in both Wnt ON and OFF states (Fiedler et al., 2015; van Tienen et al., 2017a), it would suggest that TLE3 is specifically recruited to LEF1-bound Wnt enhanceosomes, as TurboID-LEF1 failed to capture peptides from any secondary TLEs.

Interestingly, this pattern corroborates *in vivo* findings in which TLE3/4 are expressed broadly throughout early LEF1-positive domains of the primitive streak and lateral mesoderm (Koop et al., 1996; LOBE, 1997), while TLE3 is specifically expressed within tooth buds, hair follicles, and regions of epithelial-mesenchymal induction that are LEF1-exclusive and lost in LEF1$^{-/-}$ mice (Courtney van Genderen, 1994; LOBE, 1997). This would suggest that LEF1 and TLE3/4 may cooperatively establish a LEF1-only state. As K267R-LEF1 levels are rescued by the deletion of the TLE binding domain, it appears likely that TCF/LEFs lacking a central sumoylation mark may be selectively destabilized following their interaction with TLE. While this sumoylation consensus sequence is highly conserved by all four TCF/LEF family members (Fig. 27E), only LEF1 and TCF7L2 have been shown to be sumoylated at this site (Sachdev et al., 2001). Perhaps this selective sumoylation is indicative of a preceding interaction that is required for PIASy to sumoylate TCF/LEFs, and this interaction does not occur with all TCF/LEFs. To investigate these potential mechanisms additional truncations of LEF1, and the remaining TCFs, will need to be made.

There are many directions that these experiments can take us, depending on how our TCF/LEF deletions respond, but in general we will need to determine how the remaining wild-type TCFs behave in mitotic cells, and which common or unique mutations affect their mitotic localization and stability. To help guide these specific mutations we will also perform mitotic TLE3-TurboID to identify interactors which may be capable of influencing

TCF/LEF stability. Although TLEs possess no intrinsic ability to affect protein stability, a potential requirement of TLE3 binding for LEF1 destabilization suggests that secondary factors recruited by TLE3 may modulate the stability of LEF1. While TLEs have been shown to be ubiquitinated and degraded by multiple factors, they have not yet been shown to mediate TCF/LEF stability (Hanson et al., 2012; Liu et al., 2018).

However, TCF/LEF activity and stability has been shown to be affected by phosphorylation from Nemo-like Kinase (NLK) or homeodomain-interacting protein kinase 2 (HIPK2), and ubiquitination by NLK-associated RING finger protein (NARF) (Hikasa and Sokol, 2011a; Ishitani et al., 2003; Yamada et al., 2006). As such, there is precedent for mitotic depletion or inactivation of TCF/LEFs by selective PTMs, but it will require a directed effort to elucidate these mechanisms. Given the new-found function of LEF1 as a putative bookmarker, it would suggest that, like so many other things in Wnt signaling, the remaining TCFs may also bookmark in a context-dependent manner. Understanding how TCF/LEFs are selected and permitted to remain associated with mitotic chromatin will provide novel insight into critical fate-switching events throughout development and adult stem cell populations. Additionally, if TCF/LEF bookmarking is indeed regulated through selective PTMs, then our characterization of this mechanism may allow for the identification of novel drug targets capable of breaking cancer state retention by aberrantly expressed and bookmarking TCF/LEFs in cancer.

However, a point of note must be made regarding the relatively small interactome observed by our TurboID-LEF1 samples (Table 2). While our TurboID-LEF1 samples found a number of self-identifying peptides comparable to the other tagged transcription factors, suggesting that it was stable and expressed to a similar degree, it generated an

interactome roughly 10 - 15% the size of other transcription factors. By contrast Nanog had only 5 self-identified peptides and still produced an average interactome. Additionally, LEF1 has a similar length and percentage of lysines (biotinylation target) compared to the other selected transcription factors, suggesting that this restricted interactome is valid.

From our fluorescent LEF1 fusions we know that LEF1 should be enriched upon mitotic chromatin, and from our H2B-TurboID fusion identifying components of chromosomal core, we know that LEF1s interactome should not be sequestered through its participation in dense complexes or enhanceosomes. Together, these observations would suggest that TurboID-LEF1 is comparable in its expression to other fusion products, and that its reduced interactome is not the result of mis-localization or steric hindrance. However, the N-terminal domain of LEF1 binds closely with β-catenin, and as there is only a minimal G-G-S-G-G linker between LEF1 and TurboID, this linker may not afford TurboID enough mobility to adequately identify proximal interactors. While the other transcription factor fusions have disordered regions at the end where TurboID is fused, our Wnt-active culture conditions would mean that LEF1 should be in constitutive contact with β-catenin. This interaction could reduce the mobility of the TurboID fusion. Otherwise, while all samples were prepared using a common stock of buffers and reagents, and following an identical protocol, not all sample sets were prepared on the same day. To ensure that TurboID-LEF1 results were not the product of a handling error, further additional samples should be prepared and analyzed to see if they match our existing data.

	A-Peptides	M-Peptides	Length	K-count	%K	Total Interactome
H2B	18|13	16|18	127	19	15%	939
LEF1	14|15	15|18	397	25	6%	56
NANOG	5|5	5|6	305	16	5%	314
ESRRB	21|21	21|21	433	32	7%	376
OCT4	11|10	9|10	352	19	5%	501
RBPJ	21|20	21|21	526	32	6%	748

Table 2. TurboID bait peptide counts by condition.

A- and M-peptides are the number of self-identified peptides identified by each bait (ie. TurboID-LEF1 recognized 14 and 15 LEF1 peptides in either of its two runs). Length is the length of the bait protein, K-count is the number of Lysines found in each bait, %K is Kcount/Length, and Total Interactome is a count of all significant interactors identified by each bait in both asynchronous and metaphase conditions.

5.2. Improving the GLOT3-CHMIR drug screening platform

While our GLOT3-CHmiR drug screening platform identified compounds that would be missed by traditional TOP screens, its signal-to-noise ratio was lower than we had hoped. As such, while our hits were significant, they lacked the 5- to 10-fold increase observed in TOP-based screen when tested with our CHI positive control. To overcome these limitations, changes can be made to our existing GLOT3-CHmiR cell line or our culture conditions. While our choice of mAG appears comparable to most other green fluorescent proteins, the use of mKO2 seems to have not been an optimal choice. While initially chosen for its rapid maturation time, and compatibility with frequently used microscopes readily available at our institution, alternative RFPs produce spectra that much better match most existing imaging equipment in microscope facilities worldwide. An updated GLOT3-CHmiR cell line in which mKO2 has been replaced with mScarlet, an RFP that is roughly 175% the brightness of mKO2, has been generated prior to the submission of this thesis and currently only requires western blot validation. This improved GLST3-CHmiR cell line will provide better spectral separation between LEF1 and TCF7L1 fluorophores,

while the added brightness of mScarlet will improve the dynamic range of TCF7L1. However, to further boost signal intensity and provide additional biological relevance to our screening platform, our samples can be cultured and imaged on micropatterned surfaces.

The use of modified culture surfaces has already been used to generate both organ-on-a-chip platforms (An et al., 2015) and simplified 2D micropatterned screening plates (Degot et al., 2010). The main advantages of micropatterned culture surfaces are similar in this application as well, by ensuring much greater consistency in cells imaged per well and eliminating any variation in fluorescence intensity that may arise from differences in colony density or size (Degot et al., 2010). Additionally, our basal culture conditions can be optimized to induce a LEF1/TCF7L1 expression state that favours the aim of our drug screen and can be characterized by IF prior to screening. This approach will allow us to define cell fates, or even EMT events, associated with LEF1/TCF7L1 status. The consistent geometric dimensions of our micropatterns will also allow us to use image processing pipelines to quantitatively define these regions of anticipated cell fate and TCF/LEF state. All these features together will allow us to observe changes that occur not only in TCF7L1/LEF1 intensity, but also in their spatial distribution, and infer their impact on differentiation and EMT, which will in turn inform follow-up experiments. Fabrication of our existing micropatterns at a 96-well scale will, however, require cooperation with our polymer coverslip vendor (IBIDI) or operating at this scale will be unfeasible otherwise. However, screening at available 8-well or 18-well scales will also be feasible for high content screening experiments.

5.3.   CONCLUDING REMARKS

While the importance of Wnt signaling is appreciated in many fields of research, new techniques or tools capable of accurately capturing the nuances of the pathway are required to gain new mechanistic insights. The diversity in Wnt ligands and their interactions with a wide variety of Wnt cell surface receptors is further complicated by their interaction with secondary receptors that impede or promote Wnt activation. The intracellular localization and regulation of the destruction complex components adds yet another layer to the complexity of Wnt signal transduction. All these components, in the context of Wnt/β-catenin signaling, dynamically contribute towards the regulation of nuclear β-catenin translocation. However, the assembly of Wnt enhanceosome components, TCF/LEF selection/exchange, and their interactions with a variety of secondary factors that promote, impede, or bypass β-catenin interaction, all contribute towards a cellular state that is broadly referred to as Wnt "active" or "inactive". In turn this seeming "Rube Goldberg device" variety of signaling pathway is, perhaps through the advantage of its own complexity, essential for a multitude of developmental and adult tissue patterning events.

The aim of this thesis was to address how TCF/LEF expression and exchange affects Wnt-mediated cell fate decisions. To address this aim we have generated endogenously labelled cell lines and adapted micropatterning culture techniques for the isolation of homogeneous TCF/LEF-expressing populations. These platforms will allow users to track changes in Wnt transcription status in highly ordered populations by using live cell fluorescent imaging to select cell populations (Chapters 2 & 3). These populations can then be isolated and analyzed by using transcriptomic techniques to investigate how

TCF/LEFs exchange upon WREs and to identify interactors that may mediate their retention or exchange. Additionally, we devised a mitotic TurboID technique to investigate how TCF/LEF exchange may be mediated by selective mitotic retention. While we found LEF1 to be the sole TCF/LEF to remain associated with mitotic chromatin, this technique could be complemented by employing mitotic CUT & Tag to further characterize this mitotic function.

This work has established and demonstrated the efficacy of novel tools capable of disentangling the complexity of the Wnt signaling pathway by reducing the heterogeneity of sample populations, improving the relevance of biological reporters, and developing new proteomic techniques to investigate the role of Wnt in mitosis. We believe that these tools will provide new insights into the mechanisms driving TCF/LEF exchange that would not otherwise be possible to assess by using standard techniques.

REFERENCES

A. Grosberg, Y.R., S. Havlin and A. Neer (1993). Crumpled Globule Model of the ThreeDimensional Structure of DNA. Europhysics Letters *23*, 373-378.

Abou El Hassan, M., and Bremner, R. (2009). A rapid simple approach to quantify chromosome conformation capture. Nucleic Acids Research *37*, e35-e35.

Ah Cho, E., and Dressler, G.R. (1998). TCF-4 binds β-catenin and is expressed in distinct regions of the embryonic brain and limbs. Mechanisms of Development *77*, 9-18.

Al-Hajj, M., Wicha, M.S., Benito-Hernandez, A., Morrison, S.J., and Clarke, M.F. (2003). Prospective identification of tumorigenic breast cancer cells. Proceedings of the National Academy of Sciences *100*, 3983-3988.

Alan D. Agulnick, M.T., Joseph J. Breen, Tomohiro Tanaka, Igor B. Dawid & Heiner Westphal (1996). Interactions of the LIM-domainbinding factor Ldb1 with LIM homeodomain proteins. Nature *384*, 270-272.

Alghamdi, S., Khan, I., Beeravolu, N., McKee, C., Thibodeau, B., Wilson, G., and Chaudhry, G.R. (2016). BET protein inhibitor JQ1 inhibits growth and modulates WNT signaling in mesenchymal stem cells. Stem Cell Res Ther *7*, 22.

Almeida, M., Han, L., Bellido, T., Manolagas, S.C., and Kousteni, S. (2005). Wnt proteins prevent apoptosis of both uncommitted osteoblast progenitors and differentiated osteoblasts by beta-catenin-dependent and -independent signaling cascades involving Src/ERK and phosphatidylinositol 3-kinase/AKT. J Biol Chem *280*, 41342-41351.

Alver, B.H., Kim, K.H., Lu, P., Wang, X., Manchester, H.E., Wang, W., Haswell, J.R., Park, P.J., and Roberts, C.W. (2017). The SWI/SNF chromatin remodelling complex is required for maintenance of lineage specific enhancers. Nat Commun *8*, 14648.

An, F., Qu, Y., Liu, X., Zhong, R., and Luo, Y. (2015). Organ-on-a-Chip: New Platform for Biological Analysis. Anal Chem Insights *10*, 39-45.

Andersson, E.R., Sandberg, R., and Lendahl, U. (2011). Notch signaling: simplicity in design, versatility in function. Development *138*, 3593-3612.

Andersson, R., and Sandelin, A. (2020). Determinants of enhancer and promoter activities of regulatory elements. Nature Reviews Genetics *21*, 71-87.

Anup Dey, F.C., Asim Abbasi, Tom Misteli, and Keiko Ozato (2003). The double bromodomain protein Brd4 binds to acetylated chromatin during interphase and mitosis. PNAS *100*, 8758–8763.

Aragona, M., Panciera, T., Manfrin, A., Giulitti, S., Michielin, F., Elvassore, N., Dupont, S., and Piccolo, S. (2013). A mechanical checkpoint controls multicellular growth through YAP/TAZ regulation by actin-processing factors. Cell *154*, 1047-1059.

Arce, L., Pate, K.T., and Waterman, M.L. (2009). Groucho binds two conserved regions of LEF-1 for HDAC-dependent repression. BMC Cancer *9*, 159.

Arce, L., Yokoyama, N.N., and Waterman, M.L. (2006). Diversity of LEF/TCF action in development and disease. Oncogene *25*, 7492-7504.

Arnold, S.J., and Robertson, E.J. (2009). Making a commitment: cell lineage allocation and axis patterning in the early mouse embryo. Nat Rev Mol Cell Biol *10*, 91-103.

Arora, M., Packard, C.Z., Banerjee, T., and Parvin, J.D. (2016). RING1A and BMI1 bookmark active genes via ubiquitination of chromatin-associated proteins. Nucleic Acids Res *44*, 2136-2144.

Arzate-Mejia, R.G., Recillas-Targa, F., and Corces, V.G. (2018). Developing in 3D: the role of CTCF in cell differentiation. Development *145*.

Astori, A., Tingvall-Gustafsson, J., Kuruvilla, J., Coyaud, E., Laurent, E.M.N., Sunnerhagen, M., Ahsberg, J., Ungerback, J., Strid, T., Sigvardsson, M.*, et al.* (2020). ARID1a Associates with Lymphoid-Restricted Transcription Factors and Has an Essential Role in T Cell Development. J Immunol.

Atcha, F.A., Syed, A., Wu, B., Hoverter, N.P., Yokoyama, N.N., Ting, J.-H.T., Munguia, J.E., Mangalam, H.J., Marsh, J.L., and Waterman, M.L. (2007a). A Unique DNA Binding Domain Converts T-Cell Factors into Strong Wnt Effectors. Molecular and Cellular Biology *27*, 8352-8363.

Atcha, F.A., Syed, A., Wu, B., Hoverter, N.P., Yokoyama, N.N., Ting, J.H., Munguia, J.E., Mangalam, H.J., Marsh, J.L., and Waterman, M.L. (2007b). A unique DNA binding domain converts T-cell factors into strong Wnt effectors. Mol Cell Biol *27*, 8352-8363.

Azzolin, L., Panciera, T., Soligo, S., Enzo, E., Bicciato, S., Dupont, S., Bresolin, S., Frasson, C., Basso, G., Guzzardo, V.*, et al.* (2014). YAP/TAZ incorporation in the beta-catenin destruction complex orchestrates the Wnt response. Cell *158*, 157-170.

Bannister, A.J., and Kouzarides, T. (2011). Regulation of chromatin by histone modifications. Cell Research *21*, 381-395.

Beccari, L., Moris, N., Girgin, M., Turner, D.A., Baillie-Johnson, P., Cossy, A.-C., Lutolf, M.P., Duboule, D., and Arias, A.M. (2018). Multi-axial self-organization properties of mouse embryonic stem cells into gastruloids. Nature *562*, 272-276.

Belkina, A.C., and Denis, G.V. (2012). BET domain co-regulators in obesity, inflammation and cancer. Nature Reviews Cancer *12*, 465-477.

Bhanot, P., Brink, M., Samos, C.H., Hsieh, J.-C., Wang, Y., Macke, J.P., Andrew, D., Nathans, J., and Nusse, R. (1996). A new member of the frizzled family from Drosophila functions as a Wingless receptor. Nature *382*, 225-230.

Blobel, G.A., Kadauke, S., Wang, E., Lau, A.W., Zuber, J., Chou, M.M., and Vakoc, C.R. (2009). A reconfigured pattern of MLL occupancy within mitotic chromatin promotes rapid transcriptional reactivation following mitotic exit. Mol Cell *36*, 970-983.

Booth, D.G., Beckett, A.J., Molina, O., Samejima, I., Masumoto, H., Kouprina, N., Larionov, V., Prior, I.A., and Earnshaw, W.C. (2016). 3D-CLEM Reveals that a Major Portion of Mitotic Chromosomes Is Not Chromatin. Mol Cell *64*, 790-802.

Booth, D.G., and Earnshaw, W.C. (2017). Ki-67 and the Chromosome Periphery Compartment in Mitosis. Trends Cell Biol *27*, 906-916.

Borggrefe, T., and Oswald, F. (2009). The Notch signaling pathway: Transcriptional regulation at Notch target genes. Cellular and Molecular Life Sciences *66*, 1631-1646.

Branon, T.C., Bosch, J.A., Sanchez, A.D., Udeshi, N.D., Svinkina, T., Carr, S.A., Feldman, J.L., Perrimon, N., and Ting, A.Y. (2018). Efficient proximity labeling in living cells and organisms with TurboID. Nat Biotechnol *36*, 880-887.

Brantjes, H. (2001). All Tcf HMG box transcription factors interact with Groucho-related co-repressors. Nucleic Acids Research *29*, 1410-1419.

Brocardo, M., Näthke, I.S., and Henderson, B.R. (2005). Redefining the subcellular location and transport of APC: new insights using a panel of antibodies. EMBO reports *6*, 184-190.

Brzozowa, M., Wyrobiec, G., Kołodziej, I., Sitarski, M., Matysiak, N., Reichman-Warmusz, E., Żaba, M., and Wojnicz, R. (2015). The aberrant overexpression of vimentin is linked to a more aggressive status in tumours of the gastrointestinal tract. Gastroenterology Review *1*, 7-11.

Buenrostro, J.D., Giresi, P.G., Zaba, L.C., Chang, H.Y., and Greenleaf, W.J. (2013). Transposition of native chromatin for fast and sensitive epigenomic profiling of open chromatin, DNA-binding proteins and nucleosome position. Nat Methods *10*, 1213-1218.

Buenrostro, J.D., Wu, B., Chang, H.Y., and Greenleaf, W.J. (2015). ATAC-seq: A Method for Assaying Chromatin Accessibility Genome-Wide. Curr Protoc Mol Biol *109*, 21 29 21-21 29 29.

Burke, L.J., Zhang, R., Bartkuhn, M., Tiwari, V.K., Tavoosidana, G., Kurukuti, S., Weth, C., Leers, J., Galjart, N., Ohlsson, R.*, et al.* (2005). CTCF binding and higher order chromatin structure of the H19 locus are maintained in mitotic chromatin. EMBO J *24*, 3291-3300.

Butler, M.T., and Wallingford, J.B. (2017). Planar cell polarity in development and disease. Nat Rev Mol Cell Biol *18*, 375-388.

Cadigan, K.M., and Waterman, M.L. (2012). TCF/LEFs and Wnt signaling in the nucleus. Cold Spring Harb Perspect Biol *4*.

Cao, Z.-Q., Wang, Z., and Leng, P. (2019). Aberrant N-cadherin expression in cancer. Biomedicine & Pharmacotherapy *118*, 109320.

Caravaca, J.M., Donahue, G., Becker, J.S., He, X., Vinson, C., and Zaret, K.S. (2013). Bookmarking by specific and nonspecific binding of FoxA1 pioneer factor to mitotic chromosomes. Genes Dev *27*, 251-260.

Carey, M. (1998). The Enhanceosome and Transcriptional Synergy. Cell *92*, 5-8.

Carpi, N., Carpi, N., Piel, M., Azioune, A., and Fink, J. (2011). Micropatterning on glass with deep UV. Protocol Exchange.

Cartwright, P., McLean, C., Sheppard, A., Rivett, D., Jones, K., and Dalton, S. (2005). LIF/STAT3 controls ES cell self-renewal and pluripotency by a Myc-dependent mechanism. Development *132*, 885-896.

Carver, E.A., Jiang, R., Lan, Y., Oram, K.F., and Gridley, T. (2001). The mouse snail gene encodes a key regulator of the epithelial-mesenchymal transition. Mol Cell Biol *21*, 8184-8188.

Cermak, T., Doyle, E.L., Christian, M., Wang, L., Zhang, Y., Schmidt, C., Baller, J.A., Somia, N.V., Bogdanove, A.J., and Voytas, D.F. (2011). Efficient design and assembly of custom TALEN and other TAL effector-based constructs for DNA targeting. Nucleic Acids Research *39*, 7879-7879.

Chaffer, C.L., and Weinberg, R.A. (2011). A Perspective on Cancer Cell Metastasis. Science *331*, 1559-1564.

Chambers, S.M., Fasano, C.A., Papapetrou, E.P., Tomishima, M., Sadelain, M., and Studer, L. (2009). Highly efficient neural conversion of human ES and iPS cells by dual inhibition of SMAD signaling. Nat Biotechnol *27*, 275-280.

Chang, M.V., Chang, J.L., Gangopadhyay, A., Shearer, A., and Cadigan, K.M. (2008). Activation of Wingless Targets Requires Bipartite Recognition of DNA by TCF. Current Biology *18*, 1877-1881.

Chapuy, B., Michael, Charles, Monti, S., Margaretha, Qi, J., Peter, Heather, Kelly, John*, et al.* (2013). Discovery and Characterization of Super-Enhancer-Associated Dependencies in Diffuse Large B Cell Lymphoma. Cancer Cell *24*, 777-790.

Chen, D., Hinkley, C.S., Henry, R.W., and Huang, S. (2002). TBP Dynamics in Living Human Cells: Constitutive Association of TBP with Mitotic Chromosomes. Molecular Biology of the Cell *13*, 276-284.

Cheng, Y., He, C., Wang, M., Ma, X., Mo, F., Yang, S., Han, J., and Wei, X. (2019). Targeting epigenetic regulators for cancer therapy: mechanisms and advances in clinical trials. Signal Transduction and Targeted Therapy *4*.

Chittock, E.C., Latwiel, S., Miller, T.C., and Muller, C.W. (2017). Molecular architecture of polycomb repressive complexes. Biochem Soc Trans *45*, 193-205.

Chiurillo, M.A. (2015). Role of the Wnt/beta-catenin pathway in gastric cancer: An in-depth literature review. World J Exp Med *5*, 84-102.

Choi, H., Larsen, B., Lin, Z.Y., Breitkreutz, A., Mellacheruvu, D., Fermin, D., Qin, Z.S., Tyers, M., Gingras, A.C., and Nesvizhskii, A.I. (2011). SAINT: probabilistic scoring of affinity purification-mass spectrometry data. Nat Methods *8*, 70-73.

Christine Gilles, M.P., Me´lanie Mestdagt, Be´atrice Nawrocki-Raby, Philippe Ruggeri, Philippe Birembaut, and Jean-Michel Foidart (2003). Transactivation of Vimentin by beta-Catenin in Human Breast Cancer Cells. CANCER RESEARCH *63*, 2658–2664.

Christova, R., and Oelgeschlager, T. (2002). Association of human TFIID-promoter complexes with silenced mitotic chromatin in vivo. Nat Cell Biol *4*, 79-82.

Chunaram Choudhary, C.K., Florian Gnad, Michael L. Nielsen, Michael Rehman, Tobias C. Walther, Jesper V. Olsen, Matthias Mann (2009). Lysine Acetylation Targets Protein Complexes and Co-Regulates Major Cellular Functions. Science *325*, 834-840.

Coldwell, M., Cowan, J., Vlasak, M., Mead, A., Willett, M., Perry, L., and Morley, S. (2013). Phosphorylation of eIF4GII and 4E-BP1 in response to nocodazole treatment: A reappraisal of translation initiation during mitosis. Cell Cycle *12*, 3615-3628.

Cole, M.F., Johnstone, S.E., Newman, J.J., Kagey, M.H., and Young, R.A. (2008). Tcf3 is an integral component of the core regulatory circuitry of embryonic stem cells. Genes Dev *22*, 746-755.

Courtney van Genderen, R.M.O., Isabel Farinas/ Rong-Guo Quo, Tristram G. Parslow, Laurakay Bruhn, and Rudolf Grosschedl (1994). Development of several organs that require inductive epithelial-mesenchymal interactions is impaired in LEF-1deficient mice. GENES & DEVELOPMENT *8*, 2691-2703.

Cubenas-Potts, C., Srikumar, T., Lee, C., Osula, O., Subramonian, D., Zhang, X.D., Cotter, R.J., Raught, B., and Matunis, M.J. (2015). Identification of SUMO-2/3-modified proteins associated with mitotic chromosomes. Proteomics *15*, 763-772.

Cuylen, S., Blaukopf, C., Politi, A.Z., Muller-Reichert, T., Neumann, B., Poser, I., Ellenberg, J., Hyman, A.A., and Gerlich, D.W. (2016). Ki-67 acts as a biological surfactant to disperse mitotic chromosomes. Nature *535*, 308-312.

Da Costa, D., Agathanggelou, A., Perry, T., Weston, V., Petermann, E., Zlatanou, A., Oldreive, C., Wei, W., Stewart, G., Longman, J.*, et al.* (2013). BET inhibition as a single or combined therapeutic approach in primary paediatric B-precursor acute lymphoblastic leukaemia. Blood Cancer J *3*, e126.

Daniel W. Young, M.Q.H., Xiao-Qing Yang, Mario Galindo, Amjad Javed, Sayyed K. Zaidi, Paul Furcinitti, David Lapointe, Martin Montecino, Jane B. Lian, Janet L. Stein, Andre J. van Wijnen, and Gary S. Stein (2007). Mitotic retention of gene expression patterns by the cell fate-determining transcription factor Runx2. PNAS *104*, 3189–3194.

Daniels, D.L., and Weis, W.I. (2005). β-catenin directly displaces Groucho/TLE repressors from Tcf/Lef in Wnt-mediated transcription activation. Nature Structural & Molecular Biology *12*, 364-371.

David S. Parker, J.J.a.K.M.C. (2002). Pygopus, a nuclear PHD-finger protein required for Wingless signaling in Drosophila. Development *129*, 2565-2576.

Davidson, K.C., Mason, E.A., and Pera, M.F. (2015). The pluripotent state in mouse and human. Development *142*, 3090-3099.

Davies, P.S., Dismuke, A.D., Powell, A.E., Carroll, K.H., and Wong, M.H. (2008). Wnt-reporter expression pattern in the mouse intestine during homeostasis. BMC Gastroenterol *8*, 57.

Dawson, M.A., Prinjha, R.K., Dittmann, A., Giotopoulos, G., Bantscheff, M., Chan, W.-I., Robson, S.C., Chung, C.-W., Hopf, C., Savitski, M.M.*, et al.* (2011). Inhibition of BET recruitment to chromatin as an effective treatment for MLL-fusion leukaemia. Nature *478*, 529-533.

de la Roche, M., Ibrahim, A.E., Mieszczanek, J., and Bienz, M. (2014). LEF1 and B9L shield beta-catenin from inactivation by Axin, desensitizing colorectal cancer cells to tankyrase inhibitors. Cancer Res *74*, 1495-1505.

Deglincerti, A., Etoc, F., Guerra, M.C., Martyn, I., Metzger, J., Ruzo, A., Simunovic, M., Yoney, A., Brivanlou, A.H., Siggia, E.*, et al.* (2016). Self-organization of human embryonic stem cells on micropatterns. Nat Protoc *11*, 2223-2232.

Degot, S., Auzan, M., Chapuis, V., Béghin, A., Chadeyras, A., Nelep, C., Calvo-Muñoz, M.L., Young, J., Chatelain, F., and Fuchs, A. (2010). Improved Visualization and Quantitative Analysis of Drug Effects Using Micropatterned Cells. Journal of Visualized Experiments.

Deininger, M.W.N., Goldman, J.M., and Melo, J.V. (2000). The molecular biology of chronic myeloid leukemia. Blood *96,* 3343-3356.

Deluz, C., Friman, E.T., Strebinger, D., Benke, A., Raccaud, M., Callegari, A., Leleu, M., Manley, S., and Suter, D.M. (2016). A role for mitotic bookmarking of SOX2 in pluripotency and differentiation. Genes Dev *30*, 2538-2550.

Dhalluin, C., Carlson, J.E., Zeng, L., He, C., Aggarwal, A.K., Zhou, M.-M., and Zhou, M.-M. (1999). Structure and ligand of a histone acetyltransferase bromodomain. Nature *399*, 491-496.

Dostie, J., Richmond, T.A., Arnaout, R.A., Selzer, R.R., Lee, W.L., Honan, T.A., Rubio, E.D., Krumm, A., Lamb, J., Nusbaum, C.*, et al.* (2006). Chromosome Conformation Capture Carbon Copy (5C): A massively parallel solution for mapping interactions between genomic elements. Genome Research *16*, 1299-1309.

Dow, L.E., O'Rourke, K.P., Simon, J., Tschaharganeh, D.F., van Es, J.H., Clevers, H., and Lowe, S.W. (2015). Apc Restoration Promotes Cellular Differentiation and Reestablishes Crypt Homeostasis in Colorectal Cancer. Cell *161*, 1539-1552.

Doyle, E.L., Booher, N.J., Standage, D.S., Voytas, D.F., Brendel, V.P., Vandyk, J.K., and Bogdanove, A.J. (2012). TAL Effector-Nucleotide Targeter (TALE-NT) 2.0: tools for TAL effector design and target prediction. Nucleic Acids Research *40*, W117-W122.

Earnshaw, W.C., and Laemmli, U.K. (1983). Architecture of metaphase chromosomes and chromosome scaffolds. The Journal of Cell Biology *96*, 84-93.

Ermis, M., Antmen, E., and Hasirci, V. (2018). Micro and Nanofabrication methods to control cell-substrate interactions and cell behavior: A review from the tissue engineering perspective. Bioact Mater *3*, 355-369.

Estaras, C., Benner, C., and Jones, K.A. (2015). SMADs and YAP compete to control elongation of beta-catenin:LEF-1-recruited RNAPII during hESC differentiation. Mol Cell *58*, 780-793.

Etienne Labbe, A.L., and Liliana Attisano (2000). Association of Smads with lymphoid enhancer binding factor 1/T cell-specific factor mediates cooperative signaling by the transforming growth factor-b and Wnt pathways. PNAS *97*, 8358–8363

Fagotto, F. (2013). Looking beyond the Wnt pathway for the deep nature of beta-catenin. EMBO Rep *14*, 422-433.

Fan, H., and Penman, S. (1970). Regulation of protein synthesis in mammalian cells. Journal of Molecular Biology *50*, 655-670.

Farin, H.F., Jordens, I., Mosa, M.H., Basak, O., Korving, J., Tauriello, D.V., de Punder, K., Angers, S., Peters, P.J., Maurice, M.M.*, et al.* (2016). Visualization of a short-range Wnt gradient in the intestinal stem-cell niche. Nature *530*, 340-343.

Ferrer-Vaquer, A., Piliszek, A., Tian, G., Aho, R.J., Dufort, D., and Hadjantonakis, A.-K. (2010a). A sensitive and bright single-cell resolution live imaging reporter of Wnt/ß-catenin signaling in the mouse. *10*, 121.

Ferrer-Vaquer, A., Piliszek, A., Tian, G., Aho, R.J., Dufort, D., and Hadjantonakis, A.K. (2010b). A sensitive and bright single-cell resolution live imaging reporter of Wnt/ß-catenin signaling in the mouse. BMC Dev Biol *10*, 121.

Festuccia, N., Dubois, A., Vandormael-Pournin, S., Gallego Tejeda, E., Mouren, A., Bessonnard, S., Mueller, F., Proux, C., Cohen-Tannoudji, M., and Navarro, P. (2016). Mitotic binding of Esrrb marks key regulatory regions of the pluripotency network. Nat Cell Biol *18*, 1139-1148.

Festuccia, N., Gonzalez, I., Owens, N., and Navarro, P. (2017). Mitotic bookmarking in development and stem cells. Development *144*, 3633-3645.

Festuccia, N., Owens, N., Papadopoulou, T., Gonzalez, I., Tachtsidi, A., Vandoermel-Pournin, S., Gallego, E., Gutierrez, N., Dubois, A., Cohen-Tannoudji, M.*, et al.* (2019). Transcription factor activity and nucleosome organization in mitosis. Genome Res *29*, 250-260.

Fiedler, M., Graeb, M., Mieszczanek, J., Rutherford, T.J., Johnson, C.M., and Bienz, M. (2015). An ancient Pygo-dependent Wnt enhanceosome integrated by Chip/LDB-SSDP. Elife *4*.

Filippakopoulos, P., Qi, J., Picaud, S., Shen, Y., Smith, W.B., Fedorov, O., Morse, E.M., Keates, T., Hickman, T.T., Felletar, I.*, et al.* (2010). Selective inhibition of BET bromodomains. Nature *468*, 1067-1073.

Flack, J.E., Mieszczanek, J., Novcic, N., and Bienz, M. (2017). Wnt-Dependent Inactivation of the Groucho/TLE Co-repressor by the HECT E3 Ubiquitin Ligase Hyd/UBR5. Mol Cell *67*, 181-193 e185.

Fritz, A.J., Gillis, N.E., Gerrard, D.L., Rodriguez, P.D., Hong, D., Rose, J.T., Ghule, P.N., Bolf, E.L., Gordon, J.A., Tye, C.E.*, et al.* (2019). Higher order genomic organization and epigenetic control maintain cellular identity and prevent breast cancer. Genes Chromosomes Cancer *58*, 484-499.

Fuentealba, L.C., Eivers, E., Geissert, D., Taelman, V., and De Robertis, E.M. (2008). Asymmetric mitosis: Unequal segregation of proteins destined for degradation. Proceedings of the National Academy of Sciences *105*, 7732-7737.

Fyodorov, D.V., Zhou, B.-R., Skoultchi, A.I., and Bai, Y. (2018). Emerging roles of linker histones in regulating chromatin structure and function. Nature Reviews Molecular Cell Biology *19*, 192-206.

Gaarenstroom, T., and Hill, C.S. (2014). TGF-beta signaling to chromatin: how Smads regulate transcription during self-renewal and differentiation. Semin Cell Dev Biol *32*, 107-118.

Galceran, J., Farinas, I., Depew, M.J., Clevers, H., and Grosschedl, R. (1999). Wnt3a-/--like phenotype and limb deficiency in Lef1-/-Tcf1-/- mice. Genes & Development *13*, 709-717.

Galceran, J., Sustmann, C., Hsu, S.C., Folberth, S., and Grosschedl, R. (2004). LEF1-mediated regulation of Delta-like1 links Wnt and Notch signaling in somitogenesis. Genes Dev *18*, 2718-2723.

Geyer, F.C., Lacroix-Triki, M., Savage, K., Arnedos, M., Lambros, M.B., Mackay, A., Natrajan, R., and Reis-Filho, J.S. (2011). β-Catenin pathway activation in breast cancer is associated with triple-negative phenotype but not with CTNNB1 mutation. *24*, 209-231.

Ghogomu, S.M., Van Venrooy, S., Ritthaler, M., Wedlich, D., and Gradl, D. (2006a). HIC-5 Is a Novel Repressor of Lymphoid Enhancer Factor/T-cell Factor-driven Transcription. Journal of Biological Chemistry *281*, 1755-1764.

Ghogomu, S.M., van Venrooy, S., Ritthaler, M., Wedlich, D., and Gradl, D. (2006b). HIC-5 is a novel repressor of lymphoid enhancer factor/T-cell factor-driven transcription. J Biol Chem *281*, 1755-1764.

Gibcus, J.H., Samejima, K., Goloborodko, A., Samejima, I., Naumova, N., Nuebler, J., Kanemaki, M.T., Xie, L., Paulson, J.R., Earnshaw, W.C.*, et al.* (2018a). A pathway for mitotic chromosome formation. Science *359*.

Gibcus, J.H., Samejima, K., Goloborodko, A., Samejima, I., Naumova, N., Nuebler, J., Kanemaki, M.T., Xie, L., Paulson, J.R., Earnshaw, W.C.*, et al.* (2018b). A pathway for mitotic chromosome formation. Science *359*, eaao6135.

Giese, K., Amsterdam, A., and Grosschedl, R. (1991). DNA-binding properties of the HMG domain of the lymphoid-specific transcriptional regulator LEF-1. Genes & Development *5*, 2567-2578.

Giese, K., Kingsley, C., Kirshner, J.R., and Grosschedl, R. (1995). Assembly and function of a TCR alpha enhancer complex is dependent on LEF-1-induced DNA bending and multiple protein-protein interactions. Genes & Development *9*, 995-1008.

Giles, R.H., van Es, J.H., and Clevers, H. (2003). Caught up in a Wnt storm: Wnt signaling in cancer. Biochimica et Biophysica Acta (BBA) - Reviews on Cancer *1653*, 1-24.

Ginno, P.A., Burger, L., Seebacher, J., Iesmantavicius, V., and Schubeler, D. (2018). Cell cycle-resolved chromatin proteomics reveals the extent of mitotic preservation of the genomic regulatory landscape. Nat Commun *9*, 4048.

Gradl, D., König, A., and Wedlich, D. (2002). Functional Diversity ofXenopusLymphoid Enhancer Factor/T-cell Factor Transcription Factors Relies on Combinations of Activating and Repressing Elements. Journal of Biological Chemistry *277*, 14159-14171.

Graham, T.A., Weaver, C., Mao, F., Kimelman, D., and Xu, W. (2000). Crystal Structure of a β-Catenin/Tcf Complex. Cell *103*, 885-896.

Grosberg, A.Y., Nechaev, S.K., and Shakhnovich, E.I. (1988). The role of topological constraints in the kinetics of collapse of macromolecules. Journal de Physique *49*, 2095-2100.

Guo, G., Huss, M., Tong, G.Q., Wang, C., Li Sun, L., Clarke, N.D., and Robson, P. (2010). Resolution of cell fate decisions revealed by single-cell gene expression analysis from zygote to blastocyst. Dev Cell *18*, 675-685.

Gyuris, A., Donovan, D.J., Seymour, K.A., Lovasco, L.A., Smilowitz, N.R., Halperin, A.L., Klysik, J.E., and Freiman, R.N. (2009). The chromatin-targeting protein Brd2 is required for neural tube closure and embryogenesis. Biochim Biophys Acta *1789*, 413-421.

Haberland, M., Montgomery, R.L., and Olson, E.N. (2009). The many roles of histone deacetylases in development and physiology: implications for disease and therapy. Nature Reviews Genetics *10*, 32-42.

Han, W., Lee, H., and Han, J.-K. (2017). Ubiquitin C-terminal hydrolase37 regulates Tcf7 DNA binding for the activation of Wnt signalling. *7*, 42590.

Handoko, L., Kaczkowski, B., Hon, C.C., Lizio, M., Wakamori, M., Matsuda, T., Ito, T., Jeyamohan, P., Sato, Y., Sakamoto, K.*, et al.* (2018). JQ1 affects BRD2-dependent and independent transcription regulation without disrupting H4-hyperacetylated chromatin states. Epigenetics *13*, 410-431.

Hanson, A.J., Wallace, H.A., Freeman, T.J., Beauchamp, R.D., Lee, L.A., and Lee, E. (2012). XIAP monoubiquitylates Groucho/TLE to promote canonical Wnt signaling. Mol Cell *45*, 619-628.

Hart, A.H., Hartley, L., Ibrahim, M., and Robb, L. (2004). Identification, cloning and expression analysis of the pluripotency promoting Nanog genes in mouse and human. Developmental Dynamics *230*, 187-198.

Hatano, S.Y., Tada, M., Kimura, H., Yamaguchi, S., Kono, T., Nakano, T., Suemori, H., Nakatsuji, N., and Tada, T. (2005). Pluripotential competence of cells associated with Nanog activity. Mech Dev *122*, 67-79.

Hatzis, P., van der Flier, L.G., van Driel, M.A., Guryev, V., Nielsen, F., Denissov, S., Nijman, I.J., Koster, J., Santo, E.E., Welboren, W.*, et al.* (2008). Genome-wide pattern of TCF7L2/TCF4 chromatin occupancy in colorectal cancer cells. Mol Cell Biol *28*, 2732-2744.

He, T. (1998). Identification of c-MYC as a Target of the APC Pathway. Science *281*, 1509-1512.

Hermann, P.C., Huber, S.L., Herrler, T., Aicher, A., Ellwart, J.W., Guba, M., Bruns, C.J., and Heeschen, C. (2007). Distinct Populations of Cancer Stem Cells Determine Tumor Growth and Metastatic Activity in Human Pancreatic Cancer. Cell Stem Cell *1*, 313-323.

Heuberger, J., and Birchmeier, W. (2010). Interplay of cadherin-mediated cell adhesion and canonical Wnt signaling. Cold Spring Harb Perspect Biol *2*, a002915.

Heusel, M., Frank, M., Köhler, M., Amon, S., Frommelt, F., Rosenberger, G., Bludau, I., Aulakh, S., Linder, M.I., Liu, Y*., et al.* (2020). A Global Screen for Assembly State Changes of the Mitotic Proteome by SEC-SWATH-MS. Cell Systems *10*, 133-155.e136.

Hikasa, H., and Sokol, S.Y. (2011a). Phosphorylation of TCF proteins by homeodomain-interacting protein kinase 2. J Biol Chem *286*, 12093-12100.

Hikasa, H., and Sokol, S.Y. (2011b). Phosphorylation of TCF Proteins by Homeodomain-interacting Protein Kinase 2. Journal of Biological Chemistry *286*, 12093-12100.

Hirota, T. (2004). Distinct functions of condensin I and II in mitotic chromosome assembly. Journal of Cell Science *117*, 6435-6445.

Hoffman, J.A., Wu, C.I., and Merrill, B.J. (2013). Tcf7l1 prepares epiblast cells in the gastrulating mouse embryo for lineage specification. Development *140*, 1665-1675.

Hoffmeyer, K., Junghans, D., Kanzler, B., and Kemler, R. (2017). Trimethylation and Acetylation of beta-Catenin at Lysine 49 Represent Key Elements in ESC Pluripotency. Cell Rep *18*, 2815-2824.

Horne, G.A., Stewart, H.J., Dickson, J., Knapp, S., Ramsahoye, B., and Chevassut, T. (2015). Nanog requires BRD4 to maintain murine embryonic stem cell pluripotency and is suppressed by bromodomain inhibitor JQ1 together with Lefty1. Stem Cells Dev *24*, 879-891.

Horowitz, M.C., Xi, Y., Pflugh, D.L., Hesslein, D.G.T., Schatz, D.G., Lorenzo, J.A., and Bothwell, A.L.M. (2004). Pax5-Deficient Mice Exhibit Early Onset Osteopenia with Increased Osteoclast Progenitors. *173*, 6583-6591.

Hovanes, K., Li, T.W.H., Munguia, J.E., Truong, T., Milovanovic, T., Lawrence Marsh, J., Holcombe, R.F., and Waterman, M.L. (2001a). β-catenin–sensitive isoforms of lymphoid enhancer factor-1 are selectively expressed in colon cancer. Nature Genetics *28*, 53-57.

Hovanes, K., Li, T.W.H., Munguia, J.E., Truong, T., Milovanovic, T., Lawrence Marsh, J., Holcombe, R.F., and Waterman, M.L. (2001b). β-catenin–sensitive isoforms of lymphoid enhancer factor-1 are selectively expressed in colon cancer. *28*, 53-57.

Hoverter, N.P., Ting, J.H., Sundaresh, S., Baldi, P., and Waterman, M.L. (2012). A WNT/p21 circuit directed by the C-clamp, a sequence-specific DNA binding domain in TCFs. Mol Cell Biol *32*, 3648-3662.

Hoverter, N.P., Zeller, M.D., McQuade, M.M., Garibaldi, A., Busch, A., Selwan, E.M., Hertel, K.J., Baldi, P., and Waterman, M.L. (2014). The TCF C-clamp DNA binding domain expands the Wnt transcriptome via alternative target recognition. Nucleic Acids Res *42*, 13615-13632.

Howe, L.R., and Brown, A.M.C. (2004). Wnt Signaling and Breast Cancer. Cancer Biology & Therapy *3*, 36-41.

Hrckulak, D., Kolar, M., Strnad, H., and Korinek, V. (2016). TCF/LEF Transcription Factors: An Update from the Internet Resources. Cancers (Basel) *8*.

Hsu, C.-C., Huang, S.-F., Wang, J.-S., Chu, W.-K., Nien, J.-E., Chen, W.-S., and Chow, S.-E. (2016). Interplay of N-Cadherin and matrix metalloproteinase 9 enhances human nasopharyngeal carcinoma cell invasion. BMC Cancer *16*.

Huang, C., and Qin, D. (2010). Role of Lef1 in sustaining self-renewal in mouse embryonic stem cells. Journal of Genetics and Genomics *37*, 441-449.

Huang, S.-M.A., Mishina, Y.M., Liu, S., Cheung, A., Stegmeier, F., Michaud, G.A., Charlat, O., Wiellette, E., Zhang, Y., Wiessner, S.*, et al.* (2009). Tankyrase inhibition stabilizes axin and antagonizes Wnt signalling. Nature *461*, 614-620.

Hunter, J.D. (2007). Matplotlib: A 2D Graphics Environment. Computing in Science & Engineering *9*, 90-95.

Ihara, M., Yamamoto, H., and Kikuchi, A. (2005). SUMO-1 Modification of PIASy, an E3 Ligase, Is Necessary for PIASy-Dependent Activation of Tcf-4. Molecular and Cellular Biology *25*, 3506-3518.

Ishitani, T., Ninomiya-Tsuji, J., and Matsumoto, K. (2003). Regulation of lymphoid enhancer factor 1/T-cell factor by mitogen-activated protein kinase-related Nemo-like kinase-dependent phosphorylation in Wnt/beta-catenin signaling. Mol Cell Biol *23*, 1379-1389.

Ivan Olave, D.R., and Lynne D. Vales (1998). The mammalian transcriptional repressor RBP (CBF1) targets TFIID and TFIIA to prevent activated transcription. GENES & DEVELOPMENT *12*, 1621–1637.

Jain, R., Li, D., Gupta, M., Manderfield, L.J., Ifkovits, J.L., Wang, Q., Liu, F., Liu, Y., Poleshko, A., Padmanabhan, A.*, et al.* (2015). HEART DEVELOPMENT. Integration of Bmp and Wnt signaling by Hopx specifies commitment of cardiomyoblasts. Science *348*, aaa6071.

Jang, M.K., Mochizuki, K., Zhou, M., Jeong, H.S., Brady, J.N., and Ozato, K. (2005). The bromodomain protein Brd4 is a positive regulatory component of P-TEFb and stimulates RNA polymerase II-dependent transcription. Mol Cell *19*, 523-534.

Jennings, B.H., and Ish-Horowicz, D. (2008). The Groucho/TLE/Grg family of transcriptional co-repressors. Genome Biology *9*, 205.

Jiang, G., Deng, W., Liu, Y., and Wang, C. (2020a). General mechanism of JQ1 in inhibiting various types of cancer. Mol Med Rep *21*, 1021-1034.

Jiang, G., Deng, W., Liu, Y., and Wang, C. (2020b). General mechanism of JQ1 in inhibiting various types of cancer. Molecular Medicine Reports.

Jiang, X., Tan, J., Li, J., Kivimae, S., Yang, X., Zhuang, L., Lee, P.L., Chan, M.T., Stanton, L.W., Liu, E.T.*, et al.* (2008). DACT3 is an epigenetic regulator of Wnt/beta-catenin signaling in colorectal cancer and is a therapeutic target of histone modifications. Cancer Cell *13*, 529-541.

John E. J. Rasko, E.M.K., Javier Leon, Galina N. Filippova, Dmitri I. Loukinov, Sergei Vatolin, Abigail F. Robinson, Ying Jia Hu, Jonathan Ulmer, Michael D. Ward, Elena M. Pugacheva, Paul E. Neiman, Herbert C. Morse, III, Steven J. Collins, and Victor V. Lobanenkov (2001). Cell Growth Inhibition by the Multifunctional Multivalent Zinc-Finger Factor CTCF. Cancer Research *61*, 6002–6007.

Joo, S., Yeon Kim, J., Lee, E., Hong, N., Sun, W., and Nam, Y. (2015). Effects of ECM protein micropatterns on the migration and differentiation of adult neural stem cells. Sci Rep *5*, 13043.

Juan, L.J., Shia, W.J., Chen, M.H., Yang, W.M., Seto, E., Lin, Y.S., and Wu, C.W. (2000). Histone deacetylases specifically down-regulate p53-dependent gene activation. J Biol Chem *275*, 20436-20443.

Jung, Y.-S., and Park, J.-I. (2020). Wnt signaling in cancer: therapeutic targeting of Wnt signaling beyond β-catenin and the destruction complex. Experimental & Molecular Medicine *52*, 183-191.

K. Hovanes, T.W.H.L.a.M.L.W. (2000). The human LEF-1gene contains a promoter preferentially active in lymphocytes and encodes multiple isoforms derived from alternative splicing. Nucleic Acids Research *28*.

Kadauke, S., Udugama, M.I., Pawlicki, J.M., Achtman, J.C., Jain, D.P., Cheng, Y., Hardison, R.C., and Blobel, G.A. (2012). Tissue-specific mitotic bookmarking by hematopoietic transcription factor GATA1. Cell *150*, 725-737.

Kahler, R.A., Galindo, M., Lian, J., Stein, G.S., van Wijnen, A.J., and Westendorf, J.J. (2006). Lymphocyte enhancer-binding factor 1 (Lef1) inhibits terminal differentiation of osteoblasts. J Cell Biochem *97*, 969-983.

Kaplan, N., Moore, I.K., Fondufe-Mittendorf, Y., Gossett, A.J., Tillo, D., Field, Y., Leproust, E.M., Hughes, T.R., Lieb, J.D., Widom, J.*, et al.* (2009). The DNA-encoded nucleosome organization of a eukaryotic genome. Nature *458*, 362-366.

Kara, N., Hossain, M., Prasanth, S.G., and Stillman, B. (2015). Orc1 Binding to Mitotic Chromosomes Precedes Spatial Patterning during G1 Phase and Assembly of the Origin Recognition Complex in Human Cells. J Biol Chem *290*, 12355-12369.

Kaya-Okur, H.S., Wu, S.J., Codomo, C.A., Pledger, E.S., Bryson, T.D., Henikoff, J.G., Ahmad, K., and Henikoff, S. (2019). CUT&Tag for efficient epigenomic profiling of small samples and single cells. Nat Commun *10*, 1930.

Kemp, C., Willems, E., Abdo, S., Lambiv, L., and Leyns, L. (2005). Expression of all Wnt genes and their secreted antagonists during mouse blastocyst and postimplantation development. Dev Dyn *233*, 1064-1075.

Kim, C.G., Chung, I.-Y., Lim, Y., Lee, Y.H., and Shin, S.Y. (2011). A Tcf/Lef element within the enhancer region of the human NANOG gene plays a role in promoter activation. *410*, 637-642.

Kim, K., Lu, Z., and Hay, E.D. (2002). Direct evidence for a role of beta-catenin/LEF-1 signaling pathway in induction of EMT. Cell Biol Int *26*, 463-476.

King, H.W., and Klose, R.J. (2017). The pioneer factor OCT4 requires the chromatin remodeller BRG1 to support gene regulatory element function in mouse embryonic stem cells. Elife *6*.

Klarmann, G.J., Decker, A., and Farrar, W.L. (2008). Epigenetic gene silencing in the Wnt pathway in breast cancer. Epigenetics *3*, 59-63.

Klaus, A., Muller, M., Schulz, H., Saga, Y., Martin, J.F., and Birchmeier, W. (2012). Wnt/beta-catenin and Bmp signals control distinct sets of transcription factors in cardiac progenitor cells. Proc Natl Acad Sci U S A *109*, 10921-10926.

Klemm, S.L., Shipony, Z., and Greenleaf, W.J. (2019). Chromatin accessibility and the regulatory epigenome. Nature Reviews Genetics *20*, 207-220.

Knight, J.D.R., Choi, H., Gupta, G.D., Pelletier, L., Raught, B., Nesvizhskii, A.I., and Gingras, A.-C. (2017). ProHits-viz: a suite of web tools for visualizing interaction proteomics data. Nature Methods *14*, 645-646.

Kobayashi, W., and Ozawa, M. (2013). The transcription factor LEF-1 induces an epithelial-mesenchymal transition in MDCK cells independent of beta-catenin. Biochem Biophys Res Commun *442*, 133-138.

Kobayashi, W., and Ozawa, M. (2018). The epithelial-mesenchymal transition induced by transcription factor LEF-1 is independent of beta-catenin. Biochem Biophys Rep *15*, 13-18.

Kohn, A.D., and Moon, R.T. (2005). Wnt and calcium signaling: beta-catenin-independent pathways. Cell Calcium *38*, 439-446.

Koop, K.E., Macdonald, L.M., and Lobe, C.G. (1996). Transcripts of Grg4, a murine groucho-related gene, are detected in adjacent tissues to other murine neurogenic gene homologues during embryonic development. Mechanisms of Development *59*, 73-87.

Korinek, V., Barker, N., Moerer, P., Van Donselaar, E., Huls, G., Peters, P.J., and Clevers, H. (1998). Depletion of epithelial stem-cell compartments in the small intestine of mice lacking Tcf-4. Nature Genetics *19*, 379-383.

Korinek, V., Barker, N., Morin, P.J., van Wichen, D., de Weger, R., Kinzler, K.W., Vogelstein, B., and Clevers, H. (1997). Constitutive transcriptional activation by a beta-catenin-Tcf complex in APC-/- colon carcinoma. Science *275*, 1784-1787.

Kratochwil, K., Galceran, J., Tontsch, S., Roth, W., and Grosschedl, R. (2002). FGF4, a direct target of LEF1 and Wnt signaling, can rescue the arrest of tooth organogenesis in Lef1(-/-) mice. Genes Dev *16*, 3173-3185.

Kühl, M., Sheldahl, L.C., Malbon, C.C., and Moon, R.T. (2000). Ca2+/Calmodulin-dependent Protein Kinase II Is Stimulated by Wnt and Frizzled Homologs and Promotes Ventral Cell Fates inXenopus. Journal of Biological Chemistry *275*, 12701-12711.

Kunttas-Tatli, E., Zhou, M.-N., Zimmerman, S., Molinar, O., Zhouzheng, F., Carter, K., Kapur, M., Cheatle, A., Decal, R., and McCartney, B.M. (2012). Destruction Complex Function in the Wnt Signaling Pathway of Drosophila Requires Multiple Interactions Between Adenomatous Polyposis Coli 2 and Armadillo. Genetics *190*, 1059-1075.

Kurosawa, H. (2007). Methods for inducing embryoid body formation: in vitro differentiation system of embryonic stem cells. Journal of Bioscience and Bioengineering *103*, 389-398.

Kusuma, S., Smith, Q., Facklam, A., and Gerecht, S. (2017). Micropattern size-dependent endothelial differentiation from a human induced pluripotent stem cell line. J Tissue Eng Regen Med *11*, 855-861.

Kwon, C., Cheng, P., King, I.N., Andersen, P., Shenje, L., Nigam, V., and Srivastava, D. (2011). Notch post-translationally regulates beta-catenin protein in stem and progenitor cells. Nat Cell Biol *13*, 1244-1251.

Labbe, E., Letamendia, A., and Attisano, L. (2000). Association of Smads with lymphoid enhancer binding factor 1/T cell-specific factor mediates cooperative signaling by the transforming growth factor-beta and Wnt pathways. Proceedings of the National Academy of Sciences *97*, 8358-8363.

Lake, R.J., Tsai, P.F., Choi, I., Won, K.J., and Fan, H.Y. (2014). RBPJ, the major transcriptional effector of Notch signaling, remains associated with chromatin throughout mitosis, suggesting a role in mitotic bookmarking. PLoS Genet *10*, e1004204.

Lambertini, E., Franceschetti, T., Torreggiani, E., Penolazzi, L., Pastore, A., Pelucchi, S., Gambari, R., and Piva, R. (2010). SLUG: a new target of lymphoid enhancer factor-1 in human osteoblasts. *11*, 13.

Lee, C.-K., Shibata, Y., Rao, B., Strahl, B.D., and Lieb, J.D. (2004). Evidence for nucleosome depletion at active regulatory regions genome-wide. Nature Genetics *36*, 900-905.

Lei, S., Dubeykovskiy, A., Chakladar, A., Wojtukiewicz, L., and Wang, T.C. (2004). The murine gastrin promoter is synergistically activated by transforming growth factor-beta/Smad and Wnt signaling pathways. J Biol Chem *279*, 42492-42502.

Levine, M. (2010). Transcriptional Enhancers in Animal Development and Evolution. Current Biology *20*, R754-R763.

Li, L., Jothi, R., Cui, K., Lee, J.Y., Cohen, T., Gorivodsky, M., Tzchori, I., Zhao, Y., Hayes, S.M., Bresnick, E.H.*, et al.* (2011). Nuclear adaptor Ldb1 regulates a transcriptional program essential for the maintenance of hematopoietic stem cells. Nature Immunology *12*, 129-136.

Li, T.W., Ting, J.H., Yokoyama, N.N., Bernstein, A., van de Wetering, M., and Waterman, M.L. (2006). Wnt activation and alternative promoter repression of LEF1 in colon cancer. Mol Cell Biol *26*, 5284-5299.

Li, Y., Wang, L., Zhang, M., Melamed, J., Liu, X., Reiter, R., Wei, J., Peng, Y., Zou, X., Pellicer, A.*, et al.* (2009). LEF1 in Androgen-Independent Prostate Cancer: Regulation of Androgen Receptor Expression, Prostate Cancer Growth, and Invasion. *69*, 3332-3338.

Liang, K., Ashley, Brian, Jay, Andrew, Ryan, Gao, X., Jeffrey, Sue, and Shilatifard, A. (2015a). Mitotic Transcriptional Activation: Clearance of Actively Engaged Pol II via Transcriptional Elongation Control in Mitosis. Molecular Cell *60*, 435-445.

Liang, Z., Zickler, D., Prentiss, M., Chang, F.S., Witz, G., Maeshima, K., and Kleckner, N. (2015b). Chromosomes Progress to Metaphase in Multiple Discrete Steps via Global Compaction/Expansion Cycles. Cell *161*, 1124-1137.

Lieberman-Aiden, E., Van Berkum, N.L., Williams, L., Imakaev, M., Ragoczy, T., Telling, A., Amit, I., Lajoie, B.R., Sabo, P.J., Dorschner, M.O.*, et al.* (2009). Comprehensive Mapping of Long-Range Interactions Reveals Folding Principles of the Human Genome. Science *326*, 289-293.

Liefke, R., Oswald, F., Alvarado, C., Ferres-Marco, D., Mittler, G., Rodriguez, P., Dominguez, M., and Borggrefe, T. (2010). Histone demethylase KDM5A is an integral part of the core Notch-RBP-J repressor complex. *24*, 590-601.

Lin, A.Y., Chua, M.-S., Choi, Y.-L., Yeh, W., Kim, Y.H., Azzi, R., Adams, G.A., Sainani, K., Van De Rijn, M., So, S.K.*, et al.* (2011). Comparative Profiling of Primary Colorectal Carcinomas and Liver Metastases Identifies LEF1 as a Prognostic Biomarker. *6*, e16636.

Lin, S.Y., Xia, W., Wang, J.C., Kwong, K.Y., Spohn, B., Wen, Y., Pestell, R.G., and Hung, M.C. (2000). beta -Catenin, a novel prognostic marker for breast cancer: Its roles in cyclin D1 expression and cancer progression. Proceedings of the National Academy of Sciences *97*, 4262-4266.

Liu, G., and Dean, A. (2019). Enhancer long-range contacts: The multi-adaptor protein LDB1 is the tie that binds. Biochimica et Biophysica Acta (BBA) - Gene Regulatory Mechanisms *1862*, 625-633.

Liu, L.-K., Jiang, X.-Y., Zhou, X.-X., Wang, D.-M., Song, X.-L., and Jiang, H.-B. (2010). Upregulation of vimentin and aberrant expression of E-cadherin/β-catenin complex in oral squamous cell carcinomas: correlation with the clinicopathological features and patient outcome. *23*, 213-224.

Liu, L., Zhang, Y., Wong, C.C., Zhang, J., Dong, Y., Li, X., Kang, W., Chan, F.K.L., Sung, J.J.Y., and Yu, J. (2018). RNF6 Promotes Colorectal Cancer by Activating the Wnt/beta-Catenin Pathway via Ubiquitination of TLE3. Cancer Res *78*, 1958-1971.

Liu, Y., Pelham-Webb, B., Di Giammartino, D.C., Li, J., Kim, D., Kita, K., Saiz, N., Garg, V., Doane, A., Giannakakou, P.*, et al.* (2017). Widespread Mitotic Bookmarking by Histone Marks and Transcription Factors in Pluripotent Stem Cells. Cell Rep *19*, 1283-1293.

LOBE, C.L.A.C.G. (1997). Grg3, a Murine Groucho-Related Gene, is Expressed in the Developing Nervous System and in Mesenchyme-Induced Epithelial Structures. DEVELOPMENTAL DYNAMICS *208*, 11–24

Lodhi, N., Ji, Y., and Tulin, A. (2016). Mitotic bookmarking: maintaining post-mitotic reprogramming of transcription reactivation. Curr Mol Biol Rep *2*, 10-16.

Love, J.J., Li, X., Case, D.A., Giese, K., Grosschedl, R., and Wright, P.E. (1995). Structural basis for DNA bending by the architectural transcription factor LEF-1. Nature *376*, 791-795.

Lu, B., Green, B.A., Farr, J.M., Lopes, F.C., and Van Raay, T.J. (2016). Wnt Drug Discovery: Weaving Through the Screens, Patents and Clinical Trials. Cancers (Basel) *8*.

Maeshima, K., Tamura, S., Hansen, J.C., and Itoh, Y. (2020a). Fluid-like chromatin: Toward understanding the real chromatin organization present in the cell. Current Opinion in Cell Biology *64*, 77-89.

Maeshima, K., Tamura, S., Hansen, J.C., and Itoh, Y. (2020b). Fluid-like chromatin: Toward understanding the real chromatin organization present in the cell. Curr Opin Cell Biol *64*, 77-89.

Malhotra, S., and Kincade, P.W. (2009). Wnt-Related Molecules and Signaling Pathway Equilibrium in Hematopoiesis. Cell Stem Cell *4*, 27-36.

Marian A. Martinez-Balbas, A.D., Sridhar K. Rabindran,Keiko Ozato, and Carl Wu (1995). Displacement of Sequence-Specific Transcription Factors from Mitotic Chromatin. Cell *83*, 29-38.

Mariëtte Oosterwegel, M.v.d.W., Janneke Timmerman, Ada Kruisbeek, Olivier Destree, Frits Meijlink and Hans Clevers (1993). Differential expression of the HMG box factors TCF-1 and LEF-1 during murine embryogenesis. Development *118*, 439-448.

Martello, G., Sugimoto, T., Diamanti, E., Joshi, A., Hannah, R., Ohtsuka, S., Gottgens, B., Niwa, H., and Smith, A. (2012). Esrrb is a pivotal target of the Gsk3/Tcf3 axis regulating embryonic stem cell self-renewal. Cell Stem Cell *11*, 491-504.

Martyn, I., Brivanlou, A.H., and Siggia, E.D. (2019). A wave of WNT signaling balanced by secreted inhibitors controls primitive streak formation in micropattern colonies of human embryonic stem cells. Development *146*.

Martyn, I., Kanno, T.Y., Ruzo, A., Siggia, E.D., and Brivanlou, A.H. (2018). Self-organization of a human organizer by combined Wnt and Nodal signalling. Nature *558*, 132-135.

Matthews, J.M., and Visvader, J.E. (2003). LIM-domain-binding protein 1: a multifunctional cofactor that interacts with diverse proteins. EMBO reports *4*, 1132-1137.

McBeath, R., Pirone, D.M., Nelson, C.M., Bhadriraju, K., and Chen, C.S. (2004). Cell Shape, Cytoskeletal Tension, and RhoA Regulate Stem Cell Lineage Commitment. Developmental Cell *6*, 483-495.

McCormick, O.T.F. (1999). B-Catenin regulates expression of cyclinD1 in colon carcinomacells. Nature *398*, 422-426.

McDole, K., Guignard, L., Amat, F., Berger, A., Malandain, G., Royer, L.A., Turaga, S.C., Branson, K., and Keller, P.J. (2018). In Toto Imaging and Reconstruction of Post-Implantation Mouse Development at the Single-Cell Level. Cell *175*, 859-876.e833.

McKinney, W. (2010). Data Structures for Statistical Computing in Python (SciPy).

McQuin, C., Goodman, A., Chernyshev, V., Kamentsky, L., Cimini, B.A., Karhohs, K.W., Doan, M., Ding, L., Rafelski, S.M., Thirstrup, D.*, et al.* (2018). CellProfiler 3.0: Next-generation image processing for biology. PLOS Biology *16*, e2005970.

Medici, D., Hay, E.D., and Goodenough, D.A. (2006). Cooperation between snail and LEF-1 transcription factors is essential for TGF-beta1-induced epithelial-mesenchymal transition. Mol Biol Cell *17*, 1871-1879.

Menter, T., Dirnhofer, S., and Tzankov, A. (2015). LEF1: a highly specific marker for the diagnosis of chronic lymphocytic B cell leukaemia/small lymphocytic B cell lymphoma. Journal of Clinical Pathology *68*, 473-478.

Merika, M., Williams, A.J., Chen, G., Collins, T., and Thanos, D. (1998). Recruitment of CBP/p300 by the IFNβ Enhanceosome Is Required for Synergistic Activation of Transcription. Molecular Cell *1*, 277-287.

Merrill, B.J., Gat, U., DasGupta, R., and Fuchs, E. (2001). Tcf3 and Lef1 regulate lineage differentiation of multipotent stem cells in skin. Genes Dev *15*, 1688-1705.

Merrill, B.J., Pasolli, H.A., Polak, L., Rendl, M., Garcia-Garcia, M.J., Anderson, K.V., and Fuchs, E. (2004). Tcf3: a transcriptional regulator of axis induction in the early embryo. Development *131*, 263-274.

Mertz, J.A., Conery, A.R., Bryant, B.M., Sandy, P., Balasubramanian, S., Mele, D.A., Bergeron, L., and Sims, R.J. (2011). Targeting MYC dependence in cancer by inhibiting BET bromodomains. Proceedings of the National Academy of Sciences *108*, 16669-16674.

Miguel A. Andrade, P.B. (1995). HEAT repeats in the Huntington's disease protein. Nature Genetics *11*, 115-116.

Minucci, S., and Pelicci, P.G. (2006). Histone deacetylase inhibitors and the promise of epigenetic (and more) treatments for cancer. Nat Rev Cancer *6*, 38-51.

Miyamoto, D., Ohno, K., Hara, T., Koga, H., and Nakazawa, K. (2016). Effect of separation distance on the growth and differentiation of mouse embryoid bodies in micropatterned cultures. J Biosci Bioeng *121*, 105-110.

Molenaar, M., Van De Wetering, M., Oosterwegel, M., Peterson-Maduro, J., Godsave, S., Korinek, V., Roose, J., Destrée, O., and Clevers, H. (1996). XTcf-3 Transcription Factor Mediates β-Catenin-Induced Axis Formation in Xenopus Embryos. Cell *86*, 391-399.

Moore, A.C., Amann, J.M., Williams, C.S., Tahinci, E., Farmer, T.E., Martinez, J.A., Yang, G., Luce, K.S., Lee, E., and Hiebert, S.W. (2008). Myeloid Translocation Gene Family Members Associate with T-Cell Factors (TCFs) and Influence TCF-Dependent Transcription. Molecular and Cellular Biology *28*, 977-987.

Morcillo, P., Rosen, C., Baylies, M.K., and Dorsett, D. (1997). Chip, a widely expressed chromosomal protein required for segmentation and activity of a remote wing margin enhancer in Drosophila. Genes & Development *11*, 2729-2740.

Moreira, S., Polena, E., Gordon, V., Abdulla, S., Mahendram, S., Cao, J., Blais, A., Wood, G.A., Dvorkin-Gheva, A., and Doble, B.W. (2017). A Single TCF Transcription Factor, Regardless of Its Activation Capacity, Is Sufficient for Effective Trilineage Differentiation of ESCs. Cell Rep *20*, 2424-2438.

Moreira, S., Seo, C., Gordon, V., Xing, S., Wu, R., Polena, E., Fung, V., Ng, D., Wong, C.J., Larsen, B*., et al.* (2018a). Endogenous BioID elucidates TCF7L1 interactome modulation upon GSK-3 inhibition in mouse ESCs. bioRxiv, 1-14.

Moreira, S., Seo, C., Polena, E., Mahendram, S., Mercier, E., Blais, A., and Doble, B.W. (2018b). TCF7L1 and TCF7 differentially regulate specific mouse ES cell genes in response to GSK-3 inhibition. bioRxiv, 473801.

Moreira, S., Seo, C., Polena, E., Mahendram, S., Mercier, E., Blais, A., and Doble, B.W. (2018c). TCF7L1 and TCF7 differentially regulate specific mouse ES cell genes in response to GSK-3 inhibition. bioRxiv.

Morgani, S.M., Metzger, J.J., Nichols, J., Siggia, E.D., and Hadjantonakis, A.K. (2018). Micropattern differentiation of mouse pluripotent stem cells recapitulates embryo regionalized cell fate patterning. Elife *7*.

Morikawa, M., Koinuma, D., Mizutani, A., Kawasaki, N., Holmborn, K., Sundqvist, A., Tsutsumi, S., Watabe, T., Aburatani, H., Heldin, C.H.*, et al.* (2016). BMP Sustains Embryonic Stem Cell Self-Renewal through Distinct Functions of Different Kruppel-like Factors. Stem Cell Reports *6*, 64-73.

Mulas, C., Chia, G., Jones, K.A., Hodgson, A.C., Stirparo, G.G., and Nichols, J. (2018). Oct4 regulates the embryonic axis and coordinates exit from pluripotency and germ layer specification in the mouse embryo. Development *145*.

Najdi, R., Syed, A., Arce, L., Theisen, H., Ting, J.H., Atcha, F., Nguyen, A.V., Martinez, M., Holcombe, R.F., Edwards, R.A.*, et al.* (2009). A Wnt kinase network alters nuclear localization of TCF-1 in colon cancer. Oncogene *28*, 4133-4146.

Nawshad, A., and Hay, E.D. (2003). TGFbeta3 signaling activates transcription of the LEF1 gene to induce epithelial mesenchymal transformation during mouse palate development. J Cell Biol *163*, 1291-1301.

Nawshad, A., Medici, D., Liu, C.C., and Hay, E.D. (2007). TGFbeta3 inhibits E-cadherin gene expression in palate medial-edge epithelial cells through a Smad2-Smad4-LEF1 transcription complex. J Cell Sci *120*, 1646-1653.

Nemashkalo, A., Ruzo, A., Heemskerk, I., and Warmflash, A. (2017). Morphogen and community effects determine cell fates in response to BMP4 signaling in human embryonic stem cells. Development *144*, 3042-3053.

Ng, A.P., and Alexander, W.S. (2017). Haematopoietic stem cells: past, present and future. Cell Death Discovery *3*, 17002.

Nguyen, D.X., Chiang, A.C., Zhang, X.H., Kim, J.Y., Kris, M.G., Ladanyi, M., Gerald, W.L., and Massague, J. (2009). WNT/TCF signaling through LEF1 and HOXB9 mediates lung adenocarcinoma metastasis. Cell *138*, 51-62.

Ogaki, S., Shiraki, N., Kume, K., and Kume, S. (2013). Wnt and Notch Signals Guide Embryonic Stem Cell Differentiation into the Intestinal Lineages. STEM CELLS *31*, 1086-1096.

Oh, Y., and Jang, J. (2019). Directed Differentiation of Pluripotent Stem Cells by Transcription Factors. Mol Cells *42*, 200-209.

Ohnuki, Y. (1968). Morphological Studies of the Spiral Structure of Human Somatic Chromosomes. Chromosoma *25*, 402-428.

Ohta, S., Bukowski-Wills, J.C., Sanchez-Pulido, L., Alves Fde, L., Wood, L., Chen, Z.A., Platani, M., Fischer, L., Hudson, D.F., Ponting, C.P.*, et al.* (2010). The protein composition of mitotic chromosomes determined using multiclassifier combinatorial proteomics. Cell *142*, 810-821.

Olins, D.E., and Olins, A.L. (2003). Chromatin history: our view from the bridge. Nature Reviews Molecular Cell Biology *4*, 809-814.

Oliphant, T.E. (2007). Python for Scientific Computing. Computing in Science & Engineering *9*, 10-20.

Oomen, M.E., Hansen, A.S., Liu, Y., Darzacq, X., and Dekker, J. (2019). CTCF sites display cell cycle-dependent dynamics in factor binding and nucleosome positioning. Genome Res *29*, 236-249.

Orkin, S.H., Wang, J., Kim, J., Chu, J., Rao, S., Theunissen, T.W., Shen, X., and Levasseur, D.N. (2008). The Transcriptional Network Controlling Pluripotency in ES Cells. Cold Spring Harbor Symposia on Quantitative Biology *73*, 195-202.

Ota, S., Ishitani, S., Shimizu, N., Matsumoto, K., Itoh, M., and Ishitani, T. (2012). NLK positively regulates Wnt/β-catenin signalling by phosphorylating LEF1 in neural progenitor cells. The EMBO Journal *31*, 1904-1915.

Owens, N., Papadopoulou, T., Festuccia, N., Tachtsidi, A., Gonzalez, I., Dubois, A., Vandormael-Pournin, S., Nora, E.P., Bruneau, B.G., Cohen-Tannoudji, M.*, et al.* (2019). CTCF confers local nucleosome resiliency after DNA replication and during mitosis. eLife *8*.

Palozola, K.C., Donahue, G., Liu, H., Grant, G.R., Becker, J.S., Cote, A., Yu, H., Raj, A., and Zaret, K.S. (2017). Mitotic transcription and waves of gene reactivation during mitotic exit. Science *358*, 119-122.

Palozola, K.C., Lerner, J., and Zaret, K.S. (2019). A changing paradigm of transcriptional memory propagation through mitosis. Nat Rev Mol Cell Biol *20*, 55-64.

Pan, G.J., and Pei, D.Q. (2003). Identification of two distinct transactivation domains in the pluripotency sustaining factor nanog. Cell Research *13*, 499-502.

Panne, D. (2008). The enhanceosome. *18*, 236-242.

Parbin, S., Kar, S., Shilpi, A., Sengupta, D., Deb, M., Rath, S.K., and Patra, S.K. (2014). Histone deacetylases: a saga of perturbed acetylation homeostasis in cancer. J Histochem Cytochem *62*, 11-33.

Pardal, R., Clarke, M.F., and Morrison, S.J. (2003). Applying the principles of stem-cell biology to cancer. Nature Reviews Cancer *3*, 895-902.

Paridaen, J.T., Wilsch-Brauninger, M., and Huttner, W.B. (2013). Asymmetric inheritance of centrosome-associated primary cilium membrane directs ciliogenesis after cell division. Cell *155*, 333-344.

Parsons, G.G., and Spencer, C.A. (1997). Mitotic repression of RNA polymerase II transcription is accompanied by release of transcription elongation complexes. Molecular and Cellular Biology *17*, 5791-5802.

Patel, A.B., Louder, R.K., Greber, B.J., Grünberg, S., Luo, J., Fang, J., Liu, Y., Ranish, J., Hahn, S., and Nogales, E. (2018). Structure of human TFIID and mechanism of TBP loading onto promoter DNA. Science *362*, eaau8872.

Patel, J., Baranwal, S., Love, I.M., Patel, N.J., Grossman, S.R., and Patel, B.B. (2014). Inhibition of C-terminal binding protein attenuates transcription factor 4 signaling to selectively target colon cancer stem cells. Cell Cycle *13*, 3506-3518.

Pereira, L., Yi, F., and Merrill, B.J. (2006). Repression of Nanog gene transcription by Tcf3 limits embryonic stem cell self-renewal. Mol Cell Biol *26*, 7479-7491.

Perez-Salvia, M., and Esteller, M. (2017). Bromodomain inhibitors and cancer therapy: From structures to applications. Epigenetics *12*, 323-339.

Petropoulos, K., Arseni, N., Schessl, C., Stadler, C.R., Rawat, V.P., Deshpande, A.J., Heilmeier, B., Hiddemann, W., Quintanilla-Martinez, L., Bohlander, S.K.*, et al.* (2008). A novel role for Lef-1, a central transcription mediator of Wnt signaling, in leukemogenesis. J Exp Med *205*, 515-522.

Picaud, S., Da Costa, D., Thanasopoulou, A., Filippakopoulos, P., Fish, P.V., Philpott, M., Fedorov, O., Brennan, P., Bunnage, M.E., Owen, D.R.*, et al.* (2013). PFI-1, a highly selective protein interaction inhibitor, targeting BET Bromodomains. Cancer Res *73*, 3336-3346.

Pohl, S.G., Brook, N., Agostino, M., Arfuso, F., Kumar, A.P., and Dharmarajan, A. (2017). Wnt signaling in triple-negative breast cancer. Oncogenesis *6*, e310.

Prescott, D.M., and Bender, M.A. (1962). Synthesis of RNA and protein during mitosis in mammalian tissue culture cells. Experimental Cell Research *26*, 260-268.

Prieve, M.G., Guttridge, K.L., Munguia, J., and Waterman, M.L. (1998). Differential Importin-α Recognition and Nuclear Transport by Nuclear Localization Signals within the

High-Mobility-Group DNA Binding Domains of Lymphoid Enhancer Factor 1 and T-Cell Factor 1. Molecular and Cellular Biology *18*, 4819-4832.

Qi, Z., and Chen, Y.G. (2015). Regulation of intestinal stem cell fate specification. Sci China Life Sci *58*, 570-578.

Qi, Z., Li, Y., Zhao, B., Xu, C., Liu, Y., Li, H., Zhang, B., Wang, X., Yang, X., Xie, W.*, et al.* (2017). BMP restricts stemness of intestinal Lgr5(+) stem cells by directly suppressing their signature genes. Nat Commun *8*, 13824.

Raccaud, M., Friman, E.T., Alber, A.B., Agarwal, H., Deluz, C., Kuhn, T., Gebhardt, J.C.M., and Suter, D.M. (2019). Mitotic chromosome binding predicts transcription factor properties in interphase. Nat Commun *10*, 487.

Ramanuj DasGupta, E.F. (1999). Multiple roles for activated LEF/TCF transcription complexes during hair follicle development and differentiation. Development *126*, 4557-4568.

Renko, M., Fiedler, M., Rutherford, T.J., Schaefer, J.V., Pluckthun, A., and Bienz, M. (2019a). Rotational symmetry of the structured Chip/LDB-SSDP core module of the Wnt enhanceosome. Proc Natl Acad Sci U S A *116*, 20977-20983.

Renko, M., Fiedler, M., Rutherford, T.J., Schaefer, J.V., Plückthun, A., and Bienz, M. (2019b). Rotational symmetry of the structured Chip/LDB-SSDP core module of the Wnt enhanceosome. Proceedings of the National Academy of Sciences *116*, 20977-20983.

Rodenhizer, D., Dean, T., D'Arcangelo, E., and McGuigan, A.P. (2018). The Current Landscape of 3D In Vitro Tumor Models: What Cancer Hallmarks Are Accessible for Drug Discovery? Adv Healthc Mater *7*, e1701174.

Roe, J.S., Mercan, F., Rivera, K., Pappin, D.J., and Vakoc, C.R. (2015). BET Bromodomain Inhibition Suppresses the Function of Hematopoietic Transcription Factors in Acute Myeloid Leukemia. Mol Cell *58*, 1028-1039.

Ross, D.A., and Kadesch, T. (2001). The notch intracellular domain can function as a coactivator for LEF-1. Mol Cell Biol *21*, 7537-7544.

Rother, M.B., and Van Attikum, H. (2017). DNA repair goes hip-hop: SMARCA and CHD chromatin remodellers join the break dance. Philosophical Transactions of the Royal Society B: Biological Sciences *372*, 20160285.

Roux, K.J., Kim, D.I., Burke, B., and May, D.G. (2018). BioID: A Screen for Protein-Protein Interactions. Curr Protoc Protein Sci *91*, 19 23 11-19 23 15.

S.K.Nechaev, O.A.V.a. Topological correlations in trivial knots: new arguments in favor of the representation of a crumpled polymer globule. Theoretical and Mathematical Physics *134*, 142–159.

Sachdev, S. (2001). PIASy, a nuclear matrix-associated SUMO E3 ligase, represses LEF1 activity by sequestration into nuclear bodies. Genes & Development *15*, 3088-3103.

Sachdev, S., Bruhn, L., Sieber, H., Pichler, A., Melchior, F., and Grosschedl, R. (2001). PIASy, a nuclear matrix-associated SUMO E3 ligase, represses LEF1 activity by sequestration into nuclear bodies. Genes Dev *15*, 3088-3103.

Santiago, L., Daniels, G., Wang, D., Deng, F.-M., and Lee, P. (2017). Wnt signaling pathway protein LEF1 in cancer, as a biomarker for prognosis and a target for treatment. Am J Cancer Res *7*, 1389-1406.

Sasaki, T., Ito, Y., Xu, X., Han, J., Bringas, P., Jr., Maeda, T., Slavkin, H.C., Grosschedl, R., and Chai, Y. (2005). LEF1 is a critical epithelial survival factor during tooth morphogenesis. Dev Biol *278*, 130-143.

Schindelin, J., Arganda-Carreras, I., Frise, E., Kaynig, V., Longair, M., Pietzsch, T., Preibisch, S., Rueden, C., Saalfeld, S., Schmid, B.*, et al.* (2012). Fiji: an open-source platform for biological-image analysis. Nature Methods *9*, 676-682.

Schleiffer, A., Kaitna, S., Maurer-Stroh, S., Glotzer, M., Nasmyth, K., and Eisenhaber, F. (2003). Kleisins: A Superfamily of Bacterial and Eukaryotic SMC Protein Partners. Molecular Cell *11*, 571-575.

Sekiya, T., Muthurajan, U.M., Luger, K., Tulin, A.V., and Zaret, K.S. (2009). Nucleosome-binding affinity as a primary determinant of the nuclear mobility of the pioneer transcription factor FoxA. Genes Dev *23*, 804-809.

Seyfried, T.N., and Huysentruyt, L.C. (2013). On the origin of cancer metastasis. Crit Rev Oncog *18*, 43-73.

Shang, E., Wang, X., Wen, D., Greenberg, D.A., and Wolgemuth, D.J. (2009). Double bromodomain-containing gene Brd2 is essential for embryonic development in mouse. Dev Dyn *238*, 908-917.

Shcherbakova, D.M., Baloban, M., Emelyanov, A.V., Brenowitz, M., Guo, P., and Verkhusha, V.V. (2016). Bright monomeric near-infrared fluorescent proteins as tags and biosensors for multiscale imaging. Nat Commun *7*, 12405.

Shelton, D.N., Fornalik, H., Neff, T., Park, S.Y., Bender, D., Degeest, K., Liu, X., Xie, W., Meyerholz, D.K., Engelhardt, J.F.*, et al.* (2012). The Role of LEF1 in Endometrial Gland Formation and Carcinogenesis. PLoS ONE *7*, e40312.

Shi, H., Wang, X., Lu, Z., Zhao, B.S., Ma, H., Hsu, P.J., Liu, C., and He, C. (2017). YTHDF3 facilitates translation and decay of N(6)-methyladenosine-modified RNA. Cell Res *27*, 315-328.

Shtutman, M., Zhurinsky, J., Simcha, I., Albanese, C., D'Amico, M., Pestell, R., and Ben-Ze'Ev, A. (1999). The cyclin D1 gene is a target of the beta-catenin/LEF-1 pathway. Proceedings of the National Academy of Sciences *96*, 5522-5527.

Shy, B.R., Wu, C.I., Khramtsova, G.F., Zhang, J.Y., Olopade, O.I., Goss, K.H., and Merrill, B.J. (2013). Regulation of Tcf7l1 DNA binding and protein stability as principal mechanisms of Wnt/beta-catenin signaling. Cell Rep *4*, 1-9.

Sierra, R.A., Hoverter, N.P., Ramirez, R.N., Vuong, L.M., Mortazavi, A., Merrill, B.J., Waterman, M.L., and Donovan, P.J. (2018). TCF7L1 suppresses primitive streak gene expression to support human embryonic stem cell pluripotency. Development *145*.

Silva, J., Barrandon, O., Nichols, J., Kawaguchi, J., Theunissen, T.W., and Smith, A. (2008). Promotion of reprogramming to ground state pluripotency by signal inhibition. PLoS Biol *6*, e253.

Sim, Y.J., Kim, M.S., Nayfeh, A., Yun, Y.J., Kim, S.J., Park, K.T., Kim, C.H., and Kim, K.S. (2017). 2i Maintains a Naive Ground State in ESCs through Two Distinct Epigenetic Mechanisms. Stem Cell Reports *8*, 1312-1328.

Simon, John, S., Pete, Robert, Thomas, R, Tina, Sung, M.-H., Trump, S., Stafford*, et al.* (2011). Transcription Factor AP1 Potentiates Chromatin Accessibility and Glucocorticoid Receptor Binding. Molecular Cell *43*, 145-155.

Sjef Verbeek, D.l., Frans Hofhuis, Els Robanus-Maandagt, Hein te Rielet, Marc van de Wetering, Mariette Oosterwegel, Anne Wilson, H. Robson MacDonald & Hans Clevers (1995). An HMG-box-containing T-cell factor required for thymocyte differentiation. Letters to Nature *374*, 70-74.

Skene, P.J., Henikoff, J.G., and Henikoff, S. (2018). Targeted in situ genome-wide profiling with high efficiency for low cell numbers. Nat Protoc *13*, 1006-1019.

Skene, P.J., and Henikoff, S. (2017). An efficient targeted nuclease strategy for high-resolution mapping of DNA binding sites. eLife *6*.

Slusarski, D.C., Corces, V.G., and Moon, R.T. (1997). Interaction of Wnt and a Frizzled homologue triggers G-protein-linked phosphatidylinositol signalling. Nature *390*, 410-413.

Slyper, M., Shahar, A., Bar-Ziv, A., Granit, R.Z., Hamburger, T., Maly, B., Peretz, T., and Ben-Porath, I. (2012). Control of breast cancer growth and initiation by the stem cell-associated transcription factor TCF3. Cancer Res *72*, 5613-5624.

Sobecki, M., Mrouj, K., Camasses, A., Parisis, N., Nicolas, E., Lleres, D., Gerbe, F., Prieto, S., Krasinska, L., David, A.*, et al.* (2016). The cell proliferation antigen Ki-67 organises heterochromatin. Elife *5*, e13722.

Sokol, S.Y. (2011). Maintaining embryonic stem cell pluripotency with Wnt signaling. Development *138*, 4341-4350.

Song, H., Goetze, S., Bischof, J., Spichiger-Haeusermann, C., Kuster, M., Brunner, E., and Basler, K. (2010). Coop functions as a corepressor of Pangolin and antagonizes Wingless signaling. Genes & Development *24*, 881-886.

Sonnen, K.F., Lauschke, V.M., Uraji, J., Falk, H.J., Petersen, Y., Funk, M.C., Beaupeux, M., Francois, P., Merten, C.A., and Aulehla, A. (2018). Modulation of Phase Shift between Wnt and Notch Signaling Oscillations Controls Mesoderm Segmentation. Cell *172*, 1079-1090 e1012.

Spater, D., Hansson, E.M., Zangi, L., and Chien, K.R. (2014). How to make a cardiomyocyte. Development *141*, 4418-4431.

Spiegelman, B.M., and Heinrich, R. (2004). Biological Control through Regulated Transcriptional Coactivators. Cell *119*, 157-167.

Spitz, F., and Furlong, E.E.M. (2012). Transcription factors: from enhancer binding to developmental control. Nature Reviews Genetics *13*, 613-626.

Sprowl, S., and Waterman, M.L. (2013). Past visits present: TCF/LEFs partner with ATFs for beta-catenin-independent activity. PLoS Genet *9*, e1003745.

Staal, F., Famili, F., Garcia Perez, L., and Pike-Overzet, K. (2016). Aberrant Wnt Signaling in Leukemia. Cancers *8*, 78.

Staal, F.J.T., and M. Sen, J. (2008). The canonical Wnt signaling pathway plays an important role in lymphopoiesis and hematopoiesis. European Journal of Immunology *38*, 1788-1794.

Stonyte, V., Boye, E., and Grallert, B. (2018). Regulation of global translation during the cell cycle. Journal of Cell Science *131*, jcs220327.

Strickland, D., Lin, Y., Wagner, E., Hope, C.M., Zayner, J., Antoniou, C., Sosnick, T.R., Weiss, E.L., and Glotzer, M. (2012). TULIPs: tunable, light-controlled interacting protein tags for cell biology. Nat Methods *9*, 379-384.

Su, M.-C., Chen, C.-T., Huang, F.-I., Chen, Y.-L., Jeng, Y.-M., and Lin, C.-Y. (2014). Expression of LEF1 is an independent prognostic factor for patients with oral squamous cell carcinoma. *113*, 934-939.

Takada, S., Stark, K.L., Shea, M.J., Vassileva, G., McMahon, J.A., and McMahon, A.P. (1994). Wnt-3a regulates somite and tailbud formation in the mouse embryo. Genes & Development *8*, 174-189.

Tamai, K., Semenov, M., Kato, Y., Spokony, R., Liu, C., Katsuyama, Y., Hess, F., Saint-Jeannet, J.-P., and He, X. (2000). LDL-receptor-related proteins in Wnt signal transduction. Nature *407*, 530-535.

Tan, J., Yang, X., Zhuang, L., Jiang, X., Chen, W., Lee, P.L., Karuturi, R.K., Tan, P.B., Liu, E.T., and Yu, Q. (2007). Pharmacologic disruption of Polycomb-repressive complex 2-mediated gene repression selectively induces apoptosis in cancer cells. Genes Dev *21*, 1050-1063.

Tandon, B., Peterson, L., Gao, J., Nelson, B., Ma, S., Rosen, S., and Chen, Y.H. (2011). Nuclear overexpression of lymphoid-enhancer-binding factor 1 identifies chronic lymphocytic leukemia/small lymphocytic lymphoma in small B-cell lymphomas. Mod Pathol *24*, 1433-1443.

Tate, J.G., Bamford, S., Jubb, H.C., Sondka, Z., Beare, D.M., Bindal, N., Boutselakis, H., Cole, C.G., Creatore, C., Dawson, E.*, et al.* (2019). COSMIC: the Catalogue Of Somatic Mutations In Cancer. Nucleic Acids Research *47*, D941-D947.

Ten Berge, D., Brugmann, S.A., Helms, J.A., and Nusse, R. (2008). Wnt and FGF signals interact to coordinate growth with cell fate specification during limb development. *135*, 3247-3257.

ten Berge, D., Kurek, D., Blauwkamp, T., Koole, W., Maas, A., Eroglu, E., Siu, R.K., and Nusse, R. (2011). Embryonic stem cells require Wnt proteins to prevent differentiation to epiblast stem cells. Nat Cell Biol *13*, 1070-1075.

Terakawa, T., Bisht, S., Eeftens, J.M., Dekker, C., Haering, C.H., and Greene, E.C. (2017). The condensin complex is a mechanochemical motor that translocates along DNA. Science *358*, 672-676.

Teves, S.S., An, L., Bhargava-Shah, A., Xie, L., Darzacq, X., and Tjian, R. (2018). A stable mode of bookmarking by TBP recruits RNA polymerase II to mitotic chromosomes. eLife *7*.

Teves, S.S., An, L., Hansen, A.S., Xie, L., Darzacq, X., and Tjian, R. (2016). A dynamic mode of mitotic bookmarking by transcription factors. Elife *5*.

Thery, M. (2010a). Micropatterning as a tool to decipher cell morphogenesis and functions. J Cell Sci *123*, 4201-4213.

Thery, M. (2010b). Micropatterning as a tool to decipher cell morphogenesis and functions. Journal of Cell Science *123*, 4201-4213.

Thurman, R.E., Rynes, E., Humbert, R., Vierstra, J., Maurano, M.T., Haugen, E., Sheffield, N.C., Stergachis, A.B., Wang, H., Vernot, B.*, et al.* (2012). The accessible chromatin landscape of the human genome. Nature *489*, 75-82.

Tian, X., Liu, Z., Niu, B., Zhang, J., Tan, T.K., Lee, S.R., Zhao, Y., Harris, D.C.H., and Zheng, G. (2011). E-Cadherin/β-Catenin Complex and the Epithelial Barrier. Journal of Biomedicine and Biotechnology *2011*, 1-6.

Torres, J., Prieto, J., Durupt, F.C., Broad, S., and Watt, F.M. (2012). Efficient differentiation of embryonic stem cells into mesodermal precursors by BMP, retinoic acid and Notch signalling. PLoS One *7*, e36405.

Tortelote, G.G., Hernandez-Hernandez, J.M., Quaresma, A.J., Nickerson, J.A., Imbalzano, A.N., and Rivera-Perez, J.A. (2013). Wnt3 function in the epiblast is required for the maintenance but not the initiation of gastrulation in mice. Dev Biol *374*, 164-173.

Turner, D.A., Girgin, M., Alonso-Crisostomo, L., Trivedi, V., Baillie-Johnson, P., Glodowski, C.R., Hayward, P.C., Collignon, J., Gustavsen, C., Serup, P.*, et al.* (2017). Anteroposterior polarity and elongation in the absence of extra-embryonic tissues and of spatially localised signalling in gastruloids: mammalian embryonic organoids. Development *144*, 3894-3906.

Valenta, T., Lukas, J., and Korinek, V. (2003). HMG box transcription factor TCF-4's interaction with CtBP1 controls the expression of the Wnt target Axin2/Conductin in human embryonic kidney cells. Nucleic Acids Res *31*, 2369-2380.

Valls, E., Sanchez-Molina, S., and Martinez-Balbas, M.A. (2005). Role of histone modifications in marking and activating genes through mitosis. J Biol Chem *280*, 42592-42600.

Van De Wetering, M., Cavallo, R., Dooijes, D., Van Beest, M., Van Es, J., Loureiro, J., Ypma, A., Hursh, D., Jones, T., Bejsovec, A.*, et al.* (1997). Armadillo Coactivates Transcription Driven by the Product of the Drosophila Segment Polarity Gene dTCF. Cell *88*, 789-799.

Van Den Brink, S.C., Alemany, A., Van Batenburg, V., Moris, N., Blotenburg, M., Vivié, J., Baillie-Johnson, P., Nichols, J., Sonnen, K.F., Martinez Arias, A.*, et al.* (2020). Single-cell and spatial transcriptomics reveal somitogenesis in gastruloids. Nature.

van den Brink, S.C., Baillie-Johnson, P., Balayo, T., Hadjantonakis, A.K., Nowotschin, S., Turner, D.A., and Martinez Arias, A. (2014). Symmetry breaking, germ layer specification and axial organisation in aggregates of mouse embryonic stem cells. Development *141*, 4231-4242.

Van Genderen, C., Okamura, R.M., Farinas, I., Quo, R.G., Parslow, T.G., Bruhn, L., and Grosschedl, R. (1994). Development of several organs that require inductive epithelial-mesenchymal interactions is impaired in LEF-1-deficient mice. *8*, 2691-2703.

Van Hooser, A.A., Yuh, P., and Heald, R. (2005). The perichromosomal layer. Chromosoma *114*, 377-388.

van Tienen, L.M., Mieszczanek, J., Fiedler, M., Rutherford, T.J., and Bienz, M. (2017a). Constitutive scaffolding of multiple Wnt enhanceosome components by Legless/BCL9. Elife *6*.

Van Tienen, L.M., Mieszczanek, J., Fiedler, M., Rutherford, T.J., and Bienz, M. (2017b). Constitutive scaffolding of multiple Wnt enhanceosome components by Legless/BCL9. *6*.

VanderVorst, K., Hatakeyama, J., Berg, A., Lee, H., and Carraway, K.L., 3rd (2018). Cellular and molecular mechanisms underlying planar cell polarity pathway contributions to cancer malignancy. Semin Cell Dev Biol *81*, 78-87.

Varga, M., Maegawa, S., Bellipanni, G., and Weinberg, E.S. (2007). Chordin expression, mediated by Nodal and FGF signaling, is restricted by redundant function of two beta-catenins in the zebrafish embryo. Mech Dev *124*, 775-791.

Vasquez-Del Carpio, R., Kaplan, F.M., Weaver, K.L., Vanwye, J.D., Alves-Guerra, M.C., Robbins, D.J., and Capobianco, A.J. (2011). Assembly of a Notch Transcriptional Activation Complex Requires Multimerization. *31*, 1396-1408.

Veeman, M.T., Slusarski, D.C., Kaykas, A., Louie, S.H., and Moon, R.T. (2003). Zebrafish prickle, a modulator of noncanonical Wnt/Fz signaling, regulates gastrulation movements. Curr Biol *13*, 680-685.

Verbeek, S., Izon, D., Hofhuis, F., Robanus-Maandag, E., Te Riele, H., Watering, M.V.D., Oosterwegel, M., Wilson, A., Robson Macdonald, H., and Clevers, H. (1995). An HMG-box-containing T-cell factor required for thymocyte differentiation. Nature *374*, 70-74.

Walker, A., Frei, R., and Lawson, K.R. (2014). The cytoplasmic domain of N-cadherin modulates MMP-9 induction in oral squamous carcinoma cells. International Journal of Oncology *45*, 1699-1706.

Walther, N., Ulrich, A., Vockerodt, M., Von Bonin, F., Klapper, W., Meyer, K., Eberth, S., Pukrop, T., Spang, R., Trümper, L.*, et al.* (2013). Aberrant Lymphocyte Enhancer–Binding Factor 1 Expression Is Characteristic for Sporadic Burkitt's Lymphoma. The American Journal of Pathology *182*, 1092-1098.

Wang, X., and Yang, P. (2008). In vitro Differentiation of Mouse Embryonic Stem (mES) Cells Using the Hanging Drop Method. Journal of Visualized Experiments.

Wapinski, O.L., Lee, Q.Y., Chen, A.C., Li, R., Corces, M.R., Ang, C.E., Treutlein, B., Xiang, C., Baubet, V., Suchy, F.P.*, et al.* (2017). Rapid Chromatin Switch in the Direct Reprogramming of Fibroblasts to Neurons. Cell Rep *20*, 3236-3247.

Warren, David, Hnisz, D., Brian, Charles, Michael, Peter, Tong, and Richard (2013). Master Transcription Factors and Mediator Establish Super-Enhancers at Key Cell Identity Genes. Cell *153*, 307-319.

Waterman, M.L., Fischer, W.H., and Jones, K.A. (1991). A thymus-specific member of the HMG protein family regulates the human T cell receptor C alpha enhancer. Genes & Development *5*, 656-669.

Westfall, T.A., Brimeyer, R., Twedt, J., Gladon, J., Olberding, A., Furutani-Seiki, M., and Slusarski, D.C. (2003). Wnt-5/pipetail functions in vertebrate axis formation as a negative regulator of Wnt/β-catenin activity. Journal of Cell Biology *162*, 889-898.

Wheelock, M.J., Shintani, Y., Maeda, M., Fukumoto, Y., and Johnson, K.R. (2008). Cadherin switching. J Cell Sci *121*, 727-735.

White, P.H., Farkas, D.R., McFadden, E.E., and Chapman, D.L. (2003). Defective somite patterning in mouse embryos with reduced levels of Tbx6. Development *130*, 1681-1690.

Willinger, T., Freeman, T., Herbert, M., Hasegawa, H., McMichael, A.J., and Callan, M.F.C. (2006). Human Naive CD8 T Cells Down-Regulate Expression of the WNT Pathway Transcription Factors Lymphoid Enhancer Binding Factor 1 and Transcription Factor 7 (T Cell Factor-1) following Antigen Encounter In Vitro and In Vivo. The Journal of Immunology *176*, 1439-1446.

Wolf, D., Rodova, M., Miska, E.A., Calvet, J.P., and Kouzarides, T. (2002). Acetylation of beta-catenin by CREB-binding protein (CBP). J Biol Chem *277*, 25562-25567.

Wong, M.M., Byun, J.S., Sacta, M., Jin, Q., Baek, S., and Gardner, K. (2014). Promoter-bound p300 complexes facilitate post-mitotic transmission of transcriptional memory. PLoS One *9*, e99989.

Wray, J., Kalkan, T., Gomez-Lopez, S., Eckardt, D., Cook, A., Kemler, R., and Smith, A. (2011). Inhibition of glycogen synthase kinase-3 alleviates Tcf3 repression of the pluripotency network and increases embryonic stem cell resistance to differentiation. Nat Cell Biol *13*, 838-845.

Wu, C.I., Hoffman, J.A., Shy, B.R., Ford, E.M., Fuchs, E., Nguyen, H., and Merrill, B.J. (2012). Function of Wnt/beta-catenin in counteracting Tcf3 repression through the Tcf3-beta-catenin interaction. Development *139*, 2118-2129.

Wu, S.Y., and Chiang, C.M. (2007). The double bromodomain-containing chromatin adaptor Brd4 and transcriptional regulation. J Biol Chem *282*, 13141-13145.

Xing, H., Vanderford, N.L., and Sarge, K.D. (2008). The TBP–PP2A mitotic complex bookmarks genes by preventing condensin action. Nature cell biology *10*, 1318-1323.

Xing, S., Li, F., Zeng, Z., Zhao, Y., Yu, S., Shan, Q., Li, Y., Phillips, F.C., Maina, P.K., Qi, H.H.*, et al.* (2016). Tcf1 and Lef1 transcription factors establish CD8(+) T cell identity through intrinsic HDAC activity. Nat Immunol *17*, 695-703.

Yamada, M., Ohnishi, J., Ohkawara, B., Iemura, S., Satoh, K., Hyodo-Miura, J., Kawachi, K., Natsume, T., and Shibuya, H. (2006). NARF, an nemo-like kinase (NLK)-associated ring finger protein regulates the ubiquitylation and degradation of T cell factor/lymphoid enhancer factor (TCF/LEF). J Biol Chem *281*, 20749-20760.

Yamanaka, Y., Tamplin, O.J., Beckers, A., Gossler, A., and Rossant, J. (2007). Live Imaging and Genetic Analysis of Mouse Notochord Formation Reveals Regional Morphogenetic Mechanisms. Developmental Cell *13*, 884-896.

Yan, D., Wiesmann, M., Rohan, M., Chan, V., Jefferson, A.B., Guo, L., Sakamoto, D., Caothien, R.H., Fuller, J.H., Reinhard, C.*, et al.* (2001). Elevated expression of axin2 and hnkd mRNA provides evidence that Wnt/ -catenin signaling is activated in human colon tumors. Proceedings of the National Academy of Sciences *98*, 14973-14978.

Yan, J., Xu, L., Crawford, G., Wang, Z., and Burgess, S.M. (2006). The Forkhead Transcription Factor Foxl1 Remains Bound to Condensed Mitotic Chromosomes and Stably Remodels Chromatin Structure. Molecular and Cellular Biology *26*, 155-168.

Yi, F., Pereira, L., Hoffman, J.A., Shy, B.R., Yuen, C.M., Liu, D.R., and Merrill, B.J. (2011). Opposing effects of Tcf3 and Tcf1 control Wnt stimulation of embryonic stem cell self-renewal. Nat Cell Biol *13*, 762-770.

Yin, Y., White, A.C., Huh, S.-H., Hilton, M.J., Kanazawa, H., Long, F., and Ornitz, D.M. (2008). An FGF–WNT gene regulatory network controls lung mesenchyme development. Developmental Biology *319*, 426-436.

Ying, Q.L., Wray, J., Nichols, J., Batlle-Morera, L., Doble, B., Woodgett, J., Cohen, P., and Smith, A. (2008). The ground state of embryonic stem cell self-renewal. Nature *453*, 519-523.

Yochum, G.S., Sherrick, C.M., Macpartlin, M., and Goodman, R.H. (2010). A beta-catenin/TCF-coordinated chromatin loop at MYC integrates 5' and 3' Wnt responsive enhancers. Proc Natl Acad Sci U S A *107*, 145-150.

Yook, J.I., Li, X.Y., Ota, I., Fearon, E.R., and Weiss, S.J. (2005). Wnt-dependent regulation of the E-cadherin repressor snail. J Biol Chem *280*, 11740-11748.

Yoshimura, S.H., and Hirano, T. (2016). HEAT repeats - versatile arrays of amphiphilic helices working in crowded environments? J Cell Sci *129*, 3963-3970.

Yu, S., Zhou, X., Steinke, F.C., Liu, C., Chen, S.C., Zagorodna, O., Jing, X., Yokota, Y., Meyerholz, D.K., Mullighan, C.G.*, et al.* (2012). The TCF-1 and LEF-1 transcription factors have cooperative and opposing roles in T cell development and malignancy. Immunity *37*, 813-826.

Zaidi, S.K., Nickerson, J.A., Imbalzano, A.N., Lian, J.B., Stein, J.L., and Stein, G.S. (2018). Mitotic Gene Bookmarking: An Epigenetic Program to Maintain Normal and Cancer Phenotypes. Mol Cancer Res *16*, 1617-1624.

Zaidi, S.K., Young, D.W., Montecino, M., Lian, J.B., Stein, J.L., Van Wijnen, A.J., and Stein, G.S. (2010). Architectural Epigenetics: Mitotic Retention of Mammalian Transcriptional Regulatory Information. Molecular and Cellular Biology *30*, 4758-4766.

Zavadil, J., Cermak, L., Soto-Nieves, N., and Böttinger, E.P. (2004). Integration of TGF-β/Smad and Jagged1/Notch signalling in epithelial-to-mesenchymal transition. *23*, 1155-1165.

Zhan, T., Rindtorff, N., and Boutros, M. (2017). Wnt signaling in cancer. Oncogene *36*, 1461-1473.

Zhang, Y., Tian, S., Xiong, J., Zhou, Y., Song, H., and Liu, C. (2018). JQ-1 Inhibits Colon Cancer Proliferation via Suppressing Wnt/β-Catenin Signaling and miR-21. Chemical Research in Toxicology *31*, 302-307.

Zhang, Y., Yu, J., Shi, C., Huang, Y., Wang, Y., Yang, T., and Yang, J. (2013). Lef1 contributes to the differentiation of bulge stem cells by nuclear translocation and cross-talk with the Notch signaling pathway. Int J Med Sci *10*, 738-746.

Zhao, Z., Tavoosidana, G., Sjölinder, M., Göndör, A., Mariano, P., Wang, S., Kanduri, C., Lezcano, M., Singh Sandhu, K., Singh, U.*, et al.* (2006). Circular chromosome conformation capture (4C) uncovers extensive networks of epigenetically regulated intra- and interchromosomal interactions. Nature Genetics *38*, 1341-1347.

Zheng, T., Wang, A., Hu, D., and Wang, Y. (2017). Molecular mechanisms of breast cancer metastasis by gene expression profile analysis. Mol Med Rep *16*, 4671-4677.

Zhou, X., Yu, S., Zhao, D.-M., Harty, J.T., Badovinac, V.P., and Xue, H.-H. (2010). Differentiation and Persistence of Memory CD8+ T Cells Depend on T Cell Factor 1. Immunity *33*, 229-240.

Zhu, C., Yu, M., Huang, H., Juric, I., Abnousi, A., Hu, R., Lucero, J., Behrens, M.M., Hu, M., and Ren, B. (2019). An ultra high-throughput method for single-cell joint analysis of open chromatin and transcriptome. Nat Struct Mol Biol *26*, 1063-1070.

Zhuang, S. (2013). Regulation of STAT signaling by acetylation. Cellular Signalling *25*, 1924-1931.